SH
11
.A2
F53
FISH

U.S. Department
of Commerce

Volume 120
Number 2
April 2022

Fishery Bulletin

U.S. Department of Commerce

Gina M. Raimondo
Secretary

National Oceanic and Atmospheric Administration

Richard W. Spinrad
Administrator

National Marine Fisheries Service

Janet Coit
Assistant Administrator
for Fisheries

Fishery Bulletin

Scientific Editor
José I. Castro
National Marine Fisheries Service, NOAA
263 13th Avenue South
Saint Petersburg, Florida 33701

Managing Editor
Kathryn Dennis
Scientific Publications Office
National Marine Fisheries Service, NOAA
1845 Wasp Boulevard, Building 176
Honolulu, Hawaii 96818

Associate Editor
Cara Mayo
Scientific Publications Office
National Marine Fisheries Service, NOAA
7600 Sand Point Way NE
Seattle, Washington 98115-0070

Editorial Board

Henry L. Bart Jr.	Tulane University, New Orleans, Louisiana
Katherine E. Bemis	National Systematics Laboratory, Washington, DC
Matthew D. Campbell	National Marine Fisheries Service, Pascagoula, Mississippi
William B. Driggers III	National Marine Fisheries Service, Pascagoula, Mississippi
Gretchen L. Grammer	South Australian Research and Development Institute, Adelaide, Australia
Richard Langton	National Marine Fisheries Service, Walpole, Maine (retired)
J. Fernando Márquez-Farías	Universidad Autónoma de Sinaloa, Mazatlán, México
Richard S. McBride	National Marine Fisheries Service, Woods Hole, Massachusetts
Richard L. Merrick	National Marine Fisheries Service, Falmouth, Massachusetts (retired)
Richard D. Methot	National Marine Fisheries Service, Seattle, Washington
Lisa J. Natanson	National Marine Fisheries Service, Narragansett, Rhode Island (retired)
Mark S. Peterson	University of Southern Mississippi, Ocean Springs, Mississippi
André E. Punt	University of Washington, Seattle, Washington
Joseph M. Quattro	University of South Carolina, Columbia, South Carolina
John F. Walter III	National Marine Fisheries Service, Miami, Florida

***Fishery Bulletin* website: https://spo.nmfs.noaa.gov/fb.htm**

Fishery Bulletin (ISSN 0090-0656) is published quarterly by the Scientific Publications Office, National Marine Fisheries Service, NOAA, 7600 Sand Point Way NE, Seattle, WA 98115-0070.

Although the contents of this publication have not been copyrighted and may be reprinted entirely, reference to source is appreciated.

The Secretary of Commerce has determined that the publication of this periodical is necessary according to law for the transaction of public business of this Department. Use of funds for printing of this periodical has been approved by the Director of the Office of Management and Budget.

For Sale by the Superintendent of Documents, U.S. Government Publishing Office, Washington, DC 20401. Subscription price per year: $32.00 domestic and $44.80 foreign. Cost per single issue: $19.00 domestic and $26.60 foreign. **See back for order form.**

Fishery Bulletin carries original research reports on investigations in fishery science, engineering, and economics. It began as the Bulletin of the United States Fish Commission in 1881; it became the Bulletin of the Bureau of Fisheries in 1904 and the *Fishery Bulletin* of the U.S. Fish and Wildlife Service in 1941. Separates were issued as documents through volume 46; the last document was no. 1103. Beginning with volume 47 in 1931 and continuing through volume 62 in 1963, each separate appeared as a numbered bulletin. A new system began in 1963, with volume 63, in which papers are bound together in a single issue. Beginning with volume 70, number 1, January 1972, *Fishery Bulletin* became a periodical, issued quarterly. In this form, it is available by subscription from the Superintendent of Documents, U.S. Government Publishing Office, Washington, DC 20401. It is also available free in limited numbers to libraries, research institutions, and state and federal agencies and in exchange for other scientific publications.

U.S. Department of Commerce
Seattle, Washington

Volume 120
Number 2
April 2022

Fishery Bulletin

SMITHSONIAN
NOV 0 9 2022
LIBRARIES

Contents

Articles

99–112 **Daniel Pauly, Nicola Smith, and Mark Butler**

Growth and related traits of the sheepswool sponge (*Hippospongia lachne*): practical and theoretical considerations

113–124 **Sergei A. Evseenko, Dmitry V. Bolshakov, Yana Yu. Bolshakova, Yuri O. Kopylov-Guskov, Natalya V. Gordeeva, Evgeniia P. Karpova, and Alexander R. Boltachev**

New data on the morphology of the Mekong blind sole (*Typhlachirus elongatus*) indicating the need for a revision of the genus

125–137 **Lotfi Rabaoui, Lamia Yacoubi, Yu-Jia Lin, Thadickal V. Joydas, Mohammad A. Qurban, Panickan Premlal, Jinoy Gopalan, Zahid Nazeer, Manambrakat Vijayakumaran, Syed Ajmal Khan, and Rubén H. Roa-Ureta**

Ecology, life history, and fisheries potential of the flathead lobster (*Thenus orientalis*) in the Arabian Gulf

138–149 **Ross Cooper, Heidi Dewar, Barbara A. Muhling, Steven L. H. Teo, John Hyde, and Keith Bigelow**

Spatiotemporal catch patterns and population distributions of bigeye Pacific opah (*Lampris megalopsis*) and smalleye Pacific opah (*L. incognitus*) in the eastern North Pacific Ocean

150–161 **Jonathan J. Scordino, Cydni Marshall, Adrianne M. Akmajian, Daniel Shay, and Randall James**

Consumption of Pacific salmon (*Oncorhynchus* spp.) by California sea lions (*Zalophus californianus*) and Steller sea lions (*Eumetopias jubatus*) in northwest Washington during 2010–2013

The National Marine Fisheries Service (NMFS) does not approve, recommend, or endorse any proprietary product or proprietary material mentioned in this publication. No reference shall be made to NMFS, or to this publication furnished by NMFS, in any advertising or sales promotion that would indicate or imply that NMFS approves, recommends, or endorses any proprietary product or proprietary material mentioned herein or that has as its purpose an intent to cause directly or indirectly the advertised product to be used or purchased because of this NMFS publication.

The NMFS Scientific Publications Office is not responsible for the contents of the articles.

162–175 Crystal L. Hightower, J. Marcus Drymon, Amanda E. Jefferson, Matthew B. Jargowsky, Emily A. Seubert, Simon Dedman, John F. Mareska, and Sean P. Powers

Population dynamics, relative abundance, and habitat suitability for adult red drum (*Sciaenops ocellatus*) in nearshore waters of the north-central Gulf of Mexico

176–186 Megan K. McKinzie and Stephen T. Szedlmayer

Mortality estimates for gray triggerfish (*Balistes capriscus*) in the northern Gulf of Mexico based on acoustic telemetry

187–189 Errata

191–194 Guidelines for authors

National Marine
Fisheries Service
NOAA

Fishery Bulletin
established in 1881

Spencer F. Baird
First U.S. Commissioner
of Fisheries and founder
of *Fishery Bulletin*

Growth and related traits of the sheepswool sponge (*Hippospongia lachne*): practical and theoretical considerations

Daniel Pauly (contact author)[1]
Nicola Smith[2]
Mark Butler[3]

Email address for contact author: d.pauly@oceans.ubc.ca

[1] Sea Around Us
Institute for the Oceans and Fisheries
University of British Columbia
2202 Main Mall
Vancouver, British Columbia V6T 1Z4, Canada

[2] Changing Oceans Research Unit
Institute for the Oceans and Fisheries
University of British Columbia
2202 Main Mall
Vancouver, British Columbia V6T 1Z4, Canada

[3] Institute of Environment and
Department of Biological Sciences
Florida International University
3000 NE 151 Street, AC1-213
North Miami, Florida 33181

Abstract—Fisheries for Caribbean sponge species began in the mid-1800s and landings peaked around the early 1900s before crashing because of a combination of overexploitation, disease, and hurricanes as well as, later, the introduction of artificial sponges. Still, artisanal sponge fisheries remain in Florida and areas of the Caribbean like The Bahamas, but none of those fisheries or the sponges upon which they depend are well studied. On the basis of data and information published by J. Storr in 1964 as well as of our own data, von Bertalanffy growth parameters were estimated for the most commercially valuable Caribbean sponge, the sheepswool sponge or wool sponge (*Hippospongia lachne*), along with related statistics, notably longevity. Also, morphological dimensional constraints that are likely to limit the supply of oxygen deep within this and other near-spherical sponge species are presented, along with the sponges' evolutionary and ontogenic responses to these constraints. These considerations are also illustrated with data from species other than the wool sponge and are consistent with a general theory of growth for water-breathing ectotherms, the gill-oxygen limitation theory. The information provided herein should be useful for quantifying the ecosystem effect of sponge fisheries in Florida, The Bahamas, and elsewhere and for improving the management of sponge fisheries and mariculture worldwide.

Manuscript submitted 27 October 2021.
Manuscript accepted 11 March 2022.
Fish. Bull. 120:99–112 (2022).
Online publication date: 29 March 2022.
doi: 10.7755/FB.120.2.1

The views and opinions expressed or implied in this article are those of the author (or authors) and do not necessarily reflect the position of the National Marine Fisheries Service, NOAA.

This contribution addresses issues related to the growth, longevity, reproduction, and respiration of sponges, with emphasis on the sheepswool sponge (*Hippospongia lachne*), also known as and henceforth referred to as the *wool sponge*, and to the roles of sponges in fisheries, ecosystems, and ecosystem models. Emphasis is given to the relationship between growth and respiration in the wool sponge and other sponges because this issue is often overlooked in studies of water-breathing ectotherms (WBE), in which an appropriate supply of oxygen is as important for survival and growth as an appropriate amount of food (Pauly, 2021a).

Our emphasis on respiration is incorporated in the use of a growth curve, the von Bertalanffy growth function (VBGF) that is widely used in fisheries research and can be derived from the "dimensional tension" (Pauly and Cheung, 2017) between oxygen supply and demand in growing WBE.

Sponges are important if underappreciated components of marine ecosystems, including coral reefs where sponge diversity reaches its zenith (Diaz and Rützler, 2001, 2011). Many ecological functions and services, including bentho-pelagic coupling through filtration and nutrient cycling (Valentine and Butler, 2019; Pawlik and McMurray, 2020), enhancement of habitat complexity (Herrnkind et al., 1997), alterations in sediment structure (Neuweiler and Burdige, 2005), contribution to underwater soundscapes (Butler et al., 2016), provisioning of food for spongivorous species (Loh and Pawlik, 2014), and support of fisheries (Butler et al., 2017), are attributable to sponges and their associated microbiomes (Bell, 2008; Bell et al., 2017). With respect to support of fisheries, some shallow-water species are, or have been, commercially exploited, notably the wool sponge, which is also farmed (Storr, 1964; Osinga et al., 1999; McClenachan, 2008) and grown for use in habitat restoration (Butler et al., 2021).

Despite there being over 1000 genera of marine sponges (de Voogd et al., 2021; Palomares and Pauly, 2021), in the past, only 2 genera were fished

commercially, *Hippospongia* and *Spongia* (McClenachan, 2008). Because of their soft and absorbent skeletons, species of these 2 genera had, and still have, a variety of uses (McClenachan, 2008). Before the appearance of synthetic sponges, natural sponges were used for personal hygiene, house and car cleaning, medical surgery, glazing pottery, cleaning industrial machinery and railroad equipment, tile and brick laying, and dressing leather and were used as gun swabs in the army and navy and in the manufacture of hats, soldiers' helmets, and jewelry, among other things (Corfield, 1938; Stuart, 1948; Storr, 1964; McClenachan, 2008). Recently, the demand for commercially harvested sponges has extended beyond these 2 genera and has been driven primarily by the cosmetic, biomedical, and aquarium trades (Belarbi et al., 2003; Oronti et al., 2012; Mehbub et al., 2014).

The work described in this contribution is the first attempt to fit to a sponge the standard version of the VBGF, an equation commonly used in marine biology and fishery research. There are several practical reasons to fit the VBGF to a sponge. First, since the publication of the classic text of Beverton and Holt (1957), the VBGF has been and remains part of the basic toolkit of fisheries science, mainly because of its versatility and realism. As such, its parameters are components of numerous models used to understand and manage the exploitation of fish and invertebrate populations. Second, a standard growth curve should be useful for sponge mariculture, for example, to assess and compare the performance of individual sponges raised under different environmental conditions. The growth rates (in summer and winter) of 4 species of commercial sponges, the wool sponge, yellow sponge (*Spongia barbara*), glove sponge (*S. cheiris*), and grass sponge (*S. graminea*), from the Caribbean have been measured in the field, but those estimates do not include the full range of sponge sizes and ages (Butler et al., 2017).

The third reason for fitting the VBGF to sponges is theoretical. The VBGF was derived from first-order physiological principles involving the interplay of surfaces and volumes leading to asymptotic growth (see von Bertalanffy, 1938, 1951; Pauly, 2019a, 2021a). It should therefore be enlightening to test if these principles, first derived for fish, also apply to sponges, the oldest multicellular animal taxon. Also, this contribution might assist ecosystem modelers, who so far have usually neglected sponges (but see Opitz, 1996; Tudman, 2001; Butler, 2003; Pinkerton et al., 2008; Butler and Dolan, 2017).

This contribution does not address the growth of encrusting or tubular sponges that, because of their laminar bodies, may not suffer from the respiratory constraints that are emphasized later herein. Rather, this study dealt with nearly sphere-shaped species, such as the wool sponge (Fig. 1). Our use of the wool sponge as an example is also pertinent because it is one of the most valuable and abundant commercially exploited species and therefore has been better studied than many other sponge species (Stevely et al., 1978; Witzell, 1998; Butler et al., 2017, 2018; Butler et al., 2021).

Materials and methods

Growth

We fitted the VBGF to the empirical growth curve published by Storr (1964), which is based on wool sponges tagged in the upper Gulf of Mexico. Storr (1964) described the way he obtained growth data (mainly from sponges in grounds at Piney Point in Florida) as follows:

"*When the annual rates of increase between units of diameter were plotted, it was found that for growth beyond a diameter of 3-1/2 inches the growth factor could be expressed by the standard formula*:

$$y = Ae^{Bx}, \quad (1)$$

where y = *annual rate of increase—the growth factor*; [and]
x = *radius of the sponge in inches at beginning of a year and* A *and* B *are constants, while* e *is the base of the Naperian logarithms.*

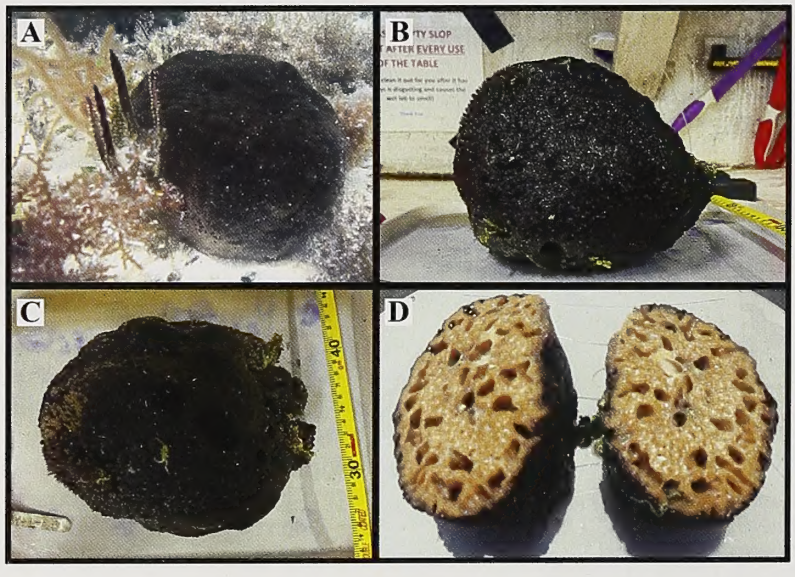

Figure 1

Images of a sheepswool sponge or wool sponge (*Hippospongia lachne*) that was 18 cm in diameter and was collected in Florida by M. Butler on 18 September 2021 and photographed by J. Butler: (**A**) shown in the wild in the Florida Keys; (**B**) side view, taken in the laboratory; (**C**) top view, taken in the laboratory; and (**D**) inside of the specimen, after horizontal sectioning in the laboratory.

This is assuming a regular spherical shape for the sponge.

For the particular values obtained on the growth rate [of sponges] *off the Piney Point area the formula, modified for ease in working, became* [as follows]:

$$y = 1 + 11.2e^{-(1.07x)} \quad (2)$$

Since the data gathered were for diameters from 2 to 7 inches, the use of this formula for extrapolation of the curve beyond 7 inches was particularly useful. . . . The formula indicates that growth will almost completely stop when the sponge reaches a 12-inch diameter."

The caveat that must be mentioned here is that it is risky to extrapolate beyond the range of one's supporting data. Storr (1964) included only data for wool sponges with diameters up to 7 in (18 cm). Therefore, his estimated asymptotic size of a diameter of 12 in (~30.5 cm) for wool sponges is tentative. Indeed, larger wool sponges exist, although from 12 inches on, they usually take a more cylindrical shape, a theme to which we return later.

Storr (1964) writes further, *"The rate of growth in diameter indicated by* [Equation 2] *appears to be valid for the first 5 or 6 years. Beyond this point the growth rate must be assumed to be somewhat less than indicated by the formula, the increase in diameter gradually approaching a uniform rate as the sponge assumes the doughnut shape."*

Using the software WebPlotDigitizer (vers. 4.5; Rohatgi, 2021), we read the size (diameter in inches) and volume (in cubic inches) from figure 7b of Storr (1964) and transposed them (Table 1). We used these data to estimate the value of the parameter a of a diameter-to-volume relationship of the following form:

$$V = aD^3, \quad (3)$$

where V = the volume;
D = the diameter; and
a = the mean value estimated by solving $a=V/D^3$ and averaging the resulting estimates of a.

The diameter-age pairs in Table 1 were then used to estimate the parameters of the VBGF (von Bertalanffy, 1938), as presented by Beverton and Holt (1957):

$$L_t = L_\infty\left(1 - e^{-K(t-t_0)}\right), \quad (4)$$

where L_t = the mean size (here: diameter) at age t of the animals in question;
L_∞ = their asymptotic size (i.e., the mean size attained after an infinitely long time);
K = a growth coefficient (here: year^{-1}); and
t_0 = the (usually negative) age they would have had at a size of zero if they had always grown in the manner predicted by the equation (which, in fish species, they usually have not; see, e.g., Pauly, 1998).

Combining Equations 3 and 4 leads to a version of the VBGF that can express growth in volume:

$$V_t = V_\infty\left(1 - e^{-K(t-t_0)}\right)^3, \quad (5)$$

where V_t = the predicted volume of wool sponge at age t; and
V_∞ = the mean volume attained after an infinitely long time.

The different forms of the VBGF are derived by integrating the differential equation posited by Pütter (1920):

$$dw/dt = HW^d - kW, \quad (6)$$

where dw/dt = the growth rate in weight (here: volume), conceived as the difference between a process adding weight and a process reducing it;
H = the rate of anabolism or the synthesis of new protein and other molecules (a process adding weight);
W = weight, representing mass and volume;
d = an exponent power <1; and
k = the rate of catabolism or molecule denaturation (a process reducing weight).

The parameter d takes a value of 2/3 when Equation 4 is integrated to produce the VBGF, and whose parameter K is $k/3$. Also note that stressful environmental factors, especially high temperatures, tend to increase k (and K) and therefore to reduce asymptotic sizes and longevity (Pauly, 2021a).

Pauly (1981, 2019a, 2021a), based on von Bertalanffy (1951), interpreted Pütter's (1920) equation such that—because oxygen is required for anabolism—the positive

Table 1

The diameter, volume, and age of sheepswool sponges (*Hippospongia lachne*), also known as wool sponges, tagged off Florida in the Gulf of Mexico, as read off the graph in figure 7b in Storr (1964). Ages in parentheses were extrapolated by using the equation $V=aD^3$ (Equation 3), where V is volume, D is diameter, and a is estimated by solving $a=V/D^3$. Volumes in parentheses were derived through Equation 2.

Age (years)	Diameter (in)	Volume (in^3)
1	2.6	8.6
2	4.3	44.2
3	5.5	88.8
4	6.6	181.9
5	7.5	269.4
6	8.2	333.3
7	8.9	388.7
(8)	9.5	434.8
(9)	10.0	480.8
(10)	10.7	(609.8)
(11)	11.3	(716.3)

term in Equation 6 corresponds to the oxygen supply to a growing fish or invertebrate, and the catabolic term corresponds to its maintenance oxygen requirements or demand, because of the fact that denatured proteins and other molecules need to be replaced for an animal's body to maintain itself. Therefore, when the anabolism exceeds the catabolism, growth occurs (given that food is also available). However, as the anabolic term grows with a power of weight d <1 (here: d=2/3), the catabolic term, which generates an oxygen demand proportional to weight, will eventually catch up—and growth will become zero, at the asymptotic volume V_∞ or the corresponding asymptotic weight W_∞.

There are various debates about this interpretation, with some arguing that the respiratory surface providing the oxygen required for anabolism is capable of growing proportionately to weight (i.e., d=1) and hence that oxygen supply cannot be limiting to the growth of fish species and other WBE. This notion was refuted by Pauly and Cheung (2017) on the basis of numerous metanalyses of gill surface areas in fish and other WBE (e.g., Hughes and Morgan, 1973; de Jager and Dekkers, 1974), which consistently have estimated d as <1, and by (Pauly, 2021a), who grouped the detractors' arguments in detailed tables depending on their nature (e.g., not appreciating the 2-D nature of gills, mistaking causes and effects, and making unfalsifiable claims) and refuted them point by point with references to the aforementioned metanalyses and other reliable peer-reviewed sources.

Surface-to-volume issues also apply to sponges, because the cumulative cross section of the pores through which water enters their bodies is a surface. This (2-D) surface, at least in compact sponges such as the wool sponge, cannot keep up with the growth of (3-D) bodies. Therefore, as a compact sponge grows, its interior will become increasingly hypoxic (Hoffmann et al., 2005; Lavy et al., 2016), and tissue maintenance will be increasingly compromised.

Sponges have therefore evolved a complex symbiotic relationship with microbes to deal with the geometric constraints imposed on sponge physiology. The sponge canal system operates as subdivided units among which pumping rates (i.e., oxygen acquisition) vary, creating spatiotemporally variable zones of hypoxia and anoxia that serve to support the respiratory activity of anaerobic symbionts (Lavy et al., 2016). Nevertheless, in some sponge species, the development of internal hypoxic zones apparently leads to tissue necrosis, as suggested by Storr (1964), who, however, attributed central tissue "death" in large wool sponges to lack of food, rather than to lack of oxygen. In comparison, in fish tissues subject to increased hypoxia, the reduced availability of oxygen leads to an increase of the role of glycolytic enzymes, which, as individual fish grow, gradually replace oxidative enzymes (Somero and Childress, 1980; Burness et al., 1999; Norton et al., 2000; Davies and Moyes, 2007).

Storr (1964), with regard to 12 in being the maximum diameter attained by spherical wool sponges, wrote the following: "*This is confirmed in the observed growth of wool sponges by the death of the central portion of the sponge when this diameter is reached. The form of the sponge from then on becomes more and more doughnut in shape. Continued growth beyond a 12-inch diameter suggests that one other growth factor operates as the sponge approaches the limit of growth indicated by the formula. Since the sponge is uniform in structure and the intake of water carrying the food is through the sides, the greatest amount of food uptake is in the periphery of the sponge. This area, therefore, continues to grow vigorously, but the rate of food intake is not sufficient nor the rate of food transfer through the sponge efficient enough to support active metabolism in the central portion of the sponge when the diameter of the sponge is 12 inches or over. The growth formula obtained would probably be directly applicable to the rate of sponge growth except for this phenomenon of sponge physiology.*"

Therefore, the growth phase documented herein pertains to spherical wool sponges; beyond this phase, wool sponges change shape, a shift that leads to different ratios between respiratory surfaces and the mass of oxygen-consuming tissues. This transition could be modeled by using a biphasic version of the VBGF (Soriano et al., 1992), but we did not attempt such modeling, mainly because the second-phase growth of this sponge species is not well documented and is of little interest to the sponge fishing and farming industries.

Longevity

Storr (1964) wrote, "*Little is known of the life span of wool sponges although the records have indicated that they can live at least 25 years. Presumably, the limiting factor to continued growth is the capability of the sponge to draw in sufficient food for self-maintenance. Any lack of food intake is counteracted in part by the dying of the central portion of the sponge so that after a certain point in growth in diameter, the volume of the sponge remains a constant in relation to the surface area.*"

In fish, it is commonly observed that the longest-lived individuals of a population reach about 95% of their L_∞ (Taylor, 1958); therefore, longevity is approximately equal to the time required to reach $0.95L_\infty$. Therefore, given Equation 4, we also have the following equation:

$$longevity \approx 3/K, \quad (7)$$

which assumes that the parameter t_0 can be neglected. A rough estimate of the uncertainty inherent in Equation 7 is provided by assuming that the longest-lived individual reaches at least 90% or at most 99% of their asymptotic length (i.e., $2.3/K$ and $4.6/K$).

Another useful model, from Hoenig (1983), links longevity with the instantaneous rate of total mortality (Z, year^{-1}) in fish, mollusks, and other marine animals (134 populations in 79 species) and which has the following form:

$$\ln(Z) = 1.44 - 0.982\ln(t_{max}), \quad (8)$$

where t_{max} = the age (in years) of the oldest individuals in a population; and

Z = the annual mortality experienced by a population (N) between time t_1 and t_2 or

$$N_2/N_1 = e^{Z(t2 - t1)}. \quad (9)$$

Note that Z, in fisheries science, is commonly thought to consist of fishing mortality (F) and natural mortality (M), in the form of $Z=F+M$.

Equation 8 was derived to estimate Z from t_{max} but can also be inverted (i.e., used to obtain rough estimates of longevity, given estimates of Z). Such estimates are available from ecosystem models, in which the ratio of production to biomass (p/b) of sponges was computed under the assumptions that the VBGF described individual growth and that population numbers decayed exponentially. Given these 2 assumptions, $p/b=Z$ (Allen, 1971), an equation that makes it easier to estimate ratios of production to biomass than the complicated approach proposed by Winberg (1971).

Reproduction

The predictability and relative fixity of the ratio between L_∞ and mean length at first maturity (L_m) of different groups of fish (Beverton and Holt, 1959) has led to the concept of "a reproductive load" (Cushing, 1981), whose values tend to range from 0.4–0.5 in large fish species, such as tuna, to 0.6–0.7 in smaller fish species, such as sardines (Beverton and Holt, 1959; Beverton, 1963; Mitani, 1970; Froese and Binohlan, 2000). This concept embodies the notion that fish and other WBE stop growing because their "energy," once L_m is reached, is channeled into reproduction rather than somatic growth (van Oosten, 1923; Hubbs, 1926; Jones, 1976; Lagler et al., 1977; Charnov, 2008; Quince et al., 2008). However, this notion is contradicted by the following facts: 1) in the majority of fish species, the females grow faster than males, even though they devote more energy to reproduction (Pauly, 2019b); 2) in long-lived fish (Liang, 2021) and other long-lived WBE, maturity is reached while growth in weight is still accelerating (Pauly, 2021b); and 3) a number of WBE continue to grow and reproduce throughout their lifetimes without suffering from senescence (Nussey et al., 2013; Gnanalingam and Butler, 2018). Still, it remains the case that L_m and L_∞ are correlated within different populations of the same species and even between species (see Pauly, 1984, 2019a).

Respiration

Sponges are considered textbook examples of animals that use current-induced flow (e.g., Vogel, 1996), but Ludeman et al. (2017) have demonstrated that at least 5 demosponge species respond to increased current velocity by reducing their filtration. The results of their study also indicate that pumping rates (mean volumetric flow rate: liters per hours per grams of dry weight), although variable, are positively correlated ($y=1.7559+x^{0.9416}$; coefficient of determination $[r^2]=0.66$) with oxygen consumed by the sponge (mean oxygen removal: micromoles per hours per grams of dry weight). Estimates of the energetic cost of pumping in demosponges varies widely from <1% for temperate sponges (Riisgård et al., 1993) to 25% or more for tropical demosponges (Hadas et al., 2008; Leys et al., 2011; Ludeman et al., 2017), such as the wool sponge.

Recall that the volume of a sphere is calculated as $V=(4/3)\pi r^3$. Therefore, the volume in a layer of a sphere can be obtained by using this equation:

$$r = (¾ \times V/\pi)^{1/3}, \quad (10)$$

where r = the radius of a spherical sponge.

Measurements of oxygen levels in the interior of a roughly spherical sponge, the Barrett's horny sponge (*Geodia barretti*), performed by Hoffmann et al. (2005) were read off their figure 2, re-expressed as fractions of ambient oxygen levels, and fitted with a logistic curve with the following form:

$$\textit{Fraction of ambient oxygen level} = 1 / \left(1 + e^{-S(I-r)}\right), \quad (11)$$

where r = the radius, measured as the depth within the sponge;
S = the slope; and
I = the inflection point at which oxygen is 50% of the ambient level.

The confidence interval (CI) of the slope S at the inflexion point I is estimated through bootstrapping (Fieberg et al., 2020).

Sponges in fisheries, ecosystems, and ecosystem models

Pending a more detailed "reconstruction" of the catches of wool sponges and other commercial sponges in the world, to match the reconstruction of the catches of exploited fish and invertebrates (Pauly and Zeller, 2016a, 2016b; see also Pauly et al.[1]), we extracted the main features of the sponge harvest data in the global fisheries catch statistics submitted by member countries to, and harmonized and disseminated by, the FAO.

In shallow-water tropical ecosystems, sponges compete for substrate with corals and algae, and they alter plankton communities in the water column and water chemistry (Peterson et al., 2006; Valentine and Butler, 2019). They also provide food and structure for animals (Herrnkind et al., 1997; Duffy, 2007; Butler et al., 2016), among other services. As such, they are frequently included in food-web models for ecosystems. However, they are usually included as a group (e.g., as a group called *sponges* in Opitz, 1996) or as part of larger groups (e.g., as *epibenthos* in Okey et al., 2004), not as distinct species, even in cases in which one species was clearly dominant.

The growth parameters presented herein, complemented by generic estimates of food consumption and turnover ratio for sponges (Table 2), may lead to better food-web models, at least for the areas of Florida and the Caribbean where sponge biomass is substantial in shallow coastal waters and on coral reefs. In the Florida Keys, a hectare of hard-bottom habitat in shallow waters harbors

[1] Pauly, D., D. Zeller, and M. L. D. Palomares (eds.). 2020. Sea Around Us concepts, design and data. [Available from website.]

Table 2

Estimates of food consumption (q) and production (p) per unit biomass (b) and trophic levels from sources by the authors of 3 Ecopath food-web models in which a *sponge* group is explicitly included. These authors sampled sponges from 3 marine ecosystems: the Virgin Islands (Opitz, 1996), the central Great Barrier Reef in Australia (Tudman, 2001), and the Te Tapuwae o Rongokako Marine Reserve (TTMR) off the North Island of New Zealand (Pinkerton et al., 2008). See tables 3 and 5 and text in Pinkerton et al. (2008) for issues with the TTMR estimate, which appears to be the most credible of the 3 estimates of p/b in this table.

Location	Trophic level	q/b (year^{-1})	p/b (year^{-1})	Source
Virgin Islands, Caribbean	2.0	4.2	1.7	Opitz (1996)
Central Great Barrier Reef	2.0	3.0	0.9	Tudman (2001)
TTMR, North Island, N.Z.	2.3	0.8	0.2	Pinkerton et al. (2008)

an estimated 47,000 individual sponges of all types with a volume of approximately 17 m^3/ha. On average, 10% of those sponges have diameters that exceed 25 cm, and wool sponges make up about 1% of the total sponge biomass (Butler et al., 2021). On coral reefs in the Caribbean, over 500 species of sponges have been identified and their average percent cover of 16% (range: 2–75%) exceeds that of corals (Miloslavich et al., 2010; Loh and Pawlik, 2014). Clearly, sponges are a major component of many tropical marine ecosystems as are their ecological ramifications, and this importance is reflected in sponges being part of published ecosystem models. We examined this issue through the coverage of sponges in successive implementations of the commonly used Ecopath food-web modeling software (Christensen and Pauly, 1992; Colléter et al., 2015).

Results

Growth

The parameters of the VBGF (Equation 4) from the diameter-at-age data in Table 1 led to the following equation:

$$D_t = 31.5\left(1 - e^{-(0.191t)}\right), \qquad (12)$$

where D_t = the predicted diameter at age t in centimeters.

The parameter t_0 (see Equation 4) is not included in this equation because it was set at zero, forcing the growth curve to start at the origin of the age scale in Figure 2. As for the value of 0.191 year^{-1} for the parameter K, its 95% CI, estimated by bootstrapping the data in Table 1, is 0.185–0.199 year^{-1}. This interval is likely to be an underestimate because the age-at-length data in Table 1 are means and therefore do not include variability in individual growth. However, even when available, data on individual growth variability are still difficult to consider when estimating VBGF parameters (Sainsbury, 1980; Wang and Thomas, 1995). The estimate of asymptotic size is close to the maximum size reported by Storr (1964), 12 in (or ~30.5 cm) up to the size at which the sponge's spherical shape is maintained.

Using Equation 3 to compute the relationship of diameter to volume indicated by the data in Table 1 leads to a mean value of parameter a of 0.55 for mediating between diameter in inches and volume in cubic inches. For the

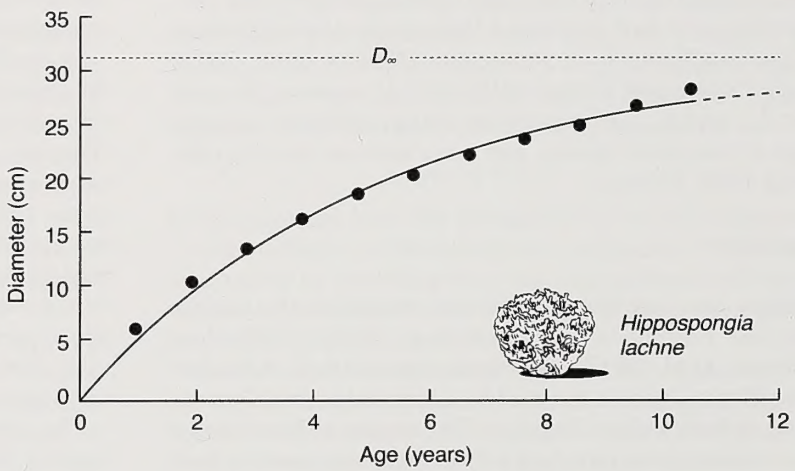

Figure 2

Growth of the sheepswool sponge (*Hippospongia lachne*), also known as the wool sponge, in the upper Gulf of Mexico as indicated by a von Bertalanffy growth curve fitted to diameter-at-age data from Storr (1964) (see Table 1). The estimates of asymptotic length (i.e., diameter) and growth coefficient are 31.5 cm and 0.191 year^{-1}, respectively. The horizontal dashed line indicates the asymptotic diameter (D_∞).

diameter in centimeters and the volume in cubic centimeters, the expression of the diameter-to-volume relationship in the wool sponge becomes

$$V = 0.055 \times D^3. \quad (13)$$

Therefore, the equation for the relationship between the age in years and the volume in cubic centimeters becomes

$$V_t = 1046\left(1 - e^{-(0.191t)}\right)^3. \quad (14)$$

Opitz (1996), for her detailed food-web model of Caribbean reefs, used a ratio of dry weight to wet weight of 333:100 and considered 22.5% of wet mass to be "*inorganic skeletal material*," on the basis of a personal communication from a scientist working mainly on deepwater or cold-water sponges.

Our own determination of the percentage of wet weight to dry weight for wool sponges collected in the Florida Keys (number of samples [n]=15) is 3.9% of wet mass. A larger percentage (11%) was estimated for another commercial sponge species that we collected in the same area (n=20): the grass sponge (*Spongia graminea*), which is the second-most valuable commercial sponge in Florida.

Longevity

The estimated longevity of the wool sponge, that is of its first, spherical phase, is as follows, given Equation 7: 3/0.191≈16 years, with uncertainty ranging from 12 to 24 years. On the other hand, the values of production per unit biomass (which can be considered equal to Z) in Table 2, used with the inverse of Equation 8, lead to estimates of longevity of 2.5 years (for Z of 1.7 year^{-1}), 4.8 year (for Z of 3.9 year^{-1}), and 22.3 years (for Z of 0.2 year^{-1}). Only the last of these estimates appears realistic, whereas the first estimate of 16 years is compatible with that of Storr (1964, p. 18–19), whose longevity estimate includes the life history phase during which wool sponges change shape (which was not considered in our study). In the meantime, however, experiments have been conducted, and their results indicate that the longevity of wool sponges is strongly influenced by environmental stress (e.g., stress caused by high temperatures, extreme levels of salinity, and phytoplankton blooms) (Butler et al., 2018).

Also note that the value of Z that was based on estimates of production per unit biomass in Table 2 and was used to produce, through Equation 8, the only reasonable estimate of t_{max} also leads to the following ratio for sponges: Z/K=0.2/0.191≈1.1. In the absence of fishing (as was the case in the model developed with data from work in the Te Tapuwae o Rongokako Marine Reserve in New Zealand; Pinkerton et al., 2008) (Table 2), Z/K is also M/K and M/K≈1.1, which is a very plausible value for low-activity or sessile animals. Therefore, for example, although M/K is 1.5 for many populations of bony fishes (Taylor, 1958; Froese et al., 2016), the mean M/K is 0.76 for 16 populations and 13 species of bivalves (from Vakily, 1992, appendix 4) and is 1.1 for 11 species of sea urchins (see Longhurst and Pauly, 1987, figure 10.2, based on Ebert, 1975), with both groups represented by both warmwater and cold-water species.

Reproduction

Butler et al. (2017) established that the number of gametocytes in tissue samples from 3 species of commercial sponges from the Florida Keys were positively and significantly related to sponge size, whether measured as sponge volume (F=4.762; df=1, 15; P=0.047; r^2=0.254) or as diameter (F=9.270; df=1, 15; P=0.009; r^2=0.398); the relationships explained ~40% of the variance in gametocyte number.

van Soest (1978) concluded that wool sponges reach a size up to 18 cm in diameter in the waters of Curaçao, where the waters are warmer than those of the upper Gulf of Mexico and where wool sponges reach diameters of over 30 cm (Storr, 1964). These numbers lead to Figure 3, which shows that maximum sizes reached by wool sponges decline with temperature (as indicated by the definition of the parameters of Equation 6) and which also illustrates the inverse relationship between minimum length at first maturity and water temperature, as has been reported for other WBE (Pauly, 2021a). This finding is supported by measurements of the growth of wool sponges in the Florida Keys, where average growth rates varied 5-fold seasonally (Butler et al., 2017).

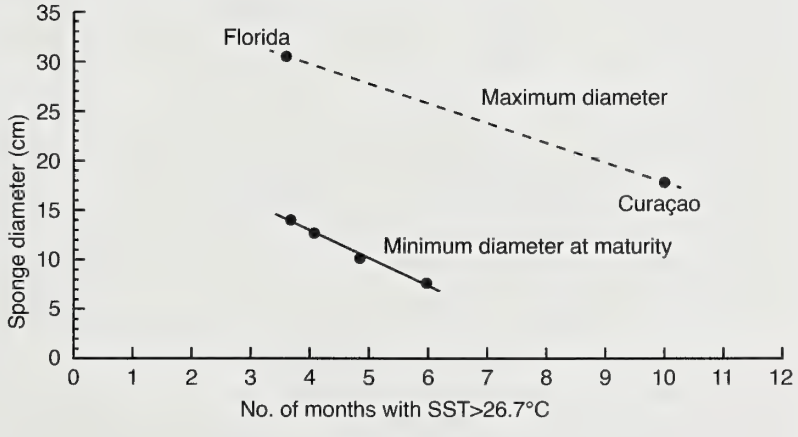

Figure 3

Apparent temperature dependence of size at first maturity (solid line) and maximum size (dashed line) for the sheepswool sponge or wool sponge (*Hippospongia lachne*) off Florida in the Gulf of Mexico (based on data from Storr, 1964) and in the waters of Curaçao in the Caribbean Sea (based on data from van Soest, 1978). SST=sea-surface temperature.

However, the mean of 0.4 for the ratio of L_m to L_∞, shown in Figure 3, cannot be used for the wool sponge to test the hypothesis in Pauly (1984) (see also Pauly, 2021a), which predicts values for this ratio in WBE. The reason is that the data in Storr (1964) do not pertain to the *mean* size at which wool sponges mature (i.e., the length at which 50% of a cohort reaches maturity) but do indicate the *minimum* size at which some of them do.

Respiration

The respiratory area of the wool sponge is not known. Measurements of the respiratory area for the European coastal sponge *Suberites massa*, taken decades ago, have been used to estimate the area at 100 cm^2/g (Pütter, 1914; von Ledebur, 1939). Gatti et al. (2002) used oxygen microprobes to measure oxygen concentrations within the tissue of the Mediterranean bacteriosponge *Suberites domuncula* and detected oxygen concentrations of approximately 50% of the surrounding ambient seawater. Weisz (2006) used oxygen microprobes and tetrazolium salts to examine oxygen concentrations and the occurrence of anoxic zones in 4 species of low-microbial-abundance and high-microbial-abundance sponges. Oxygen concentrations within the ectoderm and endoderm of low-microbial-abundance sponges were similar to ambient seawater concentrations, whereas endoderm tissues in high-microbial-abundance sponges were all hypoxic or anoxic.

The decline of the oxygen content in the interior of the near-spherical sponge Barrett's horny sponge studied by Hoffmann et al. (2005) can be re-expressed as follows:

$$\textit{Fraction of ambient oxygen level} = 1 / \left(1 + e^{-0.675(2.76 - r)}\right), \quad (15)$$

where r = the depth (in centimeters) within the sponge.

The decline of oxygen level is most rapid at the inflexion point of 2.76 cm (95% CI: 2.52–2.98), and the slope at the inflexion point (S=–0.675) has a 95% CI of –0.998 to –0.548 (Fig. 4). The generality of the numbers estimated with Equation 15 and illustrated in Figure 3 cannot currently be assessed, given that they were derived from an experiment on one species at one (low) temperature (6–15°C) (Hoffmann et al., 2003). However, the shape of this relationship is likely realistic and could be adapted to different species by increasing or decreasing the 2 parameters of Equation 15 (or Equation 10). The provided equations allow computing the oxygen level in near-spherical sponges by adding the dissolved oxygen in successive depth layers, and the oxygen level of each depth layer is the mean of the oxygen level at its outer and inner limits.

Sponges in fisheries, ecosystems and ecosystem models

Official estimates of fisheries catch of sponges are available from the FAO (available from website), originating from 25–30 countries and territories and adding up to nearly 40,000 metric tons (processed dry weight) from 1950 to 2019. However, both the number of countries exploiting sponge populations and the level of their catches are likely underestimates, requiring correction as has been recently performed through catch reconstruction for the catch of the world's marine fisheries (Pauly and Zeller, 2016a, 2016b), even if done with the exclusion of sponges.

Empirical estimates of effects of commercial fisheries on sponge communities are virtually unavailable, although in south Florida, management limitation of harvest based on the use of artisanal techniques appears to have resulted in a sustainable fishery (Butler et al., 2017). More devasting to sponges in many areas are mass die offs of sponges due to disease, cyanobacteria blooms, and poor water quality that can extend over hundreds of square kilometers with strong effects on ecosystems (Butler et al., 1995; Herrnkind et al., 1997; Webster, 2007; Gochfeld et al., 2012; Wall et al., 2012; Butler et al., 2018).

In EcoBase, a database of Ecopath food-web models (Colléter et al., 2015; available from website) that included

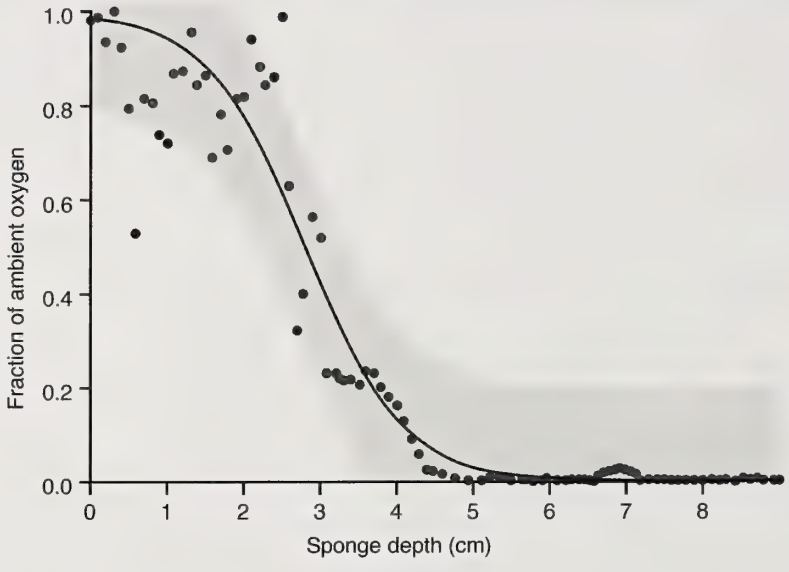

Figure 4

The decline of oxygen content inside an approximately spherical sponge, the Barrett's horny sponge (*Geodia barretti*), based on specimens sampled at depths between 100 and 200 m on the hard-bottom slope of Korsfjord near Bergen, Norway. The values were read off figure 2 in Hoffmann et al. (2005) and re-expressed as a fraction of ambient oxygen levels. The relationship between oxygen content and sponge depth is fitted with a logistic curve, and the gray shaded area represents the 95% confidence interval.

459 models as of December 2019, 84% of the models described marine ecosystems, but only 12 models included sponges. Moreover, in only 3 of those models were sponges a group of their own, not combined with corals or other benthic animals.

Table 2 presents the food consumption and production per unit biomass estimated for sponges from a variety of sources by the authors of the 3 models in which sponges were not grouped with other organisms. Other stage-based or individual-based models depicting sponge population or community stability under fishing or environmental pressure also exist (Cropper and DiResta, 1999; Butler and Dolan, 2017), but they do not explicitly incorporate food consumption or respiration in relation to production.

Discussion

We hope that the relationships given in the "Results" section will be useful to colleagues involved in the comparative study of sponges, the assessment of the status of fisheries for the wool sponge and similar sponges, the modeling of the ecosystems in which such fisheries are embedded, and the potential mariculture of sponges. There is, however, another interesting aspect to the growth and related traits of wool sponges pertaining to the first author's attempt to formulate, test, and illustrate a comprehensive theory of growth for WBE, the gill-oxygen limitation theory (Pauly and Cheung, 2017; Pauly, 2019a, 2021a).

Sponges originated approximately 800 million years ago in the Pre-Cambrian (Reitner and Wörheide, 2002; Turner, 2021); therefore, they had ample time to evolve sophisticated defenses in the form of spicules embedded in a tough matrix, which partly protects them against spongivores (Wulff, 2006; to generate a list of spongivorous fishes, select *sponges* in the drop-down list of the food item search tool on FishBase, available from website), a strategy resembling that of thorny land plants. Also, similar to plants, sponges cannot evade predators and as a result have evolved an ability to synthesize a dazzling array of complex organic molecules to protect themselves against potential consumers and pathogens (Pawlik, 2011; Loh and Pawlik, 2014; Rohde et al., 2015), and that array is the reason they are sought after as a source of potentially useful medical compounds (Blunt et al., 2003).

On the other hand, sponges did not evolve the many differentiated cells, tissues, organs, and appendages that are characteristic of other phyla, such as mollusks, arthropods, and chordates. Therefore, we can more easily detect in sponges the constraints that have shaped the transition to multicellularity in the first animals and the emergence of the first body plans. In particular, we agree with Ward (2006), who believes that "*respiration was perhaps the most important driver of animal body plans.*" Indeed, the appearance of sponges on earth, predating oxygen-producing multicellular plants by 300 million years (Brocks et al., 2017), occurred during a period when dissolved oxygen was at a premium. At that time, a day on earth was 21 h long and atmospheric oxygen levels were only about 50% of what they are today (Klatt et al., 2021). Although global oxygen stores later increased rapidly with the evolution of multicellular plants, for 500 million years sponges evolved in a world depauperate in oxygen. In the absence of tissues or organs specialized for oxygen acquisition, sponge morphology was likely strongly constrained by physiological oxygen demand.

The notion that oxygen constrains sponge energetics and morphology is contrary to the suggestion in Storr (1964) that the supply of nutrients (i.e., food) is the limiting factor to the survival and multiplication of the cells in the interior of a cell mass. In their review of food competition and limitation for coral-reef-dwelling sponges, Pawlik et al. (2015) found no evidence for food limitation of sponge growth. However, the reef sponge community is dominated by low-microbial-abundance sponges with high filtration rates and large canal volumes, and they dwell in an oxygen-enriched environment. The opposite is true for shallow-water-dwelling coastal sponges for which growth appears to be limited at high densities of sponges because of limitation of either food or oxygen (Valentine, 2019). Herein we show that oxygen supply could indeed be a primary constraint on sponge growth, at least for spherical high-microbial-abundance sponges.

The effects of a limited capacity to deliver oxygen to tissues is evidenced across many animal phyla (Heim et al., 2020). For *Homo sapiens*, effects are manifested in heart insufficiencies and attacks (Weber and Janicki, 1979) and in ischemic strokes (Janardhan and Qureshi, 2004). This phenomenon also applies to cancerous tumors whose cells shift to glycolytic metabolism when their interior is deprived of oxygen or when a temperature increase drives their oxygen demand beyond the capacity of the blood supply that they have commandeered (Warburg, 1930; Al Tameemi et al., 2019).

The fundamental reason for a limiting role of oxygen is that, because of its toxicity, molecular oxygen cannot be stored in living animal tissue (Lane, 2002); the oxygen that is stored in the mesoglea of jellyfish (Thuesen et al., 2005) is no exception because the mesoglea is not living tissue. The only way oxygen can be stored is through chemical bonding as in blood (Lenfant et al., 1970; Noren et al., 2002), and oxygen storage requires an internal circulatory system that is absent in many phyla (Heim et al., 2020), including the Porifera.

As a result, the growth of poriferans, and especially those with a spherical shape, is constrained by the aforementioned dimensional tension (Pauly and Cheung, 2017) inherent in having to supply a growing (3-D) body with oxygen in water whose flow is determined by the cumulative (2-D) cross section of the inhalant ostia (inhalant pores). This constraint remains even if a sponge's pumping rate increases with body size.

If they are limited by oxygen, we can predict that sponges, especially sphere-shaped demosponges when fully grown, will experience hypoxia and even anoxia in the central part of their bodies, as is commonly observed. Yet, this oxygen limitation also permits the presence of anaerobic bacteria and archea within the commensal community dwelling inside sponges, not too dissimilar to

the microbiome in the human gut (Cénit et al., 2014). The microbiome of sponges can be equivalent to 40% of sponge wet body weight (Lavy et al., 2016), and high densities of microbes confer multiple beneficial functions, including access to microbially mediated metabolic pathways (Hentschel et al., 2006; Weisz, 2006; Schläppy et al., 2010; Webster and Taylor, 2012; Poppell et al., 2014).

The gill-oxygen limitation theory, which building on Equations 3–6, is structured around the constraints resulting from a 2-D oxygen system having to supply the 3-D bodies of water-breathing animals (Pauly and Cheung, 2017; Pauly, 2019a, 2021a), may also apply to sponges—at least to high-microbial-abundance sponges with approximately spherical shapes.

But not all sponges are spherical. Indeed, among their various morphologies are tube-shaped sponges, vase-shaped sponges, encrusting sponges, and irregularly shaped globular sponges. Their internal structure is equally variable. The internal tissues of some are dense, whereas the extensive canal system of others makes them full of voids. There are also striking differences in the skeletal structure and makeup of spicules that define in large part sponge families. All of these characteristics play a role in water flow through sponges and influence oxygen availability.

In addition to an illustration of the gill-oxygen limitation theory, we can now consider sponges more completely in the context of ecosystem functioning. Prior to this contribution, it was difficult to accurately convert the dry weight of wool sponges into wet weight. Without these conversions, one cannot fully understand the ecological consequences of the historical collapse of the sponge fishery throughout the Americas in the early part of the 20th century, a fishery that to this day has never fully recovered (Stuart, 1948; McClenachan, 2008; Oronti et al., 2012).

The commercial export of sponges in the Americas began in The Bahamas in 1841 with the shipwreck in The Bahamas of a French merchant who later carried 500–600 specimens to Paris, where he sold them (Corfield, 1938; Stuart, 1948). Note, however, that prior to this shipment, the merchant observed "*a great number of sponges in use among the natives*" in The Bahamas, suggesting that a market for sponges might have already existed there locally before the first exports to Europe (Corfield, 1938). Additionally, Moore (1910) notes that in the Florida Keys "[*i*]*t is known that long before these* [i.e., sponges] *became an article of commerce they* [i.e., sponges] *were in limited domestic use among the inhabitants*." It is unclear when exactly sponges were first harvested in the Americas. However, it is well documented that following the first commercial export of sponges from The Bahamas in the mid-1800s, the large-scale export of sponges quickly spread throughout the Western Atlantic region, with Tarpon Springs in Florida and Batabano in Cuba becoming areas of major importance (Moore, 1910; Corfield, 1938; Bethell, 2017).

The rise and collapse of the sponge fishery in The Bahamas in many ways mirrors the events that occurred throughout the Western Atlantic region (Stuart, 1948; McClenachan, 2008; Oronti et al., 2012). At its peak in 1917, the industry employed one-third of the Bahamian workforce and included the harvesting, processing, and trading of sponges (Oronti et al., 2012; Bethell, 2017). However, by the late 1930s, a combination of disease, hurricanes, and overexploitation led to orders of magnitude decline in catches, so that by 1947, sponge exports had plummeted to 14.8 metric tons (Oronti et al., 2012). Of note is a fungal blight in the late 1930s that killed 70–95% of the already drastically reduced populations of sponges in The Bahamas before spreading to adjacent countries (Galtsoff et al., 1939). Beginning in the early 1990s, repeated phytoplankton blooms similarly destroyed up to 95% of the sponge communities over large swaths of the Florida Keys, where commercial sponge fishing continues to this day (Butler et al., 1995; Wall et al., 2012). The conversion from dry weight to wet weight that we present for the wool sponge, which was (and still is) a regionally abundant species and a commercially valuable species in the global trade (Moore, 1910; Corfield, 1938; Stuart, 1948; McClenachan, 2008), allows the quantification of the effect of the collapse of the sponge fishery in the Western Atlantic Ocean on patterns of past ecosystem biomass-dependent functions.

Conclusions

The contention, herein illustrated with the wool sponge, that the growth of large, near-spherical sponges may be limited by the oxygen supply to their interior allows a number of inferences on their likely response to ocean warming and deoxygenation, and these inferences should be important to sponge fisheries and aquaculture and to the study of sponges in their ecosystem context.

Moreover, we demonstrate that the gill-oxygen limitation theory, developed mainly with data for vertebrate, molluscan, and arthropod WBE, also applies to compact, near-spherical sponges. This demonstration provides a new avenue for their study, as it should allow the formulation of various hypotheses about their biology, notably on their shape-shifting past certain sizes, that should be straightforward to test.

Acknowledgments

We thank J. Butler for the photographs in Figure 1, E. Chu for Figures 2–4, and J. Guitton for extraction of information from EcoBase.

Literature cited

Al Tameemi, W., T. P. Dale, R. M. K. Al-Jumaily, and N. R. Forsyth.
2019. Hypoxia-modified cancer cell metabolism. Front. Cell Dev. Biol. 7:4.

Allen, K. R.
1971. Relation between production and biomass. J. Fish. Res. Board Can. 28:1573–1581.

Belarbi, E. H., M. R. Domínguez, M. C. C. García, A. C. Gómez, F. G. Camacho, and E. M. Grima.
2003. Cultivation of explants of the marine sponge *Crambe crambe* in closed systems. Biomol. Eng. 20:333–337.

Bell, J. J.
2008. The functional roles of marine sponges. Estuar. Coast. Shelf Sci. 79:341–353.
Bell, J. J., A. Biggerstaff, T. Bates, H. Bennett, J. Marlow, E. McGrath, and M. Shaffer.
2017. Sponge monitoring: moving beyond diversity and abundance measures. Ecol. Indic. 78:470–488.
Bethell, K.
2017. Revival of the sponging industry. The Tribune, 1 March 2017. [Editorial.] [Available from website.]
Beverton, R. J. H.
1963. Maturation, growth and mortality of clupeid and engraulid stocks in relation to fishing. Rapp. P.-v. Réun. Cons. Perm. Int. Explor. Mer 154:44–67.
Beverton, R. J. H., and S. J. Holt.
1957. On the dynamics of exploited fish populations, 533 p. HMSO, London.
1959. A review of the lifespans and mortality rates of fish in nature, and their relation to growth and other physiological characteristics. *In* Ciba Foundation symposium—the lifespan of animals (colloquia on ageing) (G. E.W. Wolstenholme and M. O'Connor, eds.), p. 142–180. J. and A. Churchill, London. [Available from website.]
Blunt, J. W., B. R. Copp, M. H. G. Munro, P. T. Northcote, and M. R. Prinsep.
2003. Marine natural products. Nat. Prod. Rep. 20:1–48.
Brocks, J. J., A. J. M. Jarrett, E. Sirantoine, C. Hallmann, Y. Hoshino, and T. Liyanage.
2017. The rise of algae in Cryogenian oceans and the emergence of animals. Nature 548:578–581.
Burness, G. P., S. C. Leary, P. W. Hochachka, and C. D. Moyes.
1999. Allometric scaling of RNA, DNA, and enzyme levels: an intraspecific study. Am. J. Physiol. Regul. Integr. Comp. Physiol. 277:R1164–R1170.
Butler, J., J. A. Stanley, and M. J. Butler IV.
2016. Underwater soundscapes in near-shore tropical habitats and the effects of environmental degradation and habitat restoration. J. Exp. Mar. Biol. Ecol. 479:89–96.
Butler, J., W. C. Sharp, J. H. Hunt, and M. J. Butler IV.
2021. Setting the foundation for renewal: restoring sponge communities aids the ecological recovery of Florida Bay. Ecosphere 12(12):e03876.
Butler, M. J., IV
2003. Incorporating ecological process and environmental change into spiny lobster population models using a spatially-explicit, individual-based approach. Fish. Res. 65:63–79.
Butler, M. J., IV, and T. W. Dolan III.
2017. Potential impacts of everglades restoration on lobster and hard bottom communities in the Florida Keys, FL (USA). Estuar. Coasts 40:1523–1539.
Butler, M. J., IV, J. H. Hunt, W. F. Herrnkind, M. J. Childress, R. Bertelsen, W. Sharp, T. Matthews, J. M. Field, and H. G. Marshall.
1995. Cascading disturbances in Florida Bay, USA: cyanobacteria blooms, sponge mortality, and implications for juvenile spiny lobsters *Panulirus argus*. Mar. Ecol. Prog. Ser. 129:119–125.
Butler, M. J., IV, D. C. Behringer, and M. M. Valentine.
2017. Commercial sponge fishery impacts on the population dynamics of sponges in the Florida Keys, FL (USA). Fish. Res. 190:113–121.
Butler, M. J., IV, J. B. Weisz, and J. Butler.
2018. The effects of water quality on back-reef sponge survival and distribution in the Florida Keys, Florida (USA). J. Exp. Mar. Biol. Ecol. 503:92–99.
Cénit, M. C., V. Matzaraki, E. F. Tigchelaar, and A. Zhernakova.
2014. Rapidly expanding knowledge on the role of the gut microbiome in health and disease. Biochim. Biophys. Acta 1842:1981–1992.
Charnov, E. L.
2008. Fish growth: Bertalanffy k is proportional to reproductive effort. Environ. Biol. Fishes 83:185–187.
Christensen, V., and D. Pauly.
1992. ECOPATH II—a software for balancing steady-state ecosystem models and calculating network characteristics. Ecol. Model. 61:169–185.
Colléter, M., A. Valls, J. Guitton, D. Gascuel, D. Pauly, and V. Christensen.
2015. Global overview of the applications of the Ecopath with Ecosim modeling approach using the EcoBase models repository. Ecol. Model. 302:42–53.
Corfield, G. S.
1938. Sponge industry of the Caribbean area. Econ. Geogr. 14:201–206.
Cropper, W. P., Jr., and D. DiResta.
1999. Simulation of a Biscayne Bay, Florida commercial sponge population: effects of harvesting after Hurricane Andrew. Ecol. Model. 118:1–15.
Cushing, D. H.
1981. Fisheries biology: a study in population dynamics, 2nd ed., 295 p. Univ. Wis. Press, Madison, WI.
Davies, R., and C. D. Moyes.
2007. Allometric scaling in centrarchid fish: origins of intra- and inter-specific variation in oxidative and glycolytic enzyme levels in muscle. J. Exp. Biol. 210:3798–3804.
de Jager, S., and W. J. Dekkers.
1974. Relations between gill structure and activity in fish. Neth. J. Zool. 25:276–308.
de Voogd, N. J., B. Alvarez, N. Boury-Esnault, J. L. Carballo, P. Cárdenas, M.-C. Díaz, M. Dohrmann, R. Downey, E. Hajdu, J. N. A. Hooper, et al.
2021. World Porifera database. [Available from website, accessed November 2021.]
Diaz, M. C., and K. Rützler.
2001. Sponges: an essential component of Caribbean coral reefs. Bull. Mar. Sci. 69:535–546.
2011. Biodiversity of sponges: Belize and beyond, to the greater Caribbean. *In* Too precious to drill: the marine biodiversity of Belize (M. L. D. Palomares and D. Pauly, eds.), p. 57–65. Fish. Cent. Res. Rep., vol. 19, no. 6. Univ. British Columbia, Vancouver, Canada. [Available from website.]
Duffy, J. E.
2007. Ecology and evolution of eusociality of sponge-swelling shrimp. *In* Evolutionary ecology of social and sexual systems: crustaceans as model organisms (J. E. Duffy and M. Thiel, eds.), p. 387–409. Oxford Univ. Press, New York.
Ebert, T. A.
1975. Growth and mortality of post-larval echinoids. Am. Zool. 15:755–775.
Fieberg, J. R., K. Vitense, and D. H. Johnson.
2020. Resampling-based methods for biologists. PeerJ 8:e9089.
Froese, R., and C. Binohlan.
2000. Empirical relationships to estimate asymptotic length, length at first maturity and length at maximum yield per recruit in fishes, with a simple method to evaluate length frequency data. J. Fish Biol. 56:758–773.
Froese, R., H. Winker, D. Gascuel, U. R. Sumaila, and D. Pauly.
2016. Minimizing the impact of fishing. Fish Fish. 17:785–802.
Galtsoff, P. S., H. H. Brown, C. L. Smith, and F. G. W. Smith.
1939. Sponge mortality in the Bahamas. Nature 143:807–808.

Gatti, S., T. Brey, W. Müller, O. Heilmayer, and G. Holst.
2002. Oxygen microoptodes: a new tool for oxygen measurements in aquatic animal ecology. Mar. Biol. 140:1075–1085.

Gnanalingam, G. G., and M. J. Butler IV.
2018. An examination of reproductive senescence and parental effects and reproductive senescence in Caribbean spiny lobster. Bull. Mar. Sci. 94:675–698.

Gochfeld, D. J., C. G. Easson, C. J. Freeman, R. W. Thacker, and J. B. Olson.
2012. Disease and nutrient enrichment as potential stressors on the Caribbean sponge *Aplysina cauliformis* and its bacterial symbionts. Mar. Ecol. Prog. Ser. 456:101–111.

Hadas, E., M. Ilan, and M. Shpigel.
2008. Oxygen consumption by a coral reef sponge. J. Exp. Biol. 211:2185–2190.

Heim, N. A., S. H. Bakshi, L. Buu, S. Chen, S. Heh, A. Jain, C. Noll, A. Patkar, N. Rizk, S. Sundararajan, et al.
2020. Respiratory medium and circulatory anatomy constrain size evolution in marine macrofauna. Paleobiology 46:288–303.

Hentschel, U., K. M. Usher, and M. W. Taylor.
2006. Marine sponges as microbial fermenters. FEMS Microbiol. Ecol. 55:167–177.

Herrnkind, W. F., M. J. Butler IV, J. H. Hunt, and M. Childress.
1997. Role of physical refugia: implications from a mass sponge die-off in a lobster nursery in Florida. Mar. Freshw. Res. 48:759–770.

Hoenig, J. M.
1983. Empirical use of longevity data to estimate mortality rates. Fish. Bull. 82:898–903.

Hoffmann, F., H. T. Rapp, T. Zöller, and J. Reitner.
2003. Growth and regeneration in cultivated fragments of the boreal deep water sponge *Geodia barretti* Bowerbank, 1858 (Geodiidae, Tetractinellida, Demospongiae). J. Biotechnol. 100:109–118.

Hoffmann, F., O. Larsen, V. Thiel, H. T. Rapp, T. Pape, W. Michaelis, and J. Reitner.
2005. An anaerobic world in sponges. Geomicrobiol. J. 22:1–10.

Hubbs, C. L.
1926. The structural consequences of modifications of the developmental rate in fishes, considered in reference to certain problems of evolution. Am. Nat. 60:57–81.

Hughes, G. M., and M. Morgan.
1973. The structure of fish gills in relation to their respiratory function. Biol. Rev. 48:419–475.

Janardhan, V., and A. I. Qureshi.
2004. Mechanisms of ischemic brain injury. Curr. Cardiol. Rep. 6:117–123.

Jones, R.
1976. Growth of fishes. *In* The ecology of the seas (D. H. Cushing and J. J. Walsh, eds.), p. 251–279. W. B. Saunders Co., Philadelphia, PA.

Klatt, J. M., A. Chennu, B. K. Arbic, B. A. Biddanda, and G. J. Dick.
2021. Possible link between Earth's rotation rate and oxygenation. Nat. Geosci. 14:564–570.

Lagler, K. F., J. E. Bardach, R. R. Miller, and D. R. M. Passino.
1977. Ichthyology, 2nd ed., 506 p. John Wiley and Sons, New York.

Lane, N.
2002. Oxygen: the molecule that made the world, 374 p. Oxford Univ. Press, Oxford, UK.

Lavy, A., R. Keren, G. Yahel, and M. Ilan.
2016. Intermittent hypoxia and prolonged suboxia measured *in situ* in a marine sponge. Front. Mar. Sci. 3:263.

Lenfant, C., K. Johansen, and J. D. Torrance.
1970. Gas transport and oxygen storage capacity in some pinnipeds and the sea otter. Respir. Physiol. 9:277–286.

Leys, S. P., G. Yahel, M. A. Reidenbach, V. Tunnicliffe, U. Shavit, and H. M. Reiswig.
2011. The sponge pump: the role of current induced flow in the design of the sponge body plan. PLoS ONE 6(12):e27787.

Liang, C.
2021. Relationships between W_m and W_i. *In* The gill-oxygen limitation theory (GOLT) and its critics. Sci. Adv. 7:eabc6050, supplementary materials (online only).

Loh, T.-L., and J. R. Pawlik.
2014. Chemical defenses and resource trade-offs structure sponge communities on Caribbean coral reefs. Proc. Natl. Acad. Sci. USA. 111:4151–4156.

Longhurst, A. R., and D. Pauly.
1987. Ecology of tropical oceans, 407 p. Academic Press, San Diego, CA.

Ludeman, D. A., M. A. Reidenbach, and S. P. Leys.
2017. The energetic cost of filtration by demosponges and their behavioural response to ambient currents. J. Exp. Biol. 220:995–1007.

McClenachan, L.
2008. Social conflict, over-fishing and disease in the Florida sponge fishery, 1849–1939. *In* Oceans past: management insights from the history of marine animal populations. (D. J. Starkey, P. Holm, and M. Barnard, eds.), p. 25–46. Earthscan, London.

Mehbub, M. F., J. Lei, C. Franco, and W. Zhang.
2014. Marine sponge derived natural products between 2001 and 2010: trends and opportunities for discovery of bioactives. Mar. Drugs 12:4539–4577.

Miloslavich, P., J. M. Díaz, E. Klein, J. J. Alvarado, C. Díaz, J. Gobin, E. Escobar-Briones, J. J. Cruz-Motta, E. Weil, J. Cortés, et al.
2010. Marine biodiversity in the Caribbean: regional estimates and distribution patterns. PLoS ONE 5(8):e11916.

Mitani, F.
1970. A comparative study on growth patterns of marine fishes. Bull. Jap. Soc. Sci. Fish. 36:258–265. [In Japanese.]

Moore, H. F.
1910. Commercial sponges and the sponge fisheries. Bull. Bureau Fish. 28:399–511.

Neuweiler, F. T., and D. J. Burdige.
2005. The modern calcifying sponge *Spheciospongia vesparium* (Lamarck, 1815), Great Bahama Bank: implications for ancient sponge mud-mounds. Sediment. Geol. 175:89–98.

Noren, S. R., G. Lacave, R. S. Wells, and T. M. Williams.
2002. The development of blood oxygen stores in bottlenose dolphins (*Tursiops truncatus*): implications for diving capacity. J. Zool. 258:105–113.

Norton, S. F., Z. A. Eppley, and B. D. Sidell.
2000. Allometric scaling of maximal enzyme activities in the axial musculature of striped bass, *Morone saxatilis* (Walbaum). Physiol. Biochem. Zool. 73:819–828.

Nussey, D. H., H. Froy, J.-F. Lemaitre, J.-M. Gaillard, and S. N. Austad.
2013. Senescence in natural populations of animals: widespread evidence and its implications for bio-gerontology. Ageing Res. Rev. 12:214–225.

Okey, T. A., G. A. Vargo, S. Mackinson, M. Vasconcellos, B. Mahmoudi, and C. A. Meyer.
2004. Simulating community effects of sea floor shading by plankton blooms over the West Florida Shelf. Ecol. Model. 172:339–359.

Opitz, S.
1996. Trophic interactions in Caribbean coral reefs. ICLARM Tech. Rep. 43, 341 p. [Available from website.]
Oronti, A., A. J. Danylchuk, C. E. Elmore, R. Auriemma, and G. Pesle.
2012. Assessing the feasibility of sponge aquaculture as a sustainable industry in The Bahamas. Aquac. Int. 20:295–303.
Osinga, R., J. Tramper, and R. H. Wijffels.
1999. Cultivation of marine sponges. Mar. Biotechnol. 1:509–532.
Palomares, M. L. D., and D. Pauly (eds.).
2021. SeaLifeBase, vers. 04/2021. World Wide Web electronic publication. [Available from website, accessed November 2021.]
Pauly, D.
1981. The relationships between gill surface area and growth performance in fish: a generalization of von Bertalanffy's theory of growth. Ber. Dtsch. Wiss. Komm. Meeresforsch. 28:251–282.
1984. A mechanism for the juvenile-to-adult transition in fishes. ICES J. Mar. Sci. 41:280–284.
1998. Beyond our original horizons: the tropicalization of Beverton and Holt. Rev. Fish Biol. Fish. 8:307–334.
2019a. Gasping fish and panting squids: oxygen temperature and the growth of water-breathing animals, 2nd ed., 279 p. Int. Ecol. Inst., Oldendorf/Luhe, Germany.
2019b. Female fish grow bigger—let's deal with it. Trends Ecol. Evol. 34:181–182.
2021a. The gill-oxygen limitation theory (GOLT) and its critics. Sci. Adv. 7:eabc6050.
2021b. Why do fish reach first maturity when they do? J. Fish Biol. 1–9.
Pauly, D., and D. Zeller.
2016a. Catch reconstructions reveal that global marine fisheries catches are higher than reported and declining. Nat. Commun. 7:10244.
2016b. Global atlas of marine fisheries: a critical appraisal of catches and ecosystem impacts, 520 p. Island Press, Washington, DC.
Pauly, D., and W. W. L. Cheung.
2017. Sound physiological knowledge and principles in modeling shrinking of fishes under climate change. Glob. Chang. Biol. 24:e15–e26.
Pawlik, J. R.
2011. The chemical ecology of sponges on Caribbean reefs: natural products shape natural systems. BioScience 61:888–898.
Pawlik, J. R., and S. E. McMurray.
2020. The emerging ecological and biogeochemical importance of sponges on coral reefs. Annu. Rev. Mar. Sci. 12:315–337.
Pawlik, J. R., S. E. McMurray, P. Erwin, and S. Zea.
2015. A review of evidence for food limitation of sponges on Caribbean reefs. Mar. Ecol. Prog. Ser. 519:265–283.
Peterson, B. J., C. M. Chester, F. J. Jochem, and J. W. Fourqurean.
2006. Potential role of sponge communities in controlling phytoplankton blooms in Florida Bay. Mar. Ecol. Prog. Ser. 328:93–103.
Pinkerton, M. H., C. J. Lundquist, C. A. J. Duffy, and D. J. Freeman.
2008. Trophic modelling of a New Zealand rocky reef ecosystem using simultaneous adjustment of diet, biomass and energetic parameters. J. Exp. Mar. Biol. Ecol. 367:189–203.
Poppell, E., J. Weisz, L. Spicer, A. Massaro, A. Hill, and M. Hill.
2014. Sponge heterotrophic capacity and bacterial community structure in high- and low-microbial abundance sponges. Mar. Ecol. 35:414–424.
Pütter, A.
1914. Der Stoffwechsel der Kieselschwämme. Z. Allg. Physiol. 16:65–114.
1920. Studien über physiologische Ähnlichkeit VI. Wachstumsähnlichkeiten. Pflueg. Arch. 180:298–340.
Quince, C., P. A. Abrams, B. J. Shuter, and N. P. Lester.
2008. Biphasic growth in fish I: theoretical foundations. J. Theor. Biol. 254:197–206.
Reitner, J., and G. Wörheide.
2002. Non-lithistid fossil Demospongiae—origins of their palaeobiodiversity and highlights in history of preservation. *In* Systema Porifera: a guide to the classification of sponges (J. N. A. Hooper, R. W. M. Van Soest, and P. Willenz, eds.), p. 52–68. Springer, Boston, MA.
Riisgård, H. U., S. Thomassen, H. Jakobsen, J. M. Weeks, and P. S. Larsen.
1993. Suspension feeding in marine sponges *Halichondria panicea* and *Haliclona urceolus*: effects of temperature on filtration rate and energy cost of pumping. Mar. Ecol. Prog. Ser. 96:177–188.
Rohatgi, A.
2021. WebPlotDigitizer, vers. 4.5. [Available from website, accessed October 2021.]
Rohde, S., S. Nietzer, and P. J. Schupp.
2015. Prevalence and mechanisms of dynamic chemical defenses in tropical sponges. PLoS ONE 10(7):e0132236.
Sainsbury, K. J.
1980. Effect of individual variability on the von Bertalanffy growth equation. Can. J. Fish. Aquat. Sci. 37:241–247.
Schläppy, M.-L., S. I. Schöttner, G. Lavik, M. M. M. Kuypers, D. de Beer, and F. Hoffmann.
2010. Evidence of nitrification and denitrification in high and low microbial abundance sponges. Mar. Biol. 157:593–602.
Somero, G. N., and J. J. Childress.
1980. A violation of the metabolism-size scaling paradigm: activities of glycolytic enzymes in muscle increase in larger-size fish. Physiol. Zool. 53:322–337.
Soriano, M., J. Moreau, J. M. Hoenig, and D. Pauly.
1992. New functions for the analysis of two-phase growth of juvenile and adult fishes, with application to Nile perch. Trans. Am. Fish. Soc. 121:486–493.
Stevely, J. M., J. C. Thompson, and R. E. Warner.
1978. The biology and utilization of Florida's commercial sponges. Florida Sea Grant Program, Tech. Pap. 8, 45 p. Fla. Sea Grant Coll. Program, Gainesville, FL. [Available from website.]
Storr, J. F.
1964. Ecology of the Gulf of Mexico commercial sponges and its relation to the fishery. U.S. Fish Wildl. Serv., Spec. Sci. Rep. Fish. 466, 72 p. [Available from website.]
Stuart, A. H.
1948. World trade in sponges. U.S. Dep. Commer., Ind. Ser. 82, 95 p.
Taylor, C. C.
1958. Cod growth and temperature. ICES J. Mar. Sci. 23:366–370.
Thuesen, E. V., L. D. Rutherford, Jr., P. L. Brommer, K. Garrison, M. A. Gutowska, and T. Towanda.
2005. Intragel oxygen promotes hypoxia tolerance of scyphomedusae. J. Exp. Biol. 208:2475–2482.
Tudman, P. D.
2001. Modelling the trophic effects of fishing on a midshelf coral reef of the central Great Barrier Reef. B.S. thesis, 105 p. James Cook Univ., Townsville, Australia.
Turner, E. C.
2021. Possible poriferan body fossils in early Neoproterozoic microbial reefs. Nature 596:87–91.

Vakily, J. M.
1992. Determination and comparison of bivalve growth, with emphasis on Thailand and other tropical areas. ICLARM Tech. Rep. 36, 125 p. [Available from website.]
Valentine, M. M.
2019. Sponge community biocomplexity, competition, and functional significance in hard-bottom habitats of the Florida Keys, FL (USA). Ph.D. diss., 150 p. Old Dominion Univ., Norfolk, VA. [Available from website.]
Valentine, M. M., and M. J. Butler IV.
2019. Sponges structure water-column characteristics in shallow tropical coastal ecosystems. Mar. Ecol. Prog. Ser. 608:133–147.
van Oosten, J.
1923. The whitefishes (*Coregonus clupeaformis*). A study of the scales of whitefishes of known ages. Zool. Sci. Contrib. N.Y. Zool. Soc. 2:381–412.
van Soest, R. W. M.
1978. Marine sponges from Curaçao and other Caribbean localities. Part I. Keratosa. Stud. Fauna Curaçao Other Caribb. Isl. 56(179):1–94.
Vogel, S.
1996. Life in moving fluids: the physical biology of flow, 2nd ed., 488 p. Princeton Univ. Press, Princeton, NJ.
von Bertalanffy, L.
1938. A quantitative theory of organic growth (Inquiries on growth laws. II). Hum. Biol. 10:181–213.
1951. Theoretische biologie. Zweiter Band: Stoffwechsel, Wachstum, 418 p. A. Francke Verlag, Bern, Switzerland.
von Ledebur, J. F.
1939. Über die Atmung der Schwämme und Coelenteraten. *In* Ergebnisse der biologie (K. v. Frisch, W. Ruhland, H. Stubbe, and W. Vogt, eds.), p. 262–291. Springer, Berlin, Germany.
Wall, C. C., B. S. Rodgers, C. J. Gobler, and B. J. Peterson.
2012. Responses of loggerhead sponges *Spechiospongia vesparium* during harmful cyanobacterial blooms in a subtropical lagoon. Mar. Ecol. Prog. Ser. 451:31–43.
Wang, Y.-G., and M. R. Thomas.
1995. Accounting for individual variability in the von Bertalanffy growth model. Can. J. Fish. Aquat. Sci. 52:1368–1375.
Warburg, O. H.
1930. The metabolism of tumours, 327 p. Constable, London. [Translated from the German version by F. Dickens.]
Ward, P. D.
2006. Out of thin air: dinosaurs, birds, and Earth's ancient atmosphere, 296 p. Joseph Henry Press, Washington, DC.
Weber, K. T., and J. S. Janicki.
1979. The metabolic demand and oxygen supply of the heart: physiologic and clinical considerations. Am. J. Cardiol. 44:722–729.
Webster, N. S.
2007. Sponge disease: a global threat? Environ. Microbiol. 9:1363–1375.
Webster, N. S., and M. W. Taylor.
2012. Marine sponges and their microbial symbionts: love and other relationships. Environ. Microbiol. 14:335–346.
Weisz, J.
2006. Measuring impacts of associated microbial communities on Caribbean reef sponges: searching for symbiosis. Ph.D. diss., 165 p. Univ. North Carolina, Chapel Hill, NC. [Available from website.]
Winberg, G. G. (ed.).
1971. Methods for the estimation of production of aquatic animals, 175 p. Acad. Press, London and New York.
Witzell, W. N.
1998. The origin of the Florida sponge fishery. Mar. Fish. Rev. 60(1):27–32.
Wulff, J. L.
2006. Ecological interactions of marine sponges. Can. J. Zool. 84:146–166.

National Marine Fisheries Service
NOAA

Fishery Bulletin
established in 1881

Spencer F. Baird
First U.S. Commissioner of Fisheries and founder of *Fishery Bulletin*

New data on the morphology of the Mekong blind sole (*Typhlachirus elongatus*) indicating the need for a revision of the genus

Sergei A. Evseenko (deceased)[1]
Dmitry V. Bolshakov[1]
Yana Yu. Bolshakova (contact author)[1]
Yuri O. Kopylov-Guskov[2,3]
Natalya V. Gordeeva[1,4]
Evgeniia P. Karpova[5,6]
Alexander R. Boltachev (deceased)[5,6]

Email address for contact author: yanusrunaa@mail.ru

[1] Shirshov Institute of Oceanology
Russian Academy of Sciences
36 Nakhimovsky Prospekt
Moscow 117997, Russia

[2] Lomonosov Moscow State University
Leninskiye Gory, 1, Building 12
Moscow 119234, Russia

[3] Shenzhen MSU-BIT University
1 International University Park Road
Dayun New Town
Longgang District
Shenzhen 518172, China

[4] Vavilov Institute of General Genetics
Russian Academy of Sciences
Gubkina Street, 3
Moscow 119333, Russia

[5] Kovalevsky Institute of Biology of the Southern Seas
Russian Academy of Sciences
Nakhimov Prospekt, 2
Sevastopol 299011, Russia

[6] Severtsov Institute of Ecology and Evolution
Russian Academy of Sciences
Leninskiy Prospekt, 33
Moscow 119071, Russia

Abstract—The results of analysis of 88 specimens of the Mekong blind sole (*Typhlachirus elongatus*) from the Mekong River delta in Vietnam indicate that the range of variability in meristic diagnostic characters of this species is broader than previously documented. Comparison of the new morphological data for *T. elongatus* from our analysis with data from the available literature for *T. lipophthalmus* and *T. caecus* reveals no differences between species. This fact confirms Chabanaud's conclusions about the monotypy of the genus *Typhlachirus* and indicates the need for further revision of the genus. Here, molecular data from the genes cytochrome *c* oxidase subunit 1 and 16S rRNA are presented for the first time for the genus *Typhlachirus*.

Manuscript submitted 19 November 2021.
Manuscript accepted 18 March 2022.
Fish. Bull. 120:113–124 (2022).
Online publication date: 1 April 2022.
doi: 10.7755/FB.120.2.2

The views and opinions expressed or implied in this article are those of the author (or authors) and do not necessarily reflect the position of the National Marine Fisheries Service, NOAA.

The soles of the genus *Typhlachirus* (family Soleidae) are found in marine and brackish water and distinguished by the absence of eyes. Three nominal species of the genus—*T. lipophthalmus* (Károli, 1882), *T. caecus* Hardenberg, 1931, and the Mekong blind sole (*T. elongatus*) Pellegrin and Chevey, 1940—have been described from the Indo-West Pacific. Currently, they are all considered valid (Fricke et al., 2021). Until recently, blind sole were poorly represented in ichthyological collections: a total of 15 individuals have been reported (Karoli, 1882; Hardenberg, 1931a, 1931b; Pellegrin and Chevey, 1940; Atack, 2006; Evseenko and Bolshakov, 2018; Tan and Grinang, 2020). Of these individuals, 5 specimens of *T. lipophthalmus* were caught from the coastal waters off the northwestern coast of Kalimantan, the Indonesian territory on the island of Borneo (Karoli, 1882; Atack, 2006; Tan and Grinang, 2020), 5 specimens of *T. caecus* were caught from the mouth of the Rokan River in the Strait of Malacca between Sumatra Island of Indonesia and the Malay Peninsula (Hardenberg, 1931a, 1931b), and 5 specimens of *T. elongatus* were caught from the estuarine part of the Mekong River in Vietnam (Pellegrin and Chevey, 1940; Evseenko and Bolshakov, 2018). However, Abidin and Bintoro (2014) reported about 491 blind sole from the estuarine part of the Indragiri River of Sumatra Island. This circumstance indicates that these species are relatively abundant and are frequently caught as bycatch in local fisheries.

The 3 species of blind sole are very similar in external morphology, meristic features, and body proportions; therefore, distinguishing between them is difficult. The features that the authors of the first descriptions note as diagnostic

are as follows: *T. elongatus* differs from *T. caecus* in a more elongated body shape, a more curved mouth, the shape of the nostril, the absence of pectoral fins, and coloration, and *T. elongatus* differs from *T. lipophthalmus* in coloration and smaller scales (Pellegrin and Chevey, 1940). *Typhlachirus caecus* differs from *T. lipophthalmus* in the presence of pectoral fins (Hardenberg, 1931a). In his revision of blind soles, Chabanaud (1948) carefully studied the external morphology, anatomy, and osteology of all specimens available at that time (8 specimens). He noted that there were no sufficient reasons to distinguish these 3 species and combined them into one monotypic genus *Typhlachirus*. As a species epithet, he proposed to keep the earlier synonym *T. lipophthalmus* (Chabanaud, 1939), suggested by Károli (1882).

This revision (Chabanaud, 1948) had been unknown to subsequent researchers until, in 2018, we published a work on the morphology of blind soles with a historical review of taxonomic changes in the genus *Typhlachirus* (Evseenko and Bolshakov, 2018). At the time of that writing, only 2 species had been recognized as valid: *T. caecus* and *T. elongatus* (Munroe, 2000; Desoutter et al., 2001a; Lapierre, 2007; Kottelat, 2013). However, to identify our specimens, we compared them with all species of the genus *Typhlachirus* known at that time, including the unaccepted *T. lipophthalmus* (Evseenko and Bolshakov, 2018). The purpose of the Evseenko and Bolshakov (2018) article was to discuss the problems of the taxonomy of blind soles and supplement the data on their morphology. However, in Eschmeyer's Catalog of Fishes, the work has been interpreted as a revision of the genus *Typhlachirus*. As a result, all 3 types of blind soles are currently indicated as valid in that database (Fricke et al., 2021), and the Chabanaud (1948) revision mentioned in the article (Evseenko and Bolshakov, 2018) was not taken into account again.

During an expedition to the estuarine part of the Mekong River delta, we caught 85 new specimens of blind soles. When trying to determine the species involved, we found that the diagnostic features from the first descriptions and other available literature on these species did not allow the separation of species of *Typhlachirus*. The range of meristic characters of the new specimens is much more extensive than have been noted for *T. elongatus*. In addition, a pectoral fin was found in all new specimens. Given that the absence of a pectoral fin has been reported as a diagnostic feature for *T. elongatus*, the presence of one in our specimens prompted us to reexamine the specimens of *T. elongatus* studied in our previous work (Evseenko and Bolshakov, 2018), and it also served as a reason for a more thorough study of the new specimens.

The primary purpose of the work reported here was to examine the diagnostic characters used to identify species of the genus *Typhlachirus* and to correct misunderstandings that appeared after the publication of Evseenko and Bolshakov (2018). Because there is no molecular genetic information for the genus *Typhlachirus*, we set out to fill this gap by using DNA barcoding, a tool widely used for identification of species and rapid assessment of their genetic variability (Hebert et al., 2003; Hajibabaei et al., 2007; Crawford et al., 2013; Chambers and Hebert, 2016).

Materials and methods

The materials for this work were 85 specimens of juveniles and adults of the genus *Typhlachirus*, with a range in standard body length (SL) of 14–80 mm (Suppl. Table) (online only), collected in the Mekong River delta (Fig. 1): 2 specimens (sp.) 32 mm SL, 32 mm SL, 6 April 2018, trawl no. 1, Co Chien River, 10°15′33″N, 105°57′46″E; 9 sp. 22–36 mm SL, 8 April 2018, trawl no. 5, Co Chien River, 10°10′50″N, 106°10′22″E; 2 sp. 30 mm SL, 52 mm SL, 17 April 2018, trawl no. 4, Tien River, 10°19′48′N, 106°17′38″E; 4 sp. 25–76 mm SL, 17 April 2018, 10°20′17″N, 106°19′60″E; 5 sp. 24–49 mm SL, 17 April 2018, trawl no. 1, Tien River, 10°19′37″N, 106°17′37″E; 1 sp. SL? (a question mark [?] means that the length data were lost), 17 April 2018, 10°19′80″N, 106°17′37″E; 2 sp. SL?, 4 August 2018, Tien River, 10°19′27″N, 106°00′50″E; 1 sp. SL?, 18 April 2018, 10°19′2″N, 106°10′12″E; 4 sp. 14–44 mm SL, 19 April 2018, trawl no. 1, Tien River, 10°19′19″N, 106°00′59″E; 1 sp. SL?, 11 April 2018, 10°17′23″N, 106°34′11″E; 1 sp. 46 mm SL, 24 April 2018, trawl no. 2, 10°16′26″N, 106°43′40″E; 1 sp. SL?, 11 May 2018, Tien River, 10°16′46″N, 10°50′55″E; 3 sp. SL?, 12 May 2018, Ham Luong River, 10°14′22″N, 106°13′40″E; 1 sp. 54 mm SL, 15 May 2018, trawl no. 4, Ham Luong River, 10°06′23″N, 106°24′13″E; 1 sp. 60 mm SL, 17 May 2018, trawl no. 4, Ham Luong River, 9°56′26″N, 106°39′20″E; 2 sp. 23 mm SL, 43 mm SL, 19 May 2018, trawl no. 2, Ham Luong River, 10°02′45″N, 106°27′27″E; 4 sp. 30–58 mm SL, 21 May 2018, trawl no. 2, Ba Lai River, 10°08′50′N, 106°37′57″E; 1 sp. 80 mm SL, 23 May 2018, trawl no. 1, Ba Lai River, 10°08′10″N, 106°39′00″E; 1 sp. SL?, 24 May 2018, 10°07′18″N, 106°48′26″E; 39 sp. 14–64 mm SL (capture data lost).

To study the structure of the shoulder girdle and the degree of reduction of the pectoral fins, the 49- and 53-mm-SL specimens were stained with alizarin and alcian blue and clarified according to the standard procedure (Taylor and Van Dyke, 1985). Radiographs were made and studied for almost all specimens. For comparison, we used X-rays of 2 syntypes of *T. elongatus* 28 and 33 mm SL, MNHN 1939-0270 (provided by the Muséum National d'Histoire Naturelle); 2 paratypes of *T. caecus* 76 and 83 mm SL, MNHN 1942-0080 (in Chabanaud, 1948); and 1 specimen of *T. lipophthalmus* 61 mm SL, ZRC 59653 (in Tan and Grinang, 2020). Additionally, 3 specimens, 59, 67, and 71 mm SL, described in Evseenko and Bolshakov (2018), were studied.

Information for the following features are included in the descriptions: SL, head length (HL), body depth at pectoral fin base (BD), number of rays in dorsal fin (D), number of rays in anal fin (A), number of rays in pectoral fin on the ocular (right) side of the body ($P1_d$), number of rays in pectoral fin on the blind (left) side ($P1_s$), number of rays in pelvic fin (P2), number of rays in caudal fin (C), number of vertebrae (V), number of precaudal vertebrae (PrCV),

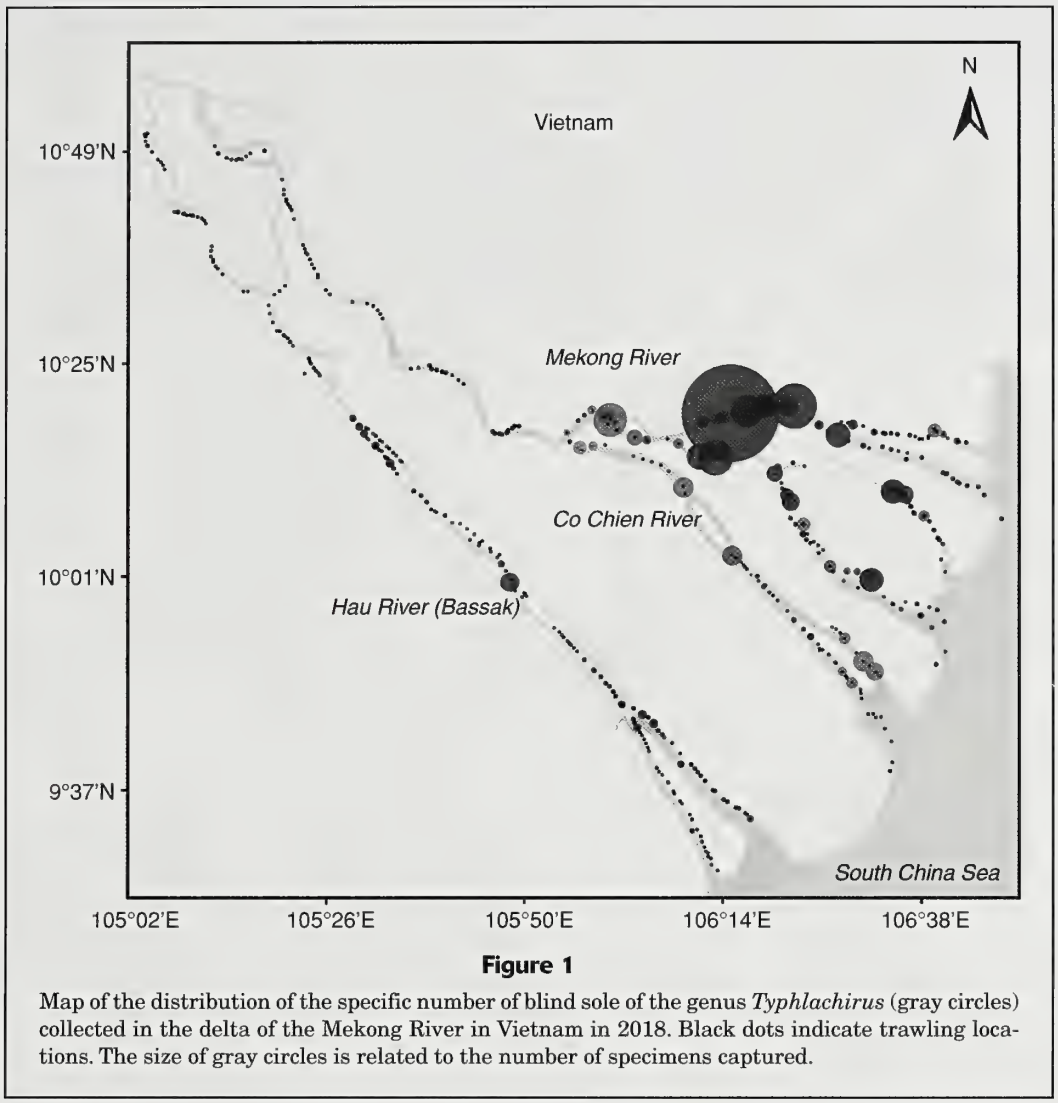

Figure 1

Map of the distribution of the specific number of blind sole of the genus *Typhlachirus* (gray circles) collected in the delta of the Mekong River in Vietnam in 2018. Black dots indicate trawling locations. The size of gray circles is related to the number of specimens captured.

number of caudal vertebrae (CV), and number of pored scales on the horizontal branch of the ocular side lateral line, not including scales on caudal fin (LL).

Statistical analysis

To check the homogeneity of our sample of specimens across all studied features, principal component analysis was performed. On the basis of analysis of combined data (from our work and published reports) on *T. elongatus*, *T. lipophthalmus*, and *T. caecus*, we excluded from further analysis both the number of rays in the pectoral fins (because of the unreliability of data in the original descriptions) and the number of vertebrae (because of the partial lack of data). Results of a preliminary normality test (Shapiro–Wilk test) indicate that all the characters except the number of pores in the lateral line had distributions that were not normal; therefore, we used Spearman's rank correlation coefficients to find linear correlations between SL and other studied features. To ensure that we had not lost any information by using this nonparametric coefficient, we also calculated Pearson correlation coefficients for our data set. To evaluate occurrence frequencies for each feature, the histograms for each character were built (Fig. 2). Principal component analysis was performed in PAST (vers. 2.17c; Hammer et al., 2001), and correlation analysis was done in R (vers. 4.0.3; R Core Team, 2020).

Molecular analysis

We extracted whole genomic DNA from muscle tissue of 14 specimens of *T. elongatus* (Suppl. Table) (online only) by using the Diatom DNA Prep 100[1] kit (Izogen Laboratory, Moscow, Russia). In total, 650 base pairs from the barcode region of the mitochondrial cytochrome *c* oxidase subunit 1 (CO1) gene were amplified with the primer set FishF1/FishR2 (Ward et al., 2005). For the subsample of 8 specimens, we amplified the segment (574 base pairs) of the 16S

[1] Mention of trade names or commercial companies is for identification purposes only and does not imply endorsement by the National Marine Fisheries Service, NOAA.

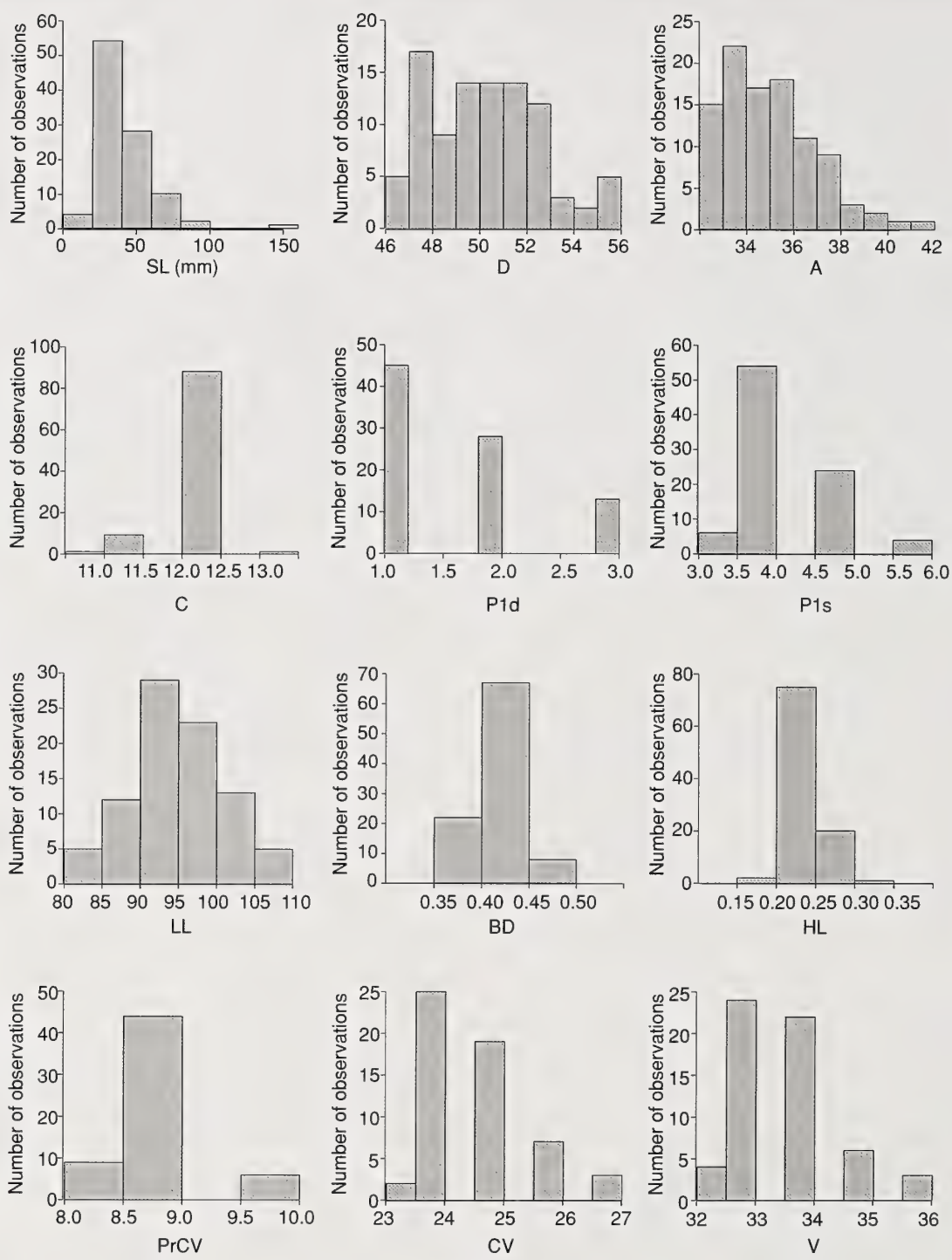

Figure 2

Frequency of occurrence of examined meristic characters and body proportions in 3 nominal species of the genus *Typhlachirus*, based on specimens captured in 2018 in the Mekong River delta of Vietnam and described in the literature (Chabanaud, 1948; Hardenberg, 1931b; Pellegrin and Chevey, 1940; Tan and Grinang, 2020). Features include standard body length (SL), number of rays in dorsal fin (D), number of rays in anal fin (A), number of rays in caudal fin (C), number of rays in pectoral fin on the ocular (right) side of the body ($P1_d$) and on the blind (left) side ($P1_s$), number of pored scales on the horizontal branch of the ocular side lateral line not including scales on caudal fin (LL), body depth at pectoral fin base (BD), head length (HL), number of precaudal vertebrae (PrCV), number of caudal vertebrae (CV), and number of vertebrae (V).

rRNA gene by using the primer set 16Sar/6Sbr (Palumbi, 1996). The choice of molecular markers was determined by the widest taxonomic representation of Soleidae species in the available databases.

Polymerase chain reaction products were purified and sequenced bidirectionally by using the same primers and an Applied Biosystems BigDye Terminator v3.1 Cycle Sequencing Kit (Thermo Fisher Scientific Inc., Waltham, MA) with an Applied Biosystems 3730 Genetic Analyzer (Thermo Fisher Scientific Inc.). All sequences were edited and aligned by using Geneious, vers. 9.1.8 (Kearse et al., 2012), to obtain consensus sequences and check the occurrence of deletions, insertions, and stop codons. Haplotypes were defined by using FaBox (Villesen, 2007) and then were deposited in GenBank (National Institutes of Health, available from website) under the following IDs: MW646924–MW646930 (CO1 haplotypes) and MW648330–MW648332 (16S rRNA haplotypes). Indices of diversity (number of polymorphic [segregating] sites, the nucleotide diversity, and the haplotype diversity; Nei, 1987) were calculated for the mtDNA CO1 gene by using DnaSP software, vers. 6.0 (Rozas et al., 2017). Tajima's D (Tajima, 1989) and Fu and Li's *F* (Fu and Li, 1993) tests of neutrality also were performed with DnaSP.

Distances between mtDNA CO1 sequences were calculated by using MEGA, vers. 6.0 (Tamura et al., 2013), under Kimura's 2-parameter substitution model commonly used for DNA barcoding in studies of fish species (Ward, 2009). A neighbor-joining (Saitou and Nei, 1987) dendrogram with 1000 bootstraps was created by using distances, calculated with Kimura's 2-parameter substitution model, in MEGA to provide a graphic representation of the divergence patterns among *Typhlachirus* and closely related species of Soleidae. We used sequences of 4 species of the genus *Brachirus*—*B. annularis*, *B. harmandi*, the black sole (*B. niger*), and the oriental sole (*B. orientalis*)—the tufted sole (*Dexillus muelleri*), *Aseraggodes kobensis*, the bamboo sole (*Heteromycteris japonicus*, the Atlantic sole (*Pegusa lascaris*), the wavyband sole (*Zebrias japonicus*), the common sole (*Solea solea*), and the tiger sole (*Soleichthys heterorhinos*) from GenBank and the Barcode of Life Data System (BOLD Systems, available from website). Additionally, for measuring intraspecific and interspecific divergence, uncorrected *p* distances, meaning the proportions of nucleotide sites at which 2 sequences being compared are different, were calculated in MEGA by dividing the number of nucleotide differences by the total number of nucleotides compared.

Results

Typhlachirus elongatus Pellegrin and Chevey, 1940

Typhlachirus elongatus Pellegrin and Chevey, 1940:155 (Fig. 1) (first description based on 2 specimens). Mekong River delta. Syntypes (2): MNHN 1939-0270 (2). Rainboth, 1996:222 (listed). Desoutter et al., 2001a:328 (listed). Evseenko and Bolshakov, 2018:553 (description). Tan and Grinang, 2020:7 (fishing localities).

Brachirus elongatus: Munroe in Randall and Lim, 2000:646 (listed). Kottelat, 2013:464 (listed).

The description of the morphology of *T. elongatus* is somewhat scattered; therefore, it is advisable to give a short but complete description here.

Key diagnostic features

D: 46–55, A: 33–40, C: 10–13, $P1_s$: 3–6, $P1_d$: (0)1–3, P_2: 3, V: 32–36, PrCV: 8–10, CV: 23–27, LL: 84–108 (Table 1). The body is right-sided, broad in front, tapered toward the tail, and strongly compressed (Fig. 3). All specimens have a right eye, but it is reduced in varying degrees. Gill rakers are absent from the gill arches. The mouth is curved to

Table 1

Meristic characters and proportional measurements of the Mekong blind sole (*Typhlachirus elongatus*) caught in the Mekong River delta in 2018 (number of specimens [*n*]=85) and from Evseenko and Bolshakov (2018) (*n*=3) in different size classes based on standard body length (SL). Features include number of rays in dorsal fin (D), number of rays in anal fin (A), number of rays in caudal fin (C), number of rays in pectoral fin on the ocular (right) side of the body ($P1_d$) and on the blind (left) side ($P1_s$), number of pored scales on the horizontal branch of the ocular side lateral line not including scales on caudal fin (LL), number of precaudal vertebrae (PrCV), number of caudal vertebrae (CV), number of vertebrae (V), body depth at pectoral fin base (BD), and head length (HL).

n	SL (mm)	D	A	C	$P1_d$	$P1_s$	LL	PrCV	CV	V	BD	HL
4	14–20	48–53	35–37	11–12	1–3	3–5	85–92	9	25	34	42–43	24–31
32	21–30	46–54	33–39	11–12	1–3	3–6	85–108	8–10	23–26	32–36	37–46	22–30
18	31–40	47–54	34–39	11–12	1–3	3–5	90–102	9	24–27	33–36	38–46	22–28
16	41–50	47–53	34–38	10–12	1–3	4–6	84–107	8–9	24–26	32–34	38–45	22–26
12	51–60	48–52	34–40	11–13	1–3	4–6	87–107	8–10	23–26	33–34	36–47	21–26
4	61–70	49–53	35–38	12	1–2	4–5	85–105	8–10	24–26	32–35	41–43	20–25
2	71–80	53–55	38–40	11–12	2	4–5	93–99	8–10	24–25	33–34	42–45	23–24

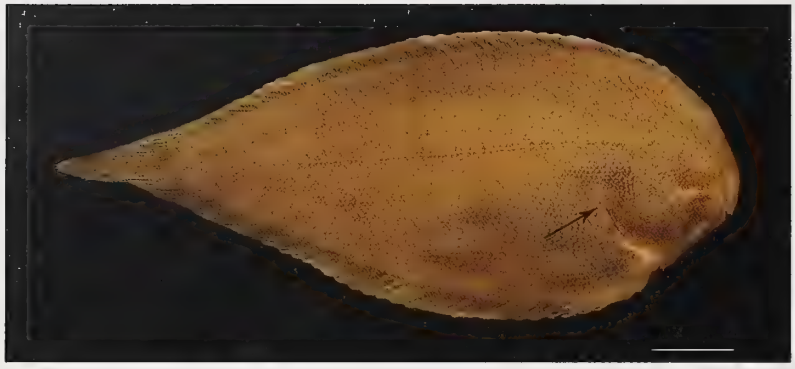

Figure 3

Photograph showing the general view of a Mekong blind sole (*Typhlachirus elongatus*), 71 mm in standard body length, caught on May 2010 in the Mekong River delta of Vietnam. The arrow points to the right pectoral fin. The scale is 1 cm.

varying degrees. The dorsal and anal fins join with the caudal fin. The pectoral fin on the right side of the body is present in all specimens. The pectoral fin on the left side is a transparent membrane; it has a wide base and 3–6 widely spaced rays, half covered by the operculum. The lateral line is straight, extending to the caudal fin on both sides of the body. Both sides of the body are covered with ctenoid scales. The right side of the body is uniformly colored pinkish brown, and the left side is pinkish white.

Morphology

Meristic characters and proportional measurements are presented in Table 1. The body is right-sided, strongly compressed, broad in front, and tapered toward the tail. The caudal fin merges with the dorsal and anal fins; the caudal peduncle is absent. The greatest body depth is 37–47% SL. The head is large, and its length is 20–31% SL. The anterior profile of the head is rounded, and the snout protrudes slightly anterior to the mouth. The epicranial complex consists of 5(6) pterygiophores associated directly with the erisma, the 0(1) pterygiophore between the erisma and second neural spine, and 6(7) pterygiophores attached between the neural spines of the second and third vertebrae. The edge of the isthmus is far behind the vertical through the corner of the mouth. The mouth is terminal, and its anterior half is curved in the ventral direction; the length of the mouth is 33–37% HL. A short dermal fringe surrounds the jaws. The teeth on the jaws are present only on the left side. The teeth on both jaws are long, thin, pointed, and slightly curved. The number of rows is from 1 to 4, and the number of rows increases from front to back.

The left eye is absent (the eye is covered under skin and muscles, and the frontal bone and lateral ethmoid bone limit the eye orbit). Only the lower (right) eye, located just above the corner of the mouth, is visible; the eye is not pigmented. The anterior nostril on the ocular side of the body is tubular and located above the edge of the maxilla; from below it is covered with a valve. The posterior nostril on the ocular side of the body is rounded, located between the eye and the anterior nostril, and covered from above by a valve. The anterior nostril on the blind side of the body is rounded, located above the middle of the maxilla, and surrounded by cilia, and it has a valve. The posterior nostril is tubular and located above the corner of the mouth.

Gill rakers are absent from the gill arches. The gill membranes are covered with skin. The upper end of the gill opens at the level of the eye. Scales are small, are ctenoid on both sides of the body, and have 5–10 cteni. On the ocular side, the largest scales are located in the anteriodorsal part of the body, size of scales decreases in the caudal direction; scales on the blind side are approximately equal to the smallest scales on the ocular side of the body.

The lateral lines on the blind side and ocular side are straight; the number of pored scales on the ocular side to the end of the scale cover is 84–108, and the number on the blind side is 120–159. The lateral line on both sides of the body continues to the caudal fin and runs between 6 and 7 rays; it additionally contains from 23 to 33 perforated scales on the ocular side and from 30 to 50 scales on the blind side. The dorsal fin begins at the most protruding part of the rostrum; the anal fin begins somewhat in front of the level of the base of the right pectoral fin. The length of the rays in the dorsal and anal fins gradually increases in the caudal direction. The caudal fin is long and pointed.

The pectoral fin on the ocular side of the body is present in all specimens; it contains from 1 to 3 unbranched rays (Fig. 4A). The fin size is comparable in size to the scales. The pectoral fin on the blind side is presented in the form of a transparent membrane with a broad base, half covered by the operculum; it contains 3–6 rays (Fig. 4B). Both rays in the pelvic fin are branched and simple. The right pelvic fin is connected to the anal fin by a membrane; the left ventral fin is free. The anus is located in the anterior quarter of the body, between the anal and pelvic fins, and is displaced to the left side. The right side of the body is uniformly colored pinkish brown, each edge of the scales is bordered in black, and the left side is pinkish white.

Biology

Little is known about the biology of this species. *Typhlachirus elongatus* is a benthic fish and lives in muddy brackish waters on soft, silty substrates. In the Mekong River delta, the locations where specimens were captured are concentrated within the estuarine ecotone formed by the 6 branches of the river. In the Hau River, *T. elongatus* were more common in the river's main course, and in the estuarine areas and the coastal sea zone, they were practically

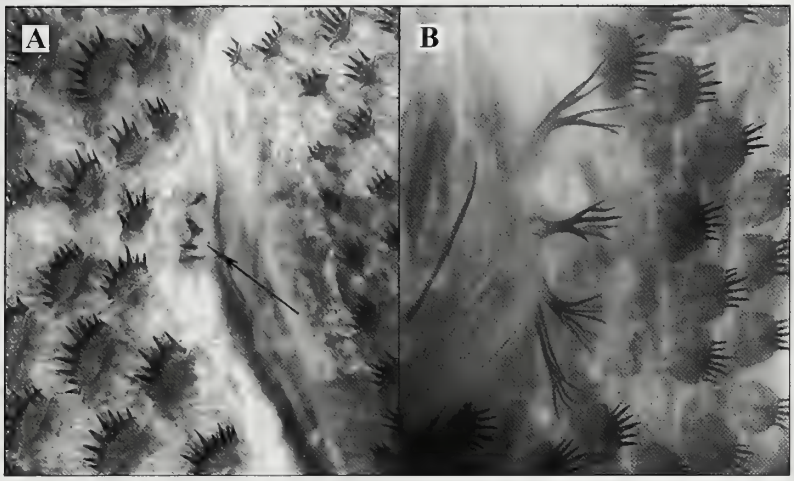

Figure 4

Photographs of the pectoral fin of a Mekong blind sole (*Typhlachirus elongatus*), 71 mm in standard body length, caught on May 2010 in the Mekong River delta of Vietnam, showing (**A**) the right (ocular) side of the body and (**B**) the left (blind) side of the body after staining with alizarin. The arrow in panel A points to the fin.

absent. In the areas where fish were caught in the Mekong River, waters in the bottom layer had temperatures of 28.2–34.1°C and salinity of 0.05–21.0. The early stages of development of this species are unknown, but metamorphosis and sinking to the bottom occur early—the smallest specimens found in collections of fish caught with trawl gear reached a size of 14 mm SL. Our new collections indicate that the species is quite numerous.

Distribution

Typhlachirus elongatus has been found in the estuarine part of the Mekong River (Pellegrin and Chevey, 1940; Evseenko and Bolshakov, 2018). Blind sole were detected in both of the main rivers of the Mekong River delta, the Co Chien (Mekong) and Hau (Bassak) Rivers (Fig. 1).

Statistical analysis

Results of the analysis of the combined sample (based on data from our work and from previous studies for all 3 species of *Typhlachirus*) reveal that all the characters, except the number of pores in the lateral line, have distributions different from normal. In this regard, we used medians and interquartile ranges to describe the average values of diagnostic features and the spread of data, respectively (Table 2). The results of principal component analysis indicate the homogeneity of the studied sample of specimens. The individuals form a single homogeneous group in the space of the first 2 principal components (PCs) (Fig. 5) that is centered around the zero coordinates. The PC1 is almost exclusively associated with the number of pores in the lateral line (loading is 0.9964), and the PC2 is associated with the number of rays in the dorsal and anal fins (loadings were 0.7963 and 0.5990, respectively) (Table 3). The PC1 and PC2 describe 96.1% of the data spread (80.6% and 15.5%, respectively). Individuals of *T. lipophthalmus* and *T. caecus* did not form separate clouds of points but found themselves on the periphery of the cloud for *T. elongatus* in the area of higher PC1 values.

We did not find linear correlations between body length and any other morphological characters: Spearman's rank correlation coefficients did not significantly differ from zero in all the cases. The Pearson's correlation coefficients were the same—all coefficients were zero.

Molecular analysis

Seven haplotypes of the mtDNA CO1 gene were found in species of *Typhlachirus* from the Mekong River delta, with

Table 2

Means, minimums (Min), maximums (Max), medians (Med), and lower interquartile (LQ) and upper interquartile (UQ) ranges of meristic characters and body proportions for the sample of 3 species of the genus *Typhlachirus* that combines data for specimens collected from the Mekong River delta in 2018 and for specimens described in literature (Chabanaud, 1948; Hardenberg, 1931a; Pellegrin and Chevey, 1940; Tan and Grinang, 2020). Features include number of rays in dorsal fin (D), number of rays in anal fin (A), number of rays in caudal fin (C), number of rays in pectoral fin on the ocular (right) side of the body ($P1_d$) and on the blind (left) side ($P1_s$), number of pored scales on the horizontal branch of the ocular side lateral line not including scales on caudal fin (LL), number of precaudal vertebrae (PrCV), number of caudal vertebrae (CV), number of vertebrae (V), body depth at pectoral fin base (BD), and head length (HL). *n*=the number of specimens used in the analysis.

Character	Mean	Min–Max	LQ–Med–UQ	*n*
D	50.8	46–56	49–51–52	95
A	36.5	33–43	35–36–38	99
C	11.9	10–13	12–12–12	99
$P1_d$	1.6	1–4	1–1–2	86
$P1_s$	4.3	3–6	4–4–5	88
LL	95.7	84–108	92–95–99	87
PrCV	8.9	8–10	9–9–9	59
CV	24.7	23–27	24–25–25	56
V	33.7	32–36	33–34–34	59
BD	42.0	37–47	41–43–44	98
HL	24.0	20–31	23–24–25	98

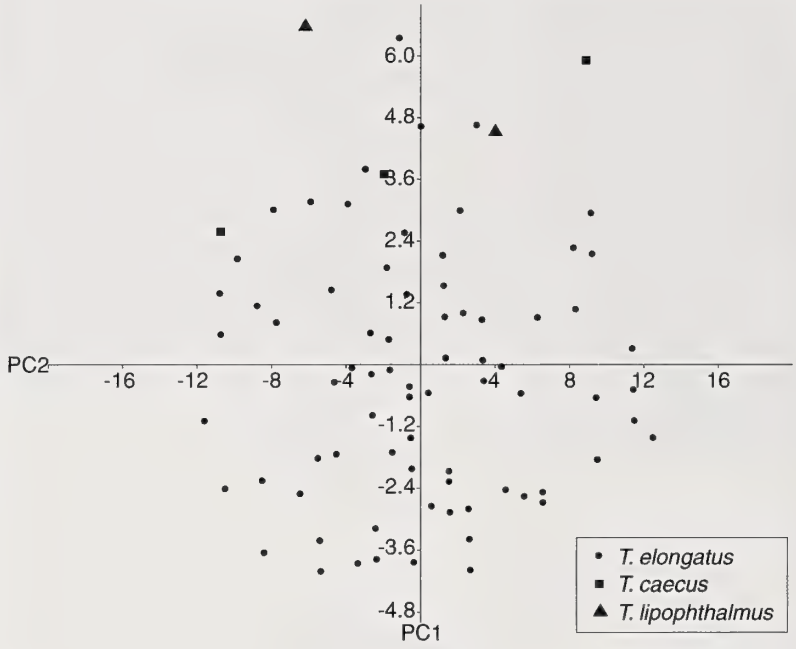

Figure 5

Plot of the principal component (PC) analysis of morphological characters and body proportions of Mekong blind sole (*Typhlachirus elongatus*) (circles), *T. lipophthalmus* (triangles), and *T. caecus* (squares). Each symbol represents a specimen captured in the Mekong River delta of Vietnam in 2018 or a specimen described in the literature (Chabanaud, 1948; Hardenberg, 1931b; Pellegrin and Chevey, 1940; Tan and Grinang, 2020).

only 2 haplotypes shared by more than 1 individual: Hap3 (MW646926) was found in 3 fish, and Hap5 (MW646928) was found in 6 fish. Results of the analysis of genetic diversity in the sample indicate a moderate degree of mtDNA COI variation: haplotype diversity is 0.802, nucleotide diversity is 0.0029, and the number of polymorphic sites is 9 (or 1.4% polymorphic sites). Estimates of Fu and Li's (1993) *F* and Tajima's (1989) D were not significant and hence do not signal selection or demographic expansion.

The final length of the mtDNA CO1 fragment after alignment of 22 sequences of *Typhlachirus* and representatives of Soleidae was 586 base pairs. All haplotypes in *Typhlachirus* were weakly distinguished (0.5% on average) and formed a single clade with high support indices (100%; Fig. 6). *Typlachirus* was obviously most closely related to species of the genus *Brachirus* and monotypic genus *Dexillus*, as predicted from their morphological similarity (Chapleau, 1989; Desoutter and Chapleau, 1997; Desoutter et al., 2001b). The distance between *Typhlachirus* and the closest species, *B. harmandi*, was 14.4%.

Discussion

Although in Eschmeyer's Catalog of Fishes 3 species of blind sole are recognized as valid (Fricke et al., 2021), our new data indicate possible monotypy of the genus *Typhlachirus*. According to the latest review of blind soles (Evseenko and Bolshakov, 2018), based on data from the literature on all known specimens of *T. lipophthalmus*, *T. caecus*, and *T. elongatus*, as well as on the study of 3 specimens of *T. elongatus* (Evseenko and Bolshakov, 2018), the species of the genus *Typhlachirus* differ mainly in meristic characters (Table 4). *Typhlachirus lipophthalmus* differs from *T. caecus* in the number of rays in the dorsal fin and from *T. elongatus* in the number of rays in the anal fin. *Typhlachirus caecus* differs from *T. elongatus* in the number of vertebrae and rays in the anal fin (Table 4). It should be noted that the revision by Chabanaud (1948)

Table 3

Loadings of the first and second principal components (PC) from principal component analysis of morphological characters of *Typhlachirus lipophthalmus*, *T. caecus*, and the Mekong blind sole (*T. elongatus*) from the sample that combines data for specimens collected in 2018 in the Mekong River delta and data from descriptions in the literature (Chabanaud, 1948; Hardenberg, 1931a; Pellegrin and Chevey, 1940; Tan and Grinang, 2020). Features include number of rays in dorsal fin (D), number of rays in anal fin (A), number of rays in caudal fin (C), body depth at pectoral fin base (BD), head length (HL), and number of pored scales on the horizontal branch of the ocular side lateral line not including scales on caudal fin (LL).

Component	D	A	C	BD	HL	LL
PC1	−0.0642	−0.0544	−0.0046	−0.0002	−0.0007	0.9964
PC2	0.7963	0.5990	0.0118	0.0013	−0.0016	0.0840

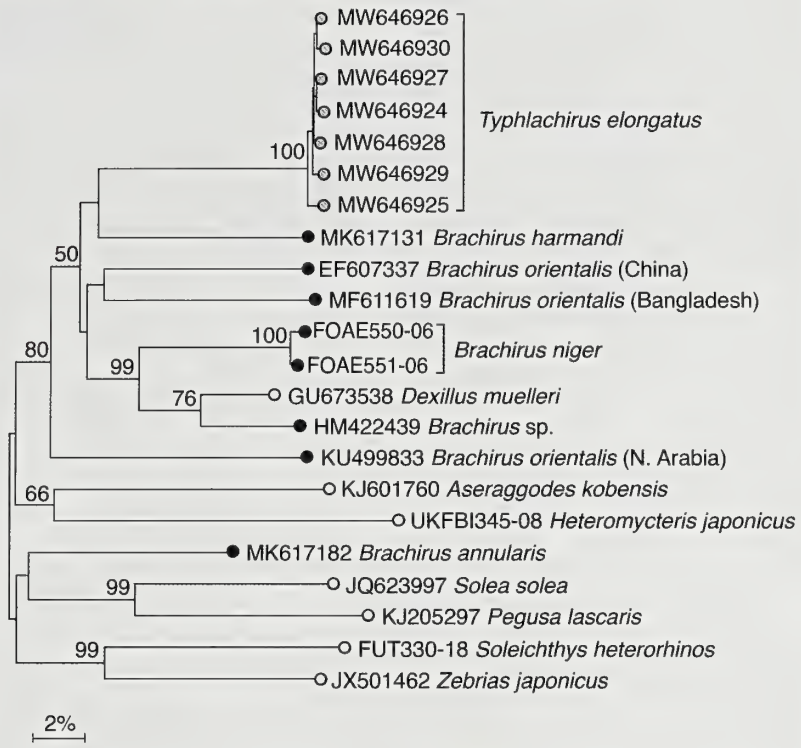

Figure 6

Neighbor-joining dendrogram created by using distances between mtDNA cytochrome *c* oxidase subunit 1 sequences calculated with Kimura's 2-parameter substitution model, showing the discrimination by distance among species of the genus *Typhlachirus*, based on sequences from molecular analysis of specimens captured in the Mekong River delta in 2018 (grey circles), and closely related species of the genus *Brachirus* (black circles) and other representatives of the family Soleidae (open circles), based on sequences available in GenBank and the Barcode of Life Data System (BOLD). Bootstrap values (≥50%) are given above branches. GenBank or BOLD numbers are given for each sequence.

and the review by Evseenko and Bolshakov (2018) were based on a small number of specimens of each species, which, in all probability, explains the registered differences in meristic characters.

We analyzed 88 specimens of *T. elongatus* from the Mekong River delta. The results indicate the homogeneity of our sample (Figs. 5 and 6). In the examined specimens of *T. elongatus*, the range of fluctuations of meristic characters is very wide and can be seen not only from the ranges of minimum and maximum values but also from the interquartile ranges (Table 2). No clear direction in the changes in meristic characters associated with the growth of fish was revealed. Despite the large spread in the number of rays in the dorsal and anal fins (D: 46–56; A: 33–43), the number of precaudal and caudal vertebrae, and the number of pores in the lateral line (PrCV: 8–10; CV: 23–27; LL: 84–108), our individuals form a homogeneous cloud (Fig. 5). Taking into account that PC1 explains a significant proportion of the total variability of the sample and is determined almost exclusively by the number of pores in the lateral line, the introduction of any apriori boundary (or boundaries) for this characteristic between the assumed taxa would automatically lead to a clear division of the sample into 2 (or more) groups. Nevertheless, such a division would be entirely artificial and would hide the objective primary result about the homogeneity of the sample. Results of molecular genetic analysis also indicate the absence of significant differences between specimens from the Mekong River delta.

The range of meristic characters of blind sole from our sample is very broad and includes the values noted in the literature for *T. lipophthalmus*, *T. caecus*, and *T. elongatus*. Several specimens of *T. lipophthalmus* and *T. caecus* turned up on the periphery of the cloud, which is mainly represented by our specimens, in the region of higher PC1 values (the number of pores in the lateral line) (Fig. 5). *Typhlachirus elongatus* from our sample had a pronounced morphological variability; therefore, it is essential to be careful about the taxonomic separation of specimens of the genus *Typhlachirus* with the limiting values of one or another feature. Hence, we explain the extreme position of *T. lipophthalmus* and *T. caecus* in Figure 5 by the small number of specimens used in the analysis. A similar broad range of meristic characters has been reported for some other species of Soleidae. For example, PrCV of 32–44 and LL of 90–133 have been suggested for zebra sole (*Zebrias zebra*) (Stephens, 2011) and PrCV of 32–35 and LL of 82–121 have been suggested for *B. panoides* (Lapierre, 2007). Therefore, such a range of characters without support by other morphological features cannot be a reason for the separation of species. As we noted earlier, the meristic characters of the 3 nominal species of *Typhlachirus* overlap, and extreme values were found even in specimens from the same sample. Accordingly, these characters cannot be used as diagnostic ones.

The presence or absence of a pectoral fin on the right side of the body is noted in several works as an important character and, in fact, the only character that distinguishes *T. lipophthalmus* and *T. elongatus* from *T. caecus* (Hardenberg, 1931a; Pellegrin and Chevey, 1940; Evseenko and Bolshakov, 2018). According to their descriptions, *T. lipophthalmus* (Pellegrin and Chevey, 1940; Chabanaud, 1948; Tan and Grinang, 2020) and *T. elongatus* (Pellegrin and Chevey, 1940; Evseenko and Bolshakov, 2018) lack the pectoral fin on the ocular side of the body. All of our specimens have a pectoral fin on the right side of the body regardless of body length. However, it is not always visible (sometimes presented as a skin outgrowth) or consists

Table 4

Meristic characters and body proportions for 3 species of the genus *Typhlachirus* based on data from the literature on all known specimens of *T. lipophthalmus*, *T. caecus*, and the Mekong blind sole (*T. elongatus*) (Chabanaud, 1948; Hardenberg, 1931a; Pellegrin and Chevey, 1940; Tan and Grinang, 2020). Features include standard body length (SL), number of rays in dorsal fin (D), number of rays in anal fin (A), number of rays in caudal fin (C), number of rays in pectoral fin on the ocular (right) side of the body ($P1_d$) and on the blind (left) side ($P1_s$), number of pored scales on the horizontal branch of the ocular side lateral line not including scales on caudal fin (LL), number of precaudal vertebrae (PrCV), number of caudal vertebrae (CV), number of vertebrae (V), body depth at pectoral fin base (BD), and head length (HL).

Species	SL (mm)	D	A	C	$P1_d$	$P1_s$	LL	PrCV	CV	V	BD	HL
T. lipophthalmus	76	56	41	12	0	5	90	–	–	–	40	25
	38	55	40	11	0	5	–	–	–	–	44	23
	33	56	39	12	0	5	–	–	–	–	39	25
	61	54	39	12	0	0	100	9	25	34	43	26
	150	56	43	12	0	0	–	–	–	–	–	–
T. caecus	93	53	42	12	3	6	105	–	–	35	46	23
	82	53	39	12	4	4	85	9	27	36	45	25
	76	52	41	12	2	4	94	8	27	35	47	23
	74	53	39	12	4	5	–	9	26	35	45	24
T. elongatus	33	56	37	12	0	5	96	–	–	33	45	24
	28	53	34	12	2	5	104	–	–	33	43	25

of only 1 ray immersed under the skin (this ray becomes noticeable only after staining) (Figs. 3 and 4).

This fact prompted us to reexamine 3 specimens of *T. elongatus* described in Evseenko and Bolshakov (2018). On each of these specimens, we found a pectoral fin presented as a skin outgrowth that did not exceed the size of scales found in all specimens (Fig. 4A). The rays in the fins of these specimens became clearly visible only after staining with alizarin. In all likelihood, authors who pointed to the absence of the pectoral fin (Károli, 1882; Pellegrin and Chevey, 1940; Tan and Grinang, 2020) did not notice the fin, or it was reduced to a greater degree than in the specimens we examined. Chabanaud (1939) also noted that the number of rays in the pectoral fin varied even in specimens from one sample. He thought that the degree of development of a pectoral fin depends on the age or sex of the fish. We suggest that the presence or absence of a pectoral fin and the number of rays in it are not species-specific features for blind soles but are demonstrations of individual variability.

We studied and compared all available X-rays of blind sole and found no difference between them. It should be noted here that some of the type specimens have been lost: the location is unknown for the holotype and 2 paratypes of *T. caecus* and the holotype of *T. lipophthalmus* (Fricke et al., 2021). On the basis of the X-ray of the paratype of *T. caecus* and non-type *T. lipophthalmus*, we measured the proportions of the body (BD and HL) and meristic characters (D, A, C, and V). We found that they were within the range of proportional measurements and characters of the studied collection of *T. elongatus*.

The body coloration of these 3 blind sole species varies somewhat but is generally similar (Károli, 1882; Hardenberg, 1931a; Pellegrin and Chevey, 1940; Evseenko and Bolshakov, 2018; Tan and Grinang, 2020). Slight variations in fish colors may be due to phenotypic plasticity or fixation—the difference is visible in photographs between the fresh and fixed specimens (Tan and Grinang, 2020). Additionally, characteristics of the substrate, food items, season, and sex can influence color differences. Noticeable variations in coloration have been reported for *B. aspilos* from different localities, and the authors suggest that these differences do not depend on sex but on the substrate (Okamoto and Motomura, 2021).

It turns out that the only thing that can be used as a diagnostic feature is the place of capture. However, it should be taken into account that all 3 locations where the type material were caught are in coastal waters of the South China Sea. The early developmental stages of blind soles are unknown. However, with a few exceptions, most soles have pelagic eggs and larvae (Ahlstrom et al., 1984), which are freely carried by currents and settle on suitable substrates. There is no geographical boundary between the regions where the type specimens were caught (Morimoto et al., 2000; Qu, 2000). Therefore, the 3 nominal species of blind sole may be local populations of the same species.

Conclusions

We analyzed our materials and found that the features thought to be diagnostic do not work for separating the 3 species of *Typhlachirus*. All the described interspecific differences are within the range of variation found in our specimens from the Mekong River. The pectoral fin on the ocular side of fish of the genus *Typhlachirus* is a reduction feature; results of data analysis for the combined

sample indicate that the fin developed to varying degrees and development did not depend on the size of the fish. Therefore, the presence of the pectoral fin and the number of rays in it cannot serve to identify species. On the basis of this result, we come to the same conclusion as Chabanaud (1948): there are no sufficient causes for saving the independence of the 3 nominal *Typhlachirus* species. Chabanaud's revision was based on a small number of specimens, and in this work, non-type specimens from only one of the type localities were examined. Therefore, to confirm our conclusion about the possible monotypy of the genus, it is necessary to study available type specimens and new specimens of *T. lipophthalmus* and *T. caecus* from the regions where the type material was captured (off the island of Borneo Island and in the Strait of Malacca).

Acknowledgments

The study was supported by the state assignment to the Shirshov Institute of Oceanology of the Russian Academy of Sciences (no. 0149-2019-0009) and work was done on the theme "Ecolan E-3.4—Ecosystem of the Mekong River in the context of global climatic changes and anthropogenic impact." The work was held within the state assignment of the Lomonosov Moscow State University (no 121032500084-6).

Literature cited

Abidin, M., and A. Bintoro.
2014. Hubungan panjang berat ikan lidah (*Typhlachirus caecus*) di perairan estuaryi Sungai Indragiri, Riau. Bul. Tek. Litkayasa 12:7–9.

Ahlstrom, E. H., K. Amaoka, D. A. Hensley, H. G. Moser, and B. Y. Sumida.
1984. Pleuronectiformes: development. *In* Ontogeny and systematics of fishes. Based on an international symposium dedicated to the memory of Elbert Halvor Ahlstrom; La Jolla, 15–18 August 1983 (H. G. Moser, W. J. Richards, D. M. Cohen, M. P. Fahay, A. W. Kendall Jr., and S. L. Richardson, eds.), p. 640–670. Am. Soc. Ichthyol. Herpetol., Spec. Publ. 1.

Atack, K.
2006. A field guide to the fishes of Kuching Rivers, Sarawak, Malaysian Borneo, 200 p. Nat. Hist. Publ. (Borneo), Kota Kinabalu, Malaysia.

Chabanaud, P.
1939. Catalogue systématique et chorologique des téléostéens dyssymétriques du globe. Bull. Inst. Oceanogr. Monaco 763:1–31.
1948. Morphologie et systematique des Soliedes affectes d'une atrophie plus ou moins complète de l'oeil migrateur. Zool. Verh. 3:1–58.

Chambers, E. A., and P. D. N. Hebert.
2016. Assessing DNA barcodes for species identification in North American reptiles and amphibians in natural history collections. PLoS ONE 11(4):e0154363.

Chapleau, F.
1989. Etude de la portion supracrânienne de la nageoire dorsale chez les Soleidae (Téléostéens, Pleuronectiformes). Cybium 13:271–279.

Crawford, A. J., C. Cruz, E. Griffith, H. Ross, R. Ibáñez, K. R. Lips, A. C. Driskell, E. Bermingham, and P. Crump.
2013. DNA barcoding applied to *ex situ* tropical amphibian conservation programme reveals cryptic diversity in captive populations. Mol. Ecol. Resour. 13:1005–1018.

Desoutter, M., and F. Chapleau.
1997. Taxonomic status of *Bathysolea profundicola* and *B. polli* (Soleidae; Pleuronectiformes) with notes on the genus. Icthyol. Res. 44:399–412.

Desoutter, M., F. Chapleau, T. A. Munroe, B. Chanet, and M. Beaunier.
2001a. Catalogue critique des types de poissons du muséum national d'histoire naturelle (suite): ordre des Pleuronectiformes. Cybium 25:299–368.

Desoutter, M., T. A. Munroe, and F. Chapleau.
2001b. Nomenclatural status of *Brachirus* Swainson, *Synaptura* Cantor and *Euryglossa* Kaup (Soleidae, Pleuronectiformes). Ichthyol. Res. 48:325–327.

Evseenko, S. A., and D. V. Bolshakov.
2018. On the morphology of Mekong blind sole *Typhlachirus elongatus* (Soleidae) with notes on the taxonomy of the genus *Typhlachirus*. J. Ichthyol. 58:688–693.

Fricke, R., W. N. Eschmeyer, and R. Van der Laan (eds.).
2021. Eschmeyer's Catalog of Fishes: genera, species, references. [Available from website, accessed October 2021.]

Fu, Y.-X., and W-H. Li.
1993. Statistical tests of neutrality of mutations. Genetics 133:693–709.

Hajibabaei, M., G. A. C. Singer, P. D. N. Hebert, and D. A. Hickey.
2007. DNA barcoding: how it complements taxonomy, molecular phylogenetics and population genetics. Trends Genet. 23:167–172.

Hammer, Ø., D. A. T. Harper, and P. D. Ryan.
2001. PAST: Paleontological statistics software package for education and data analysis. Palaeontol. Electron. 4(1):1–9.

Hardenberg, J. D. F.
1931a. Some new or rare fishes of the Indo-Australian Archipelago. Treubia 13:411–419.
1931b. The fishfauna of the Rokan Mouth. Treubia 13:81–168.

Hebert, P. D. N., A. Cywinska, S. L. Ball, and J. R. deWaard.
2003. Biological identifications through DNA barcodes. Proc. R. Soc. Lond., B 270:313–321.

Károli, J.
1882. Prodromus piscium Asiae orientalis a domine Joanne *Xantus annis* 1868–70 collectorum. Termr. Füz. 5:147–187.

Kearse, M., R. Moir, A. Wilson, S. Stones-Havas, M. Cheung, S. Sturrock, S. Buxton, A. Cooper, S. Markowitz, C. Duran, et al.
2012. Geneious Basic: an integrated and extendable desktop software platform for the organization and analysis of sequence data. Bioinformatics 28:1647–1649.

Kottelat, M.
2013. The fishes of the inland waters of Southeast Asia: a catalogue and core bibliography of the fishes known to occur in freshwaters, mangroves and estuaries. Raffles Bull. Zool., Suppl. 27:1–663.

Lapierre, K.-L.
2007. Taxonomic revision of the genera *Achiroides, Brachirus, Dexillus*, and *Paradicula* (Pleuronectiformes: Soleidae). M.S. thesis, 197 p. Univ. Ottawa, Ottawa, Canada. [Available from website.]

Morimoto, A., K. Yoshimoto, and T. Yanagi.
2000. Characteristics of sea surface circulation and eddy field in the South China Sea revealed by satellite altimetric data. J. Oceanogr. 56:331–344.

Munroe, T. A.
2000. Family Soleidae (soles). *In* A checklist of the fishes of the South China Sea (J. E. Randall and K. K. P. Lim, eds.), p. 645–646. Raffles Bull. Zool., Suppl. 8:569–667.

Nei, M.
1987. Molecular evolutionary genetics, 512 p. Columbia Univ. Press, New York.

Okamoto, J., and H. Motomura.
2021. Redescription of *Brachirus aspilos* (Bleeker 1852), a senior synonym of four nominal species, with a note on the distribution of *Dagetichthys marginatus* (Boulenger 1900) (Pleuronectiformes: Soleidae). Zootaxa 4908:354–368.

Palumbi, S. R.
1996. Nucleic acids II: the polymerase chain reaction. *In* Molecular systematics, 2nd ed. (D. M. Hillis, C. Moritz, and B. K. Mable, eds.), p. 205–247. Sinauer and Associates Inc., Sunderland, MA.

Pellegrin, J., and P. Chevey.
1940. Poissons nouveaux ou rares de Cochinchine. Descriptions de deux espèces et deux variétiés. Bull. Soc. Zool. Fr. 65:153–158.

Qu, T.
2000. Upper-layer circulation in the South China Sea. J. Phys. Oceanogr. 30:1450–1460.

R Core Team.
2020. R: a language and environment for statistical computing. R Foundation for Statistical Computing, Vienna, Austria. [Available from website, accessed October 2020.]

Rainboth, W. J.
1996. FAO species identification field guide for fishery purposes. Fishes of the Cambodian Mekong, 265 p. FAO, Rome.

Rozas, J., A. Ferrer-Mata, J. C. Sánchez-DelBarrio, S. Guirao-Rico, P. Librado, S. E. Ramos-Onsins, and A. Sánchez-Gracia.
2017. DnaSP 6: DNA sequence polymorphism analysis of large data sets. Mol. Biol. Evol. 34:3299–3302.

Saitou, N., and M. Nei.
1987. The neighbor-joining method: a new method for reconstructing phylogenetic trees. Mol. Biol. Evol. 4:406–425.

Stephens, H. R.
2011. Taxonomic revision of the flatfish genera *Zebrias* Jordan and Snyder, 1900 and *Pseudaesopia* Chabanaud, 1934 with notes on *Aesopia* Kaup, 1858 (Pleuronectiformes: Soleidae). M.S. thesis, 279 p. Univ. Ottawa, Ottawa, Canada. [Available from website.]

Tajima, F.
1989. Statistical method for testing the neutral mutation hypothesis by DNA polymorphism. Genetics 123:585–595.

Tamura, K., G. Stecher, D. Peterson, A. Filipski, and S. Kumar.
2013. MEGA6: molecular evolutionary genetics analysis version 6.0. Mol. Biol. Evol. 30:2725–2729.

Tan, H. H., and J. Grinang.
2020. *Typhlachirus lipophthalmus*, a rare eye-less sole from Borneo (Teleostei: Soleidae). Ichthyol. Explor. Freshw. 1150:1–8.

Taylor, W. R., and G. C. Van Dyke.
1985. Revised procedures for staining and clearing small fishes and other vertebrates for bone and cartilage study. Cybium 9:107–119.

Villesen, P.
2007. FaBox: an online toolbox for FASTA sequences. Mol. Ecol. Notes 7:965–968.

Ward, R. D.
2009. DNA barcode divergence among species and genera of birds and fishes. Mol. Ecol. Resour. 9:1077–1085.

Ward, R. D., T. S. Zemlak, B. H. Innes, P. R. Last, and P. D. N. Hebert.
2005. DNA barcoding Australia's fish species. Philos. Trans. R. Soc., B 360:1847–1857.

National Marine
Fisheries Service
NOAA

Fishery Bulletin
established in 1881

Spencer F. Baird
First U.S. Commissioner
of Fisheries and founder
of *Fishery Bulletin*

Ecology, life history, and fisheries potential of the flathead lobster (*Thenus orientalis*) in the Arabian Gulf

Lotfi Rabaoui (contact author)[1,2]
Lamia Yacoubi[3]
Yu-Jia Lin[1]
Thadickal V. Joydas[1]
Mohammad A. Qurban[1,2,4]
Panickan Premlal[1]
Jinoy Gopalan[1]
Zahid Nazeer[1]
Manambrakat Vijayakumaran[1]
Syed Ajmal Khan[1]
Rubén H. Roa-Ureta[5]

Email address for contact author: lrabaoui@gmail.com

[1] Center for Environment & Marine Studies
Research Institute
King Fahd University of Petroleum & Minerals
Dhahran, Eastern Province 31261, Saudi Arabia

[2] National Center for Wildlife
Riyadh 12746, Saudi Arabia

[3] University of Carthage
Amilcar, Tunis 1054, Tunisia

[4] Deputy-Ministry for Environment
Ministry of Environment, Water & Agriculture
Riyadh 11195, Saudi Arabia

[5] Centre of Marine Sciences
University of Algarve
8005-139 Faro, Portugal

Abstract—This study, which included examination of the distribution and life history and a stock assessment of the flathead lobster (*Thenus orientalis*), is the first of its kind in the waters of Saudi Arabia in the Arabian Gulf, also known as the Persian Gulf. The flathead lobster is widely distributed in this region, although it is more abundant in the central and northern Arabian Gulf. Carapace lengths at 50% and 95% maturity are 59 and 65 mm for females and 58 and 71 mm for males. The fecundity of 4 berried females ranged from 26,000 to 76,000 eggs per spawning, and the fertilization rate exceeded 97%. Length–frequency data were consistent with just 2 cohorts, indicating that this species has a short life span and high growth coefficient (K=0.846 year^{-1}). Large fishing boats (called *dhows*) accounted for more than 98% of the total landings. Estimates of natural mortality rates from use of generalized depletion models have high statistical precision and a magnitude compatible with short life history. In addition, abundance levels estimated with the depletion model are sufficient to support a sustainable small-scale fishery either as bycatch of shrimp trawlers or as a resource targeted with specialized gear. A targeted fishery for flathead lobster could be set during the off months of the shrimp trawl fishery (February–July), reducing interference with the reproduction cycle.

Manuscript submitted 2 November 2021.
Manuscript accepted 31 March 2022.
Fish. Bull. 120:125–137 (2022).
Online publication date: 20 April 2022.
doi: 10.7755/FB.120.2.3

The views and opinions expressed or implied in this article are those of the author (or authors) and do not necessarily reflect the position of the National Marine Fisheries Service, NOAA.

The flathead lobster (*Thenus orientalis*) is a highly valued commercial lobster species, with increasing importance in the world (Spanier and Lavalli, 2006). It has a wide distribution in the Arabian Gulf, also referred to as the Persian Gulf, including in waters of Saudi Arabia in the northwestern part of the gulf, where it has been traditionally captured as bycatch by local, small-scale fishing operations during the season (August–January) of the trawl fishery for the green tiger prawn (*Penaeus semisulcatus*). Landing this lobster species was forbidden by managers because of a lack of scientific knowledge for determination of sustainable catch rates and development of regulations oriented toward sustainability. This measure, implemented in 2008 and still enforced, was taken as a precautionary action pending studies of the life history and biological reference points of and a stock assessment for this species.

The distribution of species of *Thenus* and other slipper lobsters (Scyllaridae) depends on several environmental factors (Spanier and Lavalli, 1998; Wardiatno et al., 2016), as observed in palinurids (Herrnkind et al., 1997; Butler et al., 2006). The nature of sediments and the depth of water are the 2 major factors that influence the abundance of slipper lobsters (Jones, 2007; Lavalli et al., 2019). The flathead lobster prefers soft, sandy sediment areas with medium-to-coarse particle size. Tropical slipper lobsters, including species of *Thenus*, may live at densities of 1–10 individuals/ha in areas that reflect the habitat preferences of the species (Jones, 2007). There is no evidence of aggregation due to reproductive stimuli in species of *Thenus*, but the presence of other species, such as prey, predators, and competitors, may influence the density of these species in a particular habitat (Jones, 2007).

Species of *Thenus* have greater mobility because of the highly developed swimming ability that sets this

genus apart from other slipper lobsters. They are capable of moving long distances by swimming, and their life history can be described as nomadic and not directed or migratory. Jones (1988) and Courtney et al. (2001) studied the mobility of species of *Thenus* by using tagging. Data from recovery of tagged individuals indicate that individuals of *Thenus* species can move as far as 24 km in 183 d (Courtney et al., 2001). They are more active during late evening and early morning, the foraging time of the lobster (Jones, 2007).

Most of the species of *Thenus* mature in 1 year (at about 45 mm in carapace length for most species) with a fecundity of up to 67,000 eggs (Jones, 1988; Radhakrishnan et al., 2007). Like other tropical species, *Thenus* species breed almost throughout the year, with at least 2 spawning peaks, the timing of which might vary in different regions (Kagwade and Kabli, 1996; Jones, 2007; Radhakrishnan et al., 2007). Flathead lobsters carry eggs in their pleopods (swimming legs) for about 25 d before releasing phyllosoma larvae that have a larval life of 30–45 d involving 4 stages, the last one of which is the nisto stage in which larvae molt for settlement. Water currents and eddies play a role in the distribution and settlement of *Thenus* larvae because they are mostly retained within the area of release as a result of their shorter life in comparison to that of palinurid larvae, which are carried long distances offshore.

Flathead lobsters have been caught in the Saudi waters of the Arabian Gulf since 1980, yet to date little scientific information is available about the biology and population dynamics of this species and the fishery that targets it. In view of this knowledge gap, this study was carried out with the following aims: 1) to determine the spatial distribution and abundance of flathead lobsters, 2) to examine the life history of this species, and 3) to assess the stock of flathead lobsters in the waters of Saudi Arabia in the Arabian Gulf.

Material and methods

Study area

The Arabian Gulf is a semi-enclosed, shallow sea located between the Arabian Peninsula and Iran. It is bounded on the south by Oman and the United Arab Emirates, on the west by Qatar, Bahrain, and Saudi Arabia, on the north by Kuwait and Iraq, and on the east by Iran (Fig. 1). It is about 990 km long with a width of 200–370 km and an average depth of 36 m. The waters of Saudi Arabia in the Arabian Gulf host a great variety of habitats and a rich biodiversity, including nursery habitats (Rabaoui et al., 2017, 2019; Lin et al., 2021a; Rabaoui et al., 2021a), coral reefs (Lin et al., 2021b, 2021c), spawning habitats (Lin et al., 2021a), and rich pelagic habitats enhanced by manmade structures (Rabaoui et al., 2015a) with abundant mammals (Rabaoui et al., 2021b).

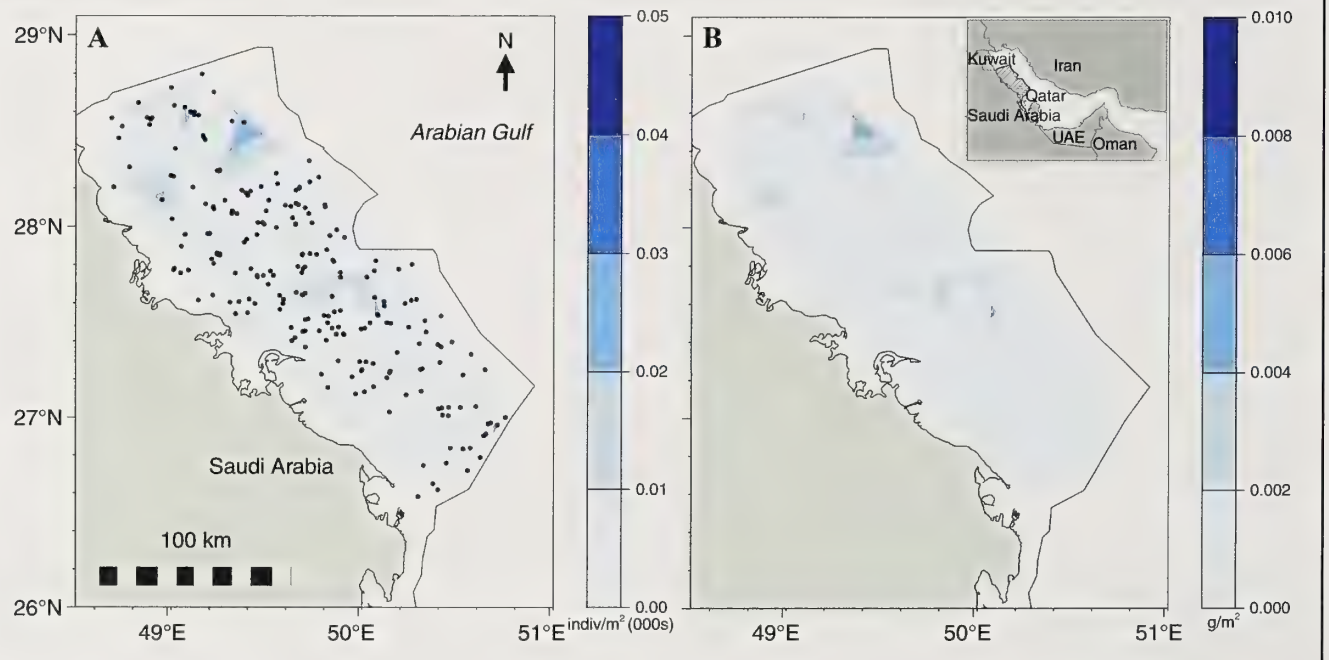

Figure 1

A map showing (**A**) abundance (in thousands of individuals per 100 square meters) and (**B**) biomass (in grams per 100 square meters) of flathead lobsters (*Thenus orientalis*) sampled in the waters of Saudi Arabia in the Arabian Gulf during trawl surveys conducted between 2013 and 2016. Dots indicate stations where surveys were conducted. In the inset, the outlined area in the Arabian Gulf indicates the study area. UAE=United Arab Emirates.

Spatial distribution and abundance

The spatial distribution and abundance of flathead lobsters were determined by using the data collected during 5 trawl surveys conducted in the waters of Saudi Arabia in the Arabian Gulf between 2013 and 2016. Three trawl surveys were conducted on the commercial outrigger *Afrah* (which had a trawl net with a knot-to-knot mesh size of 15 mm) in March and July 2013 and in May–November 2016. Two trawl surveys were completed on the Kuwaiti RV *Bahith II* (which had a trawl net with a knot-to-knot mesh size of 36 mm) in June–July 2014 and in May–June 2015. In total, trawl surveys were conducted at 189 stations (88 stations in 2013, 31 stations in 2014, 40 stations in 2015, and 30 stations in 2016).

A systematic grid design was applied for the trawling surveys. In 2013, equally spaced stations were set along predetermined transects perpendicular to the coast, covering all territorial waters of Saudi Arabia in the Arabian Gulf. In 2014 and 2015, we visited stations set as close as possible to ones we previously surveyed, with a few additions or reductions in station numbers because of constraints, such as poor weather and validity of fishing permits. In 2016, the team surveyed the locations where flathead lobsters occurred often in previous surveys, to increase sample size for biological analysis and habitat characterization. We assumed that there were no differences in size selectivity between the gears used by the 2 vessels employed for the surveys. This assumption is justified because the mesh size of both trawlers is selective for fish under 40 mm in total length, meaning carapace length plus the tail (Lin et al., 2021a), and the smallest total length of all flathead lobsters caught during surveys was 52 mm. Therefore, given this assumption of equal selectivity, we pooled the lobster catch and biological data from the surveys conducted on the 2 vessels to increase the sample size.

Standard operating procedures were applied in all surveys. In other words, the following actions were taken: 1) at each station, we recorded environmental variables, such as temperature, salinity, and depth before trawling; 2) the duration of each trawl was fixed at approximately 30 min; 3) once the catch was on deck, the bottom type (sand, mud, or rock) was determined by examining debris; 4) the entire catch was photographed and weighed; and 5) 5–100% of the catch, including the debris, was randomly sampled for further analysis in the laboratory.

The catch per unit of effort, expressed as kilograms per hour of trawling, was determined for each survey and included only the stations where at least one flathead lobster was encountered. The abundance and biomass of lobsters for the trawled area, expressed as the number of individuals per 100 square meters of trawling and grams per 100 square meters of trawling, were calculated for each survey. The spatial distributions of abundance and biomass of flathead lobsters were plotted for the cruises from 2013 through 2016 by using the packages rworldmap (vers. 1.3-6; South, 2011) and rworldxtra (vers. 1.01; South, 2012) in R, vers. 4.0.2 (R Core Team, 2020). The spatial heatmaps were plotted by using the package akima (vers. 0.6-2.1; Akima and Gebhardt, 2020) in R.

Reproductive biology and growth

A total of 302 flathead lobsters, collected during trawl surveys and from auction centers, were used for detailed morphometric studies. All collected lobsters were transported to the laboratory, where they were measured (for total length) and weighed (for total weight) and their sex was determined. The reproductive biology of the flathead lobster was studied by recording the morphological and morphometric changes that occur at maturity, the gonadosomatic index (GSI), and the maturity stages of gonads. The maturity stages of female gonads were determined following the classification proposed by Kennelly et al. (1997) and Haddy et al. (2005) (see Suppl. Table 1) (online only). Similarly, 5 maturity stages of male gonads were determined by dissecting the lobster as well as by using histology. The color and condition of the fresh gonads were noted, and their wet weight was recorded to the nearest 0.001 g after wiping water from the gonads with blotting paper. Fecundity was examined by counting the eggs in the pleopods of berried females. We estimated fecundity by taking the total weight of eggs carried by the female after stripping it, counting the eggs in a minimum of 3 samples weighing from 0.1 g to 1.0 g, and extrapolating the numbers to get the total count in the whole egg mass. The fertilization rate of eggs was estimated by counting the number of unfertilized eggs in the egg mass. Unfertilized eggs are cream or pink in color, and fertilized eggs are dark yellow or orange (Kizhakudan[1]).

The GSI was calculated for each mature female as the percentage of body weight accounted for by ovary weight. The maturity status of the lobster by carapace length was estimated by using a logistic model:

$$S(L) = \frac{1}{1 + e^{g+hL}}, \quad (1)$$

where $S(L)$ = the proportion of mature individuals at carapace length L in millimeters;
g = the intercept parameter; and
h = the slope parameter.

The model was fit to data of counts of immature and mature individuals at length categories with logistic regression. The carapace lengths at which 50% (L_{50}) and 95% (L_{95}) of individuals were mature were calculated by using the following equations (Roa et al., 1999):

$$L_{50} = \frac{-\hat{g}}{\hat{h}} \text{ and} \quad (2)$$

$$L_{95} = \frac{\ln\left(\frac{1}{19}\right) - \hat{g}}{\hat{h}}. \quad (3)$$

[1] Kizhakudan, J. K. 2016. Hatchery technology and seed production of lobsters. *In* Course manual: winter school on technological advances in mariculture for production enhancement and sustainability (I. Joseph and B. Ignatius, eds.), p. 106–113. Cent. Mar. Fish. Res. Inst., Kochi, India. [Available from website.]

The standard errors of L_{50} and L_{95} were calculated with the delta method by using the package msm (vers. 1.6.9; Jackson, 2011) in R, and a Wald-type confidence interval was also calculated. The differences between sexes in the maturity model parameters were examined by applying information theory. The Akaike information criterion (AIC) was calculated to select the best model:

$$AIC = 2p - 2\ln(Lik), \quad (4)$$

where p = the number of parameters; and
Lik = the maximum likelihood of the model.

Candidate models were fitted with data for the sexes pooled or separated, and then the AIC values for the models were compared. The model with the lowest AIC value was selected as the best working model.

Histological techniques were used to record different phases during the development of gonads. The gonads from fresh specimens were removed, weighed, and fixed in Bouin solution for 2 h and preserved thereafter in absolute ethanol. By using an ATP1 automated tissue processor, TBS[2] (VWR International, Radnor, PA), small portions (anterior, posterior, middle, oviduct, and vas deferens) of these gonads were dehydrated through the use of a series of graded ethanol solutions finalized with a clearing step in xylene. The gonad tissues were thereafter embedded in paraffin wax, sectioned at 5–6 µm with an automated TBS SHUR/Cut 4500 microtome (Cole-Parmer Instrument Co., Vernon Hills, IL), and stained with eosin and hematoxylin (Bancroft and Stevens, 1990) with a TBS SHURStain 3030 automated slide stainer (General Data Co. Inc., Cincinnati, OH). The stained sections were examined under a binocular microscope (Olympus BX51, Olympus Corp., Tokyo, Japan). The sections were photographed by using an Olympus DP72 microscope camera (Olympus Corp.). Identification and description of the different maturity stages in the ovary and testis were done on the basis of the works of Haddy et al. (2005) and Kizhakudan (2014).

Because aging data are not directly available for the flathead lobster, statistical techniques were used to determine the number of cohorts sampled over 4 years that underlie the length–frequency data. The method involves 1) a statistical model for estimating the number of cohorts underlying the length–frequency data on the basis of the multinomial distribution, 2) biological criteria to resolve the aging of the cohorts, and 3) a hierarchical statistical model based on the multivariate normal distribution to fit a growth model to the mean length and the assigned age of each cohort. Details of the mathematical and statistical models and the software used to fit the models to data have been described in Roa-Ureta (2010).

Statistical analysis of the age structure was conducted with aggregated data, without distinction by year or sex, owing to the small sample sizes (n) for all years (2013: n=21; 2014: n=15; 2015: n=31; 2016: n=235; total: n=302).

In selecting a model for estimation of the number of cohorts underlying the length–frequency data, we tested models that included 2, 3, 4, 5, 6, 7, and 8 cohorts. This wide range of hypotheses for the number of cohorts was tested because nothing was known about the age structure of the stock in waters of Saudi Arabia in the Arabian Gulf. A low number of cohorts would indicate a short-lived stock, and a high number of cohorts would point to a long-lived stock. Among the 7 models fit to the length–frequency data, the best model was selected by using the AIC. Age assignment for the resulting number of cohorts was based on previous biological knowledge about the number of spawning events, the duration of life at the larval stage, and size at settlement.

Once the number of cohorts composing the length–frequency data and associated parameters were estimated and once age assignment was completed, we fitted the following 2-parameter version of the von Bertalanffy growth function to the mean length and age data:

$$L(a) = L_\infty \left(1 - \left(\frac{L_0}{L_\infty}\right) e^{-\mathrm{Ka}}\right), \quad (5)$$

where $L(a)$ = carapace length at age a;
L_∞ = asymptotic carapace length;
L_0 = carapace length at birth; and
K = the growth coefficient.

The model is used to estimate only 2 parameters, L_∞ and K, because L_0 is assumed to be known from previous biological information and is equal to 8 mm. Both the multinomial model for length–frequency data and the multivariate normal model for the growth data were fitted by using in AD Studio, vers. 1.0, the AD Model Builder (vers. 12.0; Fournier et al., 2012) code in the supplementary material accompanying Roa-Ureta (2010).

This method has been used in many previous studies and has been useful for studying the growth of other crustaceans, such as the green tiger prawn (Rabaoui et al., 2017) and a blue swimming crab, *Portunus segnis* (Rabaoui et al., 2015b, 2021b).

Old bycatch fishery and stock assessment

The official Saudi government fisheries statistics for landings and fishing effort (MEWA[3]) that were collected for the 2 fleets of small boats (called *tarad*) and large boats (called *dhow*), in Saudi Arabia from 1995 through 2008, include landings of flathead lobster as valuable bycatch of the trawl fishery for the green tiger prawn, the main Saudi fishery in the Arabian Gulf, both by volume and value. The number of boats operating in this fishery is close to 2000 (Roa-Ureta, 2015). Almost half of them are traditional Arabic dhows with lengths ranging from 15 to 20 m, and the other half are smaller tarad boats with lengths of less

[2] Mention of trade names or commercial companies is for identification purposes only and does not imply endorsement by the National Marine Fisheries Service, NOAA.

[3] MEWA (Ministry of Environment, Water & Agriculture). 1995–2008. Official fisheries statistics of Saudi Arabia. [Available from Fish. Dep., Minist. Environ. Water Agric., Riyadh 11195, Saudi Arabia.]

than 10 m (Roa-Ureta, 2015). Dhows may remain at sea for nearly a week, and tarads conduct 1-d operations. Both fleets are motorized. The dhow fleet is more important throughout the landings time series. It accounted for an average of 93% of the monthly catch of flathead lobster along the entire time series.

We carried out a stock assessment of the flathead lobster with the method described in Roa-Ureta (2015), developed to assess data-poor fisheries. We fitted 2-fleet multiyear generalized depletion models to 14 years of monthly landings and fishing effort spanning the 168-month period from January 1995 through December 2008. Subsequent landings data were not available because landings of the flathead lobster were banned. The particular version of the model that was used is as follows:

$$C_t = \sum_l C_{t,l} = \sum_l k_l E_{t,l}^{\alpha_l} \left(N_0 e^{-Mt} - e^{\frac{-M}{2}} \left[\sum_{i=1}^{i=t-1} C_{i,l} e^{-M(t-i-1)} \right] + \sum_{j=1}^{j=P} R_{j,l} e^{-M(t-\tau_{j,l})} \right)^{\beta_l} e^{\frac{-M}{2}}, \quad (6)$$

where C_t = the true catch in numbers in month t;
l = a value of 1 or 2, and indexes the fleet;
E = the observed effort in boat-days of fishing;
N_0 = the initial abundance;
M = the natural mortality rate;
k = the scaling;
α = the effort response;
β = the abundance response;
i = the index of the time step (i=1–168);
R_j = the annual recruitment with index j (j=1,...,14 for a total of 14 annual recruitments); and
τ_j = the timing of annual recruitment with index j (in seasonal fisheries, the timing is always the first month of the season).

In these models, parameter k is similar to catchability except that it is not affected by changes because of its relationship with abundance, and the effort response α and abundance response β accommodate nonlinear dynamics, namely the potential of effort to be saturated (α<1), effort synergy (α>1), hyper-stability (β<1), and hyper-depletion (β>1).

We tried model fits with 4 alternative likelihood functions by using the data from each fleet (4 functions for each fleet data set) and 2 numerical methods to minimize the negative log-likelihood, leading to 32 model versions (4×4×2). The likelihood functions were exact normal, exact lognormal, and adjusted profile (i.e., with the dispersion parameter eliminated) approximations of the normal and lognormal. Precise formulas of these likelihoods are detailed in table 2 in Roa-Ureta (2019). Numerical procedures were the spectral projected gradient and the conjugate gradient methods. These numerical techniques have worked well with generalized depletion models because they can handle moderately large optimization problems. With 14 years of data, the 2-fleet multiyear generalized depletion models include 36 (adjusted profile approximations) or 38 (exact likelihoods) free parameters that can be estimated. The models were fit by using the package CatDyn (vers. 1.1-1; Roa-Ureta, 2019) in R.

Results

Spatial distribution of abundance and biomass

The percentage of stations where flathead lobsters were caught varied between 16% and 25% of the total number of stations sampled, during 2013–2015. The frequency of occurrence increased to 60% during the 2016 trawl survey, mainly because of the increase in the fishing effort over the areas where flathead lobsters were caught during the previous surveys. The catch per unit of effort at the stations where flathead lobsters were caught ranged from 0.434 kg/h in 2013 to 0.593 kg/h in 2014. The overall catch per unit of effort of all stations was the lowest (0.067 kg/h) in 2013 and the highest (0.339 kg/h) in 2016 (Table 1).

Results from the trawl surveys conducted from 2013 through 2016 indicate that the flathead lobsters were patchily distributed in the Arabian Gulf, from the northern border between Saudi Arabia and Kuwait to the southern border with Bahrain. The abundance and biomass of the lobsters were both higher in the central and northern parts of the western Arabian Gulf (Fig. 1). The abundance at the stations where flathead lobsters were caught ranged from 0.5×10^{-3} to 4.8×10^{-3} individuals/100 m^2 (Fig. 1A), and the biomass ranged from 0.001 to 0.800 g/100 m^2 (Fig. 1B).

Reproductive biology

The sex ratio of flathead lobsters captured in waters of Saudi Arabia was 1:1, with mature lobsters being dominant in the samples collected during November 2016. Few berried and many spent flathead lobsters were also present in the samples. Few immature flathead lobsters were collected, and most of them were above 40 mm in carapace length and were in the preadult or adult stage. Maturity data support a sex-separate maturity model for the flathead lobster with a high AIC difference of 6.01. Therefore, the maturity curve was fitted to data for females and males separately (Fig. 2). The carapace lengths at 50% and 95% maturity were 59.5 mm (standard error [SE] 0.6) and 64.6 mm (SE 1.5) for females and 57.8 mm (SE 1.1) and 71.0 mm (SE 3.0) for males. Supplementary Figures 1 and 2 (online only) show the maturity stages of female flathead lobsters, as well as the variations in their percentages. Four berried flathead lobsters (Suppl. Fig. 3) (online only) were collected during the study period, and the eggs they carried were in the advanced developmental stage (Suppl. Fig. 4) (online only). The weight of an egg mass varied from 18.74 to 60.62 g, and the weight of a single egg ranged from 796 to 849 mg. The fecundity of the 4 berried lobsters ranged from 26,000 to

Table 1

Catch per unit of effort (CPUE), mean abundance, carapace length, and weight of flathead lobsters (*Thenus orientalis*) collected during trawl surveys conducted between 2013 and 2016 in waters of Saudi Arabia in the Arabian Gulf. A range of carapace lengths is not given for 2015 because only 1 individual was measured. Standard deviations (SDs) are given in parentheses.

Year	2013	2014	2015	2016
Total no. of stations	88	31	40	30
No. of stations with lobsters	14	8	11	18
Mean lobster abundance (individuals/station)	0.278 (0.687)	0.454 (0.904)	0.026 (0.460)	0.590 (0.946)
CPUE (kg/h) of stations with lobsters	0.434	0.593	0.426	0.567
CPUE (kg/h) of all stations	0.067	0.153	0.117	0.339
Mean carapace length (mm)	90 (22)	78 (19)	95	64 (9)
Carapace length (mm) range	27–134	50–107	–	22–86
Mean total weight (g)	149 (78)	105 (74)	206 (33)	101 (180)
Total weight (g) range	3–329	24–250	46–243	97–318

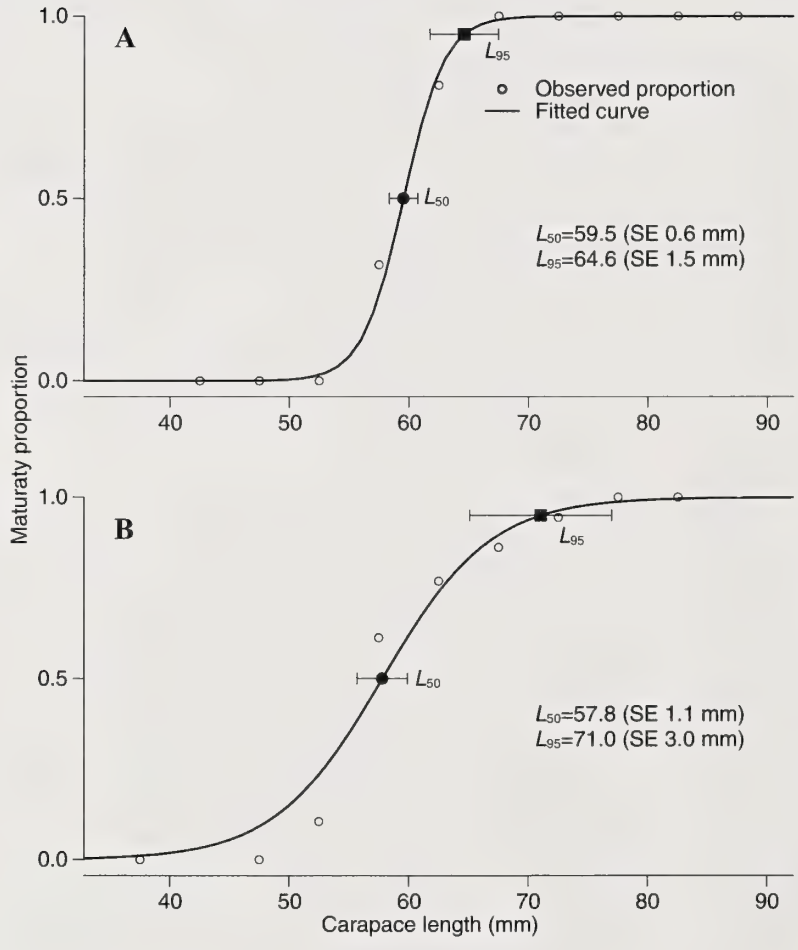

Figure 2

Maturity curves for (**A**) female and (**B**) male flathead lobsters (*Thenus orientalis*) collected between 2013 and 2016 in waters of Saudi Arabia in the Arabian Gulf. Open circles along the fitted curve indicate observed proportions. The black circle and square indicate the carapace lengths at 50% maturity (L_{50}) and 95% maturity (L_{95}), respectively. Error bars indicate the standard errors of these lengths.

76,000 eggs (Suppl. Table 2) (online only). The fertilization rate was very high, above 97% in all the lobsters.

Age and growth

Out of the 7 hypotheses tested, only 3 had successful numerical convergence under the multinomial likelihood model for the data. Those models are the ones with 2, 3, and 5 age cohorts. Of these 3 models, the best model is clearly the model with 2 cohorts, according to AIC values: −2182.1 for the 2-cohort model, −2174.4 for the 3-cohort model, and −2157.5 for the 5-cohort model. The model with the best fit to the length–frequency data is shown in Figure 3. The presence of only 2 cohorts indicates that this species has a very short lifespan and rapid growth. Estimated parameters of the best-fit normal mixture distribution model are shown in Supplementary Table 3 (online only). As can be seen in Figure 3, very few individuals belonging to the youngest cohort were observed. Nevertheless, all the parameters of the model could be estimated with satisfactory statistical precision, as evident from the low SEs. We were able to use the marginal likelihood model to estimate the parameters of the von Bertalanffy growth function in spite of the low number of cohorts estimated for the model underlying the length–frequency data (Suppl. Table 4) (online only). The growth was very rapid (with a high K of 0.846 year^{-1}). Given these results, life history theory predicts that M must be very high (Table 2).

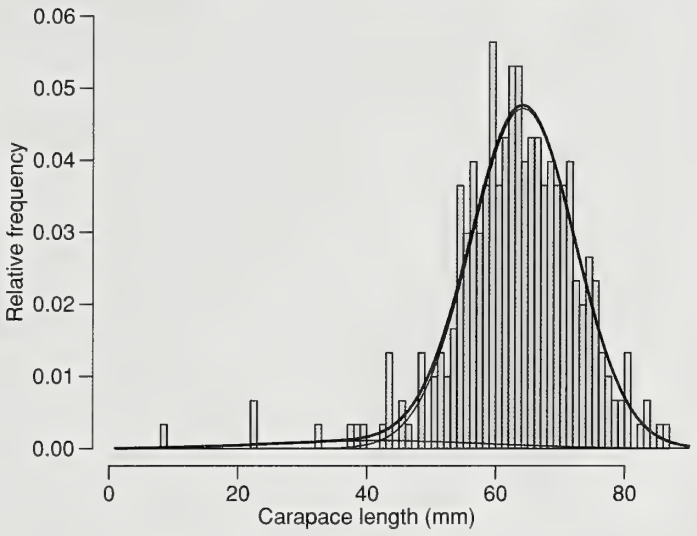

Figure 3

Aggregated length–frequency data (bars) and the fit of the model with 2 age cohorts (lines) for flathead lobsters (*Thenus orientalis*) collected from 2013 through 2016 in the waters of Saudi Arabia in the Arabian Gulf.

Lobster fishery and stock assessment

The landed catch has been increasing substantially since 2000, amounting to 43 metric tons (t) in 2008, the last year before the ban (Fig. 4A). Considering the mean weight of flathead lobsters in our sampling during 2016, that catch translates to over 200,000 individual lobsters. Dhow fleets had a dominant role in contributing to the landings, from 50% in 1995 and >98% in 2008 (Fig. 4A). The rise in landings is totally attributable to the dhow fleet, with approximately 15,000 trips per year (Fig. 4B) or 70,000 days per year (Fig. 4C) after 2003. The catch rate in kilograms per day of fishing was similar in both fleets, 0.436 kg/d for the dhow fleet and 0.300 kg/d for the tarad fleet (Fig. 4D), or around 2 flathead lobsters per day.

The best fit of the generalized depletion model to the data and the predicted biomass per month are shown in Supplementary Figure 5 (online only) (also see Supplementary Material) (online only). Estimates from the model closely follow the observed catch of both fleets (Figs. 5 and 6), although there are signs of deviation from distributional assumptions in the residual cloud for the dhow fleet, and this deviation tends to widen toward the end of the time series. Predicted biomass on the other hand indicates wide fluctuations driven by recruitment (Fig. 7) and intense M (Table 3), but the prediction is fairly imprecise, with wide statistical margins. Parameter estimates and their precision are presented in Table 3. Natural mortality is very high, at an annualized rate of 1.8 year^{-1}, and abundance inputs (N_0 and recruitment) vary widely from nearly 1 to 100 million individuals. Estimates of M, N_0, and all recruitment pulses higher than 50 million individuals have fairly good precision (coefficient of variation <50%). The operations of the dhow fleet, which accounts for over 97% of the landings in the latest years, are proportional with respect to effort and are hyperstable with respect to abundance.

Discussion

With the results of this study, we have provided for the first time the necessary scientific information for managing a sustainable fishery for flathead lobsters in waters of Saudi Arabia in the Arabian Gulf. We determined the spatial

Table 2

Published estimates of parameters of the von Bertalanffy growth function, growth coefficient (K) and asymptotic length (L_∞), and estimates of natural mortality (M) for species of *Thenus* in different regions around the world. Also provided are mean values from this study for comparison, with standard errors given in parentheses. The estimates for this study in the Arabian Gulf are based on data pooled for both sexes. Values of L_∞ for male and female *T. unimaculatus* are not provided in the consulted reference. CL=carapace length.

		K (year^{-1})		M (d^{-1})		L_∞ (mm CL)		
Species	Country	Males	Females	Males	Females	Males	Females	Source
T. australiensis	Australia	0.511	0.584	0.0022	0.0023	77.45	89.04	Courtney[4]
T. parindicus	Australia	0.949	0.834	0.0035	0.0034	61.23	72.44	Courtney[4]
T. unimaculatus	India	1.387	1.059	0.0017	0.0019	–	–	Radhakrishnan et al. (2013)
T. orientalis	Kuwait	1.789	1.679	0.0068	0.0071	71.6 (max: 74)	81.7 (max: 85)	Hussain (1996)
T. orientalis	Saudi Arabia	0.840 (1.497)		0.0048 (0.0012)		106.52 (11.06)		This study

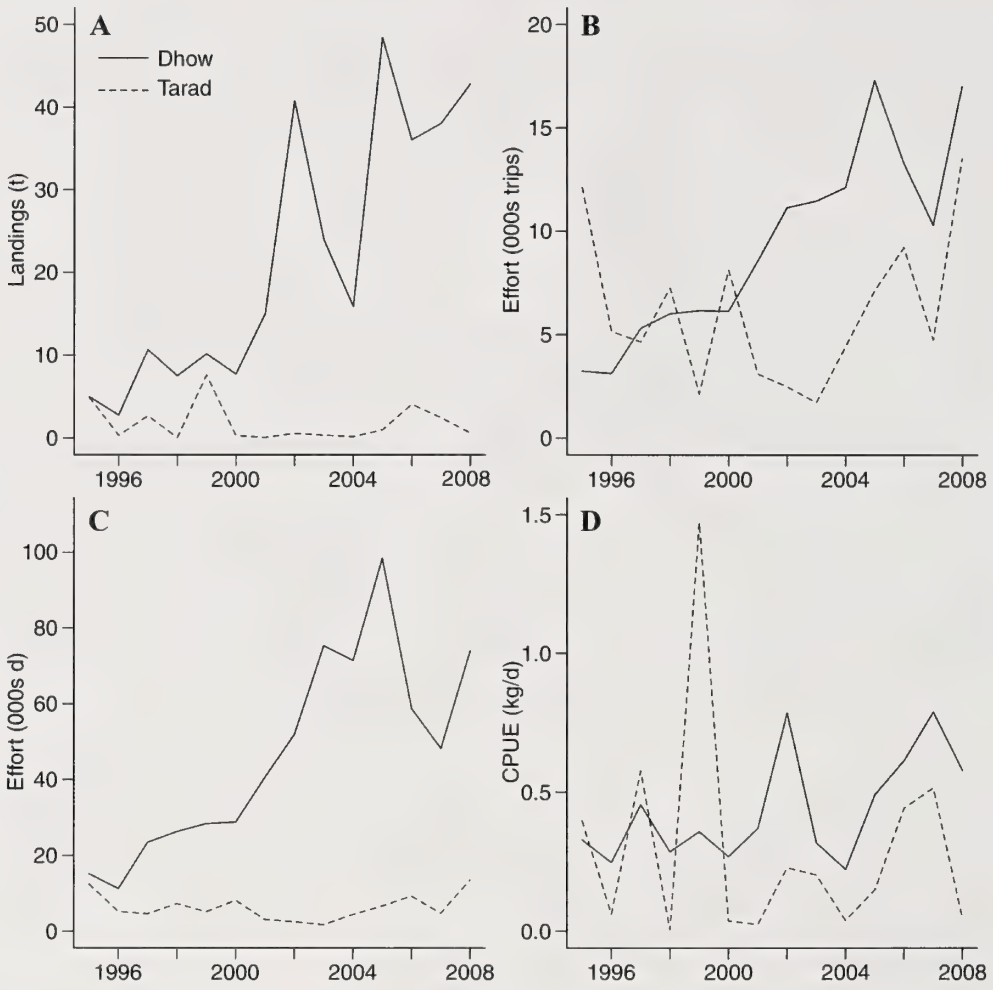

Figure 4

(**A**) Landings in metric tons (t), (**B**) fishing effort measured as the number of trips, (**C**) fishing effort measured as the number of days at sea, and (**D**) catch per unit of effort (CPUE) in kilograms per day from 1995 through 2008 for the fishery that targets flathead lobsters (*Thenus orientalis*) in the waters of Saudi Arabia in the Arabian Gulf. The fishery includes large boats called *dhow* (solid lines) and small boats called *tarad* (dashed lines).

distribution of the stock and the sexual maturity and somatic growth of the samples, and we conducted a stock assessment with a validated method that has been used for other lobster stocks (Meissa et al., 2021). The stock is distributed over the whole region at low densities, on average one order of magnitude less than those observed for *T. parindicus* and *T. australiensis* in Australia (Jones, 1988). Females and males have slightly different maturity schedules, with both sexes of flathead lobster reaching 50% maturity at about 60 mm carapace length. The growth of this species is fast, and its population structure is composed of just 2 cohorts. Recruitment dominates abundance, and the life history of this species is characterized by a short life, rapid maturation and growth, and high M.

Our findings regarding sexual maturity and somatic growth in general are fairly consistent with results from studies of other *Thenus* lobsters in regions of the Indian Ocean. Female flathead lobsters in the Arabian Gulf attain sexual maturity at a slightly higher size than the sizes reported for *T. parindicus* and *T. australiensis* (Jones, 2007). The major pulse of spawning occurred in November–December with a minor peak in May–June. Other *Thenus* species across various regions also have 2 spawning peaks (Jones, 1988; Courtney; Jones, 2007; Radhakrishnan et al., 2013). The maximum fecundity of flathead lobsters in this study (76,144 eggs) was higher than the maximum fecundity that has been reported for *T. parindicus*, *T. australiensis*, and *T. unimaculatus* (Jones, 1988; Radhakrishnan et al., 2013).

The growth rate of flathead lobsters was quite similar to the rates reported for other *Thenus* species from other regions (Table 2). The von Bertalanffy growth coefficient,

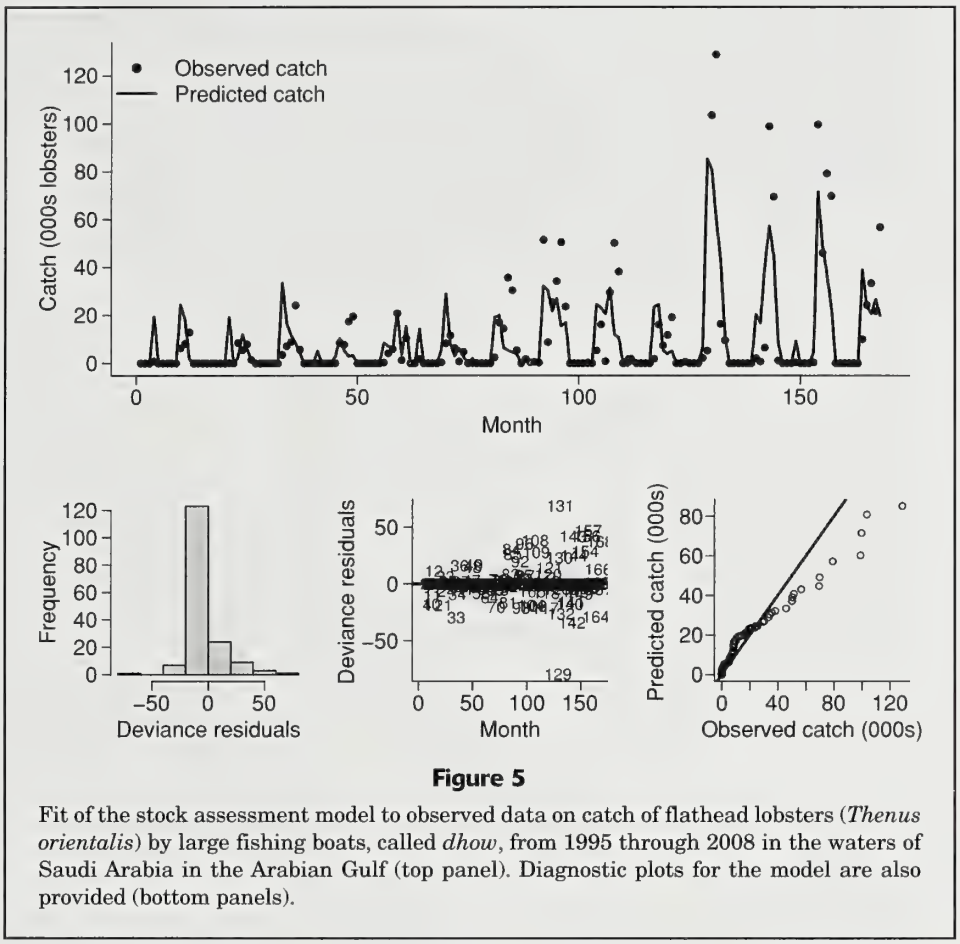

Figure 5

Fit of the stock assessment model to observed data on catch of flathead lobsters (*Thenus orientalis*) by large fishing boats, called *dhow*, from 1995 through 2008 in the waters of Saudi Arabia in the Arabian Gulf (top panel). Diagnostic plots for the model are also provided (bottom panels).

K, and M for *T. parindicus* in Australia (Courtney[4]) are fairly close to those estimated in our study, and L_∞ was lower. The K obtained in this study matches that of *T. unimaculatus* from India (Radhakrishnan et al., 2013), and M reported for the latter was lower than that of this study. On the other hand, Hussain (1996) reported higher K and M but lower L_∞ for flathead lobsters in Kuwait. Growth modeling was based on just 2 observed cohorts, with the juvenile cohort barely represented in the length–frequency data. The hierarchical method of inference accounted for the different contributions of the 2 cohorts; nevertheless, the scant information available for the juvenile cohort resulted in an imprecise estimate of K, with an SE almost double the value of the estimate (see Table 2).

There are striking similarities between the life history of flathead lobsters and that of the green tiger prawn in waters of Saudi Arabia in the Arabian Gulf. The green tiger prawn also is a short-lived, fast-growing crustacean (Rabaoui et al., 2017). One of the reasons for the fast growth of these 2 species could be the effect of temperature. Growth rates generally increase with temperature, but mortality also increases at the highest viable temperatures (Hartnoll, 1982). Located in an arid climatic zone, the western Arabian Gulf has high sea-surface temperatures of 36–40°C during summer months, with an annual sea-surface temperature of 24°C (Sheppard et al., 1992; Al-Abdulkader et al., 2019). There is a southward increase in temperature due to the greater stagnancy toward the south. Preen (2004) observed average monthly sea-surface temperatures <19°C for 4 months in Kuwait Bay, but for only 2 months 300 km farther south in Ras Tanura, Saudi Arabia, and for only 1 month at the southernmost station of Aziziah. This variation in temperature can be linked with the higher occurrence of flathead lobsters in the northern and central parts of the Saudi waters of the Arabian Gulf, indicating avoidance of high temperatures by flathead lobsters. In the Mediterranean Sea, wild slipper lobsters have been reported to migrate offshore to avoid the extreme temperatures found in shallow waters (Spanier et al., 1988; Spanier and Lavalli, 1998).

Although the availability of fisheries data ends in 2008, the fact that there has been no directed fishery for the flathead lobster since the ban supports the view that the results of our analysis presented here are relevant for the current management of flathead lobster. The most remarkable finding pertinent to the potential

[4] Courtney, A. J. 2002. The status of Queensland's Moreton Bay bug (*Thenus* spp.) and Balmain bug (*Ibacus* spp.) stocks. Queensland Dep. Prim. Ind., Inf. Ser. QI02100, 18 p. [Available from website.]

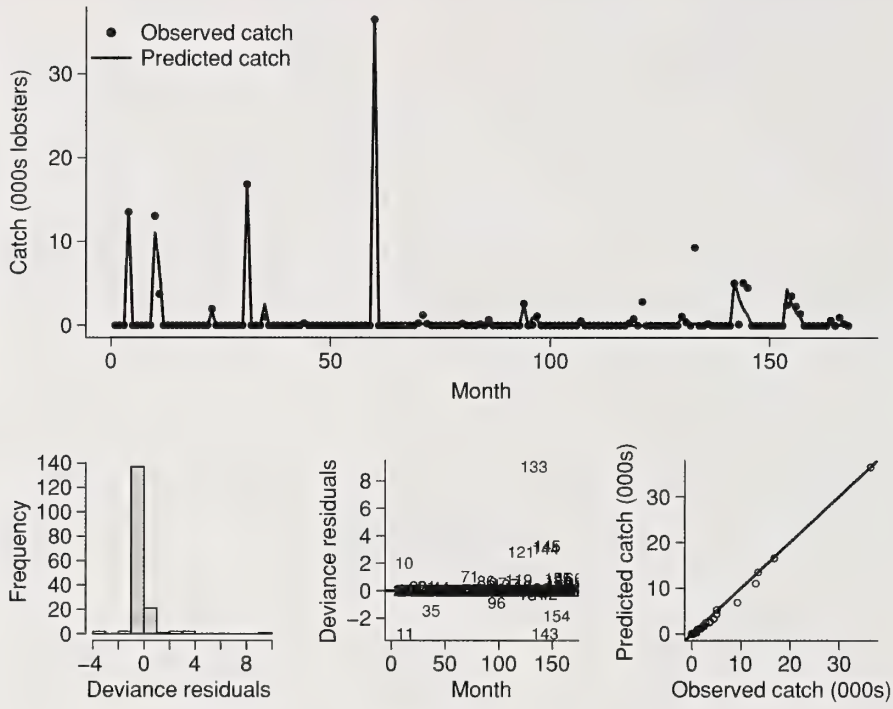

Figure 6

Fit of the stock assessment model to observed data on catch of flathead lobsters (*Thenus orientalis*) by small fishing boats, called *tarad*, from 1995 through 2008 in the waters of Saudi Arabia in the Arabian Gulf (top panel). Diagnostic plots for the model are also provided (bottom panels).

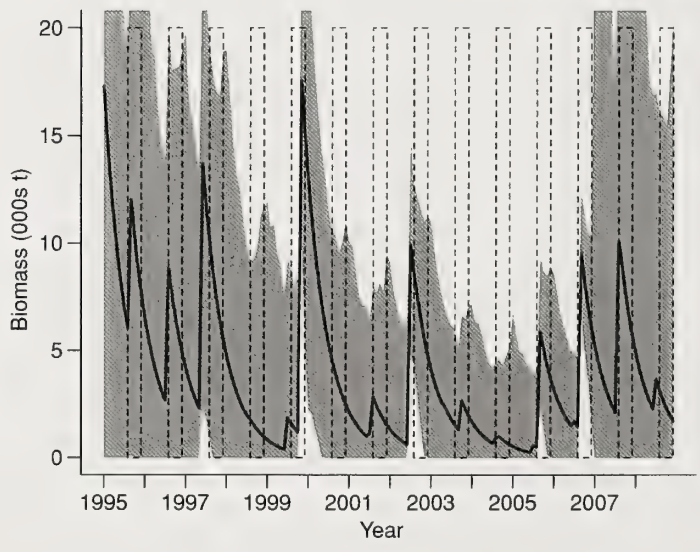

Figure 7

Predicted biomass (solid line) of flathead lobster (*Thenus orientalis*) caught in the waters of Saudi Arabia in the Arabian Gulf during 1995–2008. The gray polygon indicates the 0.5 standard error. The rectangles formed with dashed lines indicate the fishing season for the flathead lobster.

for development of a new fishery is the very wide fluctuations in abundance, driven by fluctuations of 2 orders of magnitude in recruitment and by intense M. In 8 months of the time series, stock biomass was below 500 t or 2.7 million flathead lobsters, and in the months of higher abundance the stock could have over 10,000 t or 55 million flathead lobsters. Because of the wide fluctuations in stock size, it would be necessary to adopt a precautionary stance regarding the potential to resume landings either as allowed bycatch of shrimp trawlers or as a targeted stock in a specialized small-scale fishery. Nevertheless, it should also be noted that the highest landings recorded as bycatch of the shrimp trawlers (~50 t in 2005) amount to just 10% of the minimum monthly biomass. Therefore, it should be safe to resume allowed landings of flathead lobsters as a commercially valuable bycatch of shrimp trawling, but the development of a targeted small-scale fishery would require careful fine-tuning of gear efficiency, magnitude of effort, and seasonal closures, considering that the very low biomass of the stock may drop during natural fluctuations.

Table 3

Parameter estimates from the selected best stock assessment model for flathead lobsters (*Thenus orientalis*) fished as bycatch from the trawl fishery for the green tiger prawn (*Penaeus semisulcatus*) in waters of Saudi Arabia in the Arabian Gulf from 1995 through 2008. The estimated parameters include natural mortality (M), initial abundance (N_0), recruitment for each year (in millions of individuals), scaling (k), effort response (α), abundance response (β), and dispersion. Data are from 2 fleets in the shrimp fishery: small boats (called *tarad*) and large boats (called *dhow*). CV=coefficient of variation.

	Dhow boats			Tarad boats		
Parameter	Timing (month)	Estimate	CV (%)	Timing (month)	Estimate	CV (%)
M (month^{-1})	–	0.1500	25.6	–	0.1500	25.6
N_0 (millions)	–	109.1	14.5	–	109.1	14.5
Recruitment 1995 (millions)	Oct	2.13		Oct	40.86	–
Recruitment 1996 (millions)	Sep	41.08	34.5	Nov	0.55	–
Recruitment 1997 (millions)	Sep	0.09	641.6	Jul	73.72	14.3
Recruitment 1998 (millions)	Sep	0.41	–	Jul	0.38	–
Recruitment 1999 (millions)	Aug	9.60	178.0	Dec	104.23	13.2
Recruitment 2000 (millions)	Sep	0.05	2050.4	Sep	0.05	1986.4
Recruitment 2001 (millions)	Sep	11.69	235.1	Aug	1.60	1810.1
Recruitment 2002 (millions)	Aug	59.10	23.8	Sep	1.12	460.5
Recruitment 2003 (millions)	Jun	0.95	277.6	Oct	9.62	106.6
Recruitment 2004 (millions)	Sep	2.07	137.8	Oct	1.23	164.4
Recruitment 2005 (millions)	Jul	2.24	334.5	Oct	34.30	98.2
Recruitment 2006 (millions)	Jul	2.56	182.0	Oct	52.26	21.6
Recruitment 2007 (millions)	Aug	52.14	–	Oct	1.65	–
Recruitment 2008 (millions)	Jul	8.65	210.6	Jul	1.87	799.7
k (1/number of days)	–	3.3969×10^{-8}	473.9	–	3.3420×10^{-8}	41.6
α	–	1.2433	39.2	–	0.0028	511.6
β	–	0.7138	30.4	–	3.1669	2.3
Dispersion	–	2.1160×10^{-4}	14.1	–	8.6299×10^{-7}	13.7

No targeted fishery for the flathead lobster exists anywhere in the world, and flathead lobsters form only a small percentage of the bycatch in the shrimp trawl fishery in waters of Saudi Arabia in the Arabian Gulf. Fishermen in the area have observed that flathead lobsters can be attracted to bright lights when swimming close to the surface and then caught with scoop nets. This type of fishing is done under bright illumination around oil platforms, or any other structure built in the sea that may act as a fish aggregating device. This method of fishing, which can be highly selective and non-destructive, must be scientifically studied to determine its efficiency and whether it targets a specific fraction of the population, particularly in connection with berried females. The results of our study indicate that a small-scale targeted fishery could complement landings by shrimp trawlers with a production level similar to the bycatch of flathead lobsters in the shrimp trawl fishery. This rate of exploitation would still take only 20% of the minimum biomass observed in some months during the fluctuation cycle observed in our stock assessment modeling. In addition, considering the main spawning period of November–December, a targeted fishery could be set during the off months of the shrimp trawl fishery (February–July), reducing interference with the reproduction cycle.

Conclusions

The results of this study indicate that the flathead lobster caught as bycatch in the shrimp trawl fishery in waters of Saudi Arabia in the Arabian Gulf could be the basis of a sustainable fishery connected to shrimp trawling. The percentage of juveniles in bycatch of trawl surveys was negligible, and a majority of the samples in the catch were above the size at which 50% of females attain sexual maturity. Preventing the catch of berried flathead lobsters, especially during peak spawning in November–December, would further secure sustainability. Furthermore, a targeted small-scale fishery that would operate in the off months of the shrimp trawl fishery could be developed as long as its output is similar to that of the bycatch of shrimp trawling.

Acknowledgments

The authors are grateful to the 2 anonymous reviewers who helped to improve the quality of this manuscript through their constructive comments and suggestions. We also thank all those who helped to conduct surveys in the field and process samples in the laboratory.

Literature cited

Akima, H., and A. Gebhardt.
2020. akima: interpolation of irregularly and regularly spaced data. R package, vers. 0.6-2.1. [Available from website, accessed September 2021.]

Al-Abdulkader, K. A., R. A. Loughland, and M. A. Qurban.
2019. Ecosystems and biodiversity of the Arabian Gulf. Saudi Arabian waters: fifty years of scientific research, 624 p. Saudi Aramco and King Fahd Univ. Pet. Miner., Dhahran, Saudi Arabia.

Bancroft, J. D., and A. Stevens (eds.).
1990. Theory and practice of histology techniques, 740 p. Churchill Livingstone, Edinburgh, UK.

Butler, M. J., R. S. Steneck, and W. F. Herrnkind.
2006. Juvenile and adult ecology. *In* Lobsters: biology, management, aquaculture and fisheries (B. F. Phillips, ed.), p. 263–309. Blackwell Publ., Oxford, UK.

Courtney, A. J., M. G. Cosgrove, and D. J. Die.
2001. Population dynamics of Scyllarid lobsters of the genus *Thenus* spp. on the Queensland (Australia) east coast: I. Assessing the effects of tagging. Fish. Res. 53:251–261.

Fournier, D. A., H. J. Skaug, J. Ancheta, J. Ianelli, A. Magnusson, M. N. Maunder, A. Nielsen, and J. Sibert.
2012. AD Model Builder: using automatic differentiation for statistical inference of highly parameterized complex nonlinear models. Optim. Methods Softw. 27:233–249.

Haddy, J. A., A. J. Courtney, and D. P. Roy.
2005. Aspects of the reproductive biology and growth of Balmain bugs (*Ibacus* spp.) (Scyllaridae). J. Crustac. Biol. 25:263–273.

Hartnoll, R. G.
1982. Growth. *In* The biology of crustacean: embryology, morphology, and genetics, vol. 2 (D. E. Bliss and L. G. Abele, eds.), p. 111–196. Acad. Press, New York.

Herrnkind, W. F., M. J. Butler IV, J. H. Hunt, and M. Childress.
1997. Role of physical refugia: implications from a mass sponge die-off in a lobster nursery in Florida. Mar. Freshw. Res. 48:759–770.

Hussain, M. A. M.
1996. Status of the lobster (*Thenus orientalis*) stock in Kuwaiti Waters. *In* Proceedings of the meetings of the working group on shrimp and other invertebrates and working group on demersal fishes and marine habitat; Kuwait, 11–13 May (Y. Ye and S. Almatar, eds.), p. 99–110. Kuwait Inst. Sci. Res. and Kuwait Found. Adv. Sci., Kuwait.

Jackson, C. H.
2011. Multi-state models for panel data: the msm package for R. J. Stat. Softw. 38(8):1–28.

Jones, C. M.
1988. The biology and behaviour of bay lobsters, *Thenus* spp. (Decapoda: Scyllaridae) in Northern Queensland, Australia. Ph.D. diss., 190 p. Univ. Queensland, Brisbane, Australia. [Available from website.]
2007. Biology and fishery of the bay lobster, *Thenus* spp. *In* The biology and fisheries of the slipper lobster (K. L. Lavalli and E. Spanier, eds.), p 326–358. CRC Press, Boca Raton, FL.

Kagwade, P. V., and L. M. Kabli.
1996. Reproductive biology of the sand lobster *Thenus orientalis* (Lund) from Bombay waters. Indian J. Fish. 43:13–26.

Kennelly, S. J., J. Stewart, and O. Hoegh-Guldberg.
1997. Size at sexual maturity and the reproductive biology of two species of scyllarid lobster from New South Wales and Victoria, Australia. Crustaceana 70:344–367.

Kizhakudan, J. K.
2014. Reproductive biology of the female shovel-nosed lobster *Thenus unimaculatus* (Burton and Davie, 2007) from northwest coast of India. Indian J. Geo-Mar. Sci. 43:927–935.

Lavalli, K. L., E. Spanier, and J. S. Goldstein.
2019. Scyllarid lobster biology and ecology. *In* Crustacea (G. Diarte-Plata and R. Escamilla-Montes, eds.), p. 1–26. IntechOpen, London.

Lin, Y.-J., R. H. Roa-Ureta, A. R. K. Pulikkoden, P. Premlal, Z. Nazeer, M. A. Qurban, and L. Rabaoui.
2021a. Essential fish habitats of demersal fish in the western Arabian Gulf. Mar. Pollut. Bull. 173:113013.

Lin, Y.-J., L. Rabaoui, A. U. Basali, M. Lopez, R. Lindo, P. K. Krishnakumar, M. A. Qurban, P. K. Prihartato, D. L. Cortes, A. Qasem, et al.
2021b. Long-term ecological changes in fishes and macroinvertebrates in the world's warmest coral reefs. Sci. Total Environ. 750:142254.

Lin, Y.-J., R. H. Roa-Ureta, A. U. Basali, J. F. A. Alcaria, R. Lindo, M. A. Qurban, P. K. Prihartato, A. Qasem, and L. Rabaoui.
2021c. Coarser taxonomic resolutions are informative in revealing the fish community abundance trends for the world's warmest coral reefs. Coral Reefs 40:1741–1756.

Meissa, B., M. Dia, B. C. Baye., M. Bouzouma, E. Beibou, and R. H. Roa-Ureta.
2021. A comparison of three data-poor stock assessment methods for the pink spiny lobster fishery in Mauritania. Front. Mar. Sci. 8:714250.

Preen, A.
2004. Distribution, abundance and conservation status of dugongs and dolphins in the southern and western Arabian Gulf. Biol. Conserv. 118:205–218.

R Core Team.
2020. R: a language and environment for statistical computing. R Foundation for Statistical Computing, Vienna, Austria. [Available from website, accessed July 2020.]

Rabaoui, L., Y.-J. Lin, M. A. Qurban, R. H. Maneja, J. Franco, T. V. Joydas, P. Panickan, K. Al-Abdulkader, and R. H. Roa-Ureta.
2015a. Patchwork of oil and gas facilities in Saudi waters of the Arabian Gulf has the potential to enhance local fisheries production. ICES J. Mar. Sci. 72:2398–2408.

Rabaoui, L., M. Arculeo, L. Mansour, and S. Tlig-Zouari.
2015b. Occurrence of the lessepsian species *Portunus segnis* (Crustacea: Decapoda) in the Gulf of Gabes (Tunisia): first record and new information on its biology and ecology. Cah. Biol. Mar. 56:169–175.

Rabaoui, L., Y.-J. Lin, R. H. Maneja, M. A. Qurban, P. Abdurahiman, P. Premlal, K. Al-Abdulkader, and R. H. Roa-Ureta.
2017. Nursery habitats and life history traits of the green tiger shrimp *Penaeus semisulcatus* (De Haan, 1844) in the Saudi waters of the Arabian Gulf. Fish. Res. 195:1–11.

Rabaoui, L., L. Yacoubi, D. Sanna, M. Casu, F. Scarpa, Y.-J. Lin, K.-N. Shen, T. R. Clardy, M. Arculeo, and M. A. Qurban.
2019. DNA barcoding of marine fishes from Saudi Arabian waters of the Gulf. J. Fish Biol. 95:1286–1297.

Rabaoui, L., L. Yacoubi, Y.-J. Lin, T. V. Joydas, R. H. Maneja, J. Dagoy, M. A. Qurban, and R. H. Roa-Ureta.
2021a. Distribution, abundance, and life history traits of the blue swimming crab *Portunus segnis* (Forskål, 1775) in the Saudi waters of the Arabian Gulf. Reg. Stud. Mar. Sci. 46:101895.

Rabaoui, L., R. H. Roa-Ureta, L. Yacoubi, Y.-J. Lin, R. Maneja, T. V. Joydas, P. Panickan, J. Gopalan, R. Loughland, P. K. Prihartato, et al.
2021b. Diversity, distribution, and density of marine mammals along the Saudi waters of the Arabian Gulf: update from a multi-method approach. Front. Mar. Sci. 8:687445.

Radhakrishnan, E. V., M. K. Manisseri, and V. D. Deshmukh,
2007. Biology and fishery of the slipper lobster, *Thenus orientalis*, in India. *In* The biology and fisheries of the slipper lobster (K. L. Lavalli and E. Spanier, eds.), p. 309–324. CRC Press, Boca Raton, FL.

Radhakrishnan, E. V., D. Rekha, P. K. B. Chakraborty, and M. Radhakrishnan.
2013. Fishery and population dynamics of the sand lobster *Thenus unimaculatus* (Burton & Davie, 2007) landed by trawlers at Sakthikulangara fishing harbour on the southwest coast of India. Indian J. Fish. 60(2):7–12.

Roa, R., B. Ernst, and F. Tapia.
1999. Estimation of size at sexual maturity: an evaluation of analytical and resampling procedures. Fish. Bull. 97:570–580.

Roa-Ureta, R. H.
2010. A likelihood-based model of fish growth with multiple length frequency data. J. Agric. Biol. Environ. Stat. 15:416–429.
2015. Stock assessment of the Spanish mackerel (*Scomberomorus commerson*) in Saudi waters of the Arabian Gulf with generalized depletion models under data-limited conditions. Fish. Res. 171:68–77.
2019. CatDyn: fishery stock assessment by catch dynamics models. R package, vers. 1.1-1. [Available from website, accessed February 2020.]

Sheppard, C., A. R. G. Price, and C. Roberts.
1992. Marine ecology of the Arabian region: patterns and processes in extreme tropical environments, 359 p. Acad. Press, London.

South, A.
2011. rworldmap: a new R package for mapping global data. R J. 3(1):35–43.
2012. rworldxtra: country boundaries at high resolution. R package, vers. 1.01. [Available from website, accessed March 2020.]

Spanier, E., and K. L. Lavalli.
1998. Natural history of *Scyllarides latus* (Crustacea: Decapoda): a review of the contemporary biological knowledge of the Mediterranean slipper lobster. J. Nat. Hist. 32:1769–1786.
2006. *Scyllarides* species. *In* Lobsters: biology, management, aquaculture and fisheries (B. F. Phillips, ed.), p. 462–496. Blackwell Publ., Oxford, UK.

Spanier, E., M. Tom, S. Pisanty, and G. Almog.
1988. Seasonality and shelter selection by the slipper lobster *Scyllarides latus* in the southeastern Mediterranean. Mar. Ecol. Prog. Ser. 42:247–255.

Wardiatno, Y., A. A. Hakim, A. Mashar, N. A. Butet, and L. Adrianto.
2016. Two newly recorded species of the lobster family Scyllaridae (*Thenus indicus* and *Scyllarides haanii*) from south of Java, Indonesia. HAYATI J. Biosci. 23:101–105.

National Marine Fisheries Service
NOAA

Fishery Bulletin
established in 1881

Spencer F. Baird
First U.S. Commissioner of Fisheries and founder of *Fishery Bulletin*

Spatiotemporal catch patterns and population distributions of bigeye Pacific opah (*Lampris megalopsis*) and smalleye Pacific opah (*L. incognitus*) in the eastern North Pacific Ocean

Ross Cooper (contact author)[1,2]
Heidi Dewar[2]
Barbara A. Muhling[2,3]
Steven L. H. Teo[2]
John Hyde[2]
Keith Bigelow[4]

Email address for contact author: r6cooper@ucsd.edu

[1] Scripps Institution of Oceanography
University of California San Diego
8622 Kennel Way
La Jolla, California 92037

[2] Southwest Fisheries Science Center
National Marine Fisheries Service, NOAA
8901 La Jolla Shores Drive
La Jolla, California 92037

[3] Institute of Marine Sciences
University of California Santa Cruz
1156 High Street
Santa Cruz, California 95064

[4] Pacific Islands Fisheries Science Center
National Marine Fisheries Service, NOAA
1845 Wasp Boulevard
Building 176
Honolulu, Hawaii 96818

Abstract—Opah (*Lampris* spp.) are commercially valuable, non-target fish that are regularly landed in pelagic longline fisheries in the central and eastern North Pacific Ocean. Genetic studies have confirmed 2 species in the region: bigeye Pacific opah (*L. megalopsis*) and smalleye Pacific opah (*L. incognitus*). Spatial distributions of each species are not well-defined, and little is known about species-specific catch distributions because the 2 species are difficult to distinguish visually. The objectives of this study were to characterize spatiotemporal patterns of opah landings by using catch per unit of effort (CPUE) from logbook and observer data, for the period 1995–2018, and genetics-based species identifications. Results from generalized additive models indicate that bigeye Pacific opah dominate west of 140°W and that smalleye Pacific opah dominate waters east of 130°W (dominance is defined as a proportion of catch ≥0.7). The deep-set pelagic longline fishery had higher opah CPUE than the shallow-set fishery across the geographic range of these fisheries. Opah CPUE increased from west to east on both longline gears, indicating higher overall opah CPUE in the eastern regions of both fisheries, primarily dominated by smalleye Pacific opah. Opah CPUE also increased over time as the Hawaii-based longline fisheries expanded eastward. The results of this study highlight the need for species-specific catch data and will inform management of opah species.

Manuscript submitted 19 November 2021.
Manuscript accepted 15 April 2022.
Fish. Bull. 120:138–149 (2022).
Online publication date: 29 April 2022.
doi: 10.7755/FB.120.2.4

The views and opinions expressed or implied in this article are those of the author (or authors) and do not necessarily reflect the position of the National Marine Fisheries Service, NOAA.

Opah (*Lampris* spp.), also known as moonfish, are large, laterally compressed teleosts that can reach upwards of 90 kg and 2 m fork length (Hawn and Collette, 2012). Opah occur across a broad latitudinal range in tropical, temperate, and subpolar marine regions (Hyde et al., 2014). Previous studies have found that opah have unique adaptations to retain heat created by their pectoral-fin swimming mode and distribute it throughout their entire body (Wegner et al., 2015). This full-body endothermy enhances capture of prey because opah can maintain a higher activity level and forage in cold deep water for long periods before returning to warmer surface waters (Wegner et al., 2015). Despite these intriguing discoveries, much is still unknown about the life history, distributions, and populations of opah, especially at the species level.

As recently as 2010, only 1 species of opah had been reported to reside in the North Pacific Ocean. Genetic studies, however, have confirmed the presence of 2 distinct species: the bigeye Pacific opah (*L. megalopsis*) and the smalleye Pacific opah (*L. incognitus*) (Hyde et al., 2014; Underkoffler et al., 2018). Although most biological data and studies in the North Pacific Ocean do not distinguish between the 2 species, some species-specific information is available. Results from gut content studies indicate that bigeye Pacific opah forage deeper in the water column than smalleye Pacific opah because their diet was almost entirely composed of mesopelagic species and the diet of smalleye Pacific opah included both epipelagic and mesopelagic species (Choy et al., 2013). This finding is consistent with relationships between eye size and foraging depth seen in other species (e.g., Kröger et al., 2009). In a study by Hyde et al. (2014), the spatial distribution of the 2 species were examined by using genetic analyses, and although results indicate that most smalleye Pacific opah were caught near the West Coast of the United States and that most

bigeye Pacific opah were caught near the main Hawaiian Islands (Hyde et al., 2014), there was a gap in sampling between ~140°W and 125°W. Consequently, the species distributions in the eastern North Pacific Ocean could not be determined.

Both species of opah are a relatively common incidental catch in the drift gill-net fishery targeting swordfish (*Xiphias gladius*) in the California Current system, a productive eastern boundary current system that is an important foraging ground for many highly migratory species (Block et al., 2011), and in pelagic longline fisheries targeting swordfish and bigeye tuna (*Thunnus obesus*) in the North Pacific Ocean. Although opah have not been a primary target of commercial fisheries, seafood marketing efforts and new culinary uses for previously discarded cuts of these fish have recently increased the popularity of opah, and they are an increasingly valuable secondary target. Reported landings of opah in Hawaii increased from approximately 400 metric tons (t) per year in the early 2000s to more than 800 t by 2017 (National Marine Fisheries Service, Office of Science and Technology, commercial fisheries landings, available from website, accessed May 2020). Additionally, in the California large-mesh drift gill-net fisheries, nominal catch per unit of effort (CPUE) of opah increased roughly 4-fold from 1982 to 2017 (Walker and Teo[1]).

The regions where opah are landed by U.S. fleets fall under the jurisdiction of 2 management councils: the Western Pacific Regional Fishery Management Council and the Pacific Fishery Management Council. In the Western Pacific Regional Fishery Management Council, opah are listed as a "pelagic management unit" in the fishery ecosystem plan. In contrast, they are not listed in the fishery management plan of the Pacific Fishery Management Council. There is currently no stock assessment for opah in the Pacific Ocean, nor are there any management measures in place for these species (WPRFMC, 2021).

Stock assessments are a key component of fisheries management, and any effort to assess or manage opah in the North Pacific Ocean will require species-specific information on population distributions and fisheries data such as CPUE. However, past difficulties with visual identification have led to both bigeye Pacific opah and smalleye Pacific opah being simply recorded as *opah* in fisheries records and most scientific studies. Information on the spatial distributions of bigeye and smalleye Pacific opah is limited (Hyde et al., 2014), and the species-specific CPUE is unknown. Fisheries observers are now able to more effectively identify opah in landings to species level using new visual identification keys that illustrate the differences between species in spot patterns and the trailing margin of the caudal fin. Differentiating between morphologically similar species is essential to effectively characterize the fishing mortality of each species and contribute to accurate stock assessments (Beerkircher et al., 2009).

[1] Walker, J. M., and S. L. H. Teo. In review. Distribution and relative abundance trends of opah in California waters.

The primary objectives of this study were to examine spatial and temporal patterns of catch rates of opah on pelagic longline fishing gear and to estimate the species-specific distributions and CPUE within the central and eastern North Pacific Ocean. First, we characterized the spatial and temporal patterns of fisheries effort and non-species-specific opah CPUE of the U.S. pelagic shallow- and deep-set longline fleets. We then combined the use of genetic analyses and generalized additive models (GAMs) to estimate the proportions of bigeye Pacific opah and smalleye Pacific opah caught in different areas and to estimate CPUE in regions dominated by the 2 species. Finally, patterns in species distributions and CPUE were linked to oceanography to gain insight into preferred habitat.

Materials and methods

Fisheries data

Fisheries data were obtained from pelagic longline vessels based in California and Hawaii. Since 1990, captains of vessels in the U.S. pelagic longline fleet have been required to fill out logbooks with details describing fishery-specific gear and effort, latitude and longitude, and catch information for each set (Walsh and Brodziak, 2016). In the logbook data, the species of opah that was caught on each set is not specified; instead, catch taxa are listed as *opah* or *moonfish*.

The pelagic longline vessels that operate in California and Hawaii are also required to use trained observers to document catch and bycatch, ensure regulatory compliance, and record exact catch locations. On Hawaii-based vessels, observers are present on 20% of deep-set longline trips and on 100% of shallow-set longline trips (Sippel et al.[2]). California-based vessels participate only in the deep-set fishery and have been required to have 20% observer coverage since 2016 (NMFS, 2016). Logbook and observer data for vessels based in both Hawaii and California were provided by the NOAA Pacific Islands Fisheries Science Center (Sippel et al.[2]; PIFSC[3]).

Both the logbook and observer data contained substantial fishing information. To standardize the data for analyses, the fields selected were number of opah, date of the set, effort (number of hooks), number of hooks per float (which affects fishing depth), set and haul times, and the longitude and latitude of the set.

Opah are caught on both deep- and shallow-set longline gear configurations. Both fleets operate in the eastern and central Pacific Ocean but do so with different spatial extents, reflecting the habitat of their respective target species (Figs. 1 and 2). Deep-set gear is used primarily to

[2] Sippel, T., N. Nasby-Lucas, and S. Kohin. 2014. Description of the Hawaii longline observer program. Int. Sci. Comm. Shark Work. Group ISC/14/SHARKWG-1/05, 6 p. [Available from website.]

[3] PIFSC (Pacific Island Fisheries Science Center). 2019. Hawaii longline logbook. [Available from website, accessed March 2019.]

target bigeye tuna at depths between 100 and 400 m, with a median depth of 250 m (Bigelow et al., 2006; Woodworth-Jefcoats et al., 2018). This gear has a mainline that spans an average of 65 km, with an average total number of hooks of 1700 and with 27 hooks per float (Bigelow et al., 2006). The hooks are baited with either Pacific saury (*Cololabis saira*) or Pacific sardine (*Sardinops sagax*) and generally are set in the morning and hauled in the afternoon or evening (Bigelow et al., 2006). Shallow-set gear is used primarily to target swordfish at depths between 30 and 90 m. The mainlines of this gear span 75 km, with a total of 700–1000 hooks and roughly 5 hooks per float. The hooks are baited with Pacific chub mackerel (*Scomber japonicus*) and generally are set at night when swordfish are closer to the surface (Dewar et al., 2011). In 2019, there were an estimated 22 vessels using shallow-set gear and an estimated 143 vessels using deep-set gear in the North Pacific Ocean (PIFSC[3]).

Prior to analyses, the data were filtered and separated into deep and shallow sets by using the methods of Bigelow et al. (2006), with deep-set data containing sets with 15 or more hooks per float and shallow-set data containing sets with less than 15 hooks per float. However, >95% of deep sets had 19–32 hooks per float and 500–3500 hooks per set, and >95% of shallow sets had 4–8 hooks per float and 500–1500 hooks per set. We therefore excluded sets outside these ranges, to focus our analyses on typical deep-set and shallow-set gear configurations. Data were removed from analyses if soak times (the duration over which the fishing gear is completely submerged) were outside of reasonable bounds based on knowledge of fishery operations: 2–8 h for deep sets and 2–10 h for shallow sets. Records were also removed if they were outside the general geographic range of each fishery (deep sets: 180–125°W, 0–45°N; shallow sets: 180–125°W, 15–45°N). All data from 1995 did not meet the filtration criteria and were removed, effectively

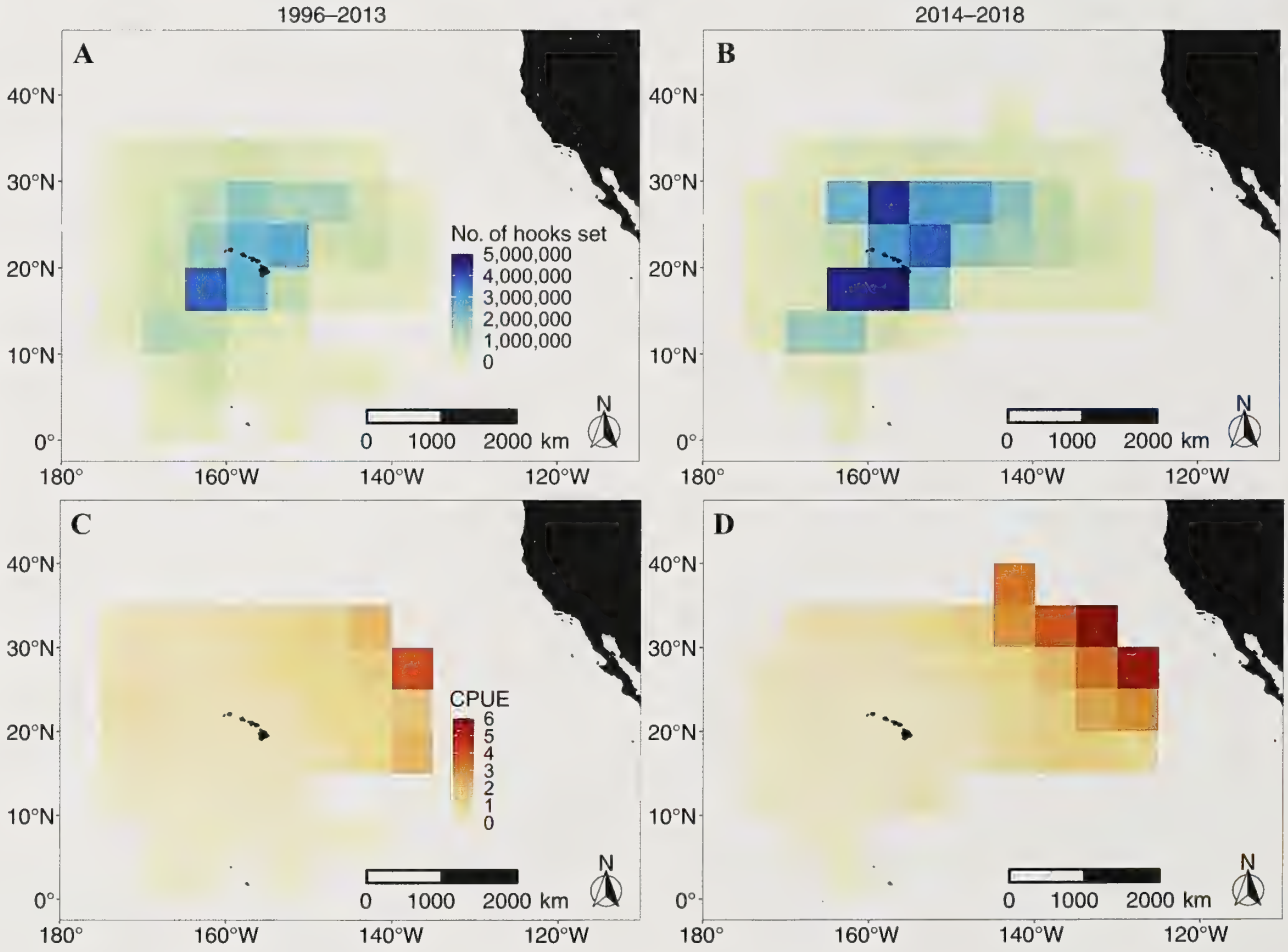

Figure 1

Map of the (**A** and **B**) average annual effort, measured as number of hooks, and (**C** and **D**) aggregate nominal catch per unit of effort (CPUE), measured as number of individuals per 1000 hooks, for opah (*Lampris* spp.) caught by the U.S. deep-set longline fishery during 1996–2013 and 2014–2018 in the central and eastern North Pacific Ocean. Logbook data are binned into 5°-by-5° blocks, and blocks with data from less than 3 vessels are not shown to maintain confidentiality.

changing the beginning of the fisheries data time series to 1996. The use of these criteria resulted in a final data set of 330,599 deep-set gear sets and 43,326 shallow-set gear sets spanning from 1996 through 2018, with 89% and 54% of data remaining from the original unfiltered data sets, respectively. Almost 40% of the shallow-set data were filtered out simply because of missing critical fields in the data set (hooks per float, hooks per set, soak time, or geographic coordinates).

The areas fished by both fleets have changed since the beginning of the longline fisheries. During the 1990s, the deep-set fishery was primarily confined to the waters around the main Hawaiian Islands, but effort began to expand eastward in the 2000s (Woodworth-Jefcoats et al., 2018). This expansion accelerated after 2013. From 1996 through 2013, only 9% of the longline sets in the deep-set fishery occurred in waters east of 150°W, and that percentage increased to 26% during 2014–2018. The percentage of sets in the shallow-set fishery that occurred east of 150°W increased from 25% to 53% over those same time frames.

Consequently, 2 periods were considered for analyses: 1996–2013 and 2014–2018. Filtered logbook data were binned into 5°-by-5° blocks to visualize effort (number of hooks set) and CPUE (number of individual opah landed per 1000 hooks). For confidentiality purposes, visualizations of effort and CPUE do not display blocks containing less than 3 unique vessels within each figure's specified period, although the data were still included in the overall calculations and analyses of fishery trends. Blocks containing less than 20 total sets of deep-set longlines or less than 10 total sets of shallow-set longlines were also removed from their respective analyses to ensure sufficient sample sizes. The shallow-set fishery had overall lower amounts of data and effort; therefore, a lower threshold was established to maximize spatial data.

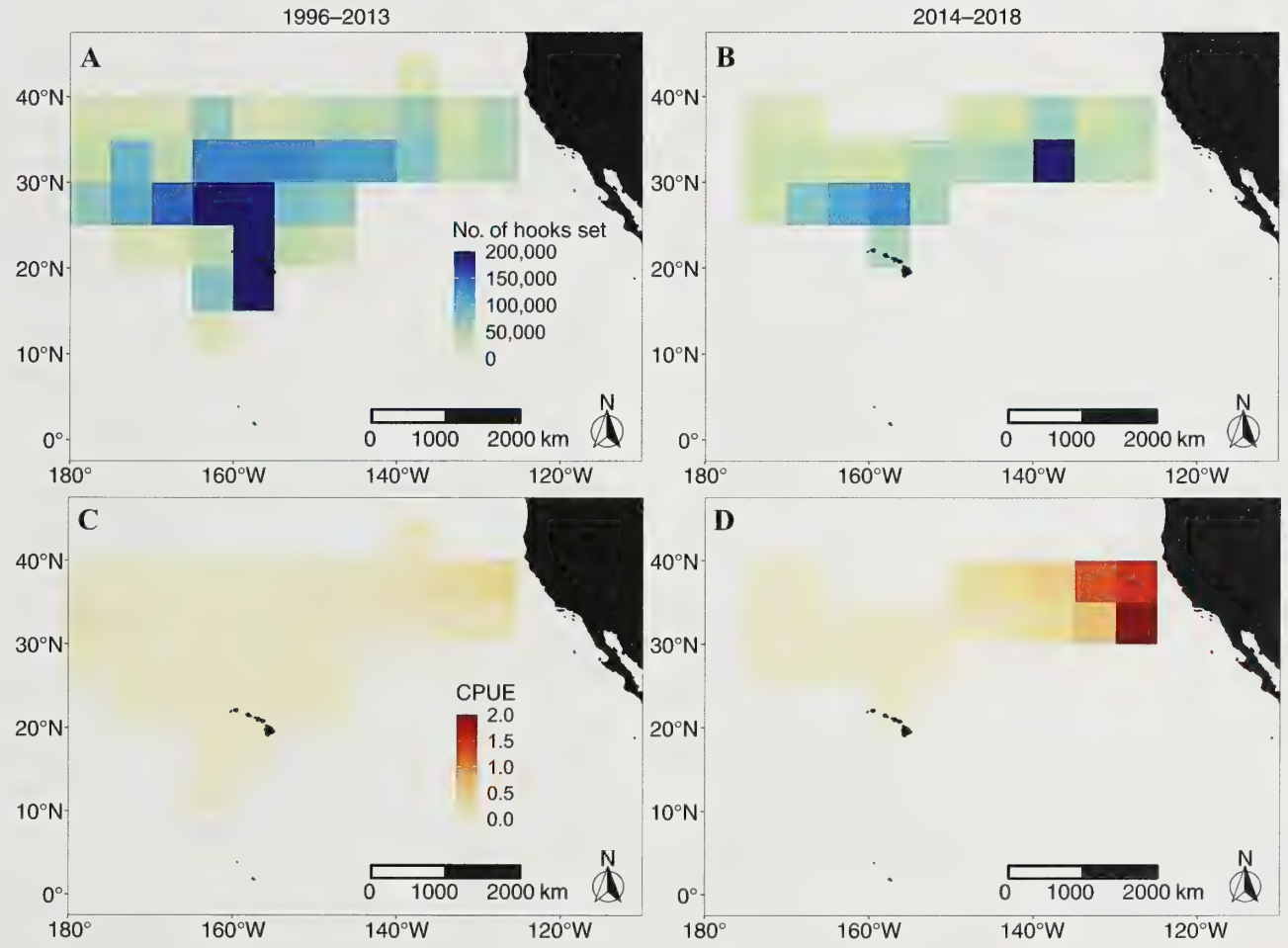

Figure 2

Map of the (**A** and **B**) average annual effort, measured as number of hooks, and (**C** and **D**) aggregate nominal catch per unit of effort (CPUE), measured as number of individuals per 1000 hooks, for opah (*Lampris* spp.) caught by the U.S. shallow-set longline fishery during 1996–2013 and 2014–2018 in the central and eastern North Pacific Ocean. Logbook data are binned into 5°-by-5° blocks, and blocks with data from less than 3 vessels are not shown to maintain confidentiality.

Genetic analyses

Genetic identification of opah was completed as described in Hyde et al. (2014). Briefly, Hyde et al. (2014) used samples of fin tissue collected either by fishery observers at sea during research cruises or by researchers after whole fish were landed in port (in either Hawaii or California) and preserved in 95% ethanol until processed. From each sample, DNA was extracted by using a boiling protocol with Chelex 100[4] resin (Bio-Rad Laboratories Inc., Hercules, CA), and a portion of the mitochondrial cytochrome *c* oxidase gene was amplified, sequenced, and compared to reference sequences for bigeye Pacific opah (accession no. JF931871, GenBank, available from website) and smalleye Pacific opah (accession no. JF931880, GenBank, available from website) to identify species.

This study incorporated samples collected by researchers and observers and used in the Hyde et al. (2014) study and samples collected by commercial fishermen since that paper was published. For samples collected by observers, sampling locations were identified to specific sets, whereas the more recent samples collected by fishermen were associated only with specific trips, not with individual sets. To standardize the spatial resolution of sampling of tissue for genetic analysis, location data for all samples were aggregated to trip level by taking the average latitude and longitude of all sets within the trip in which opah were landed (an average of 13 sets per trip), on the basis of logbook data from the same sampled trip. There were 141 deep-set and 2 shallow-set longline trips associated with genetic samples of opah. Given the lack of genetic samples from shallow-set trips, only the genetic samples from deep-set trips were retained for further analysis. In addition, 2 deep-set trips had a difference of more than 5° between the maximum and minimum latitude or longitude of a trip, and they were excluded, yielding a total of 139 deep-set longline trips that were used for estimating distribution of opah species.

Spatial distributions of species

Based on the genetic analyses described above, the proportion of bigeye Pacific opah versus smalleye Pacific opah within 5°-by-5° grid cells were calculated. A series of GAMs were then developed by using the mcgv package (vers. 1.8-33; Wood, 2017) in R, vers. 3.6.1 (R Core Team, 2019), to explain the differences in the proportions of bigeye Pacific opah. Latitude (*lat*) and longitude (*lon*) were used to predict the proportion of bigeye Pacific opah (*propnBigeye*) through beta regression, weighted by the total number of opah caught (sample size) within each grid cell:

$$propnBigeye \sim s(lon, lat),$$

where s = a thin-plate regression spline (Wood, 2017).

We tested the inclusion of season (quarter of the year) as an additional predictor in the GAMs, to assess whether spatial patterns in species distributions varied throughout the year. However, the GAMs that include season were not superior to those without that variable, with <1% difference in variance explained and higher Akaike information criteria. As such, for further analysis, we proceeded with GAMs that include just latitude and longitude as predictors.

Three GAMs were built by using identical predictor and response variables but different knot (k) values for the isotropic thin-plate regression spline: 4 (low), 6 (medium), and 8 (high). We chose to vary k to capture some of the uncertainty in the spatial prediction surface because the locations of genetically identified opah did not cover the full geographic range of the pelagic longline fleet. Values of 4, 6, and 8 allowed different patterns of spatial extrapolation outside the sampled area, without obvious overfitting.

The fitted GAMs were then used to generate maps with the expected proportions of bigeye Pacific opah over the study area and were used to identify areas dominated by either bigeye Pacific opah or smalleye Pacific opah, by using an arbitrary threshold of 0.7. Areas with expected proportions of bigeye Pacific opah ≥0.7 and ≤0.3 were classified as dominated by bigeye Pacific opah and smalleye Pacific opah, respectively. Areas with expected proportions between 0.3 and 0.7 were considered *mixed areas* without dominance of a single species of opah. The logbook data from the deep-set longline fishery were divided into 3 subsets—data for areas dominated by bigeye Pacific opah, data for areas dominated by smalleye Pacific opah, and data for mixed areas—and were used to calculate the number of sets and average CPUE in each type of area.

To estimate the uncertainty of the GAM predictions, an iterative jackknife procedure was performed. Jackknifing resamples data with a leave-one-out method; the medium (k=6) GAM with 139 trip-level data points was rerun 139 times, each time with a single trip removed (with replacement) to predict species proportion for each 1°-by-1° block in a grid spanning the study area. To visualize the uncertainty of the GAM predictions, the mean, standard deviation, and coefficient of variability were estimated for each block, with the coefficient of variability calculated as (standard deviation/mean)100.

Results

Spatial and temporal patterns: fishing effort and catch per unit of effort

A compilation of all data across the time series reveals differences in the deep- and shallow-set longline fisheries. Effort in the deep-set fishery increased from roughly 375 sets in 1996 to 18,700 sets in 2018. In contrast, effort in the shallow-set fishery peaked in 1998 at roughly 4700 sets. The shallow-set fishery was temporarily closed from 2001 through 2004 (Federal Register, 2004), and annual effort remained below 2000 sets per year from 2005 through 2018.

[4] Mention of trade names or commercial companies is for identification purposes only and does not imply endorsement by the National Marine Fisheries Service, NOAA.

The spatial range of the deep-set fishery also changed over time. In 2014–2018, the fishery expanded eastward to 125°W (compared with a limit of 135°W in 1996–2013), and less area was fished south of 10°N (Fig. 1). Even after the eastward expansion in 2014, the majority of deep-set fishery operations were still centered around the main Hawaiian Islands, with 74% of the fishery operating west of 150°W during 2014–2018 in comparison with 91% during 1996–2013.

As with effort, the spatial range of the shallow-set fishery also decreased in 2014–2018 compared with the range in 1996–2013 (Fig. 2). As with the deep-set fishery, effort for the shallow-set fishery was centralized around the Hawaiian Islands in 1996–2013 but transitioned to more of a bimodal distribution, with one peak around the Hawaiian Islands and another around 140°W, 30°N in 2014–2018.

The CPUE for opah was highest in the northeast region of both the deep-set and shallow-set fishery, roughly east of 140°W and north of 25°N, with a noticeable gradient increasing from west to east (Figs. 1 and 2). The results of comparing data between the gear types indicate that CPUE was highest in the deep-set fishery. From 2014 through 2018, CPUE of deep-set longlines in 5°-by-5° blocks ranged from 3.0 to 6.0 opah/1000 hooks in the northeast extent of the fishery and from 0.5 to 2.0 opah/1000 hooks west of 140°W. The CPUE of shallow-set longlines peaked at about 2 opah/1000 hooks in the northeast area and was generally <1 opah/1000 hooks throughout the rest of the fishery range.

Spatial distributions of species

For species identification in this study, an additional 679 samples from 37 trips were added to the 415 samples from 102 trips used in the study conducted by Hyde et al. (2014), to examine distribution in the region that overlaps with the pelagic longline fisheries. The region and time frame over which the samples were collected differed for the 2 programs (Table 1). The samples from Hyde et al. (2014) came from west of 139°42′W, whereas the more recent samples came from east of 139°6′W. Both programs sampled across months, although no samples from November were available to Hyde et al. (2014). Bigeye Pacific opah were identified in all 5°-by-5° blocks, although percent occurrence varied spatially. In the region around Hawaii and to the south, only bigeye Pacific opah were identified in the blocks. North of the Hawaiian Islands (>25°N), smalleye Pacific opah were identified in all blocks with the proportions ranging from 0.1 through 0.8 and with the highest proportional abundance in the blocks closest to the U.S. West Coast. (Fig. 3).

The Akaike information criteria for GAMs with k of 4, 6, and 8 were −2669.9, −2726.1, and −2742.0, respectively. The effective degrees of freedom for these GAMs were 2.98, 4.88, and 6.75, respectively. The effective degrees of freedom of 2.98 for the GAM with a k of 4 is very close to 3, which is 1 less than k, indicating that this GAM may be oversmoothed. The 3 GAMs explained 56.2%, 59.1%, and 60.0% of the deviance in the genetic sampling data, respectively.

Table 1

Overview of sampling of bigeye Pacific opah (*Lampris megalopsis*) and smalleye Pacific opah (*L. incognitus*) from which genetic data used in this study were obtained. Data were compiled from Hyde et al. (2014) and from genetic analyses conducted since 2014 of samples from the eastern North Pacific Ocean.

	Period	
Data type	2009–2010 (from Hyde et al.)	2017–2018
Effort (no. of trips)	102	37
Sample size	415	679
Latitude mode	30.00°N	22.45°N
Latitude range	10.68–31.72°N	19.83–33.39°N
Longitude mode	217.56°E	227.53°E
Longitude range	190.52–220.27°E	220.93–232.89°E

Model fits appeared adequate, and residuals were approximately normally distributed in each case.

All 3 GAMs predicted that bigeye Pacific opah would dominate (with proportions of bigeye Pacific opah ≥0.7) in waters west of 140°W, particularly in the southwest extent of the study area, and that smalleye Pacific opah would dominate (with proportions of bigeye Pacific opah ≤0.3) in waters east of 130°W (Fig. 4). The 2 species were predicted to co-occur in roughly equal proportions between 140°W and 130°W. Predictions from the 3 GAMs varied spatially, particularly in the area north of 25°N and east of 150°W, where fishing effort was generally lower. However, estimates from all models indicate a strong west-to-east gradient of high-to-low probability of occurrence of bigeye Pacific opah.

The results from jackknifing indicate low levels of variance over the study area, with a maximum coefficient of variability of ~4% (Fig. 5). The area with the highest coefficient of variability (155–140°W, 30–35°N) was the area with the least data, and it encompasses waters predicted to have areas dominated by bigeye Pacific opah and mixed areas. Generally, waters predicted to be dominated by one species or the other had lower variability.

Catch per unit of effort by species dominance

The results from the GAMs and the maps of CPUE were combined to examine CPUE in the 3 types of areas classified by species dominance: dominated by bigeye Pacific opah, dominated by smalleye Pacific opah, and mixed areas. The lowest CPUE was in areas predicted to be dominated by bigeye Pacific opah (west of 140°W), and the highest CPUE was in the eastern portion of the mixed area and the area predicted to be dominated by smalleye Pacific opah (east of 130°W) (Table 2, Figs. 1 and 2).

The results from comparing data for the 2 periods indicate that CPUE declined slightly in areas dominated by

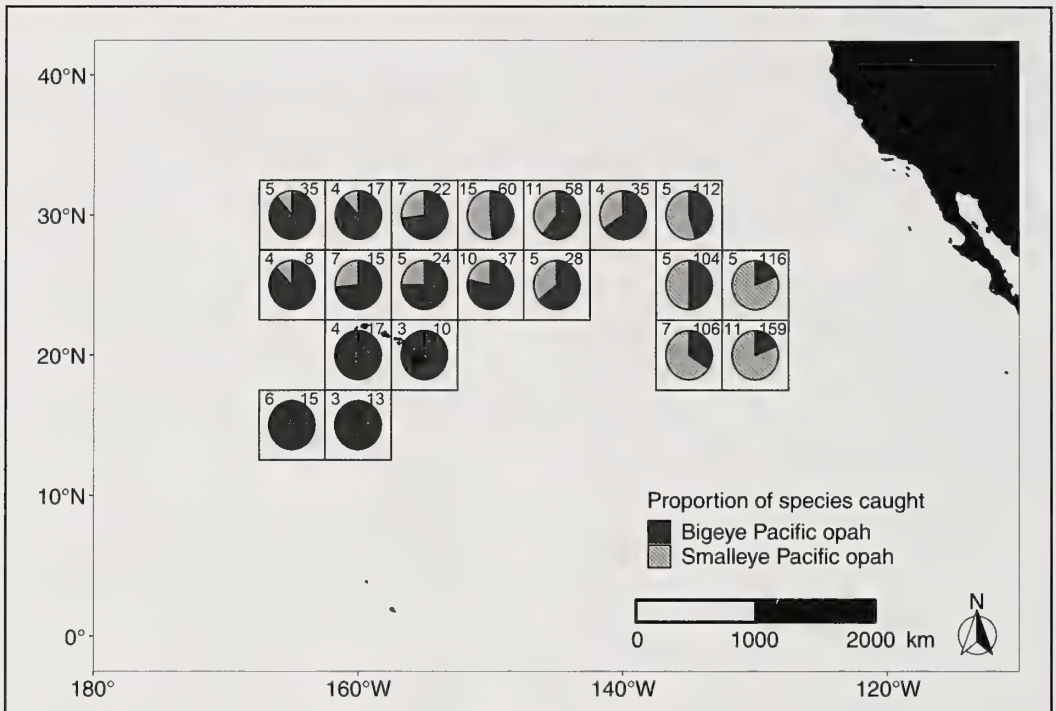

Figure 3

The proportions of genetically confirmed bigeye Pacific opah (*Lampris megalopsis*) and smalleye Pacific opah (*L. incognitus*) caught in the deep-set pelagic longline fishery for 5°-by-5° blocks in the eastern North Pacific Ocean during 2009, 2010, 2017, and 2018. In each block, the top-left number refers to the total number of trips by fishing vessels during which opah used for genetic analysis were caught, and the top-right number refers to the total number of opah caught on those trips. Blocks with data for less than 3 vessels are not shown to maintain confidentiality.

bigeye Pacific opah in 2014–2018 but remained fairly consistent in mixed areas. Because of the low effort in the eastern region during 1996–2013, it was not possible to compare CPUE across periods. It is apparent, however, that the CPUE in the region dominated by smalleye Pacific opah during 2014–2018 was consistently higher than in the regions dominated by bigeye Pacific opah and in the mixed area across both periods. Table 2 also highlights that the majority of fishing activity in this region has occurred since 2014.

Discussion

The results of this study, linking fisheries data with more detailed information on the distribution of bigeye Pacific opah and smalleye Pacific opah, advance our understanding in important ways. First, our analyses allowed examination of shifts in fisheries interactions in the context of opah distribution. Second, the results of this work provide a more complete picture of the range of the 2 species and insight into temporal and spatial patterns in catch in a species-specific context. This study represents an important step toward understanding the basic biology and fisheries interactions of the 2 opah species in the eastern North Pacific Ocean.

Fisheries distribution and catch per unit of effort

The effort and spatial distribution of both the U.S. pelagic longline fleets targeting bigeye tuna and swordfish in the Pacific Ocean have changed from 1996 to 2018. In the shallow-set fishery, the range and effort decreased. In contrast, the deep-set fishery increased in both effort and range, with substantially more effort east of 140°W. Although observations of these shifts in fisheries are not new (Woodworth-Jefcoats et al., 2018), it is important to understand the dynamics of the fishery in the context of interactions with opah. Total effort has increased in the region where the overall CPUE and proportion of smalleye Pacific opah are higher. In addition, effort has shifted from shallow-set gear to deep-set gear, and CPUE of opah is also higher in the deep-set fishery than in the shallow-set fishery. These findings are consistent with the increase in landings of opah in the deep-set longline fishery (National Marine Fisheries Service, Office of Science and Technology, commercial fisheries landings, available from website, accessed May 2020). However, variable fishing footprints, the limit of evaluation to only 2 periods, and multiple regulatory shifts make direct temporal comparisons of CPUE and effort challenging. The relative contribution of the 2 species to this increase in landings

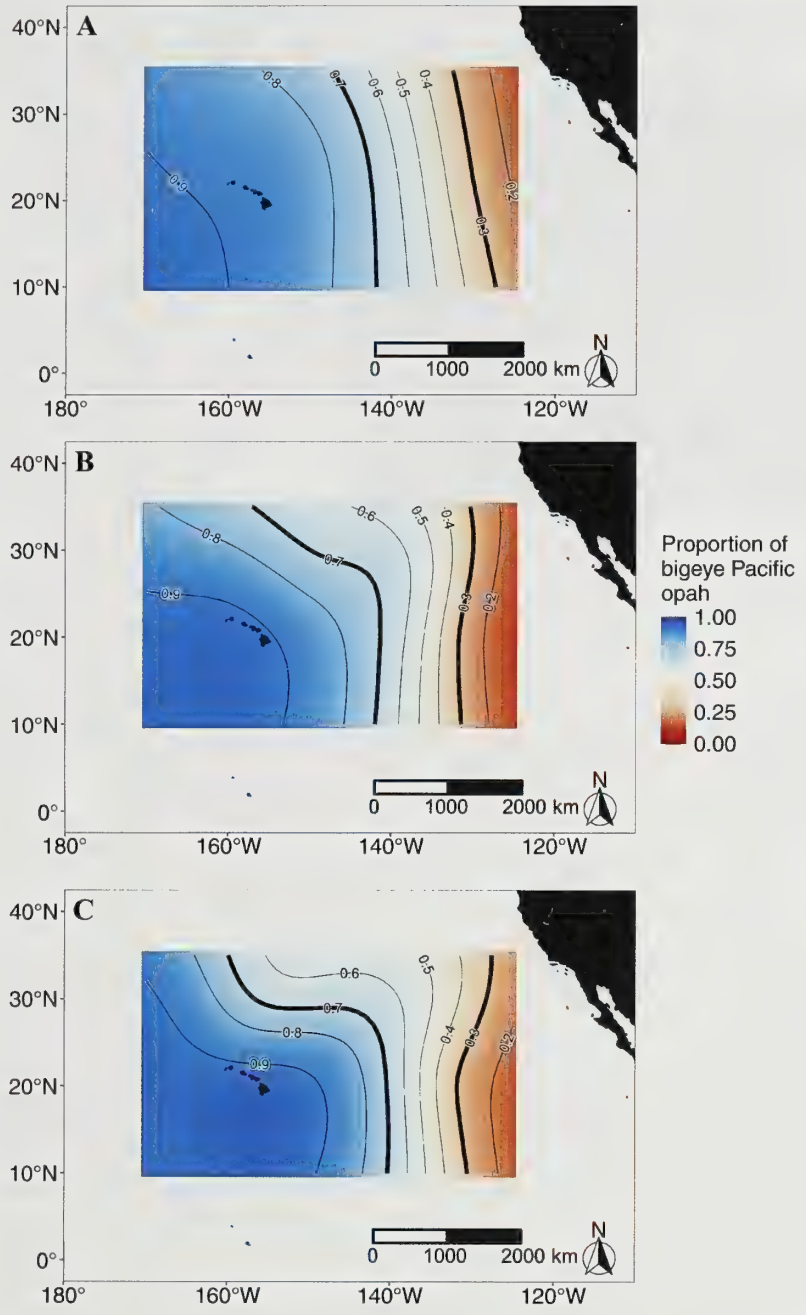

Figure 4

Contour maps of expected proportions of bigeye Pacific opah (*Lampris megalopsis*) caught during 2009, 2010, 2017, and 2018 in the eastern North Pacific Ocean in the deep-set pelagic longline fishery, generated by using generalized additive models with (**A**) 4 (low), (**B**) 6 (medium), and (**C**) 8 (high) knots for the isotropic thin-plate regression spline. Areas with expected proportions of bigeye Pacific opah of ≥0.7 (darker blue area), ≤0.3 (darker red area), and 0.3–0.7 are classified as dominated by bigeye Pacific opah, dominated by smalleye Pacific opah (*L. incognitus*), and mixed areas (no dominance), respectively. Bold contours indicate proportions of 0.7 and 0.3 to visualize the classification thresholds.

cannot be calculated because of the lack of species-specific landings data, and estimation of the relative contributions is beyond the scope of this paper.

Spatial distributions of species

Paired with data from Hyde et al. (2014), the results of the additional genetic analyses in this study have filled the gap east of 140°W, outside of the U.S. exclusive economic zone, providing a more spatially complete picture of the distributions of bigeye and smalleye Pacific opah. Results of our evaluation of species distribution indicate that, during 2009–2019, bigeye Pacific opah occurred throughout the region and smalleye Pacific opah occurred predominantly in the eastern and northern boundaries of the range of longline fisheries, with proportional abundance decreasing toward the west. There was no defined boundary between the distributions of the 2 species within the geographic scope of this study. South of 25°N, the approximate location of the North Pacific Transition Zone (Roden, 1991; Polovina et al., 2001), the transition from blocks dominated by smalleye Pacific opah to blocks dominated by bigeye Pacific opah occurred approximately between 140°W and 130°W. With the addition of new genetic samples collected for our study, the delineation of the species between 140°W and 130°W is less defined than the distributions indicated by results from Hyde et al. (2014), who reported that a number of the eastern blocks were all dominated by smalleye Pacific opah. In the North Pacific Transition Zone, the transition was even less well-defined, and smalleye Pacific opah occurred across our entire study area. Additional genetic samples from this region would allow expansion of the model into the North Pacific Transition Zone in future studies. The considerable overlap between the distributions of the 2 opah species could complicate retroactive examination of species-specific trends.

Although this study was confined to the approximate spatial extent of the U.S. pelagic longline fisheries in the North Pacific Ocean, data are available for regions outside this area and provide additional insight into the broader range of the 2 opah species in the Pacific Ocean. Results from genetic analyses of samples from the western Pacific Ocean near Japan and the southcentral Pacific Ocean near America Samoa indicate that 100% of samples are bigeye Pacific opah (Hyde et al., 2014), indicating that the dominance of bigeye Pacific opah continues both west and south

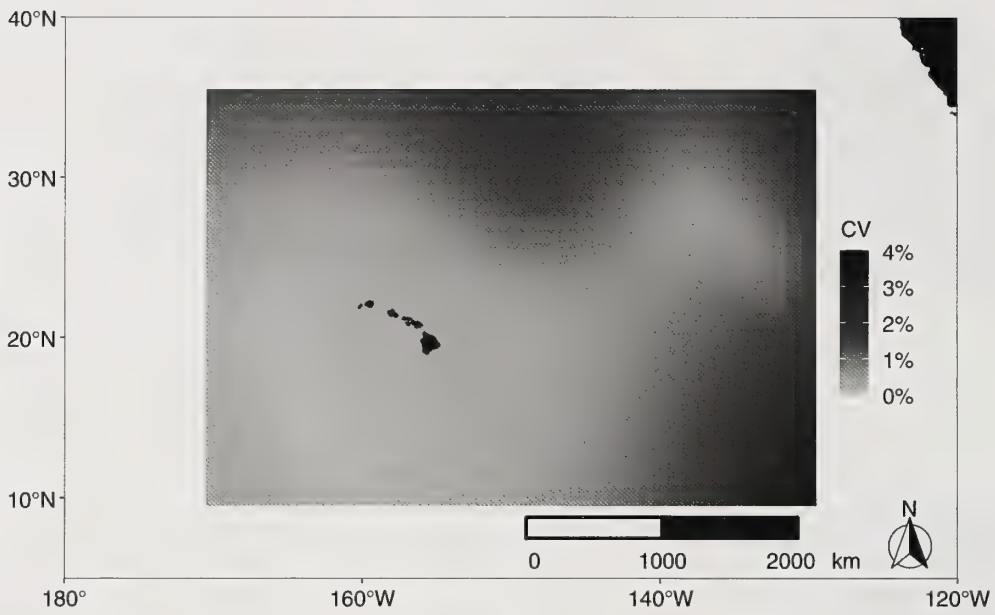

Figure 5

Coefficient of variability (CV) estimated by using a jackknife procedure and the generalized additive model with 6 knots for the thin-plate regression spline, for each 1°-by-1° block over the study area in the eastern North Pacific Ocean where opah (*Lampris* spp.) were caught with deep-set pelagic longlines during 2009, 2010, 2017, and 2018. Darker areas of the map show higher levels of variability in the data. The CVs were calculated as (standard deviation/mean)100.

Table 2

Number of sets and catch per unit of effort (CPUE), measured as number of individual opah per 1000 hooks, for the deep-set pelagic longline fishery operating in areas in the eastern North Pacific Ocean dominated by bigeye Pacific opah (*Lampris megalopsis*), smalleye Pacific opah (*L. incognitus*), or mixed species. Values are given by the number of knots (k) for the isotropic thin-plate regression spline in each generalized additive model: 4 (low), 6 (medium), and 8 (high). Some cells are blank because values are included only when data for more than 20 sets were available.

	Bigeye		Smalleye		Mixed species	
k	No. of sets	CPUE	No. of sets	CPUE	No. of sets	CPUE
Sampling period: 1996–2013						
4	236,152	0.43			3042	1.89
6	233,340	0.42			5848	1.64
8	227,167	0.40			12,028	1.22
Sampling period: 2014–2018						
4	80,382	0.34	364	4.28	10,645	1.76
6	79,114	0.32	616	2.93	11,661	1.72
8	77,311	0.31	584	2.62	13,496	1.60

of the main Hawaiian Islands and that the range of smalleye Pacific opah does not extend across the Pacific Ocean. Although pelagic longline fisheries cannot operate within 200 nautical miles of the U.S. West Coast, data are available for this region from other fisheries and research cruises. Catch composition in the California Current from the state of Washington to Mexico is nearly 100% smalleye Pacific opah (Hyde et al., 2014). It should be noted that most opah sampled were relatively large (>80 cm fork length) and presumed to be adults, and even less information is available on the geographic range of larvae and juveniles. Additional species-specific information across size classes is needed to determine the full distribution of each species.

The movement patterns of highly migratory species and the dynamic nature of their habitat make it difficult, if not impossible, to establish static boundaries of species ranges (Maxwell et al., 2015; Dunn et al., 2016). Although this study classified fixed areas for each species within the range sampled, the distribution of species can shift over time with variations in abundance, natural climate variability on interannual (e.g., El Niño–Southern Oscillation) and decadal (e.g., Pacific Decadal Oscillation) timescales, as well as with longer-term climate change.

A number of factors indicate the potential for shifts in the distribution of opah. First, the distributions of bigeye tuna and swordfish, which have habitats and diets that overlap with those of opah, have shifted with climate

variability (Bigelow et al., 1999; Howell and Kobayashi, 2006; Choy et al., 2013; Sculley and Brodziak, 2020). Second, evidence indicates that the abundance of some large pelagic predators, including opah, has decreased on the high seas. Results from both our study and that of Polovina and Woodworth-Jefcoats (2013) indicate a decline in CPUE in areas where bigeye Pacific opah are expected to dominate landings. Polovina and Woodworth-Jefcoats (2013) used longline data collected through 2011, prior to the eastward expansion of the deep-set fishery. Conversely, CPUE of opah has increased in coastal waters off California (Walker and Teo[1]). The likely influences of natural climate variability, long-term climate change, and apparent changes in abundance highlight the potential for shifts in distribution of opah and the importance of long-term monitoring of species ranges.

Opah and oceanography

Although the ecological drivers for the spatial distributions of both opah species are unknown, insights were gained by examining patterns in CPUE. Caution should be used when interpreting patterns in CPUE, but standardized CPUE trends are commonly used as indices of relative abundance for both target and non-target species (Bigelow et al., 2002; Woodworth-Jefcoats et al., 2018; Ducharme-Barth and Vincent[5]). For both pelagic longline fisheries, the highest CPUE of opah was recorded in the northeastern extent of the fishery ranges, starting at approximately 140°W.

Quantification of the relative contribution of the 2 species to the overall opah CPUE is beyond the scope of this paper; however, a number of factors may contribute to this pattern, with insights coming from the relatively high CPUE of bigeye tuna in the same region (Hanamoto, 1987; Woodworth-Jefcoats et al., 2018; Ducharme-Barth and Vincent[5]). East of ~130°W, dissolved oxygen at depth declines rapidly because of the presence of the eastern Pacific oxygen minimum zone (Karstensen et al., 2008). It has been hypothesized that, where low-oxygen waters encompass the deep scattering layer, bigeye tuna are less able to access mesopelagic prey (Hanamoto, 1987). Given that the diets and vertical habitats of bigeye tuna and opah overlap (Nakano et al., 1997; Polovina et al., 2008, Choy et al., 2013), the same forces may influence abundance of opah. East of this region, productivity is enhanced by the California Current (Rykaczewski and Checkley, 2008). Although additional research on species-specific essential habitat and gear vulnerability is needed, the apparent increase in abundance of opah in the eastern Pacific Ocean is likely linked to regional oceanography, productivity, and prey availability, as has been observed for other highly migratory species. This study did not incorporate seasonality as a predictor in the GAMs, but seasonal shifts in oceanographic conditions, and therefore potentially in distributions of opah species, could be occurring and could be revealed with additional sampling.

Insights into species-specific habitats are gained by comparing the distribution of the 2 species, particularly in regions that are dominated by a single species. Although examining the broad range of factors that influence distributions is beyond the scope of this paper, insights can come from examining distributions in the context of oceanographic conditions and prey availability.

Off the coast of California, where smalleye Pacific opah are dominant, both dissolved oxygen and temperature decline rapidly with depth, and these decreases may limit access for smalleye Pacific opah to favorable thermal habitat and mesopelagic prey species (Karstensen et al., 2008; Choy et al., 2013; Aksnes et al., 2017). At the same time, the shallow oxygen minimum zone may compress the habitat of the epipelagic species that are important prey of the smalleye Pacific opah (Prince and Goodyear, 2006; Choy et al., 2013). In contrast, in oligotrophic gyre waters south of Hawaii, where bigeye Pacific opah dominate, productivity in surface waters and epipelagic prey biomass are low (Signorini et al., 2015) and the deep scattering layer is deeper. For example, Tont (1976) listed a difference of ~100 m in the depth of the top of the deep scattering layer between the California Current and the central Pacific Ocean (an average of 282 m versus 394 m). In addition, sea-surface temperatures are warmer in the central Pacific Ocean compared with those in comparable latitudes in the California Current, and winter mixed layer depths are deeper (de Boyer Montégut et al., 2004; Deser et al., 2010). Bigeye Pacific opah tagged with pop-up archival tags north of the main Hawaiian Islands frequently occupied depths as deep as 400 m during the day, potentially reflecting targeting of mesopelagic prey (Polovina et al., 2008). Similar information on the physiological capabilities and habitat use of bigeye and smalleye Pacific opah, and their prey, will help resolve niche separation and essential habitat.

Implications of sympatric or cryptic species for fisheries management

The presence of morphologically similar species in landings can cause issues with fisheries management. For example, the population status of white marlin (*Kajikia albida*) had to be reevaluated when it was discovered that pelagic longline fisheries in the North Atlantic Ocean were unknowingly landing significant amounts of the similar-looking roundscale spearfish (*Tetrapturus georgii*) without separating them in the catch records (Beerkircher et al., 2009). Although we have studied the spatial distributions of both opah species, they are still listed as a single species in logbooks and landings data. It will, therefore, be important to collect fisheries data and conduct scientific studies for specific species. Establishing distinct, species-specific management strategies and techniques is important because changes to the fishery range, gear, or landing

[5] Ducharme-Barth, N., and M. Vincent. 2020. Analysis of Pacific-wide operational longline dataset for bigeye and yellowfin tuna catch-per-unit-effort (CPUE). Sci. Comm. sixteenth regular session; online, 11–20 August. West. Cent. Pac. Fish. Comm., Inf. Pap. WCPFC-SC16-2020/SA-IP-07, 55 p. [Available from website.]

rates may disproportionately affect 1 species and unknowingly lead to unsustainable harvest rates.

Conclusions

In this study, species-specific spatial distributions were estimated for bigeye Pacific opah and smalleye Pacific opah in U.S. longline fisheries in the North Pacific Ocean, information that has filled important knowledge gaps. Future work incorporating genetic and fisheries data—including latitude, longitude, and depth of capture—for samples collected in a broader spatial range—would help reduce uncertainty regarding the spatial distributions of and overlap between the 2 species. In addition, it would be important to determine differences and similarities between the essential habitats of each opah species, including foraging ecology, to better quantify the vulnerability of each species to different gear configurations. Better understanding of the species ranges and associations with different pelagic environments will improve efforts for management of bigeye and smalleye Pacific opah.

Acknowledgments

We recognize the data managers at the Pacific Islands Fisheries Science Center for providing data and insight on Hawaii pelagic longline fisheries, the vessel captains for providing the logbook data, and the U.S. and Pacific Islands Region Observer Programs for the observer data. We thank Catalina Offshore Products and the Honolulu Fish Auction for providing opah samples for genetic testing and L. Martin and the rest of the NOAA Southwest Fisheries Science Center genetics team for helping with collection and analysis of genetic samples. We appreciate A. Yau, K. Blincow, and E. Portner for valuable guidance and the 2 anonymous reviewers for their thorough feedback.

Literature cited

Aksnes, D. L., A. Røstad, S. Kaartvedt, U. Martinez, C. M. Duarte, and X. Irigoien.
2017. Light penetration structures the deep acoustic scattering layers in the global ocean. Sci. Adv. 3(5):e1602468.

Beerkircher, L., F. Arocha, A. Barse, E. Prince, V. Restrepo, J. Serafy, and M. Shivji.
2009. Effects of species misidentification on population assessment of overfished white marlin *Tetrapturus albidus* and roundscale spearfish *T. georgii*. Endanger. Species Res. 9:81–90.

Bigelow, K. A., C. H. Boggs, and X. He.
1999. Environmental effects on swordfish and blue shark catch rates in the US North Pacific longline fishery. Fish. Oceanogr. 8:178–198.

Bigelow, K. A., J. Hampton, and N. Miyabe.
2002. Application of a habitat-based model to estimate effective longline fishing effort and relative abundance of Pacific bigeye tuna (*Thunnus obesus*). Fish. Oceanogr. 11:143–155.

Bigelow, K., M. K. Musyl, F. Poisson, and P. Kleiber.
2006. Pelagic longline gear depth and shoaling. Fish. Res. 77:173–183.

Block, B. A., I. D. Jonsen, S. J. Jorgensen, A. J. Winship, S. A. Shaffer, S. J. Bograd, E. L. Hazen, D. G. Foley, G. A. Breed, A.-L. Harrison, et al.
2011. Tracking apex marine predator movements in a dynamic ocean. Nature 475:86–90.

Choy, C. A., E. Portner, M. Iwane, and J. C. Drazen.
2013. Diets of five important predatory mesopelagic fishes of the central North Pacific. Mar. Ecol. Prog. Ser. 492:169–184.

de Boyer Montégut, C., G. Madec, A. S. Fischer, A. Lazar, and D. Iudicone.
2004. Mixed layer depth over the global ocean: an examination of profile data and a profile-based climatology. J. Geophys. Res. 109:C12003

Deser, C., M. A. Alexander, S.-P. Xie, and A. S. Phillips.
2010. Sea surface temperature variability: patterns and mechanisms. Ann. Rev. Mar. Sci. 2:115–143.

Dewar, H., E. D. Prince, M. K. Musyl, R. W. Brill, C. Sepulveda, J. Luo, D. Foley, E. S. Orbesen, M. L. Domeier, N. Nasby-Lucas, et al.
2011. Movements and behaviors of swordfish in the Atlantic and Pacific Oceans examined using pop-up satellite archival tags. Fish. Oceanogr. 20:219–241.

Dunn, D. C., S. M. Maxwell, A. M. Boustany, and P. N. Halpin.
2016. Dynamic ocean management increases the efficiency and efficacy of fisheries management. Proc. Natl. Acad. Sci. 113:668–673.

Federal Register.
2004. Fisheries off West Coast states and in the western Pacific; western Pacific pelagic fisheries; pelagic longline fishing restrictions, seasonal area closure, limit on swordfish fishing effort, gear restrictions, and other sea turtle take mitigation measures. Fed. Regist. 69:17329–17354. [Available from website.]

Hanamoto, E.
1987. Effect of oceanographic environment on bigeye tuna distribution. Bull. Japan. Soc. Fish. Oceanogr. 51(3):203–216.

Hawn, D. R., and B. B. Collette.
2012. What are the maximum size and live body coloration of opah (Teleosti: Lampridae: *Lampris* species)? Icthyol. Res. 59:272–275.

Howell, E. A., and D. R. Kobayashi.
2006. El Niño effects in the Palmyra Atoll region: oceanographic changes and bigeye tuna (*Thunnus obesus*) catch rate variability. Fish. Oceanogr. 15:477–489.

Hyde, J. R., K. E. Underkoffler, and M. A. Sundberg.
2014. DNA barcoding provides support for a cryptic species complex within the globally distributed and fishery important opah (*Lampris guttatus*). Mol. Ecol. Resour. 14:1239–1247.

Karstensen, J., L. Stramma, and M. Visbeck.
2008. Oxygen minimum zones in the eastern tropical Atlantic and Pacific oceans. Prog. Oceanogr. 77:331–350.

Kröger, R. H. H., K. A. Fritsches, and E. J. Warrant.
2009. Lens optical properties in the eyes of large marine predatory teleosts. J. Comp. Physiol., A 195:175–182.

Maxwell, S. M., E. L. Hazen, R. L. Lewison, D. C. Dunn, H. Bailey, S. J. Bograd, D. K. Briscoe, S. Fossette, A. J. Hobday, M. Bennett, et al.
2015. Dynamic ocean management: defining and conceptualizing real-time management of the ocean. Mar. Policy 58:42–50.

Nakano, H., M. Okazaki, and H. Okamoto.
1997. Analysis of catch depth by species for tuna longline fishery based on catch by branch lines. Bull. Nat. Res. Inst. Far Seas Fish. 34:43–62.

NMFS (National Marine Fisheries Service).
2016. Endangered Species Act section 7(a)(2) biological opinion for the continued operation of the West Coast-based deep-set longline fishery managed under the fishery management plan for U.S. West Coast highly migratory species (WCR-2015-2948), 90 p. [Available from Calif. Coast. Off., West Coast Reg. Off., Natl. Mar. Fish. Serv., 501 West Ocean Blvd., Ste. 4200, Long Beach, CA 90802.]

Polovina, J. J., and P. A. Woodworth-Jefcoats.
2013. Fishery-induced changes in the subtropical Pacific pelagic ecosystem size structure: observations and theory. PLoS ONE 8(4):e62341.

Polovina, J. J., E. Howell, D. R. Kobayashi, and M. P. Seki.
2001. The transition zone chlorophyll front, a dynamic global feature defining migration and forage habitat for marine resources. Prog. Oceanogr. 49:469–483.

Polovina, J. J., D. Hawn, and M. Abecassis.
2008. Vertical movement and habitat of opah (*Lampris guttatus*) in the central North Pacific recorded with pop-up archival tags. Mar. Biol. 153:257–267.

Prince, E. D., and C. P. Goodyear.
2006. Hypoxia-based habitat compression of tropical pelagic fishes. Fish. Oceanogr. 15:451–464.

R Core Team.
2019. R: a language and environment for statistical computing. R Foundation for Statistical Computing, Vienna, Austria. [Available from website, accessed July 2019.]

Roden, G. I.
1991. Subarctic-subtropical transition zone of the North Pacific: large-scale aspects and mesoscale structure. *In* Biology, oceanography, and fisheries of the North Pacific transition zone and subarctic frontal zone (J. A. Wetherall, ed.), p. 1–38. NOAA Tech. Rep. NMFS 105.

Rykaczewski, R. R., and D. M. Checkley Jr.
2008. Influence of ocean winds on the pelagic ecosystem in upwelling regions. Proc. Natl. Acad. Sci. 105:1965–1970.

Sculley, M. L., and J. Brodziak.
2020. Quantifying the distribution of swordfish (*Xiphias gladius*) density in the Hawaii-based longline fishery. Fish. Res. 230:105638.

Signorini, S. R., B. A. Franz, and C. R. McClain.
2015. Chlorophyll variability in the oligotrophic gyres: mechanisms, seasonality and trends. Front. Mar. Sci. 2:1.

Tont, S. A.
1976. Deep scattering layers: patterns in the Pacific. CalCOFI Rep. 18:112–117.

Underkoffler, K. E., M. A. Luers, J. R. Hyde, and M. T. Craig.
2018. A taxonomic review of *Lampris guttatus* (Brünnich 1788) (Lampridiformes; Lampridae) with descriptions of three new species. Zootaxa 4413:551–565.

Walsh, W. A., and J. Brodziak.
2016. Applications of Hawaii longline fishery observer and logbook data for stock assessment and fishery research. NOAA Tech. Memo. NMFS-PIFSC-57, 62 p.

Wegner, N. C., O. E. Snodgrass, H. Dewar, and J. R. Hyde.
2015. Whole-body endothermy in a mesopelagic fish, the opah, *Lampris guttatus*. Science 348:786–789.

Wood, S. N.
2017. Generalized additive models: an introduction with R, 2nd ed., 496 p. CRC Press, Boca Raton, FL.

Woodworth-Jefcoats, P. A., J. J. Polovina, and J. C. Drazen.
2018. Synergy among oceanographic variability, fishery expansion, and longline catch composition in the central North Pacific Ocean. Fish. Bull. 116:228–239.

WPRFMC (Western Pacific Regional Fishery Management Council).
2021. Annual stock assessment and fishery evaluation report: 2020. Pacific Island pelagic fishery ecosystem plan (T. Remington, M. Fitchett, A. Ishizaki, and J. DeMello, eds.), 410 p. West. Pac. Reg. Fish. Manag. Counc., Honolulu, HI. [Available from website.]

National Marine
Fisheries Service
NOAA

Fishery Bulletin
established in 1881

Spencer F. Baird
First U.S. Commissioner
of Fisheries and founder
of *Fishery Bulletin*

Consumption of Pacific salmon (*Oncorhynchus* spp.) by California sea lions (*Zalophus californianus*) and Steller sea lions (*Eumetopias jubatus*) in northwest Washington during 2010–2013

Jonathan J. Scordino (contact author)[1]
Cydni Marshall[2]
Adrianne M. Akmajian[3]
Daniel Shay[2]
Randall James[2]

Email address for contact author: jonathan.scordino@makah.com

[1] Marine Mammal Program
Makah Fisheries Management, Makah Tribe
150 Resort Drive
Neah Bay, Washington 98357

[2] Institute of Science and Technology
North Central High School
1600 North Howard Street
Spokane, Washington 99205

[3] Marine Ecology Program
Makah Fisheries Management, Makah Tribe
150 Resort Drive
Neah Bay, Washington 98357

Abstract—Pacific salmon (*Oncorhynchus* spp.) are important to the ecology, economy, and cultures of the Pacific Northwest. Many populations of Pacific salmon in the Pacific Northwest are declining because of poor marine survival. We evaluated the role of Steller (*Eumetopias jubatus*) and California (*Zalophus californianus*) sea lions as predators of Pacific salmon. Roughly, half of the 1330 metric tons (t) of Pacific salmon eaten by Steller sea lions per year and of the 1220 t of Pacific salmon eaten by California sea lions per year in northwest Washington during 2010–2013 were coho salmon (*O. kisutch*). The response of Steller and California sea lions to the large run of pink salmon (*O. gorbuscha*) in 2011 was less than expected. Sea lions of these species rarely ate large (roughly ≥50 cm in total length) Chinook salmon (*O. tshawytscha*), indicating that they have limited direct competition for prey with the southern resident distinct population segment of killer whales (*Orcinus orca*). Combined, California and Steller sea lions in northwest Washington consumed a mass of coho salmon similar to that landed by commercial fisheries in Washington State. More work on modeling the effect of the predation by California and Steller sea lions on salmon populations, particularly for coho salmon, is needed to better evaluate the conservation and productivity of Pacific salmon.

Manuscript submitted 21 December 2021.
Manuscript accepted 27 April 2022.
Fish. Bull. 120:150–161 (2022).
Online publication date: 19 May 2022.
doi: 10.7755/FB.120.2.5

The views and opinions expressed or implied in this article are those of the author (or authors) and do not necessarily reflect the position of the National Marine Fisheries Service, NOAA.

Pacific salmon (*Oncorhynchus* spp.) are keystone species in the ecology (Willson and Halupka, 1995; Lincoln et al., 2020), economy (Amberson et al., 2016), and cultures (Butler and Campbell, 2004; Amberson et al., 2016; Korzow Richter et al., 2020; Atlas et al., 2021) of the Pacific Northwest. These species are taken by many predators (Willson and Halupka, 1995; Lincoln et al., 2020) throughout their life cycle and are important because they deliver marine-derived nutrients to freshwater (Zhang et al., 2003) and terrestrial ecosystems (Schindler et al., 2003; Walsh et al., 2020).

Many stocks of Pacific salmon along the West Coast of the United States are currently imperiled, and their important role in Pacific Northwest ecosystems is threatened (O'Higgins, 2015). Results from recent research indicate that the marine life phase of Pacific salmon plays a more important role in salmon population dynamics than had been previously recognized (Sobocinski et al., 2021; Welch et al., 2021). During the marine life phase, survival of species of Pacific salmon is affected by climatic conditions (Mueter et al., 2005; Crozier et al., 2021), interspecific and intraspecific competition with other Pacific salmon (Ruggerone and Nielsen, 2004; Kendall et al., 2020), and predators (Chasco et al., 2017a; Seitz et al., 2019; Sherker et al., 2021). Across the North Pacific Ocean, Pacific salmon are becoming smaller and are more frequently spawning at younger ages (Ohlberger et al., 2018; Losee et al., 2019), reducing their reproductive potential (Ohlberger et al., 2020; Oke et al., 2020). Manishin et al. (2021) found that these changes observed in the demographic structure of Chinook salmon (*O. tshawytscha*) could be attributed to recent increases in the mortality rate of salmon in the life stage after their first winter in the ocean and suggested that high predation rates could be a major factor in mortality. More research is needed to improve our understanding of where and when predation of Pacific salmon occurs, particularly for recovery efforts

of evolutionary significant units of salmon listed as threatened or endangered under the U.S. Endangered Species Act (ESA) (Federal Register, 1999).

In northwest Washington from 2010 through 2013, Pacific salmon made up 11.7% of the diet of Steller sea lions (*Eumetopias jubatus*) and 13.5% of the diet of California sea lions (*Zalophus californianus*), and estimates of the consumption of Pacific salmon were 1330 and 1220 metric tons (t) per year for Steller and California sea lions, respectively (Scordino et al., 2022). Counts of Steller and California sea lions in northwest Washington increased 7.9% and 7.8% per year during 2010–2018 (Allyn and Scordino, 2020). The rise in abundance of these sea lion species likely has led to a doubling of the levels of consumption of Pacific salmon estimated by Scordino et al. (2022) for Steller and California sea lions over the past decade. The method of prey identification used by Scordino et al. (2022) could not be used to reliably identify salmon to the species level (Purcell et al., 2004; Korzow Richter et al., 2020), preventing evaluation of consumption of salmon by species.

The objective of this study was to conduct genetic analysis of the salmon bones used in the work reported in Scordino et al. (2022) to determine the seasonal and annual consumption of Pacific salmon by species and size class for California and Steller sea lions in northwest Washington. Determining the species and size class of Pacific salmon consumed by these species will allow improvements in modeling of effects of this predation on species of Pacific salmon and of the competition between fisheries and Steller and California sea lions (Chasco et al., 2017a, 2017b). This information will also help in evaluation of the hypothesis by Hilborn et al. (2012) that predation by sea lions and other predators on large Chinook salmon (≥50 cm in total length [TL]) reduces the availability of this resource to killer whales (*Orcinus orca*) of the endangered southern resident distinct population segment (Federal Register, 2005) that depend on large Chinook salmon as their primary prey (Ford et al., 1998, 2016; Hanson et al., 2021). A second objective of the study described here was to document how California and Steller sea lions responded to the large increase in the number of Pacific salmon present in 2011 due to the large odd-year run of pink salmon (*O. gorbuscha*) (Losee et al., 2019).

Materials and methods

Sample collection

All scat samples analyzed in this study were collected at haul-out sites used by California and Steller sea lions in northwest Washington (Fig. 1), as reported by Scordino et al. (2022). Site selection for scat collections depended on distributions of California and Steller sea lions and on the ability of researchers to land safely at sites. Samples of Steller sea lion scat were collected primarily from haul-out sites in the Tatoosh Island Complex in the winter and spring and from Sea Lion Rock in the summer and fall; scats were obtained monthly between August 2010 and February 2013 as conditions allowed. Samples of California sea lion scat were collected primarily from East Bodelteh Island in the Bodelteh Island Complex and only in the spring, summer, and fall (Table 1).

Processing of salmon bones

Scat samples were cleaned either by washing them in paint strainer bags in a residential-style washing machine or by washing them through nested sieves (Orr et al., 2003). After cleaning, hard parts from the scat were hand-picked from the paint strainer bag or sieves and placed in a glass vial with 70% isopropyl alcohol. Hard parts were then air-dried in a heated room. S. Riemer of the Oregon Department of Fish and Wildlife identified prey hard parts to the lowest taxonomic level possible on the basis of comparisons with a reference collection of fish and cephalopod hard parts from the region (Scordino et al., 2022). Salmon bones were identified to the family level because salmon bones cannot reliably be identified to species by using morphological features (Korzow Richter et al., 2020). Identified salmon bones were separated from the rest of the prey hard parts into gelatin capsules for subsequent analysis.

Salmon bones were sorted by the size of salmon consumed on the basis of a comparison to a reference collection of salmon from estuaries and coastal areas of the Pacific Northwest. Bones from salmon consumed during their first year in the ocean, fish that were roughly less than 25 cm TL (Duffy and Beauchamp, 2011), were assigned to the small size class of salmon. The large size class of salmon corresponded with the size range of returning adult salmon, fish that were roughly 50 cm TL and greater. Recovered salmon bones that could not be definitely sorted to the large or small size class, because the bone had eroded during digestion or because the recovered type of bone (e.g., gill rakers) is known to have a wide range of sizes within a fish, were recorded as salmon of unclassified size. This unclassified size class also includes medium-sized salmon ranging roughly from 25 to 50 cm TL. Our reporting of recovered bones from salmon in the small and large size classes are minimum estimates because an unknown proportion of the unclassified size class was composed of small and large salmon.

We selected 2–3 representative salmon bones from each size class in each scat sample for genetic analysis. In the genetic analysis, a single bone from each size class was used for species determination. If the sample failed to amplify sufficiently for species identification, another representative bone was analyzed. Our research method required the assumption that the sea lions ate only 1 species of salmon per each size class of salmon observed in a scat sample because we did not have enough funding to analyze all of the salmon bones found in scat samples from the Scordino et al. (2022) study. This assumption likely is not valid given that a previous study found more than one species of salmon present in the gastrointestinal tract of 3 of 28 sea lions sampled (Roffe and Mate, 1984).

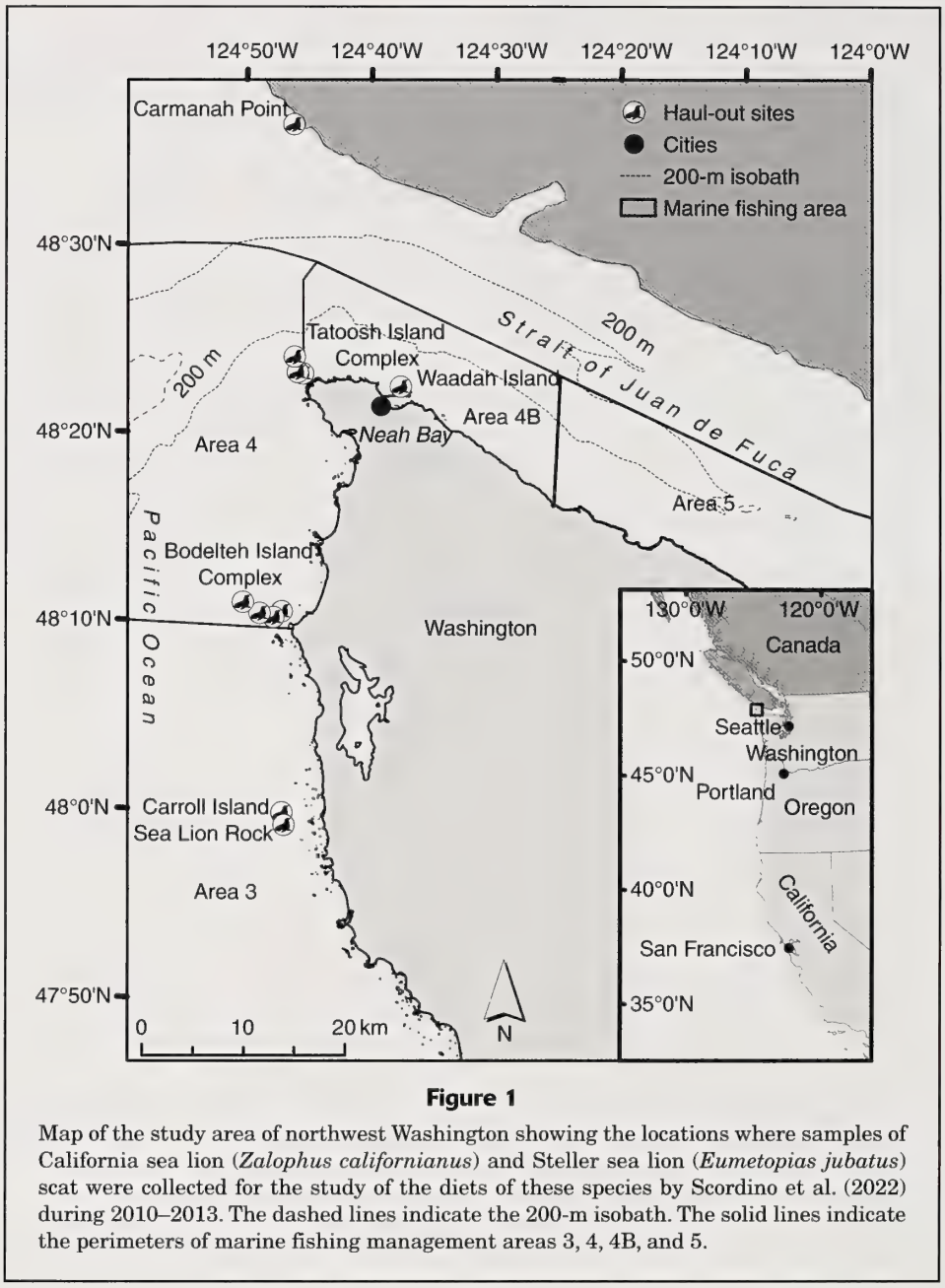

Figure 1

Map of the study area of northwest Washington showing the locations where samples of California sea lion (*Zalophus californianus*) and Steller sea lion (*Eumetopias jubatus*) scat were collected for the study of the diets of these species by Scordino et al. (2022) during 2010–2013. The dashed lines indicate the 200-m isobath. The solid lines indicate the perimeters of marine fishing management areas 3, 4, 4B, and 5.

Genetic analysis

Salmon bones were pulverized in a BeadBug[1] homogenizer (SKU D1030, Benchmark Scientific, Sayreville, NJ) by using 2-mL prefilled sterile tubes containing 3-mm zirconium beads (SKU D1032-30, Benchmark Scientific). Pulverized bone samples were then digested for 24 h at 56°C in 500 µL of extraction buffer (0.5 M EDTA pH 8, 1 M urea, and 20 mg/µL proteinase K) with constant rotation. After 24 h, digested samples were centrifuged at 1000 g for 5 min to pellet bone material. After centrifugation, the supernatant lysate was carefully pipetted into sterile 15-mL falcon tubes, and DNA was purified from the supernatant lysate by using a QIAquick PCR purification kit (catalog no. 28104, Qiagen, Hilden, Germany). To increase DNA yield, the elution buffer was heated to 60°C prior to it being adding to the column during the elution step.

We used species-specific primers and Applied Biosystems TaqMan MGB probes (minor groove binder probes, Thermo Fisher Scientific, Waltham, MA) developed by Rasmussen Hellberg et al. (2010) for identifying salmon bones as chum salmon (*O. keta*), Chinook salmon, pink salmon, steelhead (*O. mykiss*), sockeye salmon (*O. nerka*), or coho salmon (*O. kisutch*) on the basis of 915 cytochrome *c* oxidase subunit I DNA barcode sequences (Table 2). No TaqMan MGB probes were used for cutthroat trout

[1] Mention of trade names or commercial companies is for identification purposes only and does not imply endorsement by the National Marine Fisheries Service, NOAA.

Table 1

Summary of the sampling of Steller sea lion (*Eumetopias jubatus*) and California sea lion (*Zalophus californianus*) scat conducted by Scordino et al. (2022) from 2010 through 2013 in northwest Washington by year, season, and month.

		Spring			Summer			Fall			Winter			
Species	Year	Mar	Apr	May	Jun	Jul	Aug	Sep	Oct	Nov	Dec	Jan	Feb	Total
Steller sea lion	2010	0	0	0	0	0	32	3	0	27	0	0	0	62
	2011	48	18	24	35	36	42	4	31	36	0	38	0	312
	2012	38	35	34	28	36	38	35	22	38	8	0	39	351
	2013	0	0	0	0	0	0	0	0	0	0	34	17	51
California sea lion	2010	0	0	0	0	0	0	42	0	0	0	0	0	42
	2011	0	0	47	2	0	0	0	0	51	0	0	0	100
	2012	0	0	0	48	0	0	51	22	0	0	0	0	121

Table 2

Species-specific primers used to identify bones of Pacific salmon (*Oncorhynchus* spp.), found in scat of Steller sea lions (*Eumetopias jubatus*) and California sea lions (*Zalophus californianus*), to species by using real-time polymerase chain reactions. Scat samples were collected in northwest Washington from 2010 through 2013. Forward (F) and reverse (R) primers developed by Rasmussen Hellberg et al. (2010) and TaqMan minor groove binder probes were used. bp=base pair.

Species	Primer or probe	Sequence (5'–3')	Amplicon size
Chum salmon	F	TTGTCTGAGCTGTACTAATCACTG	104 bp
	R	AAGTGGTGTTTAAATTTCGATC	
	P	VIC-CAACATAGTAATACCTGCTG-MGB	
Chinook salmon	F	GATAGTAGGCACCGCCCTTAGT	183 bp
	R	CCGATCATTAGGGGAATTAATCAGT	
	P	NED-TCATAATCGGCATAACTAT-MGB	
Pink salmon	F	TACGACCATTATCAACATAAAACCA	143 bp
	R	GGTCCGTGAGCAACATAGTG	
	P	6FAM-CGGCAATCTCTCAGT-MGB	
Steelhead	F	ACCATTATTAACATAAAACCTCCAG	121 bp
	R	GTAATGCCTGCTGCCAGG	
	P	VIC-CGTTTGAGCCGTGCTA-MGB	
Sockeye salmon	F	GGAAACCTTGCCCACGCG	152 bp
	R	AAAAGTGGGGTCTGGTACTGAG	
	P	6FAM-CTCTGTTGACTTAACCATC-MGB	
Coho salmon	F	CGCTCTTCTAGGGGATGATC	95 bp
	R	CTCCGATCATAATCGGCATG	
	P	VIC-ATTTACAACGTAATCGTC-MGB	

(*O. clarkii*) or bull trout (*Salvelinus confluentus*) because they are not common in the study area relative to other salmonids (Brenkman and Corbett, 2005; Pearcy et al., 2018) and because a TaqMan MGB probe has not been developed for these species (Rasmussen Hellberg et al., 2010).

An optimized multiplexed TaqMan presence-absence assay was performed in triplicate on all purified DNA samples by using an Applied Biosystems StepOnePlus Real-Time PCR System (catalog no. 4376787, Thermo Fisher Scientific). Primer concentrations were 900 nM, and probe concentrations were 250 nM. Each run was accompanied by internal positive and negative controls. Analysis was performed by using Applied Biosystems StepOne Real-Time PCR Software, vers. 2.0 (Thermo Fisher Scientific) built into the StepOnePlus Real-Time PCR System. This software was run by using a presence-absence setting that

works by measuring the intensity of the flourogenic signal from the species-specific probes. The threshold for a positive identification was set by the StepOne software to the exponential phase of the amplification curve. Samples of salmon bones that had a single species read past a set threshold of fluorogenic signal intensity were recorded as a positive read for the species identified. Samples with no amplification or multiple signals were recorded as unidentified salmon. All parameters were set to best accommodate all primer temperature sensitivities with the optimized annealing temperature of 53°C (Rasmussen Hellberg et al., 2010).

Assessment of genotyping accuracy

We conducted a blind study of 15 samples of known Pacific salmon species provided by the NOAA Northwest Fisheries Science Center to evaluate our genotyping error rate. We provided the samples to our laboratory team (C. Marshall, R. James, and D. Shay) at the Institute of Science and Technology of North Central High School in Spokane, Washington, with unique identifiers that did not identify the species of salmon of the sample. The laboratory team ran the samples along with the salmon bones collected from samples of California and Steller sea lion scat.

Data analysis

Species of Pacific salmon identified as prey in scat samples and their size classes were tabulated for each sample. We combined the results from our genetic analysis with the sea lion diet data available from Scordino et al.[2] to calculate the split-sample frequency of occurrence (SSFO) of Pacific salmon by size class, species, and combination of species and size class. We calculated SSFO twice. In the first calculation, we included a species category of *unidentified salmon*. For the second calculation of SSFO, we assumed that the salmon bones identified in our work were a representative sample of unidentified salmon bones and incorporated the unidentified bones into data for identified prey species proportionally according to identifications within each salmon bone size class.

The following formula was used to calculate SSFO:

$$SSFO_i = \frac{\sum_{k=1}^{i} (O_{ik} / O_k)}{s} \times 100,$$

where O_{ik} = 0 if taxon i is absent in scat sample k and 1 if taxon i is present in scat sample k,

O_k = total number of all taxa present in scat sample k; and

s = total number of scat samples that contained prey (Olesiuk et al., 1990).

In many studies, SSFO has been used to reconstruct pinniped diets (Olesiuk et al., 1990; Tollit et al., 2015), but it does have the potential to overreport the importance of small prey and underreport the importance of large prey (Laake et al., 2002; Tollit et al., 2007). The resultant SSFO values were multiplied by the prey consumption estimates for California and Steller sea lions by Scordino et al. (2022) to provide an estimate of annual biomass of Pacific salmon consumed by species, by size class, and by species and size class during 2010–2013 in northwest Washington.

We used Pearson's chi-square (χ^2) and Fisher's exact tests to evaluate differences in the species and size composition of Pacific salmon consumed. First, we compared consumption of each Pacific salmon species by season and year within the diet of each sea lion species and between the diets of the 2 species of sea lions. Second, we evaluated differences in the size-class composition of Pacific salmon consumed by season and year within the diet of each sea lion species and between the diets of the 2 species. For yearly comparisons between species, only samples collected in spring, summer, and fall were used because no samples of California sea lion scat were collected during winter. Annual comparisons of Pacific salmon consumed for each species included only data for 2011 and 2012 because samples were collected in all seasons during those years. For analyses of the species composition of Pacific salmon consumed, only samples identified to species were used; we excluded unidentified salmon from these analyses.

Comparison of salmon consumption by sea lions to fishery landings

For the period from 2010 through 2013, we downloaded commercial salmon fishery data from the Pacific Fisheries Information Network APEX reporting system (available from website). The data comprise commercial landings records from both the treaty tribal fisheries and non-treaty fisheries. We calculated the average annual commercial catch of Pacific salmon from 2010 through 2013 for coastal Washington (ports along the Pacific coast, estuaries, and Neah Bay) and for all of Washington State to compare commercial catch to estimates of consumption of Pacific salmon by California and Steller sea lions.

Results

Genetic analysis was conducted on 361 samples of bones identified as those of Pacific salmon by Scordino et al. (2022). Bone samples were from 330 samples of California (93 bone samples, 89 scat samples) and Steller (268 bone samples, 241 scat samples) sea lion scat. For 4 samples of California sea lion scat and 27 samples of Steller sea lion scat, 2 size classes of salmon were identified; for all other scat samples, a single size class of salmon was identified. All data evaluated in the research described in this paper are publicly available (Scordino et al.[3]).

[2] Scordino, J., A. Akmajian, and S. Riemer. 2021. Steller and California sea lion count and diet data in northwest Washington, 2010–2013. Mendeley Data, V1. [Available from website.]

[3] Scordino, J., A. Akmajian, C. Marshall, S. Riemer, R. James, and D. Shay. 2022. Diets of Steller and California sea lions determined from scat collections in northwest Washington during 2010–2013 with genetic identification of salmon species. Mendeley Data, V2. [Available from website.]

Of the scat from California sea lions, 37 samples had remains of Pacific salmon in the large size class, 10 samples had bones of salmon in the small size class, and 46 samples had bones from salmon of an unclassified size. Of the scat from Steller sea lions, 53 samples had remains of Pacific salmon in the large size class, 59 samples had bones of salmon in the small size class, and 156 samples had bones from salmon of an unclassified size. We found a significant difference in the proportion of Pacific salmon of each size class consumed between California and Steller sea lions by pooling samples from spring, summer, and fall (Pearson's χ^2=6.64, df=2, P=0.036). California sea lions more frequently ate large salmon and less frequently ate small salmon in comparison with Steller sea lions.

Through our genetic analysis, the species was determined for 305 of the 361 salmon bones analyzed (84.5%) (Table 3). For both California and Steller sea lions, coho salmon was the most frequently identified salmon species in all 3 size classes (Table 3). Pooling bones of Pacific salmon in all size classes from scat samples collected in the spring, summer, and fall, we found significant differences in the composition of Pacific salmon species consumed by California and Steller sea lions (Pearson's χ^2=13.22, df=5, P=0.021).

Both California and Steller sea lions had significant differences in the composition of Pacific salmon species they consumed by season, with all size classes of Pacific salmon pooled (Suppl. Table 1 [online only]; Steller sea lion: χ^2=98.2, df=2, P<0.0001; California sea lion: χ^2=22.7, df=10, P=0.012). Coho salmon was the most frequently identified salmon species in samples of California sea lion scat collected in fall and winter; chum and pink salmon were the most commonly identified species from samples collected in spring. Coho salmon was the most frequently identified salmon species in samples of Steller sea lion scat collected in the fall, spring, and winter; the majority of salmon bones identified from samples collected in summer were pink salmon. We found no significant differences by size class in the species composition of Pacific salmon consumed by California and Steller sea lions (Suppl. Table 2) (online only).

We tested the responses of California and Steller sea lions to the large increase of pink salmon available in 2011 (Losee et al., 2019) by comparing the species composition of Pacific salmon consumed between 2011 and 2012. We found no significant difference in the annual species composition of Pacific salmon consumed by Steller sea lions in 2011 and 2012. We further compared Pacific salmon consumption between years by using only samples collected in summer because commercial fishery landings of adult pink salmon are typically highest in the study area in the summer. We found inconclusive but suggestive evidence of differences in the composition of Pacific salmon species consumed between summer 2011 and summer 2012 (Fisher's exact test: P=0.058), with pink salmon accounting for a larger percentage of the salmon consumed in 2011 than in 2012. We had to limit our analysis of the response of California sea lions to samples collected in the fall in 2010, 2011, and 2012 because samples were not collected in spring and summer in all years (Table 1). We found significant differences in the composition of Pacific salmon species identified by year (Fisher's exact test: P<0.001), with coho salmon being the dominant species among species identified in 2010 and 2012 and chum salmon being the dominant identified species in 2011.

Salmon consumption estimates

Data on salmon species identified from the genetic analysis in this study was combined with data on the diets of California and Steller sea lions from Scordino et al.[2] to compute the SSFO by Pacific salmon species identified and for unidentified salmon by size class. We assumed that our calculated SSFO was equivalent to percentage of diet (Olesiuk et al., 1990). Coho salmon composed the largest portion of the diets of California and Steller sea lions among the Pacific salmon species identified in scat

Table 3

Species composition of salmonids (*Oncorhynchus* spp.) identified in scat samples of California sea lions (*Zalophus californianus*) and Steller sea lions (*Eumetopias jubatus*) collected in northwest Washington from 2010 through 2013 by size class and associated sample size of identified salmon and unidentified (Unid.) bones. The size classes of prey species are large (≥50 cm in total length [TL]), small (<25 cm TL), and unclassified (could not be definitely sorted to the large or small size class).

Predator species	Size class	Prey species identified						Sample size	
		Coho	Chum	Chinook	Steelhead	Pink	Sockeye	Unid.	Identified
California sea lion	All classes	46.4%	27.4%	7.1%	3.6%	11.9%	3.6%	9	84
	Large	54.3%	22.9%	5.7%	2.9%	8.6%	5.7%	2	35
	Unclassified	43.6%	30.8%	7.7%	2.6%	15.4%	0.0%	7	39
	Small	30.0%	30.0%	10.0%	10.0%	10.0%	10.0%	0	10
Steller sea lion	All classes	57.0%	13.6%	9.5%	10.9%	8.6%	0.5%	47	221
	Large	47.7%	20.5%	6.8%	11.4%	13.6%	0.0%	9	44
	Unclassified	54.3%	14.2%	8.7%	14.2%	7.9%	0.8%	29	127
	Small	72.0%	6.0%	14.0%	2.0%	6.0%	0.0%	9	50

samples (Fig. 2). Multiplying SSFO by the estimates of consumption computed by Scordino et al. (2022), we found that Steller sea lions ate an average of 714.1 t of coho salmon per year and that California sea lions ate 550.4 t of coho salmon from spring through fall during 2010–2013 (Table 4). Chinook salmon composed 0.8% of the diet of both California and Steller sea lions (Suppl. Table 3) (online only), with average estimates of consumption of 93.6 t per year for Steller sea lions and of 74.1 t for California sea lions from spring through fall during 2010–2013 (Table 4). Proportionally assigning unidentified salmon bones to a salmon species on the basis of the frequency it was identified, we computed that Steller sea lions ate an average of 861.7 t of coho salmon and 116.4 t of Chinook salmon per year and that California sea lions ate 601.0 t of coho salmon and 80.9 t of Chinook salmon from spring through fall in each year (Suppl. Table 4) (online only).

Blind study of identification accuracy

Fifteen samples were provided to our laboratory team for a blind analysis of identification accuracy. The team was able to identify the species for 13 of the 15 samples, and the identification was accurate for all 13 samples.

Comparison of salmon consumption by sea lions to fishery landings

We compared consumption of each Pacific salmon species by California and Steller sea lions to commercial fisheries landings of Pacific salmon on the coast of Washington and in all of Washington State (Table 5). Steller sea lions consumed more coho salmon, chum salmon, pink salmon, and steelhead than were landed in commercial fisheries at coastal ports in Washington. In addition to the species listed for Steller sea lions, California sea lions also consumed more sockeye salmon per year than were landed in commercial fisheries in coastal Washington. In contrast, the combined estimates of consumption for both species of sea lions for Chinook salmon of all size classes was roughly 8.5 times less than the commercial landings of Chinook salmon in coastal Washington. To compare consumption to statewide commercial fishery landings, we combined the consumption estimates for California and Steller sea lions for all size classes of Pacific salmon. We found that California and Steller sea lions eat more steelhead than are landed in commercial fisheries throughout the state of Washington. The total estimated consumption of all size classes of coho salmon by California and Steller sea lions of 1462.8 t is similar to the statewide landings by the commercial fishery of 1646.8 t.

Fisheries generally target Pacific salmon that we would classify as large salmon in our study of consumption of salmon by California and Steller sea lions. Commercial fisheries on the Pacific coast of Washington landed more Pacific salmon of each species, with the exception of sockeye salmon, than our minimum estimate of consumption of large Pacific salmon by sea lions (Table 5).

Discussion

This study is the first to rigorously evaluate consumption of Pacific salmon by California and Steller sea lions in Washington State. We found significant differences between California and Steller sea lions in the size class of Pacific salmon consumed, with Steller sea lions more frequently consuming salmon in the small size class despite being the larger of the 2 sea lion species (Wynne, 1993). Coho salmon was the most frequently consumed salmon for both California and Steller sea lions. This result was not surprising for small Pacific salmon because coho salmon are the most abundant juvenile salmon off the coast of Washington, followed by Chinook salmon (Pearcy and Fisher, 1990). In addition to being more abundant, juvenile coho salmon are typically distributed at shallower depths in the water column than the depths at which Chinook salmon are found (Beamish et al., 2018), likely increasing their vulnerability to predation by sea lions. When consuming large Pacific salmon, California and Steller sea lions most frequently consumed coho salmon despite the greater abundance of returning adult pink, sockeye, and chum salmon migrating through the study area (Losee et al., 2019; Walters et al., 2020).

The total mass of coho salmon consumed by California and Steller sea lions in northwest Washington was similar to the mass of coho salmon landed by

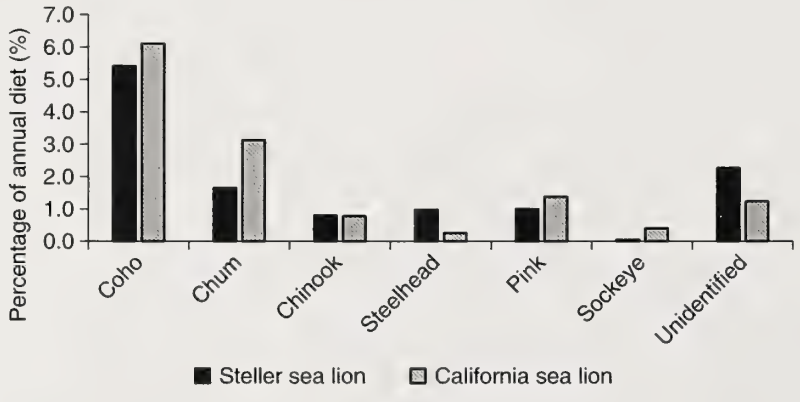

Figure 2

Split-sample frequency of occurrence of salmon species identified in samples of California sea lion (*Zalophus californianus*) and Steller sea lion (*Eumetopias jubatus*) scat collected in northwest Washington from 2010 through 2013. The *Unidentified* category is for salmon bones found in scat samples that we were unable to identify to species through genetic analysis.

Table 4

Estimated average seasonal consumption of salmon in metric tons (t) by Steller (*Eumetopias jubatus*) and California (*Zalophus californianus*) sea lions, by size class of prey and season during 2010–2013 in northwest Washington. Species of salmon were identified by analyzing bones found in sea lion scat. The size classes are small (<25 cm in total length [TL]), large (≥50 cm TL), and unclassified. The total consumption estimates for California sea lions are partial-year estimates from spring through fall (no scat of California sea lions was collected in winter). Consumption of the family Salmonidae is informed by the split-sample frequency of occurrence (SSFO) of prey taxa. The consumption of individual salmon species within size classes is informed by the SSFO of prey identified to the lowest possible taxon, with species of different size classes treated as unique species. As a result, the estimated total consumption of individual species does not equal the total estimated consumption of the family Salmonidae.

	Consumption by Steller sea lions (t)					Consumption by California sea lions (t)			
Taxon	Spring	Summer	Fall	Winter	Annual	Spring	Summer	Fall	Spring–fall
Salmon (Salmonidae)	377.1	116.2	577.0	387.6	1457.9	185.8	183.9	835.1	1204.8
Small size class	93.1	18.0	51.0	121.0	283.1	20.1	3.5	51.9	75.6
Coho salmon	60.5	4.7	22.4	88.2	175.9	0.0	3.5	15.8	19.4
Chum salmon	4.1	0.0	8.2	0.0	12.3	0.0	0.0	26.6	26.6
Chinook salmon	18.1	7.4	0.0	0.0	25.5	4.4	0.0	0.0	4.4
Steelhead	0.0	0.0	0.0	6.2	6.2	7.0	0.0	0.0	7.0
Pink salmon	0.0	3.0	0.0	10.9	13.9	0.0	0.0	9.5	9.5
Sockeye salmon	0.0	0.0	0.0	0.0	0.0	8.8	0.0	0.0	8.8
Unidentified	10.4	3.0	20.4	15.6	49.3	0.0	0.0	0.0	0.0
Unclassified	263.8	53.2	324.6	291.3	932.9	141.6	129.6	301.5	572.7
Coho salmon	120.1	6.6	114.2	159.3	400.2	43.8	58.1	107.7	209.6
Chum salmon	11.3	11.8	90.7	20.0	133.8	39.4	0.0	130.5	169.9
Chinook salmon	34.7	0.0	14.6	6.2	55.6	0.0	0.0	38.0	38.0
Steelhead	21.5	0.0	42.5	41.3	105.3	0.0	5.6	0.0	5.6
Pink salmon	8.1	19.9	10.4	15.6	54.1	40.9	21.2	12.7	74.7
Sockeye salmon	0.0	0.0	0.0	6.2	6.2	0.0	0.0	0.0	0.0
Unidentified	68.1	14.8	52.2	42.7	177.7	17.5	44.7	12.7	74.9
Large size class	37.0	46.4	222.8	7.8	314.0	26.3	49.4	463.6	539.3
Coho salmon	20.3	6.9	110.8	0.0	138.0	0.0	21.2	300.2	321.4
Chum salmon	0.0	4.4	72.3	0.0	76.7	8.8	14.1	70.3	93.2
Chinook salmon	7.3	0.0	5.2	0.0	12.5	0.0	0.0	31.7	31.7
Steelhead	9.5	2.2	0.0	7.8	19.5	8.8	0.0	0.0	8.8
Pink salmon	0.0	18.0	5.2	0.0	23.2	8.8	14.1	7.6	30.5
Sockeye salmon	0.0	0.0	0.0	0.0	0.0	0.0	0.0	28.5	28.5
Unidentified	0.0	14.8	29.2	0.0	44.0	0.0	0.0	25.3	25.3

commercial fisheries throughout the state of Washington. Roughly half of the population of Steller sea lions in Washington State haul out in our study area (Scordino et al.[4]). Furthermore, the positive trend in counts at haul-out sites in northwest Washington (Allyn and Scordino, 2020) indicates that the abundance of California and Steller sea lions has more than doubled over the past decade, and their consumption of Pacific salmon has likely also doubled. Therefore, the total mass of coho salmon consumed by California and Steller sea lions in all of Washington is likely much greater than is landed in commercial fisheries. Future efforts to model marine survival of coho salmon would benefit from inclusion of the abundance of California and Steller sea lions.

Prior to conducting our study, we hypothesized that consumption of Pacific salmon by California and Steller sea lions would be greatest during the summer of odd-numbered years, when large runs of pink salmon are available. Contrary to that expectation, the season with the lowest overall salmon consumption by Steller sea lions was summer, when many adult Pacific salmon, including pink salmon, migrate through the study area. Furthermore, Pacific salmon accounted for a smaller component of the diets of both California and Steller sea lions in 2011 than in 2012. Pink salmon were the most commonly consumed salmon by Steller sea lions during the summer, but not by as much as expected given that, during 2011, roughly 70% of the Pacific salmon returning to Puget Sound were pink salmon (Losee et al., 2019). This result is even more surprising given that results from previous diet

[4] Scordino, J. J., S. J. Jeffries, and B. A. Diehl. 2014. Steller sea lion aerial survey counts in Washington, Oregon, and northern California during the breeding season of 2011. *In* Research and education/outreach to benefit ESA listed and recently delisted marine mammals of northwest Washington (J. J. Scordino and A. M. Akmajian, eds.), p. 190–198. Final report for species recovery grant award NA10NMF4720372. [Available from Makah Fish. Manag., Makah Tribe, P.O. Box 115, Neah Bay, WA 98357.]

Table 5

Comparison of average commercial landings of salmon to salmon consumption by California sea lions (*Zalophus californianus*), Steller sea lions (*Eumetopias jubatus*), and both species combined, by species, from 2010 through 2013 in northwest Washington. Sea lion consumption estimates are reported separately for all and large (≥50 cm in total length) size classes because only large salmon are targeted by commercial fisheries. Estimates of consumption by California sea lions are partial-year estimates that do not include consumption in winter.

			Sea lions in northwest Washington					
	Commercial landings		Steller		California		Both species	
Species	Coastal Washington	All of Washington	All classes	Large class	All classes	Large class	All classes	Large class
Chinook	406.7	2421.0	116.4	14.3	80.9	33.2	197.3	47.4
Chum	143.5	4819.4	271.1	87.5	316.4	97.5	587.5	185.0
Coho	548.3	1646.8	861.7	157.4	601.0	336.5	1462.8	493.9
Pink	67.4	4911.5	116.3	26.5	125.2	31.9	241.6	58.4
Sockeye	7.8	1646.6	7.2	0.0	40.7	29.8	47.9	29.8
Steelhead	84.7	169.7	157.1	22.2	23.4	9.2	180.5	31.4

studies indicate that pinnipeds typically eat fish less than 30 cm in length (Etnier and Fowler, 2010) and that pink salmon are the smallest Pacific salmon.

California and Steller sea lions ate over 2550 t of Pacific salmon per year during 2010–2013 in northwest Washington; therefore, it is logical to examine whether these 2 species of sea lions are affecting the species of Pacific salmon listed under the ESA. The Fishery Regulation Assessment Model is used to model stock-based effects of fisheries on coho and Chinook salmon on the basis of data from recovery of coded-wire tags (Moran et al., 2018). We ran the Fishery Regulation Assessment Model by using data for marine fishing management areas 3, 4, and 4B, areas designated by the Washington Department of Fish and Wildlife that include Carroll Island, Sea Lion Rock, the Tatoosh Island Complex, the Bodelteh Island Complex, and Waadah Island (Fig. 1). We used these data from these areas in 2010–2013 to determine what proportion of the large Chinook and coho salmon consumed by sea lions were likely to be from populations listed as threatened or endangered under the ESA. We assumed for the purpose of this model that California and Steller sea lions eat a composition of stocks of coho and Chinook salmon similar to the stock composition of Pacific salmon caught in fisheries. We found that roughly 3% of the large coho salmon and 5% of the large Chinook salmon in marine fishing management areas 3, 4, and 4B during 2010–2013 were from ESA-listed populations.

The effect of predation by California and Steller sea lions on ESA-listed populations of Chinook salmon is likely less than the effect of commercial fisheries given the disparity in the metric tons of Chinook salmon landed by the fisheries and the metric tons consumed by California and Steller sea lions (Table 5). In contrast, the effect of predation by California and Steller sea lions on ESA-listed populations of coho salmon likely exceeds the effect of commercial fisheries for the reasons previously discussed. California and Steller sea lions may also be affecting the recovery of the threatened population of Lake Ozette sockeye salmon given its small size of 7000 returning adults during 2016–2019 (Haggerty[5]) and the proximity of the outfall of the Ozette River to the haul-out sites we surveyed. Ecosystem modeling that incorporates the direct effect of predation by sea lions on salmon as well as the effects on salmon predators and prey should be conducted to investigate the effect of California and Steller sea lions on populations of salmon in the Pacific Northwest.

A goal of this study was to evaluate if California and Steller sea lions in northwest Washington compete with endangered southern resident killer whales for their preferred prey of large Chinook salmon (Ford and Ellis, 2006; Hanson et al., 2021). We found that large Chinook salmon accounted for at least 0.3% and 0.1% of the diets of California and Steller sea lions, respectively. The small amount of large Chinook salmon consumed by California and Steller sea lions relative to the catch in sport and commercial fisheries in northwest Washington (Table 5) indicates that, in our study area, both species of sea lions are not major direct competitors with killer whales for prey. California and Steller sea lions likely have indirect effects on the availability of prey of killer whales because their predation on small- and medium-sized Chinook salmon reduces the number of Chinook salmon reaching the large size preferred by killer whales. The magnitude of this indirect effect is hard to evaluate because estimates of the number of Chinook salmon eaten are very sensitive to the estimated size of Chinook salmon consumed (Chasco et al., 2017a, 2017b; Nelson et al., 2021). Our size sorting allowed us to make broad interpretations of the size classes of Pacific salmon predated by

[5] Haggerty, M. 2022. Personal commun. Mike Haggerty Consulting, 242 Whiskey Creek Beach Rd., Port Angeles, WA 98363.

California and Steller sea lions, but the approach does not provide size estimates specific enough to allow computation of the number of Pacific salmon consumed. In future studies of the diets of sea lion species, all salmon bones should be measured to allow quantitative estimates of the size of salmon consumed.

Scordino et al. (2022) noted a number of caveats to their interpretation of their diet analysis that also apply to the results of this study. Most important of those caveats is that estimates from this study could overreport the consumption of small Pacific salmon and underreport the consumption of large Pacific salmon because of the use of SSFO to evaluate the diets of California and Steller sea lions (Laake et al., 2002; Tollit et al., 2007). Compounding the underreporting of large Pacific salmon is the possibility that bones from large salmon were not available in scat samples. Otariids are known to regurgitate and spew out bones from large fish (Gudmundson et al., 2006) and to not fully consume large fish, potentially reducing the availability of such bones to be identified (Tollit et al., 2017).

A second important caveat is the possibility that some of the juvenile Pacific salmon for which bones were examined in this study were consumed by another predator that was in turn eaten by a sea lion (Pierce and Boyle, 1991). Sea lions can target small-bodied prey, making it difficult to determine what portion of the bones of small Pacific salmon were from secondary consumption. Fiscus and Baines (1966) found 1280 capelin (*Mallotus villosus*) in the stomach of a juvenile Steller sea lion that had an average mass of 14.1 g, similar to the mass of juvenile Pacific salmon (Chasco et al., 2017a). For the third consideration regarding the results of this study, keep in mind that we analyzed only one bone from each size class of salmon for which bones were found in scat samples of California and Steller sea lions. This approach effectively required the assumption that California and Steller sea lions were eating only one species of Pacific salmon of a given size class during a meal. Roffe and Mate (1984) reported finding more than one species of salmon in sea lion gastrointestinal tracts, and given that result, we may not have detected all of the species of salmon present in each scat sample. Lastly, results from both captive feeding trials and studies in which genetic analysis was used for prey identification indicate that salmon bones are often not found in scat samples, even when sea lions are known to have consumed salmon (Tollit et al., 2003, 2017).

Conclusions

California and Steller sea lions depend on Pacific salmon for a portion of their diets. This dependence can create conservation concerns for depleted runs of Pacific salmon and competition with fisheries given that populations of both species of sea lions in Washington are large and growing. It was not possible to quantify the effect of predation by California and Steller sea lions on populations of Pacific salmon in this study alone. Future studies will benefit from ecosystem modeling that incorporates data on the diets of California and Steller sea lions from this study and from Scordino et al. (2022) to determine the effect of predation by both species of sea lions on populations of Pacific salmon.

Acknowledgments

Field research was conducted under marine mammal research permit no. 14326. Funding for this study was provided by the Species Recovery Grant to Tribes through the National Marine Fisheries Service. P. Gearin, M. Gosho, M. Murner, and A. Chaparro assisted with field and laboratory work. E. Iwamoto provided samples of salmon for our assessment of genotyping error and provided input on study design. T. Petersen conducted the analysis with the Fishery Regulation Assessment Model. We give a special thank you to S. Riemer for identifying and sorting the salmon bones by size class.

Literature cited

Allyn, E. M., and J. J. Scordino.
2020. Entanglement rates and haulout abundance trends of Steller (*Eumetopias jubatus*) and California (*Zalophus californianus*) sea lions on the north coast of Washington state. PLoS ONE 15(8):e0237178.

Amberson, S., K. Biedenweg, J. James, and P. Christie.
2016. "The heartbeat of our people": identifying and measuring how salmon influences Quinault tribal well-being. Soc. Nat. Resour. 29:1389–1404.

Atlas, W. I., N. C. Ban, J. W. Moore, A. M. Tuohy, S. Greening, A. J. Reid, N. Morven, E. White, W. G. Housty, J. A. Housty, et al.
2021. Indigenous systems of management for culturally and ecologically resilient Pacific salmon (*Oncorhynchus* spp.) fisheries. BioScience 71:186–204.

Beamish, R. J., L. A. Weitkamp, L. D. Shaul, and V. I. Radchenko.
2018. Ocean ecology of coho salmon. *In* The ocean ecology of Pacific salmon and trout (R. J. Beamish, ed.), p. 391–554. Am. Fish. Soc., Bethesda, MD.

Brenkman, S. J., and S. C. Corbett.
2005. Extent of anadromy in bull trout and implications for conservation of a threatened species. North Am. J. Fish. Manag. 25:1073–1081.

Butler, V. L., and S. K. Campbell.
2004. Resource intensification and resource depression in the Pacific Northwest of North America: a zooarchaeological review. J. World Prehist. 18:327–405.

Chasco, B., I. C. Kaplan, A. Thomas, A. Acevedo-Gutiérrez, D. Noren, M. J. Ford, M. B. Hanson, J. Scordino, S. Jeffries, S. Pearson, et al.
2017a. Estimates of Chinook salmon consumption in Washington State inland waters by four marine mammal predators from 1970 to 2015. Can. J. Fish. Aquat. Sci. 74:1173–1194.

Chasco, B. E., I. C. Kaplan, A. C. Thomas, A. Acevedo-Gutiérrez, D. P. Noren, M. J. Ford, M. B. Hanson, J. J. Scordino, S. J. Jeffries, K. N. Marshall, et al.
2017b. Competing tradeoffs between increasing marine mammal predation and fisheries harvest of Chinook salmon. Sci. Rep. 7:15439.

Crozier, L. G., B. J. Burke, B. E. Chasco, D. L. Widener, and R. W. Zabel.
2021. Climate change threatens Chinook salmon throughout their life cycle. Commun. Biol. 4:222.

Duffy, E. J., and D. A. Beauchamp.
2011. Rapid growth in the early marine period improves the marine survival of Chinook salmon (*Oncorhynchus tshawytscha*) in Puget Sound, Washington. Can. J. Fish. Aquat. Sci. 68:232–240.

Etnier, M. A., and C. W. Fowler.
2010. Size selectivity in marine mammal diets as a guide to evolutionarily enlightened fisheries management. North Am. J. Fish. Manag. 30:588–603.

Federal Register.
1999. Endangered and threatened species; threatened status for three Chinook salmon evolutionarily significant units (ESUs) in Washington and Oregon, and endangered status for one Chinook Salmon ESU in Washington. Fed. Regist. 64:14308–14328. [Available from website.]

Federal Register.
2005. Endangered and threatened wildlife and plants: endangered status for southern resident killer whales. Fed. Regist. 70:69903–69912. [Available from website.]

Fiscus, C. H., and G. A. Baines.
1966. Food and feeding behavior of Steller and California sea lions. J. Mammal. 47:195–200.

Ford, J. K. B., and G. M. Ellis.
2006. Selective foraging by fish-eating killer whales *Orcinus orca* in British Columbia. Mar. Ecol. Prog. Ser. 316:185–199.

Ford, J. K. B., G. M. Ellis, L. G. Barrett-Lennard, A. B. Morton, R. S. Palm, and K. C. Balcomb III.
1998. Dietary specialization in two sympatric populations of killer whales (*Orcinus orca*) in coastal British Columbia and adjacent waters. Can. J. Zool. 76:1456–1471.

Ford, M. J., J. Hempelmann, M. B. Hanson, K. L. Ayres, R. W. Baird, C. K. Emmons, J. I. Lundin, G. S. Schorr, S. K. Wasser, and L. K. Park.
2016. Estimation of a killer whale (*Orcinus orca*) population's diet using sequencing analysis of DNA from feces. PLoS ONE 11(1):e0144956.

Gudmundson, C. J., T. K. Zeppelin, and R. R. Ream.
2006. Application of two methods for determining diet of northern fur seals (*Callorhinus ursinus*). Fish. Bull. 104:445–455.

Hanson, M. B., C. K. Emmons, M. J. Ford, M. Everett, K. Parsons, L. K. Park, J. Hempelmann, D. M. Van Doornik, G. S. Schorr, J. K. Jacobsen, et al.
2021. Endangered predators and endangered prey: seasonal diet of southern resident killer whales. PLoS ONE 16(3):e0247031.

Hilborn, R., S. P. Cox, F. M. D. Gulland, D. G. Hankin, N. T. Hobbs, D. E. Schindler, and A. W. Trites.
2012. The effects of salmon fisheries on southern resident killer whales: final report of the independent science panel, 61 p. Prepared with the assistance of D. R. Marmorek and A.W. Hall, ESSA Technologies Ltd., Vancouver, B.C., for National Marine Fisheries Service, Seattle, WA, and Fisheries and Oceans Canada, Vancouver, BC. [Available from website.]

Kendall, N. W., B. W. Nelson, and J. P. Losee.
2020. Density-dependent marine survival of hatchery-origin Chinook salmon may be associated with pink salmon. Ecosphere 11:e03061.

Korzow Richter, K., K. McGrath, E. Masson-MacLean, S. Hickinbotham, A. Tedder, K. Britton, Z. Bottomley, K. Dobney, A. Hulme-Beaman, M. Zona, et al.
2020. What's the catch? Archaeological application of rapid collagen-based species identification for Pacific salmon. J. Archaeol. Sci. 116:105116.

Laake, J. L., P. Browne, R. L. DeLong, and H. R. Huber.
2002. Pinniped diet composition: a comparison of estimation models. Fish. Bull. 100:434–447.

Lincoln, A. E., R. Hilborn, A. J. Wirsing, and T. P. Quinn.
2020. Managing salmon for wildlife: do fisheries limit salmon consumption by bears in small Alaskan streams? Ecol. Appl. 30:e02061.

Losee, J. P., N. W. Kendall, and A. Dufault.
2019. Changing salmon: an analysis of body mass, abundance, survival, and productivity trends across 45 years in Puget Sound. Fish Fish. 20:934–951.

Manishin, K. A., C. J. Cunningham, P. A. H. Westley, and A. C. Seitz.
2021. Can late stage marine mortality explain observed shifts in age structure of Chinook salmon? PLoS ONE 16(2):e0247370.

Moran, P., J. Dazey, L. LaVoy, and S. Young.
2018. Genetic mixture analysis supports recalibration of the Fishery Regulation Assessment Model. Fisheries 43:83–97.

Mueter, F. J., B. J. Pyper, and R. M. Peterman.
2005. Relationships between coastal ocean conditions and survival rates of Northeast Pacific salmon at multiple lags. Trans. Am. Fish. Soc. 134:105–119.

Nelson, B. W., S. F. Pearson, J. H. Anderson, S. J. Jeffries, A. C. Thomas, W. A. Walker, A. Acevedo-Gutiérrez, I. M. Kemp, M. M. Lance, A. Louden, and M. R. Voelker.
2021. Variation in predator diet and prey size affects perceived impacts to salmon species of high conservation concern. Can. J. Fish. Aquat. Sci. 78:1661–1676.

O'Higgins, T.
2015. It's not easy being green: a systems approach to environmental management, 120 p. Dunedin Acad. Press, Edinburgh, UK.

Ohlberger, J., E. J. Ward, D. E. Schindler, and B. Lewis.
2018. Demographic changes in Chinook salmon across the Northeast Pacific Ocean. Fish Fish. 19:533–546.

Ohlberger, J., D. E. Schindler, R. J. Brown, J. M. S. Harding, M. D. Adkison, A. R. Munro, L. Horstmann, and J. Spaeder.
2020. The reproductive value of large females: consequences of shifts in demographic structure for population reproductive potential in Chinook salmon. Can. J. Fish. Aquat. Sci. 77:1292–1301.

Oke, K. B., C. J. Cunningham, P. A. H. Westley, M. L. Baskett, S. M. Carlson, J. Clark, A. P. Hendry, V. A. Karatayev, N. W. Kendall, J. Kibele, et al.
2020. Recent declines in salmon body size impact ecosystems and fisheries. Nat. Commun. 11:4155.

Olesiuk, P. F., M. A. Bigg, G. M. Ellis, S. J. Crockford, and R. J. Wigen.
1990. An assessment of the feeding habits of harbour seals (*Phoca vitulina*) in the Strait of Georgia, British Columbia, based on scat analysis. Can. Tech. Rep. Fish. Aquat. Sci. 1730, 135 p.

Orr, A. J., J. L. Laake, M. I. Dhruv, A. S. Banks, R. L. DeLong, and H. R. Huber.
2003. Comparison of processing pinniped scat samples using a washing machine and nested sieves. Wildl. Soc. Bull. 31:253–257.

Pearcy, W. G, and J. P. Fisher.
1990. Distribution and abundance of juvenile salmonids off Oregon and Washington, 1981–1985. NOAA Tech. Rep. NMFS 93, 83 p.

Pearcy, W. G., R. D. Brodeur, S. M. McKinnell, and J. P. Losee.
2018. Ocean ecology of anadromous coastal cutthroat trout. *In* The ocean ecology of Pacific salmon and trout (R. J. Beamish, ed.), p. 905–930. Am. Fish. Soc., Bethesda, MD.

Pierce, G. J., and P. R. Boyle.
1991. A review of methods for diet analysis in piscivorous marine mammals. Oceanogr. Mar. Biol., Annu. Rev. 29:409–486.

Purcell, M., G. Mackey, E. LaHood, H. Huber, and L. Park.
2004. Molecular methods for the genetic identification of salmonid prey from Pacific harbor seal (*Phoca vitulina richardsi*) scat. Fish. Bull. 102:213–220.

Rasmussen Hellberg, R. S., M. T. Morrissey, and R. H. Hanner.
2010. A multiplex PCR method for the identification of commercially important salmon and trout species (*Oncorhynchus* and *Salmo*) in North America. J. Food Sci. 75:C595–C606.

Roffe, T. J., and B. R. Mate.
1984. Abundances and feeding habits of pinnipeds in the Rogue River, Oregon. J. Wildl. Manag. 48:1262–1274.

Ruggerone, G. T., and J. L. Nielsen.
2004. Evidence for competitive dominance of pink salmon (*Oncorhynchus gorbuscha*) over other salmonids in the North Pacific Ocean. Rev. Fish Biol. Fish. 14:371–390.

Schindler, D. E., M. D. Scheuerell, J. W. Moore, S. M. Gende, T. B. Francis, and W. J. Palen.
2003. Pacific salmon and the ecology of coastal ecosystems. Front. Ecol. Environ. 1:31–37.

Scordino, J. J., A. M. Akmajian, and S. L. Edmondson.
2022. Dietary niche overlap and prey consumption for the Steller sea lion (*Eumetopias jubatus*) and California sea lion (*Zalophus californianus*) in northwest Washington during 2010–2013. Fish. Bull. 120:39–54.

Seitz, A. C., M. B. Courtney, M. D. Evans, and K. Manishin.
2019. Pop-up satellite archival tags reveal evidence of intense predation on large immature Chinook salmon (*Oncorhynchus tshawytscha*) in the North Pacific Ocean. Can. J. Fish. Aquat. Sci. 76:1608–1615.

Sherker, Z. T., K. Pellett, J. Atkinson, J. Damborg, and A. W. Trites.
2021. Pacific great blue herons (*Ardea herodias fannini*) consume thousands of juvenile salmon (*Oncorhynchus* spp.). Can. J. Zool. 99:349–361.

Sobocinski, K. L., C. M. Greene, J. H. Anderson, N. W. Kendall, M. W. Schmidt, M. S. Zimmerman, I. M. Kemp, S. Kim, and C. P. Ruff.
2021. A hypothesis-driven statistical approach for identifying ecosystem indicators of coho and Chinook salmon marine survival. Ecol. Indic. 124:107403.

Tollit, D. J., M. Wong, A. J. Winship, D. A. S. Rosen, and A. W. Trites.
2003. Quantifying errors associated with using prey skeletal structures from fecal samples to determine the diet of Steller's sea lion (*Eumetopias jubatus*). Mar. Mamm. Sci. 19:724–744.

Tollit, D. J., S. G. Heaslip, R. L. Barrick, and A. W. Trites.
2007. Impact of diet-index selection and the digestion of prey hard remains on determining the diet of the Steller sea lion (*Eumetopias jubatus*). Can. J. Zool. 85:1–15.

Tollit, D. J., M. A. Wong, and A. W. Trites.
2015. Diet composition of Steller sea lions (*Eumetopias jubatus*) in Frederick Sound, southeast Alaska: a comparison of quantification methods using scats to describe temporal and spatial variabilities. Can. J. Zool. 93:361–376.

Tollit, D., L. Fritz, R. Joy, K. Miller, A. Schulze, J. Thomason, W. Walker, T. Zeppelin, and T. Gelatt.
2017. Diet of endangered Steller sea lions (*Eumetopias jubatus*) in the Aleutian Islands: new insights from DNA detections and bioenergetic reconstructions. Can. J. Zool. 95:853–868.

Walsh, J. C., J. E. Pendray, S. C. Godwin, K. A. Artelle, H. K. Kindsvater, R. D. Field, J. N. Harding, N. R. Swain, and J. D. Reynolds.
2020. Relationships between Pacific salmon and aquatic and terrestrial ecosystems: implications for ecosystem-based management. Ecology 101(9):e03060.

Walters, C. J., M. K. McAllister, and V. Christensen.
2020. Has Steller sea lion predation impacted survival of Fraser River sockeye salmon? Fisheries 45:597–604.

Welch, D. W., A. D. Porter, and E. L. Rechisky.
2021. A synthesis of the coast-wide decline in survival of West Coast Chinook salmon (*Oncorhynchus tshawytscha*, Salmonidae). Fish Fish. 22:194–211.

Willson, M. F., and K. C. Halupka.
1995. Anadromous fish as keystone species in vertebrate communities. Conserv. Biol. 9:489–497.

Wynne, K.
1993. Guide to marine mammals of Alaska, 75 p. Alsk. Sea Grant Coll. Program, Univ. Alsk. Fairbanks, Fairbanks, AK.

Zhang, Y., J. N. Negishi, J. S. Richardson, and R. Kolodziejczyk.
2003. Impacts of marine-derived nutrients on stream ecosystem functioning. Proc. R. Soc. Lond., B 270:2117–2123.

National Marine
Fisheries Service
NOAA

Fishery Bulletin
established in 1881

Spencer F. Baird
First U.S. Commissioner
of Fisheries and founder
of *Fishery Bulletin*

Population dynamics, relative abundance, and habitat suitability for adult red drum (*Sciaenops ocellatus*) in nearshore waters of the north-central Gulf of Mexico

Crystal L. Hightower[1,2]
J. Marcus Drymon[3,4]
Amanda E. Jefferson[3,4]
Matthew B. Jargowsky[3,4]
Emily A. Seubert[3]
Simon Dedman[5]
John F. Mareska[6]
Sean P. Powers (contact author)[1,2]

Email address for contact author: spowers@disl.edu

[1] Department of Marine Sciences
University of South Alabama
5871 USA Drive North
Mobile, Alabama 36688

[2] Dauphin Island Sea Lab
101 Bienville Boulevard
Dauphin Island, Alabama 36528

[3] Coastal Research and Extension Center
Mississippi State University
1815 Popp's Ferry Road
Biloxi, Mississippi 39532

[4] Mississippi-Alabama Sea Grant Consortium
703 East Beach Drive
Ocean Springs, Mississippi 39564

[5] Hopkins Marine Station
Stanford University
120 Oceanview Boulevard
Pacific Grove, California 93950

[6] Marine Resources Division
Alabama Department of Conservation and Natural Resources
PO Box 189
Dauphin Island, Alabama 36528

Abstract—In the Gulf of Mexico, the red drum (*Sciaenops ocellatus*) is an immensely popular sportfish, yet the Gulf of Mexico stock is currently managed as data-limited in federal waters. The results of the federal stock assessment conducted in 2016 for Gulf of Mexico red drum were not recommended for providing management advice. Consequently, we sought to address data gaps highlighted in the assessment by producing up-to-date overall and sex-specific growth models, standardized indices of relative abundance, and predictions of habitat suitability and by updating estimates of natural mortality. Using a time series for the period of 2006–2018, we assigned ages of 0–36 years to 1178 red drum. A negative binomial generalized linear model including variables for year, depth, surface temperature, dissolved oxygen, and bottom salinity was used to standardize an index of relative abundance. Examination of catch per unit of effort revealed that adult red drum were significantly more abundant in state waters than in federal waters. These findings were explained by habitat suitability models, which were used to identify surface current velocity, surface temperature, and depth as the strongest predictors of relative abundance. The results of our investigation reveal that the adult spawning stock of red drum in the Gulf of Mexico is not fully protected by the catch moratorium in federal waters.

Manuscript submitted 1 November 2021.
Manuscript accepted 9 May 2022.
Fish. Bull. 120:162–175 (2022).
Online publication date: 19 May 2022.
doi: 10.7755/FB.120.2.6

The views and opinions expressed or implied in this article are those of the author (or authors) and do not necessarily reflect the position of the National Marine Fisheries Service, NOAA.

Advances in approaches to data collection and statistical techniques have ushered in the next generation of stock assessments (Lynch et al., 2018). For data-rich species, stock assessments can incorporate ecosystem-based inputs (Lynch et al., 2018), often through the use of spatially explicit approaches (e.g., Goethel et al., 2011; Berger et al., 2017). Despite these advances, more than half of U.S. stocks remain data-limited (Newman et al., 2015). Enhancing basic data inputs is imperative for improving assessments for these stocks. For stocks under aggressive rebuilding schedules, those for which catch data may not reflect population trends or for which catch is completely restricted, the need for reliable time series that track abundance is even more critical.

In the Gulf of Mexico (GOM), the red drum (*Sciaenops ocellatus*) is a highly prized species supporting valuable recreational fisheries. Recreational catch of red drum is permitted in all state waters in the GOM (out to 3 nautical miles [nmi] in Louisiana, Mississippi, and Alabama and out to 9 nmi in Texas and Florida), but a catch moratorium in federal waters has been in place since 1987. In addition, commercial fishing of this species is prohibited in all GOM states except Mississippi. Consequently, the data sources that would be useful for assessing GOM red drum (e.g., commercial landings) are lacking (Powers et al., 2012). Therefore, despite a wealth of knowledge on population connectivity (e.g., Rooker et al., 2010), movement and recruitment (e.g., Burnsed et al., 2020), and

spawning (e.g., Lowerre-Barbieri et al., 2019), the red drum in the Gulf of Mexico is classified by the National Marine Fisheries Service as a "data-limited species" (SEDAR, 2016).

The reauthorization in 2006 of the Magnuson-Stevens Fishery Conservation and Management Act (Magnuson-Stevens . . . 2021) required development and implementation of annual catch limits for all federally managed stocks, a mandate that spurred significant advances in the development of methods for assessment of data-limited stocks (Newman et al., 2015). One of these methods, as implemented in the R package DLMtool (vers. 3.2.1; Carruthers and Hordyk, 2018), was recently used to assess a suite of data-limited species in the GOM, including the lane snapper (*Lutjanus synagris*), wenchman (*Pristipomoides aquilonaris*), yellowmouth grouper (*Mycteroperca interstitialis*), speckled hind (*Epinephelus drummondhayi*), snowy grouper (*Hyporthodus niveatus*), almaco jack (*Seriola rivoliana*), lesser amberjack (*S. fasciata*), and red drum (SEDAR, 2016). During this assessment, at least one method for data-limited species was identified as having preferable performance compared to the status quo for every species examined, with the notable exception of red drum (SEDAR, 2016). Therefore, despite new tools tailored to the assessment of data-limited species and a wealth of information about the population biology and ecology of red drum, the results from this assessment were not recommended for providing management advice for red drum (SEDAR, 2016).

Careful consideration of existing data sets can improve our ability to assess stocks like the GOM stock of red drum. Specific data recommendations from the most recent assessment of red drum include 1) expansion of efforts to collect samples, for analysis of age and length, at varying sizes, seasons, months, and locations, particularly for offshore fish; 2) identification or optimization of fishery-independent surveys to characterize relative abundance in federal waters; and 3) exploration of ways to increase data collection from existing fishery-independent surveys (SEDAR, 2016). To those ends, the goals of this study were to combine data from fishery-independent surveys operating throughout the year and across the continental shelf to produce up-to-date overall and sex-specific growth models, update estimates of the instantaneous natural mortality rate (M), generate standardized indices of relative abundance, and provide predictions of habitat suitability for red drum in the north-central GOM, with the expectation that the results of these efforts can be used to optimize future fishery-independent surveys.

Materials and methods

Data collection

Catch data for adult red drum were collected during fishery-independent bottom longline surveys conducted in all seasons in the north-central GOM during 2006–2018 (Fig. 1). The locations for bottom longline surveys were selected by using a stratified-random sampling design and were sampled following standardized methods described in Drymon et al. (2013, 2020). Briefly, the mainline consisted of 1.85 km (1 nmi) of 4-mm monofilament (545 kg test) that was set with 100 gangions. Gangions consisted of a longline snap and a 15/0 circle hook baited with Atlantic mackerel (*Scomber scombrus*). Each gangion was made of 3.66 m of 3-mm monofilament (320 kg test). All sets were soaked for 1 h, and mid-set measurements of surface and bottom temperatures (in degrees Celsius), salinity, and bottom dissolved oxygen (in milligrams per liter), as well as of depth at the start and end of each set (in meters), were recorded. During the retrieval of the bottom longline, all red drum encountered were measured to the nearest millimeter (maximum total length [TL]), weighed, and retained, and their sex was determined. Sagittal otoliths were extracted for age and growth analyses. Catch data were converted to catch per unit of effort (CPUE), expressed as the number of individuals per 100 hooks per hour.

To augment the samples of adult red drum from the bottom longline survey, smaller red drum were collected from the monthly gill-net survey of the Alabama Department of Conservation and Natural Resources, Marine Resources Division, during 2006–2018; these additional samples were aged. This survey includes areas of coastal Alabama from eastern Mississippi Sound to western Perdido Bay and Mobile Bay (Fig. 1) (Livernois et al., 2020). The gill-net survey of the Marine Resources Division involves 2 different nets: a small-mesh gill net and a large-mesh gill net. The small-mesh gill net consists of 5 panels that are 45.0 m long by 2.4 m deep, each containing stretch meshes in sizes of 5.1–10.2 cm. The large-mesh gill net consists of 4 panels that are also 45.0 m long by 2.4 m deep, with stretch meshes in sizes of 11.4–15.2 cm. Red drum caught in either gill net were measured to the nearest millimeter (maximum TL) and weighed, and their sex was determined. Sagittal otoliths were extracted for age and growth analyses.

For fish of all ages combined (from both longline and gill-net surveys), 2-sample Kolmogorov–Smirnov tests were used to examine differences in length and weight distributions between sexes. Some red drum collected with longlines were not measured for TL. For red drum from longline surveys that had both maximum total and fork length (FL) measurements, linear regression was used to examine the relationship of maximum TL to FL, resulting in this equation:

$$TL = 1.04(FL) + 23.53, \quad (1)$$

where TLs and FLs are expressed in millimeters (number of samples [n]=346, coefficient of multiple determination [R^2]=0.96). This regression was used to estimate the TLs of red drum from the longline survey that were lacking a maximum TL measurement (n=238). Differences in sex ratio were tested by using a chi-square test (Pearson, 1900) against an expected 1:1 male-to-female ratio.

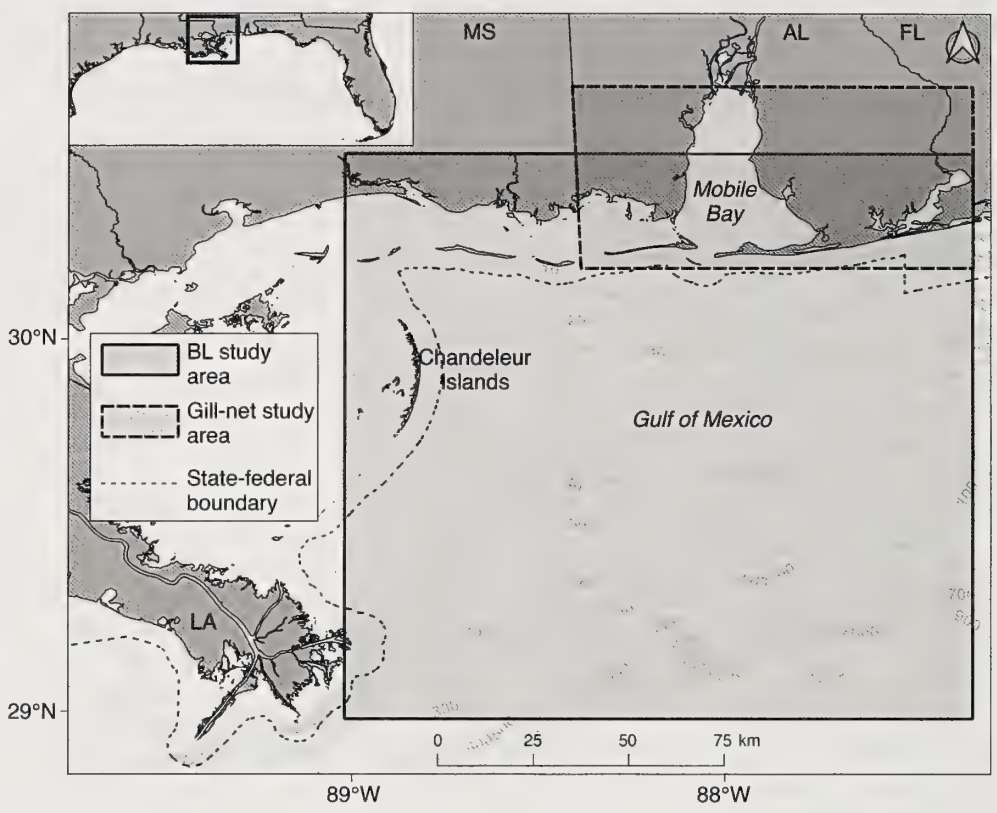

Figure 1

Map of the study areas in the north-central Gulf of Mexico where red drum (*Sciaenops ocellatus*) were collected during fishery-independent bottom longline (BL) and gill-net surveys from 2006 through 2018. The dashed line that follows the coastline indicates the boundary between state and federal waters. Gray lines indicate depth contours. LA=Louisiana; MS=Mississippi; AL=Alabama; FL=Florida.

Otolith processing and aging

All otoliths were processed following procedures detailed in Powers et al. (2012) and VanderKooy et al.[1] A portion of the fish aged in Powers et al. (2012) were also included in our study; however, these fish were aged again as part of this study for consistency. Once otoliths were processed, aging was conducted by 2 readers independently (without consultation between readers) and blindly (without knowledge of fish capture date or size). Each otolith section was viewed with an Olympus[2] SZX16 stereomicroscope (Olympus Corp., Tokyo, Japan) with transmitted light (brightfield illumination). The number of opaque zones was counted along the ventral edge of the sulcus acusticus. A margin code (1–4) was assigned to the otolith margin, according to the otolith manual of the Gulf States Marine Fisheries Commission (VanderKooy et al.[1]).

Whole age, in years, was calculated for each fish according to guidelines of the Gulf States Marine Fisheries Commission. If the collection month was January–June and the margin code was 3 or 4, the whole age equaled the number of opaque zones, plus 1. If the collection month was October–December and the margin code was 1 or 2, the whole age equaled the number of opaque zones, minus 1. For all other combinations of capture month and margin code, the whole age equaled the number of opaque zones. Next, the number of days between the capture date and October 1 (the assumed birth date of red drum; Ditty, 1986) of the previous year was calculated. This number was then divided by the total number of days in the capture year, and the result was added to the whole age to yield the fractional age.

If the readers assigned different whole ages to any otolith, the readers consulted with each other or a third reader aged the otolith. If the 2 initial readers did not reach an agreement or if the third reader did not agree with 1 of the 2 initial ages, the otolith was excluded from further analysis. Average percent error was calculated for all whole ages to

[1] VanderKooy, S., J. Carroll, S. Elzey, J. Gilmore, and J. Kipp (eds.). 2020. A practical handbook for determining the ages of Gulf of Mexico and Atlantic Coast fishes, 3rd ed. Gulf States Mar. Fish. Comm., Publ. 300, 248 p. [Available from website.]

[2] Mention of trade names or commercial companies is for identification purposes only and does not imply endorsement by the National Marine Fisheries Service, NOAA.

evaluate between-reader precision (Beamish and Fournier, 1981; Campana, 2001). Two-sample Kolmogorov–Smirnov tests were used to examine differences in fractional age distributions between sexes.

Modeling growth

To estimate growth parameters for red drum in this study, the von Bertalanffy growth function (VBGF) was fit to female and male red drum and to red drum of unknown sex for the complete data set, the fishery-independent Marine Resources Division gill-net data set, and the bottom longline data set, by using the following equation (von Bertalanffy, 1938):

$$L_t = L_\infty(1 - e^{-K(t - t_0)}), \quad (2)$$

where L_t = the predicted TL in millimeters;
L_∞ = the mean asymptotic length in millimeters;
K = the Brody growth coefficient (years^{-1});
t = the time (fractional age) in years; and
t_0 = the hypothetical age in years at which length equals 0.

The VBGF was used to model sex-specific growth. Eight candidate versions of the VBGF were fit to the sex-specific fractional age data: a general version, where all 3 parameters (L_∞, K, and t_0) could vary between sexes; 3 versions where 2 of the 3 parameters could vary between sexes; 3 versions where only 1 parameter could vary between sexes; and a common version where all 3 parameters were held constant between sexes (Ogle, 2016; Nelson et al., 2018; Jefferson et al., 2019). Akaike information criterion (AIC) values were used to rank these models on the basis of fit and to identify the best-fitting version (Akaike, 1998; Katsanevakis and Maravelias, 2008; Ogle, 2016). All growth parameters were modeled in statistical software R, vers. 4.1.0 (R Core Team, 2021), with the add-on packages FSA (vers. 0.9.1; Ogle et al., 2021) and nlstools (vers. 1.0-2; Baty et al., 2015).

Estimating mortality

By using whole ages of fish sampled in bottom longline surveys, an age-based catch curve (Chapman and Robson, 1960) was created for calculating total mortality; however, graphical examination of the catch curve revealed that critical assumptions necessary for estimating instantaneous total mortality had been violated (Tuckey et al., 2007; Smith et al., 2012). Specifically, red drum did not appear to fully recruit to the gear until age 20; therefore, any mortality estimates generated from this catch curve would not be representative of the stock. Although total mortality estimates were unattainable, M was calculated by using 3 empirical methods (Then et al., 2015; Ogle, 2016):

1. Hoenig$_{\text{fishes}}$, Hoenig's (1983) log-transformed linear regression for fish species,

$$M = e^{1.46 - 1.01\log_e(t_{max})}, \quad (3)$$

where t_{max} = the maximum age of the animal in years;

2. the Hoenig$_{\text{nls}}$ (nonlinear least squares) estimator (Then et al., 2015),

$$M = 4.899t_{max}^{-0.916}; \text{ and} \quad (4)$$

3. the Pauly$_{\text{nls–T}}$ (nonlinear least squares, omitting temperature) estimator (Pauly, 1980; Then et al., 2015),

$$M = 4.118K^{0.73}L_\infty^{-0.333}, \quad (5)$$

where K and L_∞ are parameters from the combined VBGF. All mortality analyses were conducted with FSA in R.

Relative abundance

Yearly changes in CPUE for red drum sampled during bottom longline surveys were examined by generating a nominal index of relative abundance. To standardize the index of relative abundance, a negative binomial generalized linear model (Hardin and Hilbe, 2007) was fit to the CPUE data by using the glmmTMB package (vers. 1.1.2; Brooks et al., 2017) in R. Abiotic variables thought to influence CPUE were added to the model by using forward stepwise model selection. Akaike information criterion values were used to identify the best-fitting model. Model fit was examined by using the DHARMa package (vers. 0.4.3; Hartig, 2021) in R to check for uniformity, outliers, dispersion, and zero inflation. Multicollinearity was tested by using the performance package (vers. 0.7.3; Lüdecke et al., 2021) in R, with variance inflation factors less than 10 signifying low correlation (Dormann et al., 2013). To create a standardized yearly index, the abiotic variables thought to influence CPUE were set to their median values.

Spatial analysis

The index of relative abundance generated as described above was used to examine trends in relative abundance of red drum. First, minimum distance from shore (in kilometers) was calculated in QGIS, vers. 3.8.1 (QGIS Development Team, 2019). Then, nominal CPUE was calculated for 4 discrete areas: <3 nmi from shore (i.e., state waters), 3–6 nmi from shore, 6–9 nmi from shore, and >9 nmi from shore. Finally, a one-way analysis of variance, followed by a Tukey's multiple-pairwise-comparison test, was used to test for differences in nominal CPUE between these 4 areas. Age and length were examined in relation to distance from shore to identify the composition of red drum vulnerable to recreational fishermen in state waters versus that of those protected in federal waters.

Habitat modeling

Boosted regression trees (BRTs) were used to describe the relationships between the CPUE of red drum from bottom longline surveys and environmental variables potentially influencing distribution and abundance. Specifically, BRTs were fit for 3 seasons (meteorological spring, summer, and autumn); winter data were not included in BRT analysis

given that few red drum were captured (n=35) and effort was relatively low (70 stations). Boosted regression trees use machine learning to fit complex, nonlinear relationships and to offer predictive advantages over generalized linear or additive models. For a complete description of BRTs and the methods used in this study, see Drymon et al. (2020).

Results of preliminary analyses indicate a high proportion of zero values (i.e., zero-inflated data). To account for the preponderance of zeros, a 2-step (i.e., delta or hurdle) process was chosen to model catch data. Probability of presence and absence was modeled by using a BRT with a binary distribution, and continuous non-zero (i.e., abundance) probability was modeled by using a BRT with a Gaussian distribution. Because the catch data also contain some instances of anomalously high catch (i.e., long-tailed data), non-zero data were natural log-transformed. Predictions were reverse log-transformed so that the final model is a product of the binary and Gaussian BRTs (Lo et al., 1992).

Sixteen variables with data from multiple sources were considered for the BRTs (see table 1 in Drymon et al., 2020). Although data for some variables (e.g., temperature, salinity, and dissolved oxygen) were collected on-site during bottom longline sampling, all predictor data were obtained following methods outlined in Drymon et al. (2020) to facilitate comparisons with previous habitat modeling in the same region. Surface and bottom temperatures (in degrees Celsius), salinity, and 3-dimensional surface and bottom current velocities (surface, northward, and upward, in meters per second), as well as sea-surface height (in meters), were obtained from the Hybrid Coordinate Ocean Model data server (4-km resolution; HYCOM consortium, available from website, accessed January 2020). Bottom dissolved oxygen (in milligrams per liter) was obtained from Gulf of Mexico Hypoxia Watch maps (NOAA National Centers for Environmental Information, available from website, accessed January 2020) and interpolated across ~100–250 survey stations (the number of stations varied by year). Depth (in meters) and substrate grain size (in millimeters) were obtained from the Coastal Relief Model bathymetry for the Gulf of Mexico (resolution of 0.33 arc seconds or ~10 m; Buczkowski et al., 2006; U.S. Geological Survey, gmx_grd.zip, available from website). Day length (in minutes) was calculated in R by using code by S. Dedman (available from GitHub, accessed January 2020).

Given the quantity of potential predictor data considered within the BRTs, some degree of spatial autocorrelation was anticipated (e.g., between distance from shore and depth, between surface and bottom temperatures); however, BRTs are robust despite autocorrelation among independent variables (Abeare, 2009). All BRTs were fit by using the package gbm.auto (vers. 1.4.1; Dedman et al., 2017) in R. Learning rate, bag fraction, and tree contribution are parameters that are used in concert to determine minimum predictive error (Elith et al., 2008). These parameters were optimized by using gbm.auto for the model run for each season.

Model performance and interpretation

The BRT modeling approach allowed automatic partitioning of the data into training and testing sets, at a ratio dictated by the bag fraction. Ten-fold cross validation was then performed, with the members of the training and testing sets randomized each time. Performance metrics included training and testing correlation, cross-validation deviance (and standard error [SE]), and correlation (and SE), as well as area under receiver-operator curve (AUC) (Hanley and McNeil, 1982) and its cross-validation and cross-validation SE for the binary models (Parisien and Moritz, 2009). The final Gaussian fitted functions from the BRT were visualized by using marginal effect plots to indicate the effect of a particular variable on the response after accounting for the average effects of other model variables (Elith et al., 2008).

Habitat suitability

The distribution of suitable habitat was predicted by using the BRTs described previously. Environmental data for model predictions were obtained as detailed previously, except that Hybrid Coordinate Ocean Model data were extracted for one representative date per season (the monthly groupings for the seasons were March–May, June–August, and September–November). Representative dates for environmental data were selected by ranking the absolute value of the differences between values for all sites for all variables against the mean for those variables, then by identifying the date within each season that most closely matched those values. The BRTs then were used to predict CPUE values for each 2-by-2-km cell. These values were then then mapped in QGIS by using the heatmap setting to produce color points weighted by the predicted abundances generated from the BRT. By using gbm.auto, the coefficient of variance was calculated for the predicted abundance values for each 2-by-2-km cell to represent model variance.

Results

Catch data

Between May 2006 and November 2018, 1296 bottom longline sets were conducted and 815 red drum were caught (Fig. 2), with 741 of those red drum measured and 472 fish kept for otolith collection. Approximately 100 stations were sampled each year (mean: 100 stations [standard deviation 22]; range: 80–143 stations), and survey effort (number of sets) was relatively well distributed across the 3 seasons examined in the BRTs: spring (460 sets), summer (405 sets), and autumn (361 sets). Red drum caught on bottom longlines were primarily encountered in state waters across all seasons (Fig. 2) and were exclusively larger than the size at 50% maturity reported by Bennetts et al. (2019) (Fig. 3A).

To supplement the otoliths taken from the 472 red drum retained from the bottom longline surveys, otoliths from

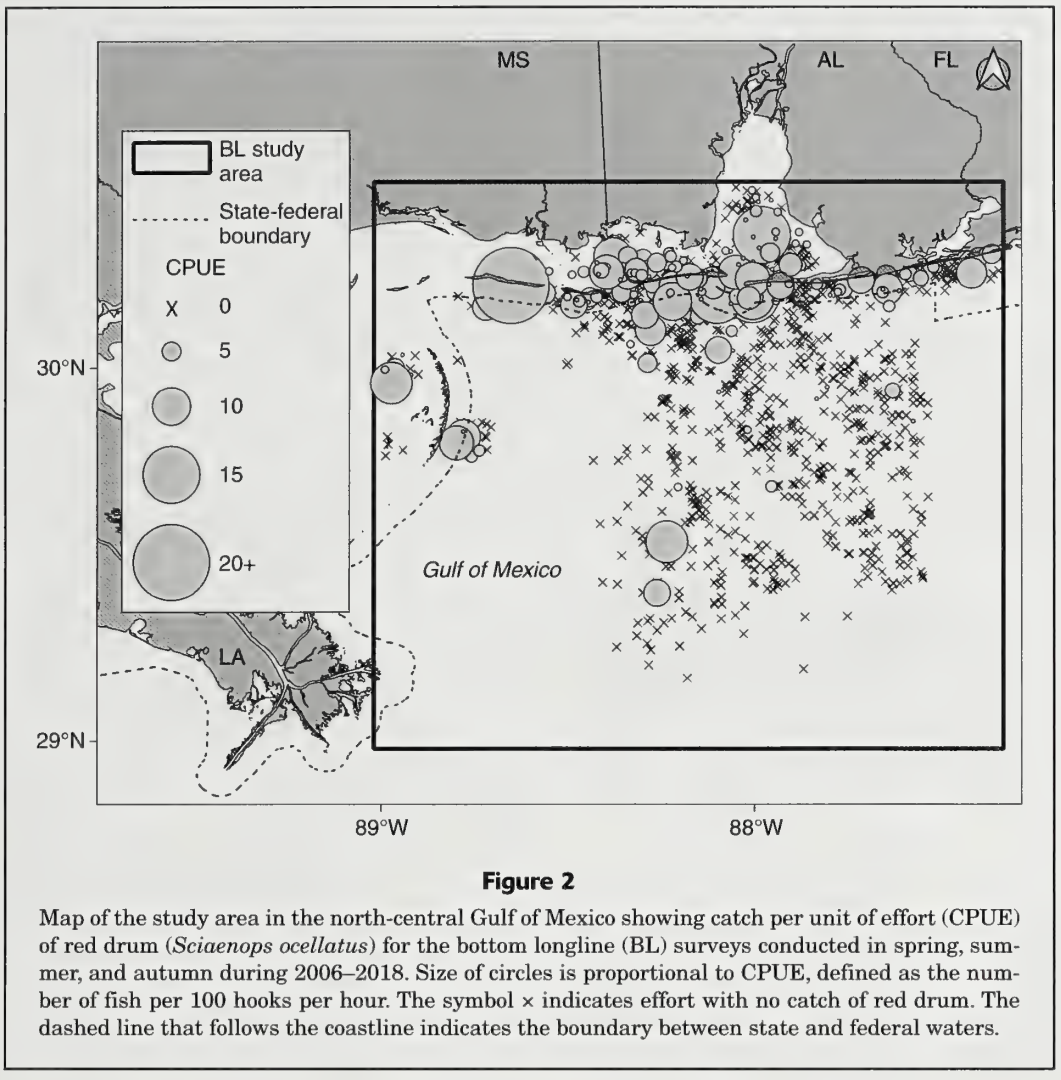

Figure 2

Map of the study area in the north-central Gulf of Mexico showing catch per unit of effort (CPUE) of red drum (*Sciaenops ocellatus*) for the bottom longline (BL) surveys conducted in spring, summer, and autumn during 2006–2018. Size of circles is proportional to CPUE, defined as the number of fish per 100 hooks per hour. The symbol × indicates effort with no catch of red drum. The dashed line that follows the coastline indicates the boundary between state and federal waters.

an additional 709 red drum captured in gill nets were analyzed; therefore, a total of 1181 red drum were used for age and growth analyses. Of these fish, 392 red drum were female, 369 fish were male, and 420 fish were of unknown sex. The female-to-male ratio was 1.06:1.00 and did not differ significantly from a 1:1 ratio (χ^2=0.70, df=1, P=0.40). Total lengths of red drum were 80–1102 mm (Fig. 3B). The average TL of all fish examined (those caught with bottom longlines and gill nets combined) was 619.13 mm (SE 8.22). Results from Kolmogorov–Smirnov tests indicate that females were significantly longer (D=0.20, P<0.01) and heavier (D=0.18, P<0.01) than males.

Age

Ages were assigned to 1178 red drum. Otoliths from the remaining 3 fish (0.25% of all red drum from which otoliths were taken) were deemed unreadable and were omitted from further analysis. Four fish had no length measurements and were also omitted from further analysis. The between-reader percent agreement was 93.46%, and the between-reader average percent error was 4.52%; these estimates are largely driven by differences in the margin codes assigned to age-0 fish. Whole ages ranged from 0 to 36 years, and fractional ages ranged from 0.37 to 36.53 years. The maximum age of both sexes was 36 years; however, results of Kolmogorov–Smirnov tests indicate that fractional age distributions differed significantly by sex (D=0.15, P<0.01). The mean ages of females and males were 11.72 and 9.90 years, respectively.

Growth and mortality

The VBGF for all age data combined (including females, males, and fish of unknown sex) is as follows:

$$L_t = 950.45(1 - e^{-0.31(t-(-0.26))}) \text{ (Fig. 4A).} \quad (6)$$

For the sex-specific data, the model version that allowed L_∞ and t_0 to vary by sex best fit the data. This model version was followed closely by the version in which L_∞ and K vary (difference in AIC values [ΔAIC] between these 2 models: 1.7) and the version that allowed all parameters to vary (ΔAIC for the best fit version and this version: 1.7). On the basis of predictions from the best-fit model, females

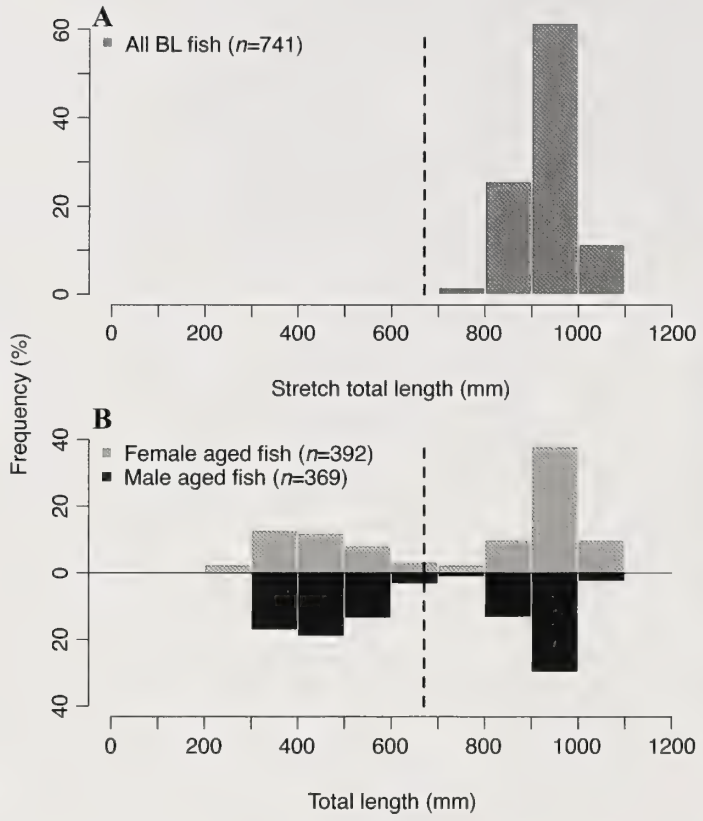

Figure 3

Length–frequency distributions for (**A**) red drum (*Sciaenops ocellatus*) encountered during bottom longline (BL) surveys (sexes combined) and (**B**) red drum encountered during BL and gill-net surveys (by sex) in the north-central Gulf of Mexico from 2006 through 2018. The vertical dashed line represents size at 50% maturity, reported by Bennetts et al. (2019). *n*=number of samples.

have a higher L_∞ value compared with that of males. The VBGF versions for female (F) and male (M) red drum, respectively, are as follows:

$$L_{t(F)} = 969.63(1 - e^{-0.30(t-(-0.35))}); \text{ and} \quad (7)$$

$$L_{t(M)} = 932.71(1 - e^{-0.30(t-(-0.45))}) \text{ (Fig. 4B).} \quad (8)$$

All VBGF parameter estimates from this study are listed in Table 1. Estimates of M were 0.12 for the $\text{Hoenig}_{\text{fishes}}$ method, 0.14 for the $\text{Hoenig}_{\text{nls}}$ method, and 0.39 for the $\text{Pauly}_{\text{nls-T}}$ method.

Relative abundance

The final version of the negative binomial generalized linear model included variables for year, depth, surface temperature, dissolved oxygen, and bottom salinity. The variables for latitude, longitude, bottom temperature, surface salinity, and day length were also tested but were excluded from the final version of the model. Model fit was deemed appropriate because the model did not suffer from deviations from uniformity, outliers (Suppl. Fig. 1) (online only), dispersion (P=0.92), or zero inflation (P=0.87). The results of the variance inflation factor analysis indicate a lack of multicollinearity, given that all variance inflation factors were less than 2. The variable for year was not significant (P=0.13), and there were no trends within the standardized index (Fig. 5), indicating that the declines in the nominal CPUE data for 2007–2010 reflect increases in offshore sampling effort beginning in 2010 rather than changes in relative abundance of red drum.

Spatial analysis

During 2006–2018, bottom longline sets were distributed fairly evenly between state (46%) and federal (54%) waters. Nominal CPUE was highest less than 3 nmi from shore (1.13 [SE 0.10], 602 stations), followed by 3–6 nmi from shore (0.72 [SE 0.18], 103 stations), 6–9 nmi from shore (0.35 [SE 0.19], 58 stations), and greater than 9 nmi from shore (0.08 [SE 0.03], 533 stations). The one-way analysis of variance found that distance from shore was significant (P<0.01). The results from the Tukey's multiple-pairwise-comparison test indicate that nominal CPUE was significantly higher less than 3 nmi from shore compared with 6–9 nmi from shore (P<0.01) and greater than 9 nmi from shore (P<0.01). Nominal CPUE was also significantly higher 3–6 nmi from shore than greater than 9 nmi from shore (P<0.01). Both ages (D=0.41, P<0.01) and length distributions (D=0.42, P<0.01) were significantly different for red drum caught in state versus federal waters. Notably, fish were older and larger in state waters (average age of 18 years and average total length of 938 mm) than in federal waters (average age of 12 years and average total length of 887 mm). Further examination revealed a negative correlation between age and distance from shore (coefficient of correlation [r]=–0.239, P<0.01) and between size and distance from shore (r=–0.274, P<0.01).

Model performance and interpretation

Model performance was assessed for all red drum across the 3 sampling seasons: spring, summer, and autumn. The AUC scores for training data were high across all seasons (0.90), indicating "very good" model performance according to criteria defined in Lane et al. (2009) (Table 2). Cross-validated AUC scores were 0.85–0.86 (SE 0.01), indicating that model overfitting was negligible (Hijmans and Elith, 2013).

Habitat suitability

Across all seasons, northward velocity of the surface current, surface temperature, and depth were the 3 most influential predictors of abundance of red drum (Table 2).

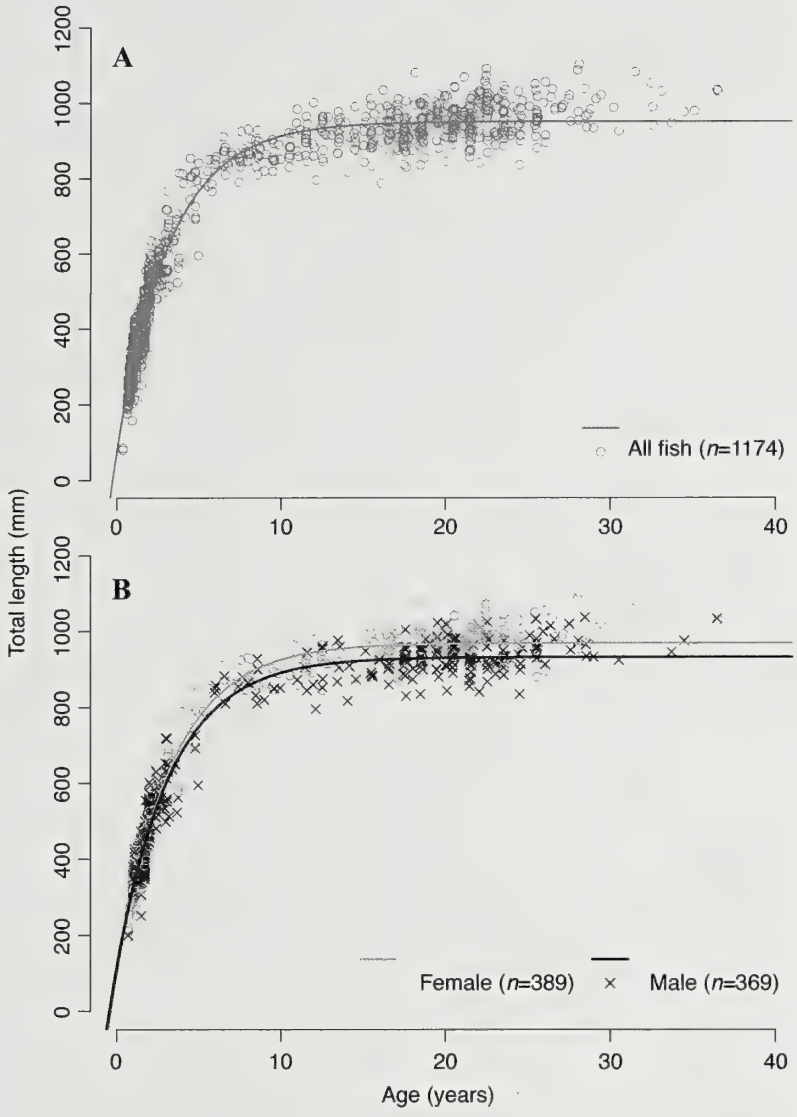

Figure 4

von Bertalanffy growth curves for red drum (*Sciaenops ocellatus*) sampled in the north-central Gulf of Mexico from 2006 through 2018, (**A**) for sexes combined, including fish of unknown sex, and (**B**) for males and females separately. *n*=number of samples.

In particular, red drum had a preference for surface current northward velocities greater than 0 m/s, with high preferences for velocities greater than 0.1 m/s (Fig. 6, A, D, and G). Preferences for surface temperatures less than 22°C (Fig. 6, B, E, and H) and depths between 5 and 17 m (Fig. 6, C, F, and I) were also apparent. These predictors were consistent across seasons. In general, the most suitable habitat for red drum was predominately within state waters. A seasonal shift in predicted habitat suitability was detected, indicating that red drum prefer shallow (<10 m) habitats in the spring and autumn and deep (>30 m) waters during the summer (Fig. 7). Coefficients of variance of the predicted relative abundance were low, but were highest in deep waters (Suppl. Fig. 2) (online only). Because all fish in the BRT analysis were larger than the estimated size at 50% maturity (Fig. 3A), we are confident that these results do not confound localized spatial preferences with life history shifts in habitat use.

Discussion

Our findings, based on a large sample size and broad size distribution, support results of previous studies indicating that the red drum is a relatively long-lived, slow-growing species in the GOM. Perhaps not surprisingly, our findings are most similar to those of Bennetts et al. (2019); 3-parameter VBGFs were used in both studies to model sex-specific growth from a similar number and size range of fish collected in Mississippi and Alabama. However, the maximum age in our study is notably older than the maximum age reported by Bennetts et al. (2019) (36 years

Table 1

Mean estimates for parameters of the von Bertalanffy growth function, by sex, based on age data for red drum (*Sciaenops ocellatus*) collected from 2006 through 2018 during fishery-independent bottom longline and gill-net surveys in the north-central Gulf of Mexico. Parameters include mean asymptotic length (L_∞), Brody growth coefficient (K), and hypothetical age at which length equals 0 (t_0). The category for sexes combined includes fish of unknown sex. Standard errors of the mean (SE) are provided in parentheses.

Sex	L_∞ (mm)	K (years^{-1})	t_0 (years)
Combined	950.45 (2.35)	0.31 (0.01)	−0.26 (0.03)
Female	969.63 (3.42)	0.30 (0.01)	−0.35 (0.05)
Male	932.71 (3.78)	0.30 (0.01)	−0.45 (0.06)

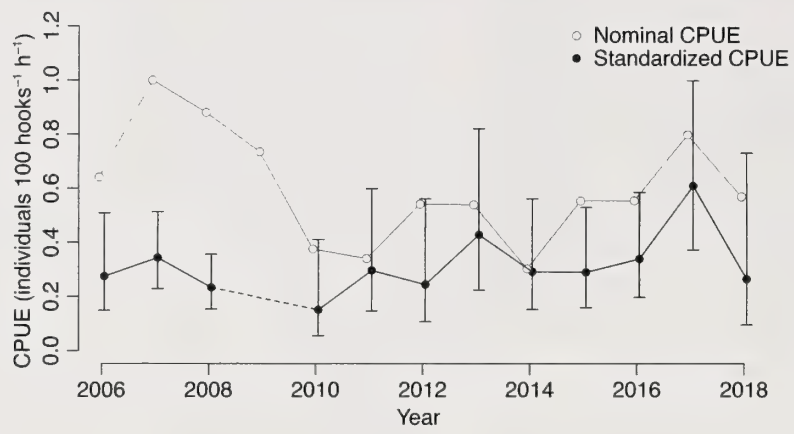

Figure 5

Nominal and standardized catch per unit of effort (CPUE) of red drum (*Sciaenops ocellatus*) from bottom longline surveys conducted in the north-central Gulf of Mexico during 2006–2018. A mean of 100 stations (standard deviation 22) were sampled per year (range: 80–143 stations). Median values are shown in the index standardized by fitting a negative binomial generalized linear model to the CPUE data. For 2009, there is no standardized CPUE estimate because of a lack of positive catch data with corresponding data for abiotic variables from that year. Error bars indicate 95% confidence intervals of standardized CPUE.

versus 31 years), a difference that illustrates the importance of sampling enough large, presumably old individuals. Specifically, we collected more than 4 times more individuals larger than 1000 mm TL than Bennetts et al. (2019); 2 of these fish, 1 male and 1 female, were assigned ages of 36 years. Although fish older than 36 years are likely rare off Mississippi and Alabama, future efforts to model age and growth for red drum should consider collections that span the entirety of the range of the species. Future research also should account for the effects of gear selectivity, temporal or spatial changes in age structure, variable recruitment, and unexplained variance arising from individuals of undetermined sex, all of which are potential sources of bias in growth model parameters in this study.

Despite the large sample size and broad size distribution of red drum captured by using 2 fishery-independent gear types, individuals between 600 and 800 mm TL (ages 3–6) were notably rare in our study. Interestingly, it is in this size range that red drum in this region undergo maturation, according to mean estimates of size and age at maturity from Bennetts et al. (2019). Specifically, mean age at 50% maturity for males and females is approximately 3 years, with fully mature individuals (spawning capable and elevated gonadosomatic index) undetected until ages 5 and 6 (Bennetts et al., 2019). Therefore, although a multi-panel gill net can adequately sample fish of ages 0–2 and the bottom longline can adequately sample fish of age 7 and older, fish between the ages of 3 and 6 years are not selected by either gear type. Similar size selectivity has been reported for red drum off the West Florida Shelf. Using 3 fishery-independent gear types (haul seine, trammel net, and purse seine), Winner et al. (2014) demonstrated that red drum that were 600–800 mm TL were not well represented in the catch in either haul seines or purse seines, yet they were dominant in trammel-net surveys. These examples illustrate that population dynamics are difficult to assess for red drum and that multiple gear types are needed to describe population dynamics across all life stages of this species.

Surprisingly, a comprehensive review of life history studies of red drum revealed that recent age-based estimates of M are not available for this species (SEDAR, 2016). During the most recent stock assessment, it was concluded that the updated Hoenig equation using longevity (Then et al., 2015) was the most robust approach for red drum. Our estimate of annual M based on the Then et al. (2015) approach was 0.14 year^{-1}, a rate that is similar to the range of values used in

Table 2

Percentage of contribution of the 3 variables identified through analysis with boosted regression trees as the most influential on relative abundance of red drum (*Sciaenops ocellatus*) in the north-central Gulf of Mexico between 2006 and 2018. The area under receiver-operator-curve (AUC) and cross-validated (CV) AUC scores, with standard errors (SEs), were used to assess the model's ability to discriminate between species presence and absence.

Season	Training data AUC score	CV AUC score (SE)	Marginal Effect 1		Marginal Effect 2		Marginal Effect 3	
			Variable	%	Variable	%	Variable	%
Spring	0.90	0.86 (0.01)	Northward velocity of surface current	26.2	Surface temperature	20.7	Depth	14.7
Summer	0.90	0.85 (0.01)	Northward velocity of surface current	25.8	Surface temperature	20.4	Depth	14.6
Autumn	0.90	0.86 (0.01)	Northward velocity of surface current	25.8	Surface temperature	20.4	Depth	14.4

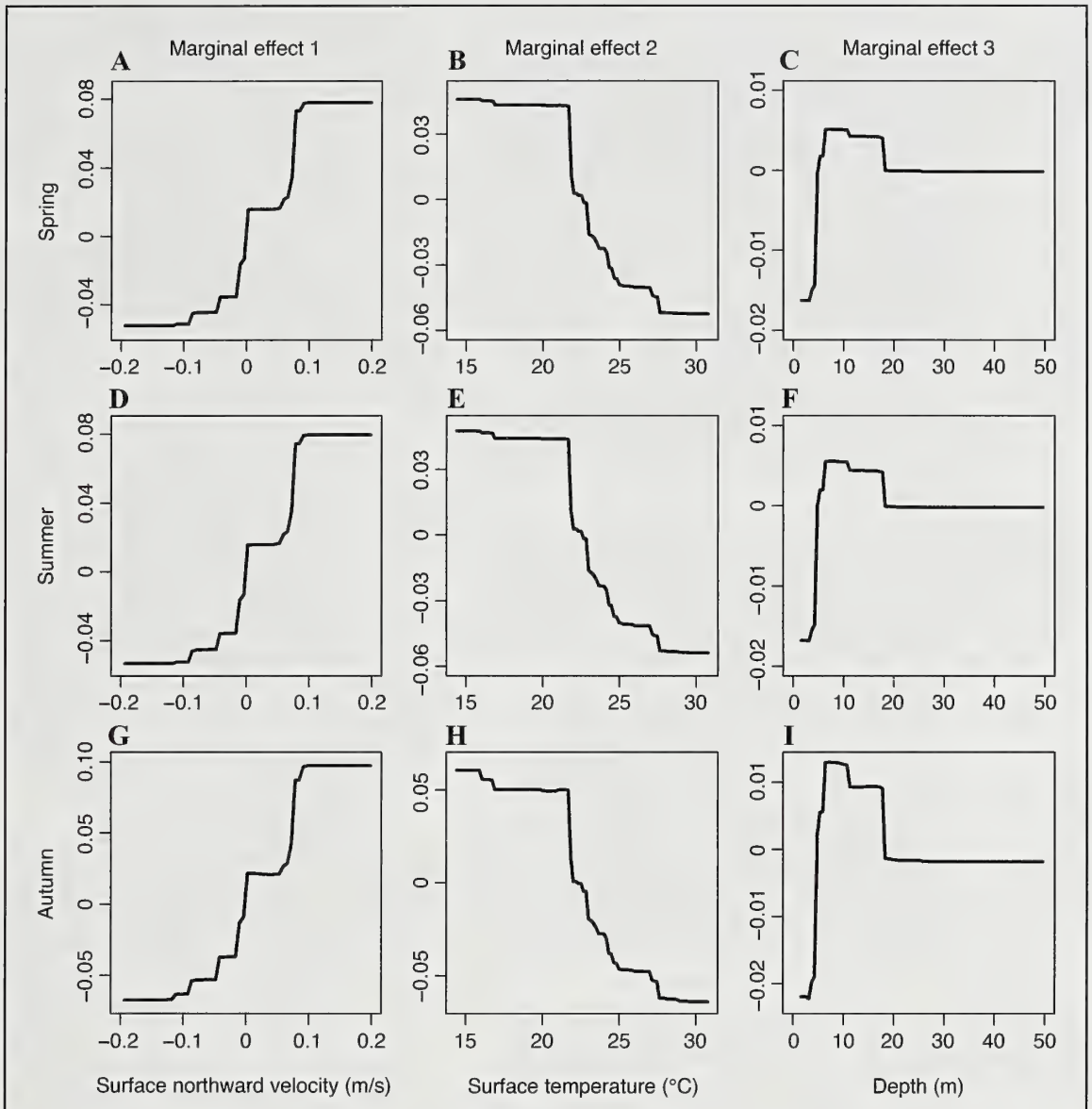

Figure 6

Marginal effect plots for the 3 variables identified through analysis with boosted regression trees (BRTs) as the most influential in predicting relative abundance of red drum (*Sciaenops ocellatus*) in (**A–C**) spring, (**D–F**) summer, and (**G–I**) autumn in the north-central Gulf of Mexico: northward velocity of the surface current, surface temperature, and depth. Data used in the BRT analysis were from surveys conducted in 2006–2018.

the assessment (0.16–0.18 year^{-1}). Unfortunately, the current approach for stock assessments (DLMtool; Carruthers and Hordyk, 2018) does not allow for age-dependent estimates of M. The inability to model age-dependent mortality is potentially problematic for red drum because fishing pressure is higher for juveniles, which likely experience different M than that experienced by older individuals. As the red drum becomes less data-limited, development of the ability to account for age-based differences in M should be prioritized.

The development of a Gulf-wide index of relative abundance generated from fishery-independent bottom longline surveys is critical for future assessments of red drum. During the last stock assessment, 6 potential methods were considered for generating catch advice. The only method to meet the performance criteria was Islope, which is solely based on an index of relative abundance (Carruthers and Hordyk, 2018). For GOM red drum, the index of relative abundance deemed most representative of the adult spawning stock was the index based on data from our bottom longline survey. Therefore, the index of relative abundance generated in this study is an important step toward producing catch advice for this data-limited species. This index indicates that the relative abundance of red drum has varied little over the past 13 years. However, given the long life span of red drum,

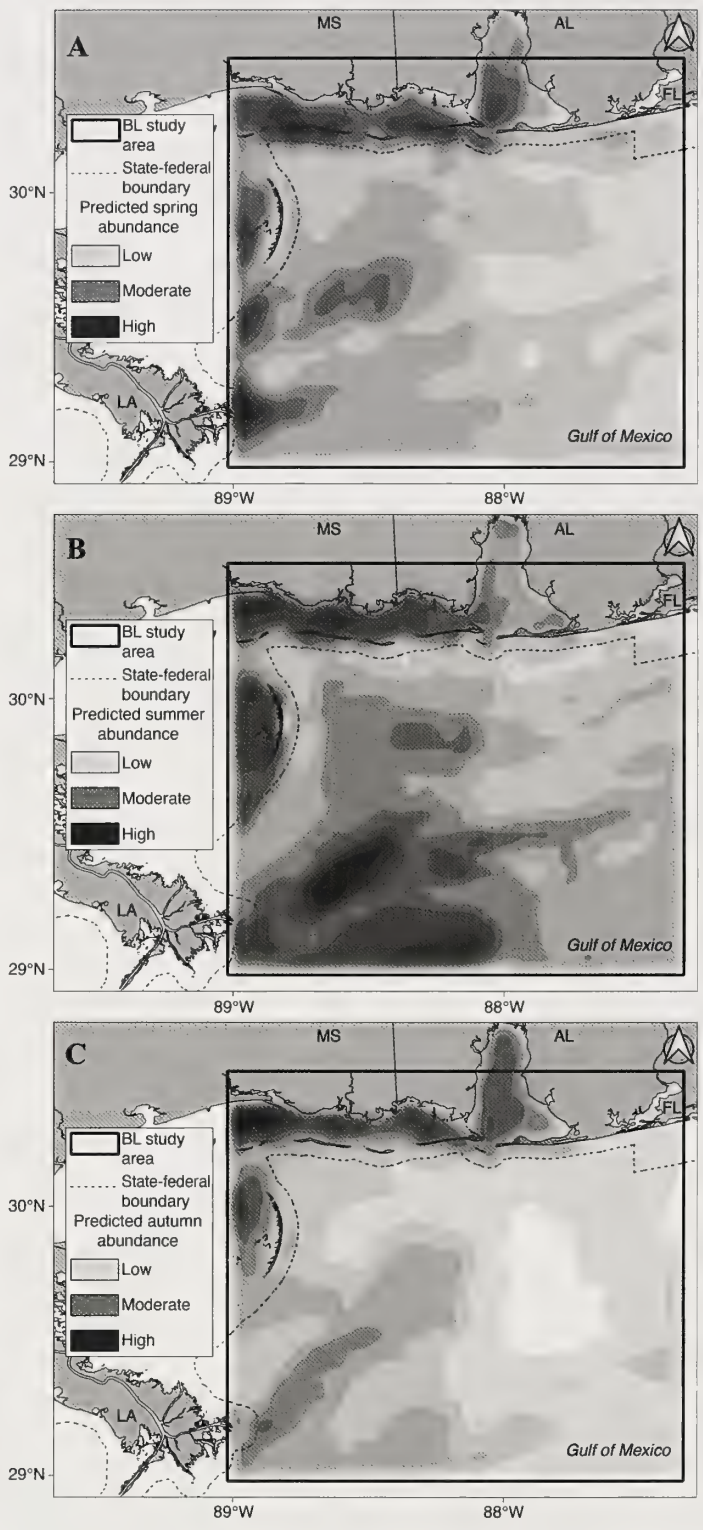

Figure 7

Maps of the study area showing predicted relative abundance from boosted regression trees (BRTs) for red drum (*Sciaenops ocellatus*) collected in (**A**) spring, (**B**) summer, and (**C**) autumn during bottom longline (BL) surveys in the north-central Gulf of Mexico. Light shades indicate areas of low predicted abundance, and dark shades indicate areas of high predicted abundance. The dashed line that follows the coastline indicates the boundary between state and federal waters. Data used in the BRT analysis were from surveys conducted in 2006–2018.

changes in relative abundance for this species are likely to be delayed and gradual. Consequently, continued fishery-independent monitoring is essential, both for characterizing changes in the population and for increasing the stability of catch advice generated from future stock assessments that apply the Islope approach (Sagarese et al., 2019).

Management of red drum in the GOM currently relies on each GOM state meeting an escapement goal (30%) of 4-year-old red drum (SEDAR, 2016). The premise of this management scheme is that most of these fish would enter the offshore adult population where the federal moratorium on GOM red drum protects the adult spawning stock. However, CPUE for adult red drum in the north-central GOM has been substantially higher in state waters than in federal waters (Powers et al., 2012). Similar differences in CPUE between jurisdictions has been observed in other areas of the GOM (e.g., Winner et al., 2014) and along the east coast of Florida (Reyier et al., 2011), particularly from August through November when adults return to state waters to spawn (Lowerre-Barbieri et al., 2016, 2019). These individuals travel to natal areas where they are targeted within spawning aggregations (Burnsed et al., 2020).

Although state-level management of red drum is primarily focused on regulating the catch of juveniles by using slot limits, the current management plans for 4 out of 5 GOM states (i.e., all GOM states except Florida) also afford opportunities to keep a red drum larger than the slot limit. For example, landings data from the NOAA Marine Recreational Information Program (recreational fisheries statistics, available from website, accessed September 2021) indicate that nearly 20% of red drum taken from Mississippi and Alabama state waters have been greater than 762 mm FL (30 in FL), whereas no fish larger than this size have been landed in Florida (Fig. 8). Our findings clearly indicate that off the coast of Alabama, the federal moratorium does not protect the larger, older age classes of red drum from exploitation. Adequately protecting these fish will require state management measures that either completely prohibit the catch of large individuals (e.g., as is done in Florida) or impose a tag system that allows a single over-slot fish per year (e.g., as is done in Texas).

The catch data support the outputs from the BRTs, and the results of BRT analysis indicate that adult red drum prefer inshore, state waters. It has been long established that schools of spawning red drum aggregate near tidal passes (Lowerre-Barbieri et al., 2008; Reyier et al., 2011); the results of our analysis indicate a mechanistic explanation for this observation, confirming the

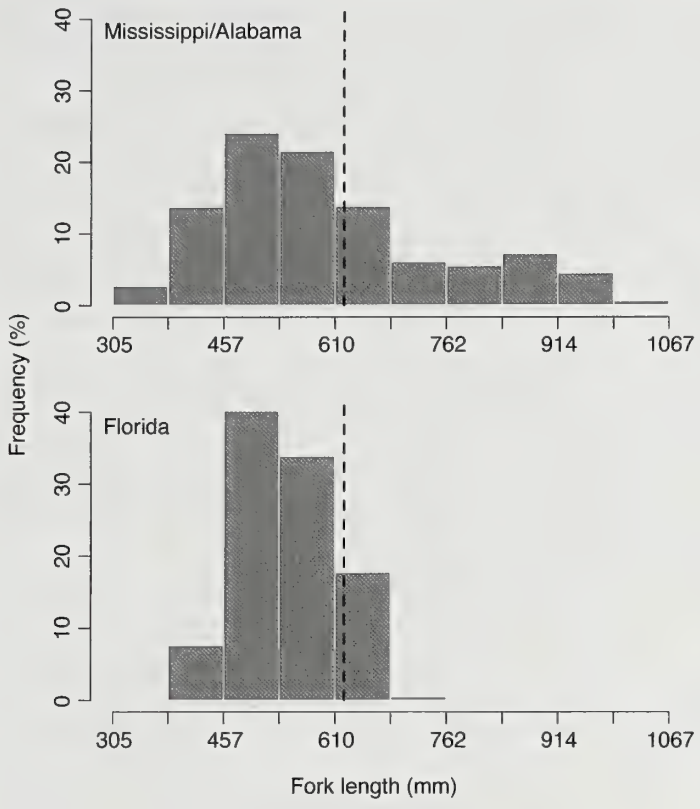

Figure 8

Length–frequency distributions for red drum (*Sciaenops ocellatus*) caught in waters off Mississippi and Alabama and off Florida between 2006 and 2018. Data are from the NOAA Marine Recreational Information Program. The vertical dashed line represents size at 50% maturity, reported by Bennetts et al. (2019).

importance of surface current velocity when defining suitable habitat for red drum. Temperature is also a well known and strong predictor of habitat use of red drum. In previous work in this region, bimodal peaks in relative abundance in the spring and autumn were documented as was the correspondence of these seasonal peaks to temperatures of 21°C and 20°C, respectively (Powers et al., 2012), which are consistent with the temperatures identified in this study as those preferred by red drum. On the basis of habitat suitability predictions from the BRTs, we speculate that during the summer, adult red drum may be using deep (>30 m), cool (~20°C) waters as a thermal refuge.

Conclusions

Clearly, assessing a stock under a complete catch moratorium presents distinct challenges. Nonetheless, when the data typically used to assess the status of a stock (e.g., commercial catch data) are lacking, an opportunity exists to consider alternative data sources, which can sometimes provide new information about stock dynamics (Olney and Hoenig, 2001). Such is the case for GOM red drum. In addition to updated ages, growth models, and M estimates, the results of our investigation reveal that the adult spawning stock is not fully protected by the federal catch moratorium. Moreover, through use of our habitat suitability models, we identified factors that may predict suitable habitat for red drum in other regions of the GOM. Collectively, the findings from this study, in concert with those from future efforts to combine nearshore indices of relative abundance from standardized bottom longline surveys throughout the region (e.g., the surveys of the Southeast Area Monitoring and Assessment Program), will be critical for advancing the stock of red drum in the GOM from its status as data-limited.

Acknowledgments

We thank Dauphin Island Sea Lab captains and crew, especially Captains T. Guoba and J. Wittmann, for their help with the bottom longline survey. We thank A. Kroetz, T. Spearman, T. Nelson, and others for their help with field collections, otolith processing, and aging. Thanks to the Marine Resources Division, Alabama Department of Conservation and Natural Resources, for collecting and sharing data on red drum from gill-net surveys. This work was conducted in accordance with Institutional Animal Care and Use Committee protocol no. 1562086 and was funded in part by the Gulf of Mexico Fishery Management Council.

Literature cited

Abeare, S. M.
2009. Comparisons of boosted regression tree, GLM and GAM performance in the standardization of yellowfin tuna catch-rate data from the Gulf of Mexico lonline [sic] fishery. M.S. thesis, 71 p. La. State Univ., Baton Rouge, LA. [Available from website.]

Akaike, H.
1998. Information theory and an extension of the maximum likelihood principle. *In* Selected papers of Hirotugu Akaike (E. Parzen, K. Tanabe, and G. Kitagawa, eds.), p. 199–213. Springer, New York.

Baty, F., C. Ritz, S. Charles, M. Brutsche, J.-P. Flandrois, and M.-L. Delignette-Muller.
2015. A toolbox for nonlinear regression in R: the package nlstools. J. Stat. Softw. 66(5):1–21.

Beamish, R. J., and D. A. Fournier.
1981. A method for comparing the precision of a set of age determinations. Can. J. Fish. Aquat. Sci. 38:982–983.

Bennetts, C. F., R. L. Leaf, and N. J. Brown-Peterson.
2019. Sex-specific growth and reproductive dynamics of red drum in the northern Gulf of Mexico. Mar. Coast. Fish. 11:213–230.

Berger, A. M., D. R. Goethel, and P. D. Lynch.
2017. Introduction to "space oddity: recent advances incorporating spatial processes in the fishery stock assessment and management interface." Can. J. Fish. Aquat. Sci. 74:1693–1697.

Brooks, M. E., K. Kristensen, K. J. van Benthem, A. Magnusson, C. W. Berg, A. Nielsen, H. J. Skaug, M. Mächler, and B. M. Bolker.
2017. glmmTMB balances speed and flexibility among packages for zero-inflated generalized linear mixed modeling. R J. 9(2):378–400.

Buczkowski, B. J., J. A. Reid, C. J. Jenkins, J. M. Reid, S. J. Williams, and J. G. Flocks.
2006. usSEABED: Gulf of Mexico and Caribbean (Puerto Rico and U.S. Virgin Islands) offshore surficial sediment data release. U.S. Geol. Surv. Data Ser. 146. Woods Hole Sci. Cent., Coast. Mar. Program, U.S. Geol. Surv., Woods Hole, MA. [Available from website.]

Burnsed, S. W., S. Lowerre-Barbieri, J. Bickford, and E. H. Leone.
2020. Recruitment and movement ecology of red drum *Sciaenops ocellatus* differs by natal estuary. Mar. Ecol. Prog. Ser. 633:181–196.

Campana, S. E.
2001. Accuracy, precision and quality control in age determination, including a review of the use and abuse of age validation methods. J. Fish Biol. 59:197–242.

Carruthers, T. R., and A. R. Hordyk.
2018. The data-limited methods toolkit (DLM tool): an R package for informing management of data-limited populations. Methods Ecol. Evol. 9:2388–2395.

Chapman, D. G., and D. S. Robson.
1960. The analysis of a catch curve. Biometrics 16:354–368.

Dedman, S., R. Officer, M. Clarke, D. G. Reid, and D. Brophy.
2017. Gbm.auto: a software tool to simplify spatial modelling and marine protected area planning. PLoS ONE 12(12):e0188955.

Ditty, J. G.
1986. Ichthyoplankton in neritic waters of the northern Gulf of Mexico off Louisiana: composition, relative abundance, and seasonality. Fish. Bull. 84:935–946.

Dormann, C. F., J. Elith, S. Bacher, C. Buchmann, G. Carl, G. Carré, J. R. G. Marquéz, B. Gruber, B. Lafourcade, P. J. Leitão, et al.
2013. Collinearity: a review of methods to deal with it and a simulation study evaluating their performance. Ecography 36:27–46.

Drymon, J. M., L. Carassou, S. P. Powers, M. Grace, J. Dindo, and B. Dzwonkowski.
2013. Multiscale analysis of factors that affect the distribution of sharks throughout the northern Gulf of Mexico. Fish. Bull. 111:370–380.

Drymon, J. M., S. Dedman, J. T. Froeschke, E. A. Seubert, A. E. Jefferson, A. M. Kroetz, J. F. Mareska, and S. P. Powers.
2020. Defining sex-specific habitat suitability for a northern Gulf of Mexico shark assemblage. Front. Mar. Sci. 7:35.

Elith, J., J. R. Leathwick, and T. Hastie.
2008. A working guide to boosted regression trees. J. Anim. Ecol. 77:802–813.

Goethel, D. R., T. J. Quinn II, and S. X. Cadrin.
2011. Incorporating spatial structure in stock assessment: movement modeling in marine fish population dynamics. Rev. Fish. Sci. 19:119–136.

Hanley, J. A., and B. J. McNeil.
1982. The meaning and use of the area under a receiver operating characteristic (ROC) curve. Radiology 143:29–36.

Hardin, J. W., and J. M. Hilbe.
2007. Generalized linear models and extensions, 2nd ed., 387 p. Stata Press, College Station, TX.

Hartig, F.
2021. DHARMa: residual diagnostics for hierarchical (multi-level/mixed) regression models. R package, vers. 0.4.3. [Available from website, accessed August 2021.]

Hijmans, R. J., and J. Elith.
2013. Species distribution modeling with R. *In* Spatial data science with R. R CRAN Proj., R Found. Stat. Comput., Vienna, Austria. [Available from website.]

Hoenig, J. M.
1983. Empirical use of longevity data to estimate mortality rates. Fish. Bull. 82:898–903.

Jefferson, A. E., R. J. Allman, A. E. Pacicco, J. S. Franks, F. J. Hernandez, M. A. Albins, S. P. Powers, R. L. Shipp, and J. M. Drymon.
2019. Age and growth of gray triggerfish (*Balistes capriscus*) from a north-central Gulf of Mexico artificial reef zone. Bull. Mar. Sci. 95:177–195.

Katsanevakis, S., and C. D. Maravelias.
2008. Modelling fish growth: multi-model inference as a better alternative to *a priori* using von Bertalanffy equation. Fish Fish. 9:178–187.

Lane, J. Q., P. T. Raimondi, and R. M. Kudela.
2009. Development of a logistic regression model for the prediction of toxigenic *Pseudo-nitzschia* blooms in Monterey Bay, California. Mar. Ecol. Prog. Ser. 383:37–51.

Livernois, M. C., S. P. Powers, M. A. Albins, and J. F. Mareska.
2020. Habitat associations and co-occurrence patterns of two estuarine-dependent predatory fishes. Mar. Coast. Fish. 12:64–77.

Lo, N. C.-H., L. D. Jacobson, and J. L. Squire.
1992. Indices of relative abundance from fish spotter data based on delta-lognormal models. Can. J. Fish. Aquat. Sci. 49:2515–2526.

Lowerre-Barbieri, S. K., L. R. Barbieri, J. R. Flanders, A. G. Woodward, C. F. Cotton, and M. K. Knowlton.
2008. Use of passive acoustics to determine red drum spawning in Georgia waters. Trans. Am. Fish. Soc. 137:562–575.

Lowerre-Barbieri, S. K., S. L. W. Burnsed, and J. W. Bickford.
2016. Assessing reproductive behavior important to fisheries management: a case study with red drum, *Sciaenops ocellatus*. Ecol. Appl. 26:979–995.

Lowerre-Barbieri, S. K., M. D. Tringali, C. P. Shea, S. W. Burnsed, J. Bickford, M. Murphy, and C. Porch.
2019. Assessing red drum spawning aggregations and abundance in the eastern Gulf of Mexico: a multidisciplinary approach. ICES J. Mar. Sci. 76:516–529.

Lüdecke, D., M. S. Ben-Shachar, I. Patil, P. Waggoner, and D. Makowski.
2021. performance: an R package for assessment, comparison and testing of statistical models. J. Open Source Softw. 6(60):3139.

Lynch, P. D., R. D. Methot, and J. S. Link (eds.).
2018. Implementing a next generation stock assessment enterprise: an update to the NOAA Fisheries stock assessment improvement plan. NOAA Tech. Memo. NMFS-F/SPO-183, 127 p.

Magnuson-Stevens Fishery Conservation and Management Act, 16 U.S. Code Sect. 1801–1891d. (2020). [Available from website.]

Nelson, T. R., A. E. Jefferson, P. T. Cooper, C. A. Buckley, K. L. Heck Jr., and J. Mattila.
2018. Eurasian perch *Perca fluviatilis* growth and fish community structure, inside and outside a marine-protected area in the Baltic Sea. Fish. Manag. Ecol. 25:172–185.

Newman, D., J. Berkson, and L. Suatoni.
2015. Current methods for setting catch limits for data-limited fish stocks in the United States. Fish. Res. 164:86–93.

Ogle, D. H.
2016. Introductory fisheries analyses with R, 338 p. CRC Press, Boca Raton, FL.
Ogle, D. H., P. Wheeler, and A. Dinno.
2021. FSA: fisheries stock analysis. R package, vers. 0.9.1. [Available from website, accessed August 2021.]
Olney, J. E., and J. M. Hoenig.
2001. Managing a fishery under moratorium: assessment opportunities for Virginia's stocks of American shad. Fisheries 26(2):6–12.
Parisien, M.-A., and M. A. Moritz.
2009. Environmental controls on the distribution of wildfire at multiple spatial scales. Ecol. Monogr. 79:127–154.
Pauly, D.
1980. On the interrelationships between natural mortality, growth parameters, and mean environmental temperature in 175 fish stocks. ICES J. Mar. Sci. 39:175–192.
Pearson, K.
1900. On the criterion that a given system of deviations from the probable in the case of a correlated system of variables is such that it can be reasonably supposed to have arisen from random sampling. Lond. Edinb. Dublin Philos. Mag. J. Sci. 50(302):157–175.
Powers, S. P., C. L. Hightower, J. M. Drymon, and M. W. Johnson.
2012. Age composition and distribution of red drum (*Sciaenops ocellatus*) in offshore waters of the north central Gulf of Mexico: an evaluation of a stock under a federal harvest moratorium. Fish. Bull. 110:283–292.
QGIS Development Team.
2019. QGIS Geographic Information System. Open Source Geospatial Foundation Project. [Available from website, accessed July 2019.]
R Core Team.
2021. R: a language and environment for statistical computing. R Found. Stat. Comput., Vienna, Austria. [Available from website, accessed July 2021.]
Reyier, E. A., R. H. Lowers, D. M. Scheidt, and D. H. Adams.
2011. Movement patterns of adult red drum, *Sciaenops ocellatus*, in shallow Florida lagoons as inferred through autonomous acoustic telemetry. Environ. Biol. Fishes 90:343–360.
Rooker, J. R., G. W. Stunz, S. A. Holt, and T. J. Minello.
2010. Population connectivity of red drum in the northern Gulf of Mexico. Mar. Ecol. Prog. Ser. 407:187–196.
Sagarese, S. R., W. J. Harford, J. F. Walter, M. D. Bryan, J. J. Isely, M. W. Smith, D. R. Goethel, A. B. Rios, S. L. Cass-Calay, C. E. Porch, et al.
2019. Lessons learned from data-limited evaluations of data-rich reef fish species in the Gulf of Mexico: implications for providing fisheries management advice for data-poor stocks. Can. J. Fish. Aquat. Sci. 76:1624–1639.
SEDAR (Southeast Data, Assessment, and Review).
2016. SEDAR 49 stock assessment report. Gulf of Mexico data-limited species: red drum, lane snapper, wenchman, yellowmouth grouper, speckled hind, snowy grouper, almaco jack, lesser amberjack, 81 p. SEDAR, North Charleston, SC. [Available from website.]
Smith, M. W., A. Y. Then, C. Wor, G. Ralph, K. H. Pollock, and J. M. Hoenig.
2012. Recommendations for catch-curve analysis. North Am. J. Fish. Manag. 32:956–967.
Then, A. Y., J. M. Hoenig, N. G. Hall, D. A. Hewitt, and E. Jardim (handling ed.).
2015. Evaluating the predictive performance of empirical estimators of natural mortality rate using information on over 200 fish species. ICES J. Mar. Sci. 72:82–92.
Tuckey, T., N. Yochum, J. Hoenig, J. Lucy, and J. Cimino.
2007. Evaluating localized vs. large-scale management: the example of tautog in Virginia. Fisheries 32:21–28.
von Bertalanffy, L.
1938. A quantitative theory of organic growth (inquiries on growth laws. II). Hum. Biol. 10:181–213.
Winner, B. L., K. E. Flaherty-Walia, T. S. Switzer, and J. L. Vecchio.
2014. Multidecadal evidence of recovery of nearshore red drum stocks off west-central Florida and connectivity with inshore nurseries. North Am. J. Fish. Manag. 34:780–794.

National Marine
Fisheries Service
NOAA

Fishery Bulletin
established in 1881

Spencer F. Baird
First U.S. Commissioner
of Fisheries and founder
of *Fishery Bulletin*

Mortality estimates for gray triggerfish (*Balistes capriscus*) in the northern Gulf of Mexico based on acoustic telemetry

Megan K. McKinzie
Stephen T. Szedlmayer (contact author)

Email address for contact author: szedlst@auburn.edu

School of Fisheries, Aquaculture and Aquatic Sciences
Auburn University
8300 State Highway 104
Fairhope, Alabama 36532

Abstract—Gray triggerfish (*Balistes capriscus*) is a common resident of reef habitats in the northern Gulf of Mexico. It is targeted by fishermen and recently considered not overfished. However, stock status is highly dependent on indirect mortality estimates from sport and commercial fishery landings that may have errors. To enhance management efforts, we used acoustic telemetry to directly estimate fishing mortality (F), natural mortality (M), and total mortality (Z) for gray triggerfish on artificial reefs in the northern Gulf of Mexico. Over the study period, 30 fish emigrated, 4 fish were caught by fishermen, 4 fish died of natural causes, 8 fish were active when their transmitter battery expired, and 3 fish were still active at the end of the study. Annual F was 0.23 (95% confidence interval [CI]: 0.07–0.50) and was lower than in past stock assessments. This rate indicates that earlier management efforts were successful. However, our F estimate is possibly greater than a recent management goal of 0.17 based on a 30% spawning potential ratio. Therefore, gray triggerfish stocks may still be experiencing overfishing. Annual M was 0.25 (95% CI: 0.07–0.57) and supports the management applied M of 0.28. Annual Z was 0.48 (95% CI: 0.18–0.85), which was not considered sustainable under the most recent stock assessment and supports the management decision to increase fishery restrictions.

Manuscript submitted 3 January 2022.
Manuscript accepted 23 May 2022.
Fish. Bull. 120:176–186 (2022).
Online publication date: 3 June 2022.
doi: 10.7755/FB.120.2.7

The views and opinions expressed or implied in this article are those of the author (or authors) and do not necessarily reflect the position of the National Marine Fisheries Service, NOAA.

Gray triggerfish (*Balistes capriscus*) is exploited by sport and commercial fisheries throughout the northern Gulf of Mexico and southeastern United States (SEDAR, 2015). Historically, this species was neither heavily targeted nor considered an important food resource. However, its value has increased in recent years as fishing restrictions on red snapper (*Lutjanus campechanus*) and other important species of reef fish have increased (SEDAR, 2013). This rising interest has also led to increased concern about the status of the stock of gray triggerfish in the Gulf of Mexico.

In 2011, the Gulf of Mexico stock of gray triggerfish was considered overfished and experiencing overfishing (SEDAR, 2011). As a result, the Gulf of Mexico Fishery Management Council reduced the annual catch limit, set a spawning season closure from 1 June through 31 July, a sport bag limit of 2 gray triggerfish per fishermen per day, and a commercial trip limit of 12 gray triggerfish per trip (GMFMC, 2012). A more recent stock assessment in 2015 indicated that the gray triggerfish stock was no longer experiencing overfishing, but the stock was still overfished (SEDAR, 2015). In 2017, a new rebuilding plan for gray triggerfish was developed, and through this plan a less restrictive definition of *overfished* was adopted and characterized the stock as no longer overfished but still rebuilding (GMFMC, 2017a). The new rebuilding plan further reduced the recreational bag limit to 1 gray triggerfish per fishermen per day, increased the recreational minimum size limit for gray triggerfish to 381 mm fork length (FL) (15 in FL), increased the commercial trip limit for gray triggerfish to 16 fish per trip, and added in an additional seasonal closure from 1 January through 28 February (GMFMC, 2017b). Therefore, questions concerning the stock status of the gray triggerfish remain, reinforcing the need for a new benchmark stock assessment.

Especially important for gray triggerfish stock assessments are estimates of mortality. Prior to the implementation of the fishery management plan for reef fish resources of the Gulf of Mexico in 1984 (GMFMC, 1981), the total mortality (Z) for this stock of gray triggerfish was estimated to range from 0.40 to 0.67 during 1979–1982 (Johnson and Saloman, 1984). More recent estimates based on catch-curve analyses indicate that the mean Z for the period of 1986–2011 was 0.95 (Burton et al., 2015), which exceeds the estimated maximum sustainable Z of 0.45 (with fishing mortality [F] of 0.17, based on a 30% spawning potential ratio, and

natural mortality [M] of 0.28; i.e., $Z=F+M$) determined from the 2015 stock assessment (SEDAR, 2015). From this 2015 assessment, the estimated F for 2013 was 0.12, but previous estimates indicate that F exceeded sustainable levels and ranged from 0.35 to 0.67 in that year (SEDAR, 2011; Burton et al., 2015). Estimates of M have been relatively constant over time, ranging from 0.27 to 0.28 (SEDAR, 2011; Burton et al., 2015; SEDAR, 2015; GMFMC, 2017b).

Estimates of F, M, and Z for gray triggerfish are critical for management but are highly dependent on fishery-dependent data from the Marine Recreational Information Program, which is known to have difficulties (NASEM, 2017). Also, it is relatively easy for management to estimate Z from age–frequency analyses, but it is more difficult to separate Z into F and M for an exploited stock (Ricker, 1975). Some authors have proposed methods to estimate M with equations that attempt to relate M to life history characteristics, such as maximum length, maximum age, or growth rates (Hewitt and Hoenig, 2005; Charnov et al., 2013). Mortality can also be estimated through mark-recapture studies on the basis of the number of tagged fish that were caught and reported by fishermen (Pine et al., 2012). However, there are inherent caveats with conventional mark-recapture studies; for example, fishermen not reporting catch of tagged fish, fish shedding tags, and fish emigrating from study areas (Schwartz, 2000; Pollock et al., 2001; Denson et al., 2002; Pine et al., 2003, 2012).

Telemetry methods have been used in terrestrial animals for some time (Trent and Rongstad, 1974; Pollock et al., 1995) and more recently have been applied to aquatic organisms (Hightower et al., 2001; Heupel and Simpfendorfer, 2002; Pollock et al., 2004; Starr et al., 2005; Knip et al., 2012). In the northern Gulf of Mexico, telemetry methods have been successfully used to estimate F and M of red snapper residing on natural and artificial reefs, independent of tag returns by fishermen (Topping and Szedlmayer, 2013; Williams-Grove and Szedlmayer, 2016a; Mudrak and Szedlmayer, 2020). Telemetry can also be used to estimate non-reporting by fishermen and tagging mortality (Hightower et al., 2001; Williams-Grove and Szedlmayer, 2016a; Mudrak and Szedlmayer, 2020). In previous studies, telemetry methods have been applied to gray triggerfish to estimate movement patterns (Herbig and Szedlmayer, 2016; McKinzie, 2018; Bacheler et al., 2019a, 2019b), and responses to baited fish traps (Bacheler et al., 2018), but have not been reported for mortality estimations. In our study, we applied telemetry methods to estimate mortality of gray triggerfish from artificial reef habitats in the northern Gulf of Mexico from 2013 through 2017. We estimated M, F, and Z with a known-fate model (Kaplan and Meier, 1958; Pollock et al., 1989) on the basis of fine-scale positions obtained from Vemco Positioning Systems[1] (VPS; Innovasea Systems, Boston, MA) composed of acoustic receivers and transmitters, and these estimates can potentially enhance management efforts for this species.

Materials and methods

Study area and array design

Covering 64 km^2, the study area was located 23–35 km south of Dauphin Island, Alabama, in the northern Gulf of Mexico. The study area contained 26 steel-cage artificial reefs (2.5 × 1.3 × 2.4 m), each positioned 1.4–1.6 km apart at depths of 18–35 m (Fig. 1). The artificial reefs were deployed at unpublished locations from 2006 through 2010 within a designated reef building zone (Hugh Swingle General Permit Area; Syc and Szedlmayer, 2012). A VPS array of acoustic receivers (VR2W, Innovasea Systems; 69 Hz) and synchronization transmitters (V16-6x, Innovasea Systems; 69 kHz, transmission delay of 540–720 s) was deployed at each of 5 reef sites to monitor patterns of fine-scale movements (in meters) and to estimate mortality of gray triggerfish tagged with acoustic transmitters (V13-1L or V13P-1L, Innovasea Systems; 69 kHz, transmission delay of 40–80 s, battery life of 566–991 d). The depths at the 5 reef sites were 18, 23, 25, 26, and 35 m. In addition, a single VR2W acoustic receiver was placed at each of 21 surrounding reef sites to detect large-scale movements (in kilometers) and emigrations away from VPS sites (Fig. 1).

Each of the 5 VPS sites consisted of 5 acoustic receivers: a center receiver placed 10–20 m north of the reef site and 4 receivers placed 300 m north, south, east, and west of the center receiver (Piraino and Szedlmayer, 2014). The V16-6x synchronization transmitters were attached 1 m above each receiver to standardize the internal receiver clocks (Piraino and Szedlmayer, 2014). The design of the receiver arrays at VPS sites permitted high detection efficiency of tagged gray triggerfish (≥88%; McKinzie, 2018). Every 4–6 months, data were downloaded and all receivers were exchanged. Data from the VPS receivers were sent to Innovasea Systems for post-processing after every download. A stationary control transmitter (V13-1L) was placed at a known location within each VPS array to validate the accuracy of Innovasea-derived positions and to ensure continuous data collection throughout the study period.

Each of the 21 surrounding reef sites contained a single VR2W receiver that detected presence and absence of tagged fish. Every 6–12 months, data were downloaded and these single receivers were exchanged. The maximum radius for transmitter detection around each receiver was estimated to be 770 m (McKinzie, 2018). Therefore, tagged gray triggerfish were detected in 82% (53 km^2) of the area within the array of 21 receivers used to monitor large-scale movements, leaving 18% (11 km^2) of the area with little coverage. The areas of low detection occurred over paths that were 100–300 m wide between the coverage areas of single receivers at surrounding reef sites (McKinzie, 2018).

[1] Mention of trade names or commercial companies is for identification purposes only and does not imply endorsement by the National Marine Fisheries Service, NOAA.

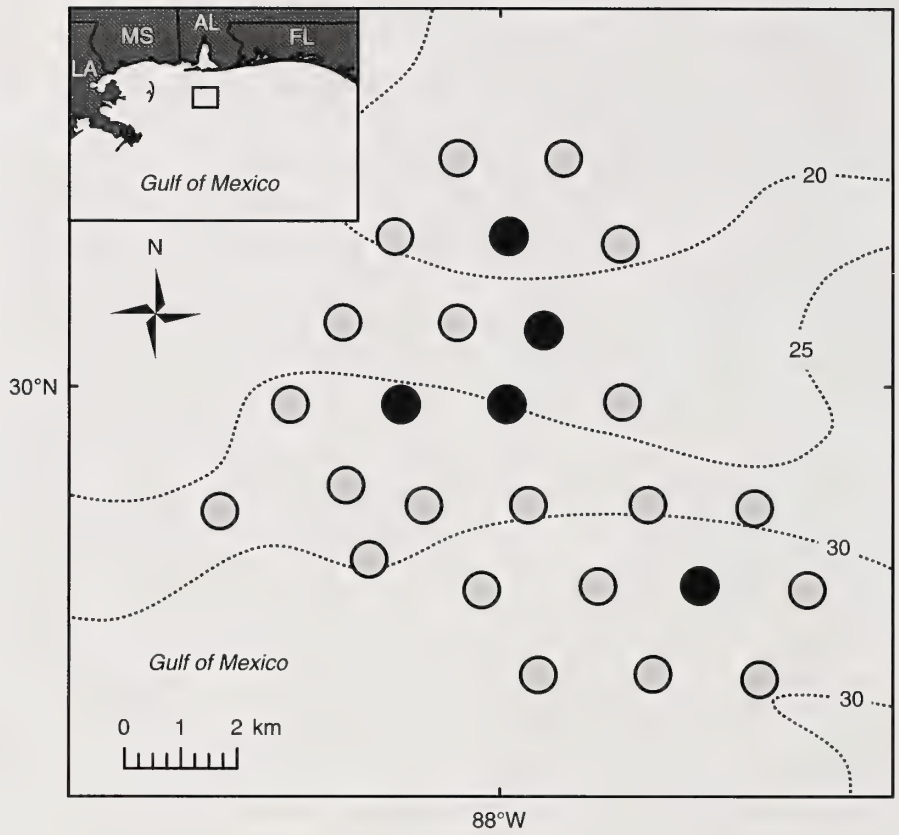

Figure 1

Map of the locations of 5 artificial reef sites where a Vemco Positioning System (VPS) was deployed (black circles) and of 21 surrounding reef sites where an acoustic receiver was deployed (gray circles) within the Hugh Swingle General Permit Area (black square outline in inset) in the northern Gulf of Mexico. Gray triggerfish (*Balistes capriscus*) were tagged and released at the VPS sites from 23 January 2013 through 16 June 2017. Fish movements were monitored at all sites until 5 September 2017. The dotted lines indicate 5-m depth contours.

Fish tagging and cage-release method

We tagged and released adult gray triggerfish (sample size [*n*]=56) on artificial reef sites from 23 January 2013 through 16 June 2017 and monitored movements until 5 September 2017. Prior to tagging, we measured dissolved oxygen concentration and temperature throughout the water column using a multiparameter water-quality sonde (YSI Model 6920, YSI Inc., Yellow Springs, OH). Fish were tagged and released if dissolved oxygen levels were >2.5 mg/L. If water temperatures at the surface exceeded 27°C, ice was added to the holding tanks during sedation and recovery to reduce stress from high temperatures.

Gray triggerfish were captured with hook-and-line gear baited with squid (*Loligo* spp. or *Lolliguncula* spp.) at 5 VPS sites (Fig. 1). On the research vessel, adult fish ≥250 mm FL (Kelly-Stormer et al., 2017) were anesthetized in 70-L containers with 150 mg tricaine methanesulfonate (MS-222)/L seawater (Munday and Wilson, 1997; Cho and Heath, 2000) for 80 s to level 4 of sedation (loss of equilibrium, fin movement stopped; Summerfelt and Smith, 1990). After anesthesia, fish were weighed (to the nearest 0.1 kg) and measured to the nearest millimeter in total length, FL, and standard length. An acoustic transmitter (V13-1L or V13P-1L) was surgically implanted within the peritoneal cavity through a vertical incision of 1–2 cm on the ventral left side. The incision was then closed with 2–3 discontinuous, dissolvable sutures (chromic gut surgical sutures, Ethicon Inc., Raritan, NJ). Povidone-iodine (Betadine, Avrio Health L.P., Stamford, CT) was applied over the incision to reduce the risk of infection. Fish were also tagged with an external anchor tag (FM-95W, Floy Tag & Manuf. Inc., Seattle, WA) inserted 1–2 cm posterior to the incision, with a unique identification number, contact information, and reward notice for later identification by fishermen or scuba divers (Herbig and Szedlmayer, 2016).

After tagging, fish were transferred to a 185-L recovery tank with aerated seawater. During the recovery period, fish were monitored for increased opercular pumping, control

of body orientation, and resumption of normal swimming motion. Recovered fish were then placed into a weighted rectangular cage (46 × 61 × 61 cm) made of plastic-coated 13-gauge wire and quickly lowered to the seafloor (depths: 19–31 m) within 10 m of the capture site. Once the cage reached the seafloor, a door automatically opened, allowing the tagged fish to leave on its own initiative (Williams et al., 2015). Any tagged fish that did not leave the cage after 20 min on the seafloor were not released.

Validation of detection data

Acoustic receivers can generate false detections that are not from valid transmitters in tagged fish (Pincock[2]). False detections can result from incomplete transmission due to interference (noise) or collision of signals when 2 or more transmitters simultaneously reach a receiver (Pincock[2]). To reduce the potential for data loss due to signal collisions, no more than 10 transmitters (tagged fish plus a control transmitter) were deployed at any individual VPS site at any one time (Topping and Szedlmayer, 2011; Piraino and Szedlmayer, 2014; McKinzie, 2018). False detections that resulted in the production of unknown tag IDs were removed from all subsequent analyses. Transmitter detections of known tags were screened before they were accepted as valid. Transmitter detections were accepted as valid if there were a minimum of 2 detections for a single transmitter ID and if there was at least one short interval between detections and more short intervals than long intervals. The short interval time was set at 30 min (30 times the nominal ping interval of 60 s). The long interval was set at 12 h (720 times the nominal ping interval of 60 s; Pincock[2]). All false detections of valid transmitters were removed from analysis.

Survival and mortality estimates

Fish positions (latitude and longitude) were calculated by Innovasea Systems from the time differential of signal arrival at 3–5 receivers. Status of each fish tagged with a transmitter was based on positions and the time interval between detections after a 3-d post-tagging recovery period. Any fish that remained stationary after exiting their release cage or that permanently emigrated away from the VPS site within the 3-d recovery period were considered lost and were removed from analyses. After 3 d, tagged gray triggerfish were categorized as active (continuously swimming around a VPS site), emigrated (progressively moving farther away from a VPS site until it was lost or had moved to a surrounding reef site), dead as a result of natural causes (M, tag became stationary or data indicates erratic large-scale movements, e.g., shark movement patterns; Altobelli and Szedlmayer, 2020), or dead or removed from stock as a result of fishing (F, suddenly disappeared from a VPS site).

[2] Pincock, D. G. 2012. False detections: what they are and how to remove them from detection data. Amirix Syst. Doc. DOC-004691, vers. 3, 11 p. [Available from website, accessed February 2022.]

Fish that emigrated were frequently detected with receivers at surrounding reef sites, and fish that experienced a mortality event were not detected at surrounding sites. Fishing mortalities were also confirmed by tags returned by fishermen. To increase the probability that fishermen would return tags, a high monetary reward was offered ($150). Posters describing the study and reward offer were posted at marinas, bait shops, and other public sites and on the Auburn University fish tagging website. It was assumed that tagged gray triggerfish active within the VPS sites where they were tagged and released experienced similar mortality rates to untagged fish outside of these VPS sites (Williams-Grove and Szedlmayer, 2016a; Mudrak and Szedlmayer, 2020).

A known-fate model was applied in the program MARK (vers. 8.2, available from website; White and Burnham, 1999) to estimate probabilities of conditional survival and total survival, as well as standard errors and 95% confidence intervals (CIs) (Schroepfer and Szedlmayer, 2006; Topping and Szedlmayer, 2013; Herbig and Szedlmayer, 2016; Williams-Grove and Szedlmayer, 2016a, 2016b; Mudrak and Szedlmayer, 2020). Annual estimates were based on weekly time intervals for each year of the study (2013–2017). The program MARK was used to calculate estimates of survival based on the maximum likelihood binomial (Edwards, 1992). The probability of surviving a mortality event was determined by calculating the number of individuals at risk of dying and the number of individuals that survived for that time interval. Fish that emigrated or suffered a mortality event not under consideration were removed (right censored). For example, when F was estimated, all data for fish that emigrated or died as a result of natural causes were removed (Williams-Grove and Szedlmayer, 2016a).

Instantaneous annual mortality rates were based on total survival (S) throughout the entire study period (241 weeks) adjusted to 52 weeks ($annual\ S = total\ S^{(52/241)}$) for each type of mortality. For example, the following equations were used for adjustments: $annual\ F = -\ln S^{(52/241)}$ for fishing mortality, $annual\ M = -\ln S^{(52/241)}$ for natural mortality, and $annual\ Z = -\ln S^{(52/241)}$ for total mortality (Starr et al., 2005). Confidence limits for instantaneous mortality rates were calculated from the 95% CIs estimated from the maximum-likelihood estimator of the survival functions at 1 year (52 weeks) (Klein and Moeschberger, 2003; Topping and Szedlmayer, 2013; Williams-Grove and Szedlmayer, 2016a; Mudrak and Szedlmayer, 2020). The reported sample sizes for the mortality estimates were the number of tagged gray triggerfish at risk during the time interval under analysis (Klein and Moeschberger, 2003).

Results

Mean fish size was 395 mm FL (standard deviation 52) and ranged from 276 to 535 mm FL. Most tagged gray triggerfish (86%) were above the legal sport and commercial size limit (356 mm FL). Five fish (9%) left their

VPS site within 3 d post-release, and 2 additional fish (3%) did not move after exiting their release cage. Data for these 7 individuals were removed from all analyses. The remaining individuals (n=49, 88%) were categorized as active, caught, emigrated, or deceased, and data for them were included in all subsequent estimates of mortality.

Movement patterns of gray triggerfish that remained after the 3-d recovery period (n=49) were monitored for 4–622 d. Among these tracked individuals, 30 fish had a final status of emigrated, 4 fish were caught by fishermen, 4 fish died of natural causes, and 11 fish were active when either their transmitter battery failed (n=8) or the study period ended (n=3) (Fig. 2). These fish were considered

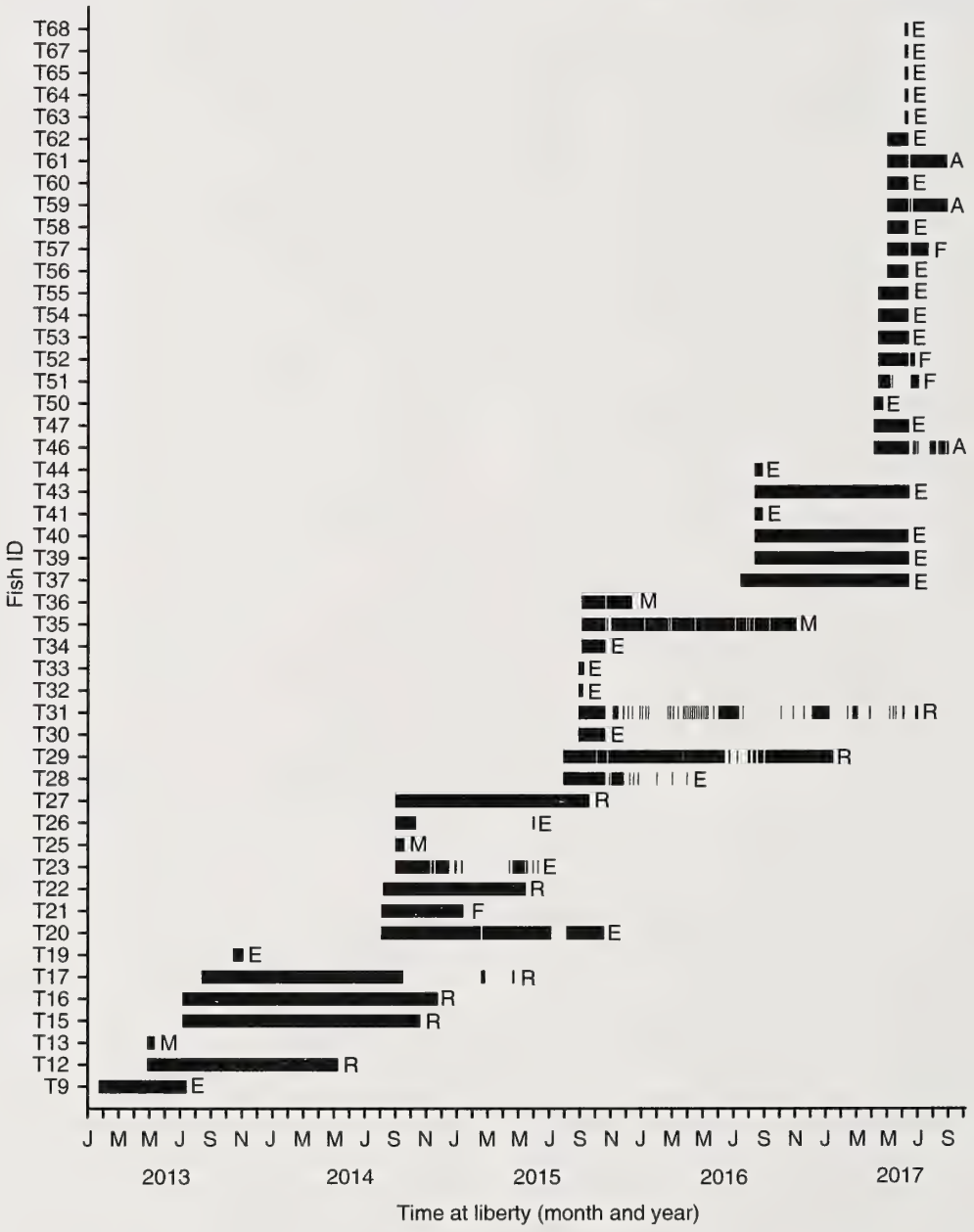

Figure 2

Duration of detections of 49 gray triggerfish (*Balistes capriscus*) (black bars) tagged with transmitters and tracked at artificial reef sites in the northern Gulf of Mexico from January 2013 through September 2017. Letters at the end of the bars denote the final fate of fish at sites where a Vemco Positioning System (VPS) was deployed: emigrated (E), fishing mortality (F), natural mortality (M), unknown (U), active as of the end of the study on 5 September 2017 (A), and resident at VPS site when transmitter battery failed (R).

active while residing at their respective VPS sites and were removed (right censored) from the data set when they emigrated away from their VPS sites.

Fishing mortality occurred for 4 tagged gray triggerfish (8%) while they resided at their VPS site (Fig. 2). All events of fishing mortality identified with telemetry were verified by reports of recapture by fishermen (a 100% reporting rate). Two additional fish (T20 and T28) were reported as captured by fishermen in 2016 after they emigrated from their VPS site. Fish T20 was detected and tracked intermittently for 443 d at the VPS site where it was tagged and released, and then it emigrated and was caught 693 d after release 2.2 km northwest of its VPS site. Fish T28 emigrated from its VPS site 12 d after release and was caught 249 d after release 0.9 km west of its VPS site. Total S from F (S_F) within the VPS sites over the 241-week study period was 0.35 (95% CI: 0.10–0.73). Total S adjusted to annual S, calculated as $S_F=0.35^{(52/241)}$, was 0.80; therefore, annual F, calculated as $F=-\ln 0.80$, was 0.23 (95% CI: 0.07–0.50) (Fig. 3). In 2015, 1 gray triggerfish was caught, among the 15 fish available for recapture at the VPS sites, and F was 0.29 (95% CI: 0.03–1.44). In 2017, 3 gray triggerfish were caught, among the 26 fish available for recapture, and F was 1.13 (95% CI: 0.29–2.87). No fishing mortalities were detected in 2013 (7 fish at liberty), 2014 (11 fish at liberty), or 2016 (9 fish at liberty) (Table 1). However, CIs overlap and indicate no significant differences in F among years.

During this study, natural mortalities were detected for 4 fish (8%), while they were active at their VPS site (Fig. 2). One additional natural mortality was detected for fish T34 outside the VPS site 199 d after it emigrated, but this fish had been removed from analysis. Total S from M (S_M) over the entire study period was 0.32 (95% CI: 0.07–0.74). Total S adjusted to annual S, calculated as $S_M=0.32^{(52/241)}$, was 0.78; therefore, annual M, calculated as $-\ln 0.78$, was 0.25 (95% CI: 0.07–0.57) (Fig. 4). One natural mortality occurred in each of the following years: 2013 (M=0.42; 95%

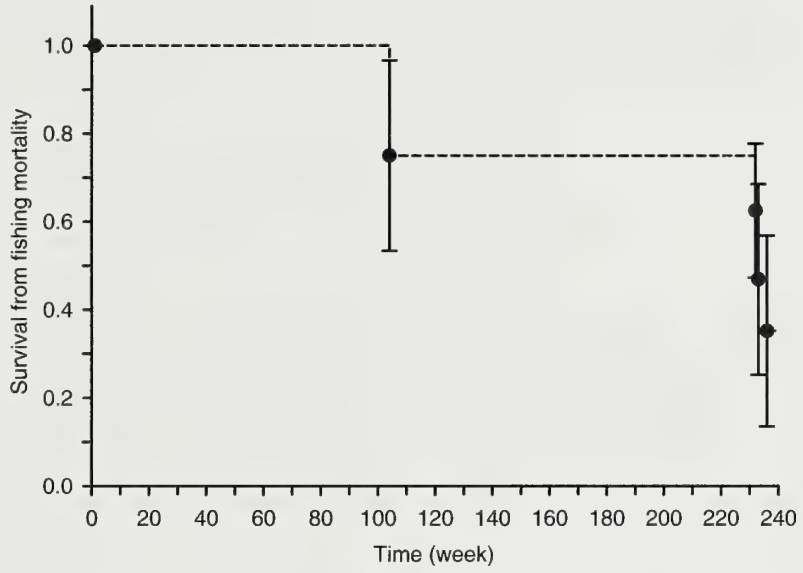

Figure 3

Weekly survival (S) of gray triggerfish (*Balistes capriscus*) from fishing mortality in the northern Gulf of Mexico from 2013 through 2017. The dashed lines indicate the proportions of fish surviving fishing mortality after each weekly interval. Instantaneous fishing mortality rates were calculated from S after 1 year at liberty. Black points indicate conditional estimates of S for weekly time intervals when a mortality occurred. Error bars indicate standard errors. The annual fishing mortality rate, calculated as $-\ln 0.35^{(52/241)}$, was 0.23 (95% confidence interval: 0.07–0.50) during the 241-week study period.

Table 1

Estimates of instantaneous annual total (Z), fishing (F), and natural (M) mortality rates of gray triggerfish (*Balistes capriscus*) from the use of telemetry methods with Vemco Positioning Systems at reef sites in the northern Gulf of Mexico from 2013 through 2017. Mortality rates were estimated for each year and for all 5 years combined by using the number of tagged fish available for recapture during each year (n) and the number of days in the fishing season for each year. The 95% confidence intervals for mortality rates are provided in parentheses.

Year	n	Z	F	M	Season	No. of days
2013	7	0.42 (0.05–1.95)	0.00	0.42 (0.05–1.95)	1 Jan–9 Jun; 1 Aug–15 Oct	236
2014	12	0.12 (0.02–0.69)	0.00	0.12 (0.02–0.69)	1 Jan–30 Apr	120
2015	15	0.69 (0.13–2.09)	0.29 (0.03–1.44)	0.41 (0.04–1.87)	1 Jan–6 Feb	37
2016	9	0.22 (0.03–1.17)	0.00	0.22 (0.03–1.17)	1 Jan–31 May	152
2017	26	1.13 (0.29–2.87)	1.13 (0.29–2.87)	0.00	Closed	0
Total	49	0.48 (0.18–0.85)	0.23 (0.07–0.50)	0.25 (0.07–0.57)	–	545

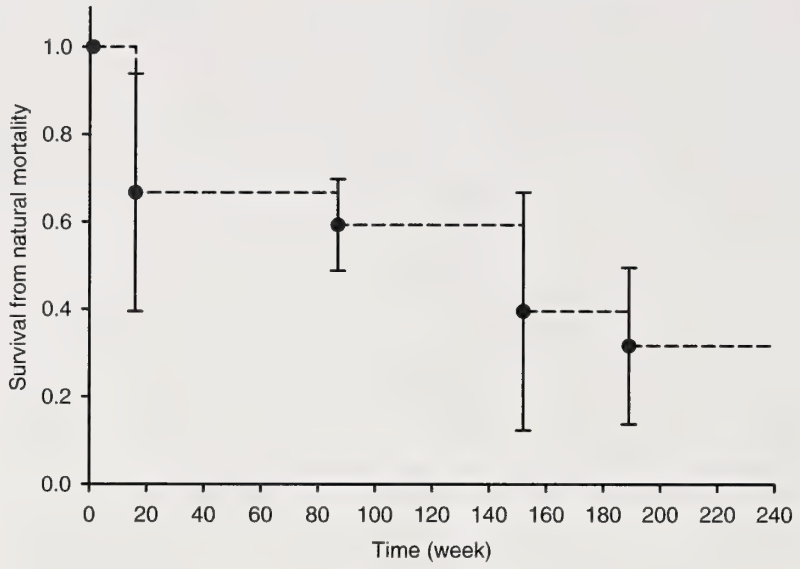

Figure 4

Weekly survival (S) of gray triggerfish (*Balistes capriscus*) from natural mortality in the northern Gulf of Mexico from 2013 through 2017. The dashed lines indicate the proportions of fish surviving after each weekly interval. Instantaneous natural mortality rates were calculated from S after 1 year at liberty. Black points indicate conditional estimates of S for weekly time intervals when a mortality occurred. Error bars indicate standard errors. The annual natural mortality rate, calculated as $-\ln 0.32^{(52/241)}$, was 0.25 (95% confidence interval: 0.07–0.57) during the 241-week study period.

CI: 0.05–1.95), 2014 (M=0.12; 95% CI: 0.02–0.69), 2015 (M=0.41; 95% CI: 0.04–1.87), and 2016 (M=0.22; 95% CI: 0.03–1.17). Again, CIs overlap and indicate no significant difference in M among years. No natural mortalities were detected in 2017 (Table 1).

Total S from Z (S_Z) for all years of the study was 0.11 (95% CI: 0.02–0.44), S_Z adjusted to annual S, calculated as $S_Z=0.11^{(52/241)}$, was 0.62, and annual Z, calculated as $-\ln 0.62$, was 0.48 (95% CI: 0.18–0.85) (Fig. 5). Total mortality ranged from 0.12 (in 2014) to 1.13 (in 2017), but again CIs overlap and indicate no significant difference in Z among years (Table 1). No false detections were recorded by receivers at VPS sites or surrounding reef sites after mortalities occurred. The lack of false detections, along with reports from fishermen of recaptured fish, verify all mortalities determined with the VPSs (deaths resulting from both natural causes and fishing).

Discussion

In this study, acoustic telemetry was applied to directly estimate instantaneous rates of F, M, and Z for gray triggerfish. The arrays of receivers at VPS sites allowed continuous, long-term (up to 662 d), highly accurate (to ≤3 m) tracking of tagged gray triggerfish that resided around artificial reefs in the northern Gulf of Mexico. Importantly, the number of mortalities were estimated directly, independent of the number of tags returned by fishermen, because the fates of tagged individuals were known while they resided at VPS-monitored reef sites (Hightower et al., 2001; Heupel and Simpfendorfer, 2002; Bacheler et al., 2009; Topping and Szedlmayer, 2013; Williams-Grove and Szedlmayer, 2016a).

The estimated annual F from this study is 0.23 for the period of 2013–2017, a level lower than that from the previous stock assessment in 2015, indicating that management efforts of amendment 37 have been successful in reducing F (GMFMC, 2012). However, the F of 0.23 from this study is still greater than the F of 0.12 estimated for 2013 in the previous stock assessment (SEDAR, 2015). The greater F in this study indicates that the Gulf of Mexico stock of gray triggerfish may still be experiencing overfishing because the value is greater than the maximum F threshold of 0.17 from the stock assessment in 2015; the threshold was based on a spawning potential ratio of 30% (SEDAR, 2015). The rebuilding plan developed in 2017 also noted that the Gulf of Mexico stock of gray triggerfish was not rebuilding on target, possibly as a result of the sport fishery often exceeding annual catch limits, incompatibilities between the federal and state fishing seasons, and low annual recruitment (GMFMC, 2017b).

Limits on catch of gray triggerfish were unchanged over the study period of 2013–2017. However, sport fishery accountability measures led to seasons of varying lengths (from 37 to 236 d) during 2013–2016, with a complete closure in 2017 because of landings in 2016 exceeding the catch limit by 245% (GMFMC, 2017b). In this study, we did not detect a significant difference in annual F, as indicated by overlapping CIs. It is possible that no trends were observed because fishermen were unaware of season length and closure dates prior to the start of the annual fishing season because they were announced mid-season once annual catch limits were estimated to have been reached. Yet, as has been the case with most telemetry tagging studies, sample sizes were small in this study. Therefore, annual comparisons of F should be treated with caution because of the limited number of tagged fish that were available for recapture each year.

Fishery regulations for target and non-target species may have unexpected consequences (Gislason, 2003; Walters et al., 2005). In this study, although no significant differences were detected for F among years, the trend in F indicates that the highest annual rate was 1.13 in 2017. Surprisingly, this level of F occurred when the federal sport fishery for gray triggerfish was completely closed because fishermen exceeded the quota for 2016 (GMFMC, 2017b).

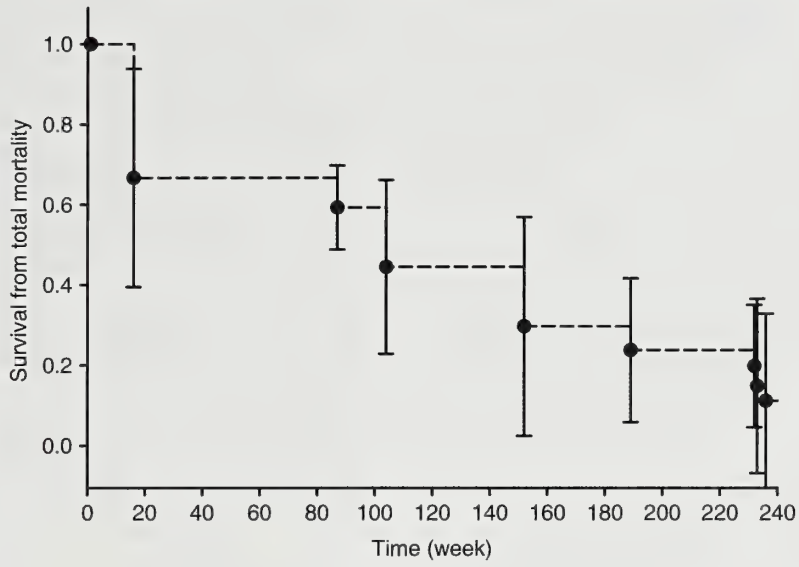

Figure 5

Weekly survival (S) of gray triggerfish (*Balistes capriscus*) from total mortality in the northern Gulf of Mexico from 2013 through 2017. The dashed lines indicate the proportions of fish surviving after each weekly interval. Instantaneous total mortality rates were calculated from S after 1 year at liberty. Black points indicate conditional estimates of S for weekly time intervals when a mortality occurred. Error bars indicate standard errors. The annual total mortality rate, calculated as $-\ln 0.11^{(52/241)}$, was 0.48 (95% confidence interval: 0.18–0.85) during the 241-week study period.

All fishing mortalities of gray triggerfish in 2017 occurred in July during the extended sport fishery season for red snapper (NMFS[3]). Therefore, we suggest that the sport fishery for red snapper affected a non-target species, gray triggerfish, because of their shared dependence on natural and artificial reef habitats (Simmons and Szedlmayer, 2011, 2018; Jaxion-Harm et al., 2018). Previous telemetry studies have confirmed that both species are reef dependent, maintain long-term residencies, and have high site fidelity to individual reef structures (Szedlmayer and Schroepfer, 2005; Topping and Szedlmayer, 2011; Piraino and Szedlmayer, 2014; Herbig and Szedlmayer, 2016; Williams-Grove and Szedlmayer, 2016b, 2017; McKinzie, 2018). Increased F has also been linked to fish species that congregate at predictable or known locations (Roughgarden and Smith, 1996; Hutchings, 2000; Worm et al., 2009; Williams-Grove and Szedlmayer, 2016a).

At the time of our study, the Gulf of Mexico stock of gray triggerfish was overfished and not rebuilding on target. In addition, the population size and spawning stock biomass were near historic lows (GMFMC, 2017b). However, because of recent changes to the minimum stock size threshold, the stock is no longer considered overfished, but it is still not rebuilding on target (GMFMC, 2017a). Any additional fishing pressure on gray triggerfish, particularly during critical periods, such as spawning when the fishery is closed, could further slow stock recovery (van Overzee and Rijnsdorp, 2015).

Historically, rates for reporting of tagged fish by fishermen were indirectly measured with secretly implanted tags, port or processor surveys, landings data, and multiple-tag studies (Pollock et al., 2001; Pine et al., 2003). In multiple-tag studies, reporting of recovery of high-reward tags is assumed to be 100%, and the difference between the reporting for recovery of standard tags and that for high-reward tags is used to adjust the reporting rate (Pollock et al., 2001; Bacheler et al., 2009; Hightower and Pollock, 2013). In this study, we used a high reward ($150) for all tags, and reporting rates were 100%, based on the number of fishing mortalities determined by using telemetry. However, these results should be interpreted with caution because of small sample sizes, and always assuming 100% return rates for high-reward tags may cause underestimates of F (Pollock et al., 2001; Pine et al., 2003). For example, in previous telemetry studies in which tag reporting rates were directly estimated, reporting rates were <100%: 17% (Hightower et al., 2001), 89% (Topping and Szedlmayer, 2013), 63% (Williams-Grove and Szedlmayer, 2016a), and 77.1% (Mudrak and Szedlmayer, 2020).

[3] NMFS (National Marine Fisheries Service). 2017. NOAA announces the 2017 Gulf of Mexico red snapper recreational seasons. FB17-023 Gulf of Mexico Fishery Bulletin. [Available from website, accessed February 2022.]

Reporting rates less than 100% were attributed to tag shedding, unintentional noncompliance, or intentional nonreporting due to disagreements over management restrictions (Schwartz, 2000; Pollock et al., 2001; Denson et al., 2002; Gaertner and Pierre-Hallier, 2015; Williams-Grove and Szedlmayer, 2016a).

Another advantage of telemetry is that it can be used to provide fishery-independent estimates of F and M, but reports of recaptured fish by fishermen are still important for validating the telemetry-based estimates (Hightower and Pollock, 2013; Topping and Szedlmayer, 2013; Williams-Grove and Szedlmayer, 2016a; Mudrak and Szedlmayer, 2020). In addition, data on tag returns by fishermen provide a rare opportunity to understand fishermen behavior (Pine et al., 2003) and can be used to generate species-specific reporting rates of tagged fish (Mudrak and Szedlmayer, 2020).

In this study, one natural mortality event was observed during each year of the study, except in 2017. The overall annual estimate of M was 0.25 (95% CI: 0.07–0.57) for all years of the study (2013–2017) and was similar to the M of 0.28 that was used in the stock assessment model for 2015 (Burton et al., 2015; SEDAR, 2015). Both the 2015 stock assessment and the telemetry approach used in this study are validated by the similarity of the values of M estimated with the 2 totally different methods.

Interestingly, one gray triggerfish (T35) was identified as a fish that experienced natural mortality rather than as an emigrated fish on the basis of patterns of detections with receivers at surrounding reef sites after the fish left the VPS site. Detections of fish T35, after almost continuous tracking for 426 d at the VPS site where it was tagged and released (Fig. 2), were recorded at 15 different surrounding reef sites and indicate that 38 directed movements occurred over a 5-d period, with a total distance moved of 91 km. This pattern of substantially increased horizontal movement matches movement patterns of a tagged sandbar shark (*Carcharhinus plumbeus*) and a tagged bull shark (*C. leucas*) detected with telemetry in the same study area (Altobelli and Szedlmayer, 2020). Therefore, these detections of fish T35 indicate the movements of a predator rather than of a gray triggerfish.

Conclusions

In this study, we successfully identified the fates of 100% of tagged gray triggerfish residing on artificial reefs in the northern Gulf of Mexico after a 3-d recovery period, independent of tag returns by fishermen, and used telemetry from VPS sites for direct estimation of F, M, and Z. Valid detections from receivers at surrounding reef sites were used to successfully verify that fish emigrated. Mortalities identified with telemetry were confirmed by using information on tag returns by fishermen, on the lack of detections with single receivers after fish were caught, or on detection patterns that indicate predator movements. The estimate of M from this study supports values applied in management efforts, and the F from this study indicates that previous management efforts have been successful in reducing F but that the stock may still be experiencing overfishing. This study also highlights the importance of bycatch mortality of gray triggerfish (i.e., as fishermen pursue other species, such as red snapper, gray triggerfish are caught despite a closed season for this species).

One difficulty in this study was comparing mortality estimates for a relatively small area off the coast of Alabama to estimates for the entire Gulf of Mexico. Therefore, the telemetry estimates from this study may be limited. Still, estimates of mortality based on telemetry methods are likely more accurate than estimates based on landings data from phone or mail surveys (i.e., based on fishery-dependent data from the Marine Recreational Information Program; SEDAR, 2015). Therefore, the expansion of the use of acoustic telemetry for estimation of mortality rates could improve the management of gray triggerfish.

Acknowledgments

We thank A. Altobelli, R. Beyea, L. Biermann, A. Everett, E. Fedewa, J. Grove, J. Herbig, S. Landers, E. Levine, P. Mudrak, A. Osowski, C. Roberts, M. Szczebak, and N. Wilson for their assistance with fieldwork. This project was supported by Sport Fish Restoration funding through the Marine Resources Division of the Alabama Department of Conservation and Natural Resources. This is a contribution of the Alabama Agricultural Experiment Station, and the School of Fisheries, Aquaculture, and Aquatic Sciences, Auburn University.

Literature cited

Altobelli, A. N., and S. T. Szedlmayer.
2020. Migration and residency of sandbar, Atlantic sharpnose, bull, and nurse sharks in the northern Gulf of Mexico. North Am. J. Fish. Manag. 40:1324–1343.

Bacheler, N. M., J. A. Buckel, J. E. Hightower, L. M. Paramore, and K. H. Pollock.
2009. A combined telemetry - tag [sic] return approach to estimate fishing and natural mortality rates of an estuarine fish. Can. J. Fish. Aquat. Sci. 66:1230–1244.

Bacheler, N. M., K. W. Shertzer, J. A. Buckel, P. J. Rudershausen, and B. J. Runde.
2018. Behavior of gray triggerfish *Balistes capriscus* around baited fish traps determined from fine-scale acoustic tracking. Mar. Ecol. Prog. Ser. 606:133–150.

Bacheler, N. M., T. Michelot, R. T. Cheshire, and K. W. Shertzer.
2019a. Fine-scale movement patterns and behavioral states of gray triggerfish *Balistes capriscus* determined from acoustic telemetry and hidden Markov models. Fish. Res. 215:76–89.

Bacheler, N. M., K. W. Shertzer, R. T. Chesire, and J. H. MacMahan.
2019b. Tropical storms influence the movement behavior of a demersal oceanic fish species. Sci. Rep. 9:1481.

Burton, M. L., J. C. Potts, D. R. Carr, M. Cooper, and J. Lewis.
2015. Age, growth, and mortality of gray triggerfish (*Balistes capriscus*) from the southeastern United States. Fish. Bull. 113:27–39.

Charnov, E. L., H. Gislason, and J. G. Pope.
2013. Evolutionary assembly rules for fish life histories. Fish Fish. 14:213–224.

Cho, G. K., and D. D. Heath.
2000. Comparison of tricaine methanesulphonate (MS222) and clove oil anaesthesia effects on the physiology of juvenile chinook [sic] salmon *Oncorhynchus tshawytscha* (Walbaum). Aquac. Res. 31:537–546.

Denson, M. R., W. E. Jenkins, A. G. Woodward, and T. I. J. Smith.
2002. Tag-reporting levels for red drum (*Sciaenops ocellatus*) caught by anglers in South Carolina and Georgia estuaries. Fish. Bull. 100:35–41.

Edwards, A. W. F.
1992. Likelihood, expanded ed., 296 p. Johns Hopkins Univ. Press, Baltimore, MD.

Gaertner, D., and J. Pierre-Hallier.
2015. Tag shedding by tropical tunas in the Indian Ocean and other factors affecting the shedding rate. Fish. Res. 163:98–105.

Gislason, H.
2003. The effects of fishing on non-target species and ecosystem structure and function. *In* Responsible fisheries in the marine ecosystem (M. Sinclair and G. Valdimarsson, eds.), p. 255–274. FAO, Rome.

GMFMC (Gulf of Mexico Fisheries Management Council).
1981. Environmental impact statement and fishery management plan for the reef fish resources of the Gulf of Mexico, 216 p. Gulf Mex. Fish. Manag. Counc., Tampa, FL. [Available from website.]
2012. Modifications to the gray triggerfish rebuilding plan including adjustments to the annual catch limits and annual catch targets for the commercial and recreational sectors: final amendment 37 to the fishery management plan for the reef fish resources of the Gulf of Mexico, including environmental assessment, fishery impact statement, regulatory impact review, and Regulatory Flexibility Act analysis, 140 p. Gulf Mex. Fish. Manag. Counc., Tampa, FL. [Available from website.]
2017a. Minimum stock size threshold (MSST) revision for reef fish stocks with existing status determination criteria: final amendment 44 (revised) to the fishery management plan for the reef fish resources of the Gulf of Mexico, 104 p. Gulf Mex. Fish. Manag. Counc., Tampa, FL. [Available from website.]
2017b. Gray triggerfish rebuilding plan: final amendment 46 to the fishery management plan for the reef fish resources of the Gulf of Mexico, including environmental assessment, fishery impact statement, regulatory impact review, and Regulatory Flexibility Act analysis, 149 p. Gulf Mex. Fish. Manag. Counc., Tampa, FL. [Available from website.]

Herbig, J. L., and S. T. Szedlmayer.
2016. Movement patterns of gray triggerfish, *Balistes capriscus*, around artificial reefs in the northern Gulf of Mexico. Fish. Manag. Ecol. 23:418–427.

Heupel, M. R., and C. A. Simpfendorfer.
2002. Estimation of mortality of juvenile blacktip sharks, *Carcharhinus limbatus*, within a nursery area using telemetry data. Can. J. Fish. Aquat. Sci. 59:624–632.

Hewitt, D. A., and J. M. Hoenig.
2005. Comparison of two approaches for estimating natural mortality based on longevity. Fish. Bull. 103:433–437.

Hightower, J. E., and K. H. Pollock.
2013. Tagging methods for estimating population size and mortality rates of inland striped bass populations. Am. Fish. Soc. Symp. 80:249–262.

Hightower, J. E., J. R. Jackson, and K. H. Pollock.
2001. Use of telemetry methods to estimate natural and fishing mortality of striped bass in Lake Gaston, North Carolina. Trans. Am. Fish. Soc. 130:557–567.

Hutchings, J. A.
2000. Collapse and recovery of marine fishes. Nature 406:882–885.

Jaxion-Harm, J., S. T. Szedlmayer, and P. A. Mudrak.
2018. A comparison of fish assemblages according to artificial reef attributes and seasons in the northern Gulf of Mexico. Am. Fish. Soc. Symp. 86:23–45.

Johnson, A. G., and C. H. Saloman.
1984. Age, growth, and mortality of gray triggerfish, *Balistes capriscus*, from the northeastern Gulf of Mexico. Fish. Bull. 82:485–492.

Kaplan, E. L., and P. Meier.
1958. Nonparametric estimation from incomplete observations. J. Am. Stat. Assoc. 53:457–481.

Kelly-Stormer, A., V. Shervette, K. Kolmos, D. Wyanski, T. Smart, C. McDonough, and M. J. M. Reichert.
2017. Gray triggerfish reproductive biology, age, and growth off the Atlantic coast of the southeastern USA. Trans. Am. Fish. Soc. 146:523–538.

Klein, J. P., and M. L. Moeschberger.
2003. Survival analysis: techniques for censored and truncated data, 2nd ed., 538 p. Springer-Verlag, New York.

Knip, D. M., M. R. Heupel, and C. A. Simpfendorfer.
2012. Mortality rates for two shark species occupying a shared coastal environment. Fish. Res. 125–126:184–189.

McKinzie, M. K.
2018. Horizontal and vertical movement, residency and mortality of gray triggerfish (*Balistes capriscus*) on artificial reefs in the northern Gulf of Mexico. Ph.D. diss., 146 p. Auburn Univ., Auburn, AL. [Available from website.]

Mudrak, P. A., and S. T. Szedlmayer.
2020. Fishing mortality estimates for red snapper, *Lutjanus campechanus*, based on acoustic telemetry and conventional mark-recapture. *In* Red snapper biology in a changing world (S. T. Szedlmayer and S. A. Bortone, eds.), p. 75–94. CRC Press, Boca Raton, FL.

Munday, P. L., and S. K. Wilson.
1997. Comparative efficacy of clove oil and other chemicals in anaesthetization of *Pomacentrus amboinensis*, a coral reef fish. J. Fish Biol. 51:931–938.

NASEM (National Academies of Sciences, Engineering, and Medicine).
2017. Review of the Marine Recreational Information Program, 198 p. Natl. Acad. Press, Washington, DC. [Available from website.]

Pine, W. E., K. H. Pollock, J. E. Hightower, T. J. Kwak, and J. A. Rice.
2003. A review of tagging methods for estimating fish population size and components of mortality. Fisheries 28:10–23.

Pine, W. E., J. E. Hightower, L. G. Coggins, M. V. Lauretta, and K. H. Pollock.
2012. Design and analysis of tagging studies. *In* Fisheries techniques, 3rd ed. (A. V. Zale, D. L. Parrish, and T. M. Sutton, eds.), p. 521–572. Am. Fish. Soc., Bethesda, MD.

Piraino, M. N., and S. T. Szedlmayer.
2014. Fine-scale movements and home ranges of red snapper around artificial reefs in the northern Gulf of Mexico. Trans. Am. Fish. Soc. 143:988–998.

Pollock, K. H., S. R. Winterstein, C. M. Bunck, and P. D. Curtis.
1989. Survival analysis in telemetry studies: the staggered entry design. J. Wildl. Manag. 53:7–15.

Pollock, K. H., C. M. Bunck, S. R. Winterstein, and C.-L. Chen.
1995. A capture-recapture survival analysis model for radio-tagged animals. J. Appl. Stat. 22:661–672.
Pollock, K. H., J. M. Hoenig, W. S. Hearn, and B. Calingaert.
2001. Tag reporting rate estimation: 1. An evaluation of the high-reward tagging method. North Am. J. Fish. Manag. 21:521–532.
Pollock, K. H., H. Jiang, and J. E. Hightower.
2004. Combining telemetry and fisheries tagging models to estimate fishing and natural mortality rates. Trans. Am. Fish. Soc. 133:639–648.
Ricker, W. E.
1975. Computation and interpretation of biological statistics of fish populations. Bull. Fish. Res. Board Can. 191, 382 p.
Roughgarden, J., and F. Smith.
1996. Why fisheries collapse and what to do about it. Proc. Natl. Acad. Sci. U.S.A. 93:5078–5083.
Schroepfer, R. L., and S. T. Szedlmayer.
2006. Estimates of residence and site fidelity for red snapper *Lutjanus campechanus* on artificial reefs in the northeastern Gulf of Mexico. Bull. Mar. Sci. 78:93–101.
Schwartz, F. J.
2000. Anglers and tagging programs: another perspective. Fisheries 25(12):36–37.
SEDAR (Southeast Data, Assessment, and Review).
2011. SEDAR 9 update stock assessment report: Gulf of Mexico gray triggerfish, 266 p. Gulf Mex. Fish. Manag. Counc., Tampa, FL. [Available from website.]
2013. SEDAR 31—Gulf of Mexico red snapper stock assessment report, 1103 p. SEDAR, North Charleston, SC. [Available from website.]
2015. SEDAR 43 stock assessment report: Gulf of Mexico gray triggerfish, 174 p. SEDAR, North Charleston, SC. [Available from website.]
Simmons, C. M., and S. T. Szedlmayer.
2011. Recruitment of age-0 gray triggerfish to benthic structured habitat in the northern Gulf of Mexico. Trans. Am. Fish. Soc. 140:14–20.
2018. Competitive interactions between gray triggerfish (*Balistes capriscus*) and red snapper (*Lutjanus campechanus*) in laboratory and field studies in the northern Gulf of Mexico. Can. J. Fish. Aquat. Sci. 75:1313–1318.
Starr, R. M., V. O'Connell, S. Ralston, and L. Breaker.
2005. Use of acoustic tags to estimate natural mortality, spillover, and movements of lingcod (*Ophiodon elongatus*) in a marine reserve. Mar. Technol. Soc. J. 39:19–30.
Summerfelt, R. C., and L. S. Smith.
1990. Anesthesia, surgery, and related techniques. *In* Methods for fish biology (C. B. Schreck and P. B. Moyle, eds.), p. 213–272. Am. Fish. Soc., Bethesda, MD.
Syc, T. S., and S. T. Szedlmayer.
2012. A comparison of size and age of red snapper (*Lutjanus campechanus*) with the age of artificial reefs in the northern Gulf of Mexico. Fish. Bull. 110:458–469.
Szedlmayer, S. T., and R. L. Schroepfer.
2005. Long-term residence of red snapper on artificial reefs in the northeastern Gulf of Mexico. Trans. Am. Fish. Soc. 134:315–325.
Topping, D. T., and S. T. Szedlmayer.
2011. Site fidelity, residence time and movements of red snapper *Lutjanus campechanus* estimated with long-term acoustic monitoring. Mar. Ecol. Prog. Ser. 437:183–200.
2013. Use of ultrasonic telemetry to estimate natural and fishing mortality of red snapper. Trans. Am. Fish. Soc. 142:1090–1100.
Trent, T. T., and O. J. Rongstad.
1974. Home range and survival of cottontail rabbits in southwestern Wisconsin. J. Wildl. Manag. 38:459–472.
van Overzee, H. M. J., and A. D. Rijnsdorp.
2015. Effects of fishing during the spawning period: implications for sustainable management. Rev. Fish Biol. Fish. 25:65–83.
Walters, C. J., V. Christensen, S. J. Martell, and J. F. Kitchell.
2005. Possible ecosystem impacts of applying MSY policies from single-species assessment. ICES J. Mar. Sci. 62:558–568.
White, G. C., and K. P. Burnham.
1999. Program MARK: survival estimation from populations of marked animals. Bird Study 46(sup1):S120–S139.
Williams-Grove, L. J., and S. T. Szedlmayer.
2016a. Mortality estimates for red snapper based on ultrasonic telemetry in the northern Gulf of Mexico. North Am. J. Fish. Manag. 36:1036–1044.
2016b. Acoustic positioning and movement patterns of red snapper *Lutjanus campechanus* around artificial reefs in the northern Gulf of Mexico. Mar. Ecol. Prog. Ser. 553:233–251.
2017. Depth preferences and three-dimensional movements of red snapper, *Lutjanus campechanus*, on an artificial reef in the northern Gulf of Mexico. Fish. Res. 190:61–70.
Williams, L. J., J. L. Herbig, and S. T. Szedlmayer.
2015. A cage release method to improve fish tagging studies. Fish. Res. 172:125–129.
Worm, B., R. Hilborn, J. K. Baum, T. A. Branch, J. S. Collie, C. Costello, M. J. Fogarty, E. A. Fulton, J. A. Hutchings, S. Jennings, et al.
2009. Rebuilding global fisheries. Science 325:578–585.

Errata

Fishery Bulletin 118:145–156 (2020).
Langan, Joseph A., M. Conor McManus, Douglas R. Zemeckis, and Jeremy S. Collie
Abundance and distribution of Atlantic cod (*Gadus morhua*) in a warming southern New England

Corrections

Please note that a minor coding error affected several of the values reported in the text and in Figures 3, 5, and 6 in this manuscript. Importantly, this error does not affect any of the reported patterns or conclusions of the work. All changes to statistical results are within the confidence bounds of the original reported values (i.e., there are no significant change in values). The revised sentences and figures provided here include corrected values.

On Page 150, in the last paragraph in the right column, the second sentence should read as follows, with corrected coefficients of correlation (r) and P-values:

When compared with the VTR landings data, YOY mean annual CPUE in the RIDEM trawl survey was significantly correlated at a lag of 2 years both to future landings by the party and charter fleets (r=0.666, P=0.007) and to future landings by commercial vessels (r=0.582, P=0.023).

On Page 151, in Line 3 of the right column, the value for deviance explained is reported as *27.2%* but should be given as *27.6%*.

On Page 150, Figure 3 should read as follows, with corrected values in panel A:

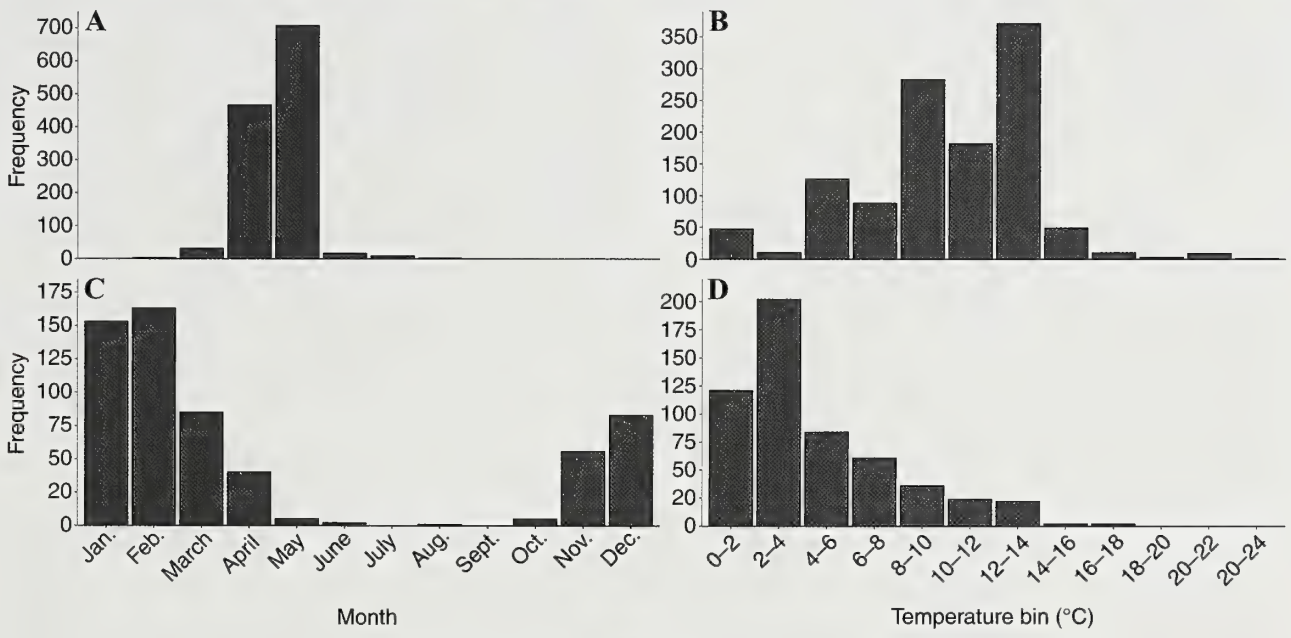

Figure 3

Frequency distributions of the months during and bottom water temperatures at which (**A** and **B**) young-of-the-year (YOY) Atlantic cod (*Gadus morhua*) and (**C** and **D**) those age 1 or older (age 1+) were captured in Rhode Island. The YOY Atlantic cod were sampled during a monthly trawl survey conducted by the Rhode Island Department of Environmental Management in 1979–2018, and age-1+ Atlantic cod were sampled during the trawl surveys conducted by the Graduate School of Oceanography, University of Rhode Island, in 1959–2018.

On Page 152, Figure 5 should read as follows, with corrected values in panels B and C:

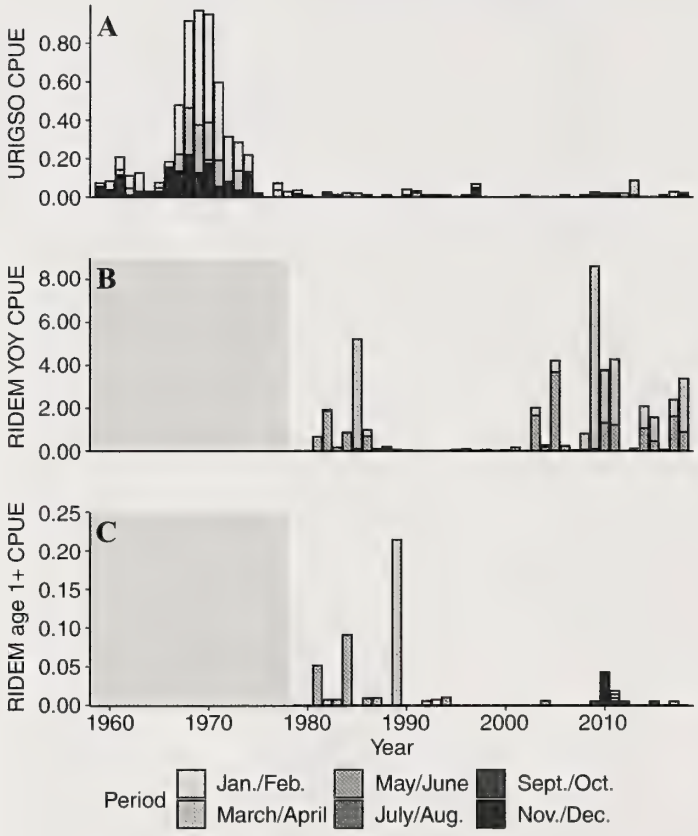

Figure 5

Abundance of Atlantic cod (*Gadus morhua*) in waters of Rhode Island from fishery-independent sources of catch-per-unit-of-effort (CPUE) data, separated into bimonthly bins. Abundances shown include the following data: (**A**) annual CPUE of Atlantic cod in the trawl survey conducted by the University of Rhode Island Graduate School of Oceanography (URIGSO) in 1959–2018, (**B**) CPUE of young-of-the-year Atlantic cod in the seasonal and monthly trawl surveys conducted by the Rhode Island Department of Environmental Management (RIDEM) in 1979–2018, and (**C**) CPUE of Atlantic cod that were age 1 or older (age 1+) in the RIDEM seasonal and monthly trawl surveys conducted in 1979–2018. Gray shaded areas indicate the periods for which no data are available.

On Page 153, Figure 6 should read as follows, with corrected values in the figure and with corrected *P*-value and coefficient of multiple determination in the third sentence of the legend:

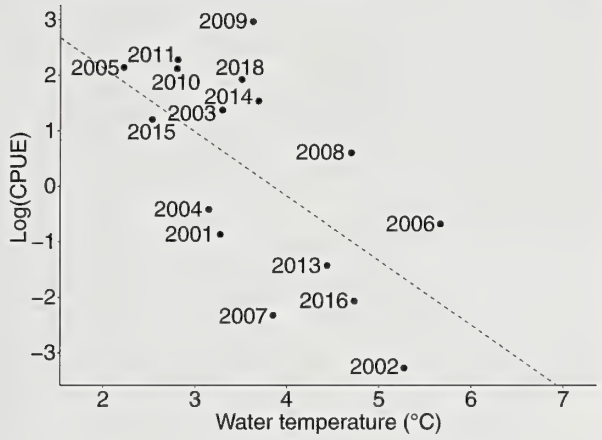

Figure 6

The approximately log-linear relationship between mean bottom water temperature in February and log-transformed mean catch per unit of effort (CPUE) of young-of-the-year (YOY) Atlantic cod (*Gadus morhua*) in March–July, during the period of observed increase in CPUE in Rhode Island state waters in 2001–2018. Water temperatures in February were recorded during trawl surveys conducted by the University of Rhode Island Graduate School of Oceanography and are used to represent values for each year, and CPUE data are from trawl surveys conducted by the Rhode Island Department of Environmental Management. The diagonal dashed line depicts a linear regression fit to the data (P=0.006, coefficient of multiple determination=0.383). Data from the surveys conducted in 2017 were omitted because of missing temperature measurements. Data from surveys conducted in 2012 were omitted because no YOY Atlantic cod were captured.

Fishery Bulletin

Guidelines for authors

Contributions published in *Fishery Bulletin* describe original research in marine fishery science, fishery engineering and economics, and marine environmental and ecological sciences (including modeling). Preference will be given to manuscripts that examine processes and underlying patterns. Descriptive reports, surveys, and observational papers may occasionally be published but should appeal to an audience outside the locale in which the study was conducted.

Although all contributions are subject to peer review, responsibility for the contents of papers rests upon the authors and not on the editor or publisher. *Submission of an article implies that the article is original and is not being considered for publication elsewhere.*

All submissions are subject to a double-blind review to remove the identity of author and reviewer during the review process.

Plagiarism and double publication are considered serious breaches of publication ethics. To verify the originality of the research in papers and to identify possible previous publication, manuscripts may be screened with plagiarism-detection software.

Manuscripts must be written in English; authors whose native language is not English are strongly advised to have their manuscripts checked by English-speaking colleagues before submission.

Once a paper has been accepted for publication, online publication takes approximately 2 weeks.

There is no cost for publication in *Fishery Bulletin*.

Types of manuscripts accepted by the journal

Articles generally range from 20 to 30 double-spaced typed pages (12-point font) and describe an original contribution to fisheries science, engineering, or economics. Tables and figures are not included in this page count, but the number of figures should not exceed 1 figure for every 4 pages of text. Articles contain the following divisions: abstract, introduction, methods, results, discussion, and conclusions.

Notes are generally less than 10 double-spaced typed pages (12-point font), including the Literature cited section. Like articles, notes describe an original contribution to fisheries science. They follow a format similar to that for articles: abstract, introduction, methods, results, and discussion, but the results and discussion sections may be combined and a conclusions section should not be included. They should include no more than 2 figures or tables (2 of each would be too many). They are distinguished from full articles in that they report a noteworthy new observation or discovery—such as the first report of a new species, a unique finding, condition, or event that expands our knowledge of fisheries science, engineering, or economics—and do not require a lengthy discussion. Manuscripts on range extensions will not be considered.

Companion articles should be submitted together and are published together as a scientific contribution. Both articles should address a closely related topic and may be articles that result from a workshop or conference.

Review articles of exceptional quality may be considered occasionally for publication on a case-by-case basis. They address a timely topic that is relevant to aspects of fisheries science. They should include an abstract, but the format of the article, per se, will be up to the author. Please contact the scientific editor to discuss your ideas regarding a potential review article before embarking on such a project.

Perspective essays generally are less than 5 double-spaced typed pages (12-point font) and provide clarification of misused terms or misunderstood topics in fisheries science. Essays are accepted at the discretion of the scientific editor. Opinion pieces on policy will not be considered. They should include an abstract and a list of the literature cited, but no other sections should divide the article. Please contact the scientific editor to discuss your idea before making a submission.

Preparation of manuscript

Title page should include authors' full names, affiliations, mailing addresses, and the senior author's email address.

Abstract should be limited to 200 words (one-half typed page), state the main scope of the research, and emphasize the authors' conclusions and relevant findings. Do not review the methods of the study or list the contents of the paper. Because abstracts are circulated by abstracting agencies, it is important that they represent the research clearly and concisely.

General text must be typed in 12-point Times New Roman font throughout. A brief introduction should convey the broad significance of the paper; the remainder of the paper should be divided into the following sections: Materials and methods, Results, Discussion, Conclusions, and Acknowledgments. Headings within each section must be short, reflect a logical sequence, and follow the rules of subdivision (i.e., there can be no subdivision without at least 2 subheadings). The entire text should be intelligible to interdisciplinary readers; therefore, all acronyms, abbreviations, and technical terms should be written out in full and defined the first time they are mentioned. Abbreviations should be used sparingly because they are not carried over to indexing databases and slow readability for those readers

outside a discipline. They should never be used for the main subject (e.g., species or method) of a paper.

For general style, follow the U.S. Government Publishing Office *Style Manual* (2016, available at website) and *Scientific Style and Format: the CSE Manual for Authors, Editors, and Publishers* (2014, 8th ed.) published by the Council of Science Editors. For scientific nomenclature, use the current edition of the American Fisheries Society's (AFS) *Common and Scientific Names of Fishes from the United States, Canada, and Mexico* and its companion volumes (*Crustaceans, Mollusks, Cnidaria and Ctenophora*, and *World Fishes Important to North Americans*). For species not found in the previously mentioned AFS publications and for more recent changes in nomenclature, use the Integrated Taxonomic Information System (ITIS, available at website), or, secondarily, the California Academy of Sciences *Catalog of Fishes* (available at website) for species names not included in ITIS. Common (vernacular) names of species should be lowercase. Citations must be given for the identification of specimens. For example, "Fish species were identified according to Collette and Klein-MacPhee (2002); sponges were identified according to Stone et al. (2011)."

Dates should be written as follows: 11 November 2018. Measurements should be expressed in metric units, for example, "58 metric tons (t);" if other units of measurement are used, please make this fact explicit to the reader. Use numerals, not words, to express whole and decimal numbers in the general text, tables, and figure captions (except at the beginning of a sentence). For example, "We considered 3 hypotheses. We collected 7 samples in this location." Use American spelling. Refrain from using the shorthand slash (/), an ambiguous symbol, in the general text.

Cite all software, special equipment, and chemical solutions used in the study within parentheses in the general text, including the version number, company name, and the city and state (or nation) of the company headquarters, for example, "SAS, vers. 9.4 (SAS Institute Inc., Cary, NC)."

Word usage and grammar that may be useful are the following:

- *Aging*
  For our journal, the word *aging* is used to mean both age determination and the aging process (senescence). Authors should make clear which meaning is intended where ambiguity may arise.

- *Fish and fishes*
  The plural of the word fish (a collective noun that implies individuals without regard to species) is *fish*.
  Example: The *fish* were collected by trawl net.
  Example: The numbers of *fish* collected that season were less than the numbers from previous years.

  The plural for *fish species* is *fishes* (a contrived plural used by taxonomists to mean several or more *fish species*) or one can use *fish species* (which is preferred in this journal for clarity across disciplines).
  Example: The *fishes* of Puget Sound [biodiversity is implied] or
  Example: The *fish species* of Puget Sound [preferred plural for clarity across disciplines].

- *Crab and crabs, squid and squids, etc.*
  The plural of the word *crab* (i.e., many individuals without regard to species) is *crab*.
  Example: The crab were sorted by weight.
  Example: Many red king *crab* were dying [Many individuals of one species of crab.]

  The plural of *crab species* is *crabs* (a word used by taxonomists) or *crab species* (the latter is preferred in this journal for clarity).
  Example: These *crabs* were selected for treatment. [Different crab species are implied.]
  Example: These *crab species* were selected for treatment. [Preferred word choice for clarity.]
  Example: Snow *crabs* are found throughout the North Pacific Ocean and Bering Sea. [There are 2 species of snow crab; therefore the word *crabs* can be used here.]
  Example: *Two species* of snow *crab* are found throughout the North Pacific Ocean and Bering Sea. [Preferred usage for clarity.]
  Example: Three crabs were selected for treatment. [3 species of crab are implied.]
  Example: Three crab species were selected for treatment. [Preferred word choice for clarity.]

- We use *fisherman* and *fishermen*, not *fisher* and *fishers*, in this journal. One can always use crew member, vessel operator, and angler (the latter for recreational fishing).

- *The definite article with common names of species*
  When the singular common name of a species represents the entire class or group to which it belongs, use the definite article.
  Example: Only one species of the genus *Salmo* is found in the Atlantic Ocean—*the* Atlantic salmon (*Salmo salar*).
  Example: The sonic emissions of *the* bottlenose dolphin are complex.

  For plural common names, this rule does not apply.
  Example: Chinook salmon are found throughout the Pacific Ocean.
  Example: Bottlenose dolphins are found in temperate and tropical waters.

- *Sex*
  For the meaning of male and female, use the word *sex*, not *gender*. Do not write, "fish were sexed." Write, "sex was determined."

- *Participles*
  As adjectives, participles must modify a specific noun or pronoun.
  Example: Using mark-recapture methods, these scientists determined the size of the population. [Correct. The participle *using* modifies the word *scientists*.]

Example: These scientists, based on the collected data, concluded that the mortality rate of these fish had increased. [Incorrect. The scientists were not based on the collected data.]

Example: These scientists concluded, on the basis of collected data, that the mortality rate of these fish had increased. [Correct. The offending participle has been eliminated and an adverbial phrase modifies the verb *concluded*.]

Equations and mathematical symbols should be set from a standard mathematical program (MathType or Equation Editor). Equations formatted in LaTex are not acceptable. For mathematical symbols in the general text (α, χ^2, π, $\pm$, etc.), use the symbols provided by the MS Word program and italicize all variables, except those variables represented by Greek letters and the superscript and subscript parts of variables and expressions. Do not use photo mode when creating these symbols in the general text, and do not cut and paste equations, letters, or symbols from a different software program.

Number equations (if there are more than one) for future reference by scientists; place the number within parentheses at the end of the first line of the equation.

Literature cited section comprises published works and those accepted for publication (in press) in peer-reviewed journals. Follow the name and year system for citation format in this section (i.e., citations should be listed alphabetically by the authors' last names, and then by year if there is more than one citation by the same author. A list of abbreviations for citing journal titles can be found on our website.

Authors are responsible for the accuracy and completeness of all citations. Avoid the use of multiple citations when a single citation sufficiently supports a statement; cite the work that first reported the information that supports a statement, not all of the subsequent works. Literature citation format: Authors (last name, followed by initials for first name and, if given, middle name of first author; then list names of additional authors with initials before last names). Year. Title of article. Abbreviated title of the journal in which it was published. Always include either the range of page numbers (for a journal article) or a total number of pages (for a book or other type of publication). List a sequence of citations in the general text chronologically, for example, "(Smith, 1932; Green, 1998; Smith and Jones, 2015)."

Acknowledgments should be no more than 6 lines of text. Only those who have contributed in an outstanding way should be acknowledged by name. For recognition of other persons or groups, use a general term, such as *crew*, *observers*, or *research coordinators*, and do not include names with these terms.

Digital object identifier (doi) code ensures that a publication has a permanent location online. A doi link (which may include a doi code) should be included at the end of citations of published literature. Authors are responsible for submitting accurate doi links. Faulty links will be deleted at the page-proof stage.

Footnotes are used for all documents that have not been formally peer reviewed and for observations and personal communications, but these types of references should be cited sparingly in manuscripts submitted to the journal.

All reference documents, administrative reports, internal reports, progress reports, project reports, contract reports, personal observations, personal communications, unpublished data, manuscripts in review, and council meeting notes are footnoted in 10-point font and placed at the bottom of the page on which they are first cited. Footnote format is the same as that for formal literature citations. A link to the online source (e.g., [Available from http://www... , accessed July 2017.]), or the mailing address of the agency or department holding the document, should be provided so that readers may obtain a copy of the document.

Tables are often overused in scientific papers; it is seldom necessary to present all the data associated with a study. Tables should not be excessive in size and must be cited in numerical order in the text. Headings should be short but ample enough to allow the table to be intelligible on its own.

All abbreviations and unusual symbols must be explained in the table legend. Other incidental comments may be footnoted with numeral footnote markers. Use asterisks only to indicate significance in statistical data. Do not put a table legend on a page separate from the table; place the legend above the table. *Do not submit tables in photo mode.*

- Note probability with a capital, italic *P*.
- Provide a zero before all decimal points for values less than one (e.g., 0.07).
- Round all values to 2 decimal points.
- Use a comma in numbers of 5 digits or more (e.g., 13,000 but 3000).

Figures must be cited in numerical order in the text. Graphics should aid in the comprehension of the text, but they should be limited to presenting patterns rather than raw data. The number of figures should not exceed 1 figure for every 4 pages of text.

Figure legends should explain all symbols and abbreviations seen in the figure and should be double spaced on a separate page at the end of the manuscript.

Line art and halftone figures should be saved at resolutions >600 dots per inch (dpi) and >300 dpi, respectively. Color is allowed in figures to show morphological differences among species (for species identification), to show stain reactions, to show gradations (such as those of temperature and salinity within maps), and to distinguish

between numerous lines and symbols in graphs. Figures approved for color should be saved in CMYK format.

All figures must be submitted as PDF, TIFF, or EPS files.

- Capitalize only the first letter of the first word and proper nouns in all labels within figures.
- Do not use overly large font sizes for labels in maps and for axis labels in graphs.
- Use the same point size for all labels, except for panel labels (e.g., **A**), which should be slightly larger than other labels (e.g., 11 point versus 8 point).
- Use a sans serif font for all labels. Panel labels (e.g., **A**), however, should be in Times New Roman font.
- Do not use bold fonts or bold lines in figures. Do not use italic fonts. Exceptions include use of italic fonts for labels of bodies of water in maps and a bold font for panel labels (e.g., **A**).
- Do not place outline rules around graphs.
- Do not include vertical and horizontal lines in the background of graphs. Ticks for values on the x-axis and y-axis will suffice.
- Place a north arrow and label degrees latitude and longitude (e.g., 170°E) in all maps. If scale of map requires more than degrees, use degrees minutes, not decimal degrees.
- Place panel labels (e.g., **A**, **B**, **C**) within the upper-left area of each graph or photo in a multi-panel figure, from left to right, then top to bottom. If the letter is not visible against a dark background, put a white box behind it. Do not use white labels.
- Avoid placing labels vertically or diagonally. Y-axis labels can be vertical. Words in horizontal labels can be stacked vertically to fit.
- Use symbols, shading, or patterns (not clip art) in maps and graphs.
- For scale bars in maps, use kilometers. Use the label *km* or *kilometers* (lowercased).

Supplementary materials that are considered essential, but are too large or impractical for inclusion in a paper (e.g., metadata, figures, tables, videos, and websites), may be provided at the end of an article. These materials are subject to the editorial standards of the journal. A URL to the supplementary material and a brief explanation for including such material should be sent at the time of initial submission of the paper to the journal.

- **Metadata, figures, and tables** should be submitted in standard digital format (MS Word or PDF file) and should be cited in the general text, for example, as ". . . was determined (Suppl. Table 3, Suppl. Fig. 1)."
- **Websites** should be cited with a URL in the general text.
- **Videos** must not be larger than 30 MB to allow a swift technical response for viewing the video. Authors should consider whether a short video uniquely captures what text alone cannot capture for the understanding of a process or behavior under examination in the article. Supply an online link to the location of the video.

Copyright law does not apply to *Fishery Bulletin*, which falls within the public domain. However, if an author reproduces any part of an article from *Fishery Bulletin*, reference to source is considered correct form (e.g., Source: Fish. Bull. 117:105).

Failure to follow these guidelines and failure to correspond with editors in a timely manner will delay publication of a manuscript.

Submission of manuscript

Submit a manuscript online at the ScholarOne Manuscripts website for *Fishery Bulletin*. Commerce Department authors must provide proof of internal clearance of their manuscripts with either a completed and signed NOAA Form 25-700 or a copy of the clearance email from the Research Publication Tracking System. For further details on electronic submission, please contact the associate editor, Cara Mayo, at

cara.mayo@noaa.gov.

When requested, the text and tables should be submitted in MS Word format. Each figure should be sent as a separate PDF, TIFF, or EPS file. Send a copy of a figure in the original software if conversion to any of these formats yields a degraded version of the figure.

Questions? If you have questions regarding these guidelines, please contact the managing editor, Kathryn Dennis, at

kathryn.dennis@noaa.gov.

Questions regarding manuscripts under review should be addressed to Associate Editor Cara Mayo.

Fishery Bulletin

Subscription form

Superintendent of Documents **Publications** Order Form

*5178

☐ YES, please send me the following publications:

____ Subscriptions to *Fishery Bulletin*
for $32.00 per year ($44.80 foreign)

The total cost of my order is $ _____ . Prices include regular domestic postage and handling and are subject to change.

_____
(Company or Personal Name) (Please type or print)

_____
(Additional address/attention line)

_____
(Street address)

_____
(City, State, ZIP Code)

_____
(Daytime phone including area code)

_____
(Purchase Order No.)

Charge your order.
IT'S EASY!

VISA

MasterCard

Please Choose Method of Payment:

☐ Check payable to the Superintendent of Documents
☐ GPO Deposit Account ☐☐☐☐☐☐☐–☐
☐ VISA or MasterCard Account
☐☐☐☐☐☐☐☐☐☐☐☐☐☐☐☐
☐☐☐☐ (Credit card expiration date)

To fax your orders (202) 512-2104

_____
(Authorizing Signature)

Mail to: Superintendent of Documents
P.O. Box 979050, St. Louis, Missouri 63197
Tel. no. (U.S. callers): 866-512-1800
Tel. no. (International callers): 1-202-512-1800

Thank you for your order!

Also available online at
https://bookstore.gpo.gov/products/fishery-bulletin
email: ContactCenter@gpo.gov

SMITHSONIAN LIBRARIES
3 9088 02039 9580